PFC/RR-83-08 DOE UC-20, C, D, E

MODELING OF LITHIUM AND LITHIUM-LEAD REACTIONS IN AIR USING LITFIRE

Victor J. Gilberti

and

Mujid S. Kazimi

January 1983

Plasma Fusion Center

and the

Department of Nuclear Engineering

Massachusetts Institute of Technology
Cambridge, Massachusetts 02139

Prepared for

E.G. & G. Idaho, Inc.

and

The U.S. Department of Energy
Idaho Operations Office

under

DOE Contract #DE-AP07-79ID0019

LITHIUM AND LITHIUM-LEAD MODELING IN MULTI-COMPARTMENT SYSTEMS

by

Victor J. Gilberti

and

Mujid S. Kazimi

ABSTRACT

LITFIRE is a computer code that simulates the combustion of lithium in various containment schemes. The accuracy of LITFIRE in predicting thermal and pressure responses of containment atmosphere and structures has been tested against small scale (100 kg. Li) spills performed at the Hanford Engineering Development Laboratory. The agreement between experiment and LITFIRE prediction was within 10%

Modifications to the code have been made to increase its utility in modeling fires in fusion reactor containments. The ability to monitor lithium-lead alloy reactions in air has been incorporated into LITFIRE. Also, the geometry has been made more flexible and the available options made compatible with one another. Preliminary comparisons indicate that lithium-lead alloys are less reactive than pure lithium and generate maximum cell gas temperatures that are nearly a factor of two lower than those resulting from pure lithium fires, for the same volume of liquid metal spilled.

Application of LITFIRE to fires in a prototypical fusion reactor was made. The predictions of LITFIRE indicate that fires limited to the torus of a tokamak fusion reactor would be much less severe than fires resulting from spills directly onto the containment building floor. However, the primary wall and surrounding structures would become hotter in spills inside the torus because they are directly exposed to radiative heating by the fire.

PUBLICATIONS UNDER CONTRACT #K-1702

ON FUSION SAFETY

1. M. S. Kazimi et al., "Aspects of Environmental Safety Analysis of Fusion Reactors," MITNE-212, Dept. of Nuclear Engineering, M.I.T., October 1977.

2. R. W. Sawdye, J. A. Sefcik, M. S. Kazimi, "Reliability Requirements for Admissible Radiological Hazards from Fusion Reactors," Trans. Am. Nucl. Soc. 27, 65-66, November 1977.

3. D. A. Dube, M. S. Kazimi and L. M. Lidsky, "Thermal Response of Fusion Reactor Containment to Lithium Fire," 3rd Top. Meeting in Fusion Reactor Technology, May 1978.

4. R. W. Sawdye and M. S. Kazimi, "Application of Probabilistic Consequence Analysis to the Assessment of Potential Radiological Hazards of Potential Hazards of Fusion Reactors," MITNE-220, Dept. of Nuclear Engineering, M.I.T., July 1978.

5. D. A. Dube and M. S. Kazimi, "Analysis of Design Strategies for Mitigating the Consequences of Lithium Fire within Containment of Controlled Thermonuclear Reactors," MITNE-219, Dept. of Nuclear Engineering, M.I.T., July 1978.

6. R. W. Sawdye and M. S. Kazimi, "Fusion Reactor Reliability Requirements Determined by Consideration of Radiological Hazards," Trans. Am. Nucl. Soc. 32, 66, June 1979.

7. R. W. Green and M. S. Kazimi, "Safety Considerations in the Design of Tokamak Toroidal Magnet Systems," Trans. ANS 32, 69, June 1979.

8. R. W. Green and M. S. Kazimi, "Aspects of Tokamak Toroidal Magnet Protection," PFC/TR-79-6, Plasma Fusion Center, M.I.T., July 1979.

9. S. J. Piet and M. S. Kazimi, "Uncertainties in Modeling of Consequences of Tritium Release from Fusion Reactors," PFC/TR-79-5, Plasma Fusion Center, M.I.T., July 1979.

10. M. J. Young and S. J. Piet, "Revisions to AIRDOS-II," PFC/TR-79-8, Contract #K-1702, Plasma Fusion Center, M.I.T., August 1979.

11. S. J. Piet and M. S. Kazimi, "Implications of Uncertainties in Modeling of Tritium Releases from Fusion Reactors," Proc. Tritium Technology in Fission, Fusion and Isotopic Applications, April 1980.

12. M. S. Tillack and M. S. Kazimi, "Development and Verification of the LITFIRE Code for Predicting the Effects of Lithium Spills in Fusion Reactor Containments, PFC/RR-80-11, Plasma Fusion Center, M.I.T., July 1980.

Publications Under Contract #K-1702 (continued)

13. M. S. Kazimi and R. W. Sawdye, "Radiological Aspects of Fusion Reactor Safety: Risk Constraints in Severe Accidents," J. of Fusion Energy, Vol. 1, No. 1, pp. 87-101, January 1981.

14. P. J. Krane and M. S. Kazimi, "An Evaluation of Accidental Water-Reactions with Lithium Compounds in Fusion Reactor Blankets," PFC/RR-81-26, Plasma Fusion Center, M.I.T., July 1981.

15. D. R. Hanchar and M. S. Kazimi, "Tritium Permeation Modelling of a Conceptual Fusion Reactor Design," PFC/RR-81-27, Plasma Fusion Center, M.I.T., July 1981.

16. M. S. Kazimi, "IAEA Workshop on Fusion Safety March 23-27, 1981, Vienna, Austria," J. of Fusion Energy, Vol. 1, No. 3, ppl 241-243, 1981.

17. M. S. Tillack and M. S. Kazimi, "Modelling of Lithium Fires," Nuclear Technology/Fusion, Vol. 2, No. 2, pp. 233-245, April 1982.

18. S. J. Piet, M. S. Kazimi and L. M. Lidsky, "Potential Consequences of Tokamak Fusion Reactor Accidents: The Materials Impact," PFC/RR-82-19, Plasma Fusion Center, M.I.T., June 1982.

19. S. J. Piet, V. J. Gilberti, "FUSECRAC: Modifications of CRAC for Fusion Application," Nuclear Eng. Dept. and Plasma Fusion Center, M.I.T., PFC/RR-82-20, June 1982.

20. M. S. Kazimi, "Safety and Risk Targets for Fusion Energy," Societe Francaise de Radioprotection 10th Annual Congres, Avignon, France Oct. 18-22, 1982.

21. V. J. Gilberti and M. S. Kazimi, "Modeling of Lithium and Lithium-Lead Reactions in Air Using LITFIRE," PFC/RR-83-08, Plasma Fusion Center, M.I.T., January 1983.

ACKNOWLEDGEMENTS

The personal interest in this work of G. Nardella of DOE and J. Crocker and S. Cohen of E.G. & G., Idaho is much appreciated. Several discussions with D. W. Jepson of HEDL were also helpful in understanding the experimental results used in this report.

We are grateful to Gail Jacobson for her assistance in typing the tables and figures; to Joe Johnson for helping Victor discover the joys of text editing and the frustrations of computing; and to Mark Tillack for making sense of LITFIRE when it seemed an impossible task.

This report is based on a thesis submitted by the first author to M.I.T. in fulfillment of the requirements of an M.S. Degree in Nuclear Engineering.

TABLE OF CONTENTS

LIST OF FIGURES

LIST OF TABLES

1. INTRODUCTION

1.1. Background on Lithium Fire Modeling

The study of lithium fires is primarily due to lithium's presence in proposed fusion reactors as a tritium breeder and/or coolant. A major safety concern of using lithium is the potentially large amount of energy that could be released into the containment from lithium-air or lithium-water chemical reactions. This energy may be sufficient to cause melting and/or volitalization of structural materials as well as substantial pressurization of the containment building. Aside from the structural damage itself, another safety concern is volatilization of radioactive structural materials, such as the first wall of a tokamak torus. The high temperatures, coupled with possible pressurization of the containment, may lead to failure of the containment integrity. Therefore, lithium fires are a possible mechanism for release of radioactive particles outside the containment [1]. In addition, the reaction products of lithium air or water interactions (LiOH, Li_3N, Li_2O) are themselves corrosive and can also damage the reactor's structural materials.

As a result of these safety concerns with pure lithium, other lithium based alloys have been proposed as coolants and/or breeders. Among these are several lithium-lead alloys (Li_7Pb_2, $Li_{17}Pb_{83}$, $LiPb_4$), as well as LiAl and Li_2O. Limited preliminary studies indicate that these alloys are less reactive and may be safer to use than pure lithium [2]. A comparison of alternate coolants and breeders appears in Table 1.1. For an extensive analysis of the relative hazards associated with many of the proposed breeder/coolant combinations see the discussion in chapter five of Piet, et. al., [3]. Table 1.2 lists the important chemical reactions with lithium or LiPb compounds.

Several experiments of lithium combustion in various atmospheres have been performed to determine the consequences of such reactions as well as to formulate an engineering database for the combustion of lithium. These experiments are on a small scale (1 to 100 kg.-Li burned) when compared to a fusion reactor inventory of approximately 400,000 kg.-Li (for UWMAK-III) [4]. The results of these experiments were used to calibrate many of the empirical relations found in LITFIRE, the computer code that is the basis for the present work.

Since the lead component of LiPb is effectively inert, these compounds are expected to react with the same materials as pure lithium. Experiments using LiPb as reactant have been limited to small tests (0.05 kg.-LiPb) in water and one test in air using a blow torch as the heat source [5]. Other experiments involving LiPb combustion in an air atmosphere are in progress but data from these will not be available in time for use in the present work [6].

The properties of lithium and lithium-lead compounds are not completely known over the temperature range of interest. For LiPb the data is minimal and is summarized in section 4.2 of

TABLE 1.1

Comparison of Alternate Coolants and Breeders

Material	(B = Breeder) (C = Coolant)	Advantages	Disadvantages
Lithium	B & C	Excellent heat transfer High boiling point Low melting point High specific heat Low viscosity Good neutron moderator No long-term activation products No neutron damage High breeding ratio possible Low density	Highly reactive with: air water concrete High electrical conductivity
Li_aPb_b	B	Lower chemical reactivity than lithium High breeding ratio possible Lead is a good neutron shield for magnets Tritium recovery feasible	Poor technology base High density Activation product: Pb^{205} Reactive with water or lithium coolant
Flibe (34 BeF_2: 66 LiF)	B + C	Good neutron moderator Low vapor pressure Low electrical conductivity Low tritium solubility Low chemical reactivity (expected)	Scarcity of berylium
$LiAlO_2$	B	Chemical stability	Requires neutron multiplication
Water	C	Substantial engineering experience and database	Reacts with Li, and LiPb alloys High pumping power High operating pressure

TABLE 1.2

Lithium Reactions of Interest

	Heat of Reaction, ΔH_{298} kcal/mole of product
In Air	
$4Li + O_2 \longrightarrow 2Li_2O$	-43
$2Li + O_2 \longrightarrow Li_2O_2$	-152
$6Li + N_2 \longrightarrow 2Li_3N$	-48
$2Li + 2H_2O \longrightarrow 2LiOH + H_2$	-49
$2Li + H_2 \longrightarrow 2LiH$	
$2Li + LiOH \longrightarrow 2LiO_2 + H_2$	
Note: Li_2O_2 is unstable above 250 °C	-151.3 (magnetite)
In Concrete	
$8Li + Fe_3O_4 \longrightarrow 3Fe + 4Li_2O$	-151.3 (magnetite)
$4Li + SiO_2 \longrightarrow Si + 2Li_2O$	(basalt)
$2Li + H_2 \longrightarrow 2LiH$	
Others	
$4Li + 3CO_2 \longrightarrow 2Li_2CO_3 + C$	-45
$nLi + mPb \longrightarrow Li_n Pb_m$	$-13n$ for $\frac{n}{m} < 1$

this report. However, work is continuously being done to expand the database, and two reports have been published that review the state of knowledge of these materials [7,8]. Property data in the present calculations have been taken from these two reports unless otherwise specified.

1.2. LITFIRE History and Development

The computer code LITFIRE, developed at MIT, is an analytic tool for calculating the consequences of lithium fires in various containment schemes. In its original form, LITFIRE was a modified version of SPOOL-FIRE [9] which modeled liquid-metal sodium fires in containment. The adaptation of SPOOL-FIRE to LITFIRE incorporated several major changes. These include allowance for nitrogen and water vapor reactions as well as changing sodium properties implicit in the code to lithium properties. In addition, the effect of aerosols in the containment on radiative heat transfer was included. By far the most important change to the modeling was the incorporation of a "combustion zone" above the lithium pool. It is in this zone that lithium combustion takes place, according to mass and heat transfer mechanisms described by Dube [1].

With these changes in tact LITFIRE was used to predict the consequences of a postulated lithium fire in a prototypical fusion reactor geometry. A sensitivity analysis was performed on many of the important parameters in LITFIRE and best estimates for these parameters were adopted. An analysis of strategies for mitigating the consequences of lithium fires was performed and found to have significant effects [1].

After the original study was completed, lithium combustion experiments were conducted at the Hanford Engineering Development Laboratory (HEDL). The geometry of these experiments differed significantly from the capabilities of LITFIRE and useful comparisons were not readily attainable. Several changes were made to LITFIRE to model the experimental setup and the predictions of LITFIRE were then compared to the experimental data. The new modifications brought the temperature field predictions to within 30% of the HEDL experimental results for a variety of lithium reactions. Details of the experiments and LITFIRE changes were documented by Tillack [10]. Other unverified extensions of the code were also developed at that time. They include the capacity for lithium-concrete reactions and a two compartment containment scheme with combustion in one cell and mass and heat transfer between the two cells.

The inclusion of LiPb-water reactions in a prototypical breeder element was next incorporated into LITFIRE [2]. This modeling is substantially different from the combustion zone model for pool fires and has therefore been separated from the rest of the lithium fire modeling. As a result there are now two versions of LITFIRE, (LITFIRE-A) treating lithium-air and lithium-concrete reactions; and (LITFIRE-B) treating LiPb-water reactions. The addition of LiPb-air reactions is

part of the present work and will be incorporated into LITFIRE-A since much of the combustion zone modeling is identical to that of lithium-air reactions. Table 1.3 lists the versions and options of LITFIRE that are presently available and their state of verification with respect to experiment.

1.3. LITFIRE Model Description

LITFIRE generates the temperature and pressure profiles in an idealized geometry with a single heat source and various heat sinks. The heat source term represents the combustion of lithium. When combustion has ceased, or the reaction does not ignite, the hottest structural component (or the lithium pool itself) will act as a decaying heat source until all the temperatures reach equilibrium with ambient. The heat flow between nodes is one-dimensional and consists of conductive, convective, and radiative components when appropriate.

convection	$\frac{dq}{dt} = h A (T_1 - T_2)$	Newton's Law of Cooling $h = h(\mathrm{Gr},\mathrm{Pr})$ = heat transfer coefficient	(1.1)
conduction	$\frac{dq}{dt} = k A \frac{dT}{dx}$	Fourier's Conduction Equation $k = k(T)$ = thermal conductivity	(1.2)
radiation	$\frac{dq}{dt} = \sigma A (T_1^4 - T_2^4)$	Stephan- Boltzman Law σ = Stephan-Boltzman Constant	(1.3)

In some cases one of the channels may be ignored if it is not of significant magnitude with respect to the other components.

Correlations for the heat transfer mechanisms are fairly simple and the combustion source term is highly idealized in order to: 1) permit greater flexibility for users; 2) base the calculations on available data, and; 3) to reduce computation time and costs. For a given geometry, there are enough user defined coefficients to accurately model the principal heat transfer mechanisms. However, the combustion zone model is fairly inflexible and is also the most simplified part of the LITFIRE model. The effect of surface layer formation, wicking, product buildup in the pool, and multiple species reactant competition are ignored or very crudely modeled. Significant improvements to multiple species combustion were added by Tillack [10] and are further discussed in chapter 2 of this report.

The idealized energy flows in LITFIRE (one and two cell versions) are shown in Figures 1.1 and 1.2. Each node has a heat capacity approximating that of its physical counterpart (average specific heat of the material times the total mass of the node) and a single, bulk averaged temperature. Heat transfer between two nodes is a function of temperature difference and the equivalent thermal resistance (for each heat transfer mechanism) of that specific pair of nodes.

Mass flows in LITFIRE are also lumped and are principally between the two cell gas nodes, the combustion zone and lithium pool, and the combustion zone and primary cell gas. These are

TABLE 1.3

LITFIRE Versions and Available Options

Version	Reaction Modeled	Available Options	State of Verification
LITFIRE-A	Li-Air	One or two cells Pan geometry Gas injections Emergency cooling of floor or cell gas SI or English units	Compared to small scale HEDL tests. (less than 100kg. Li)
LITFIRE-A	Li-Concrete	All of above except pan geometry	Unverified
LITFIRE-A	LiPb-Air	Same as Li-Air reactions	Unverified
LITFIRE-B	LiPb-Water	One cell SI or English units	Unverified

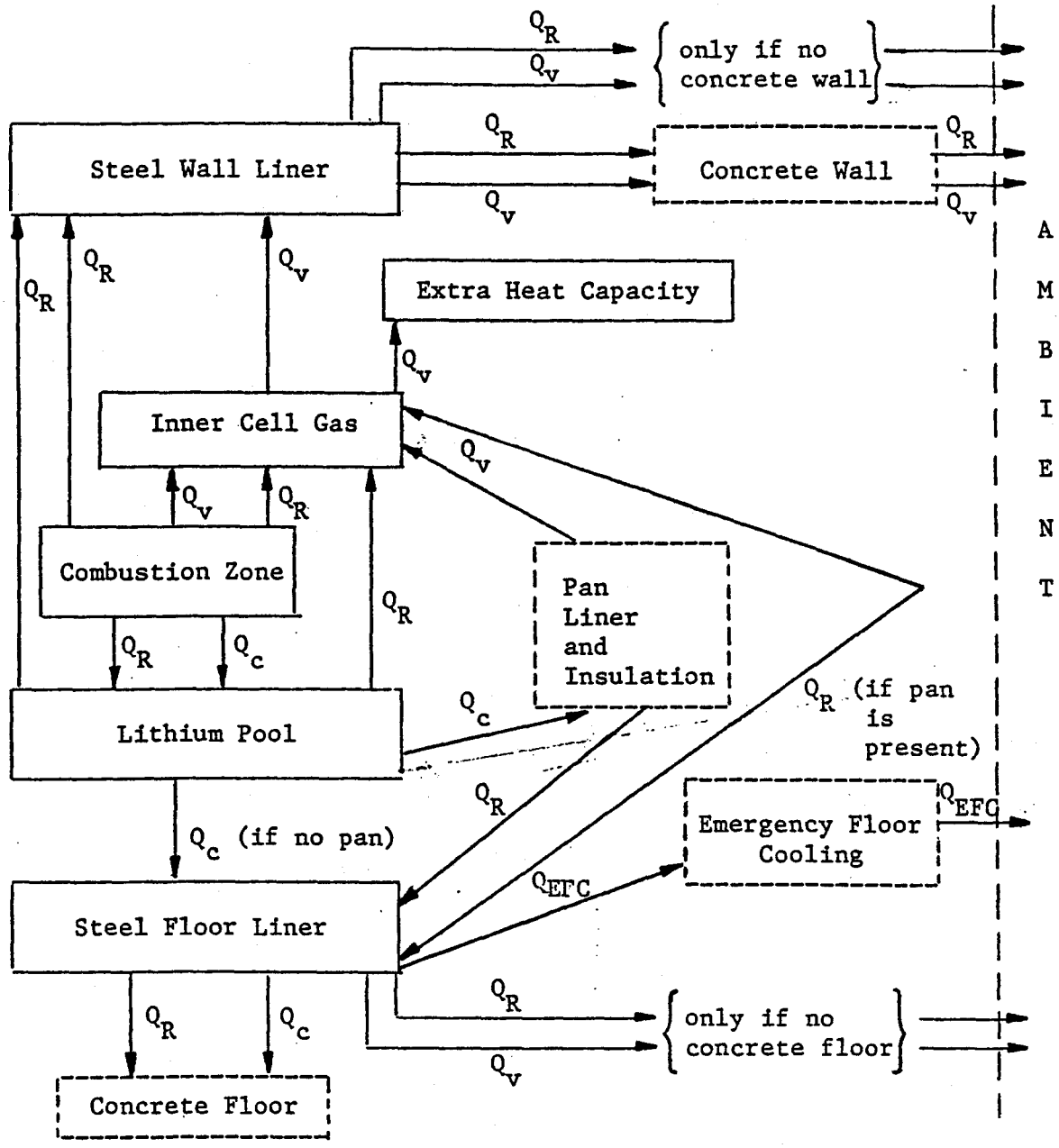

dashed lines indicate optional node

Q_R = radiative heat transfer

Q_v = convective heat transfer

Q_c = conductive heat transfer

Figure 1.1: Energy flow in single cell LITFIRE

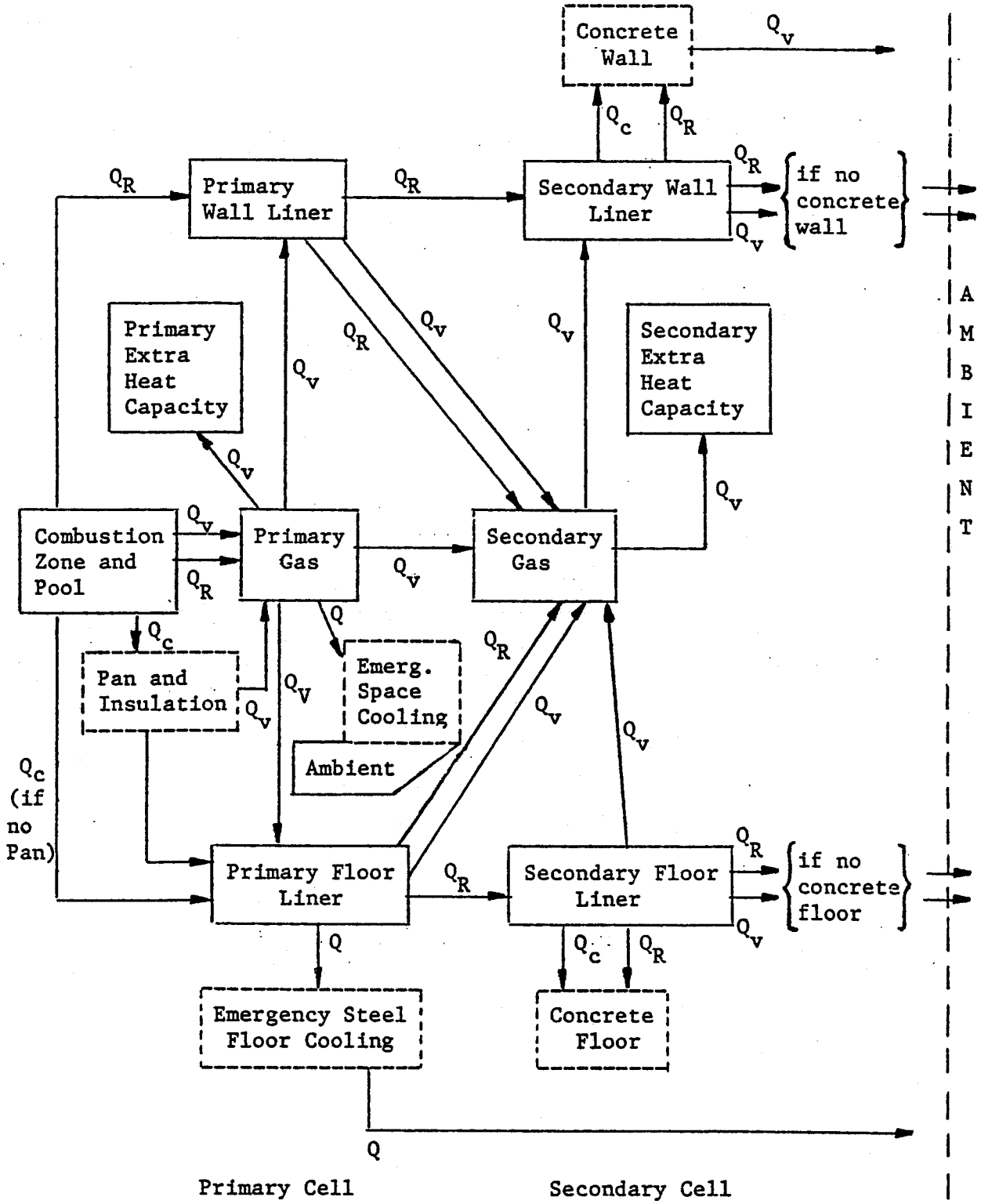

Figure 1.2: Energy flow in two-cell LITFIRE

shown schematically in Figure 1.3. Structural materials are not allowed to participate in the mass flows and are considered stable at any temperature. Therefore, LITFIRE is not capable of predicting the effects of volatilization or melting of structural components and the user should be aware that the predictions of LITFIRE will be inaccurate in this regime. More detailed descriptions of the mass flows are given in chapters 3 (two cell exchange) and 4 (combustion zone-pool transport).

The time history in LITFIRE is determined by a set of simultaneous coupled differential equations. For each thermal element in the model the temperature history is calculated by a set of numerical integration subroutines that use the methods of finite differences in the spatial regime and either Simpson's rule or a fourth-order Runge-Kutta method in the time domain [1]. The actual integration is of the form

$$Y(t) = Y(t_0) + \int_{t_0}^{t} dt' \, \frac{dY}{dt'} \qquad (1.4)$$

where the time rates of change (dY/dt') are calculated in the main LITFIRE program for each node by finite differencing. The program solves for each node simultaneously during each time step and has a capacity of 100 separate nodes. The numerical stability during each time step determined form the fractional temperature change at certain nodes during a single time step (different from integration time step). LITFIRE uses the most sensitive nodes to determine the stability criteria, but it is still possible that under certain regimes the code may produce nonphysical results. Experience has shown that this can happen when a node is given too thin a thickness or too high a conductivity. Recommended values are listed in the user's guide [11] and were used in the present calculations. Another numerical instability can occur if there is an oscillatory solution to a given node that has a period of the same magnitude of the time step. In LITFIRE, this has been found to occur on occasion when an orifice is used in the two cell option. This phenomena is discussed in more detail in chapter 3.

The program flow has been reorganized to promote clarity and facilitate modification to the existing coding as well as reduce computation time. Nine subroutines have been added to the body of the program that represent options available with LITFIRE. Specifically, these are two cell, LiPb combustion, pan geometry, concrete wall, concrete floor, concrete combustion, gas injection, and SI units subroutines. (Appendix D contains a listing of the version of LITFIRE used in the present calculations.) In addition, many of the variable names and intermediate program calculations have been changed for greater clarity. Appendix F contains a glossary of all variables presently used in LITFIRE.

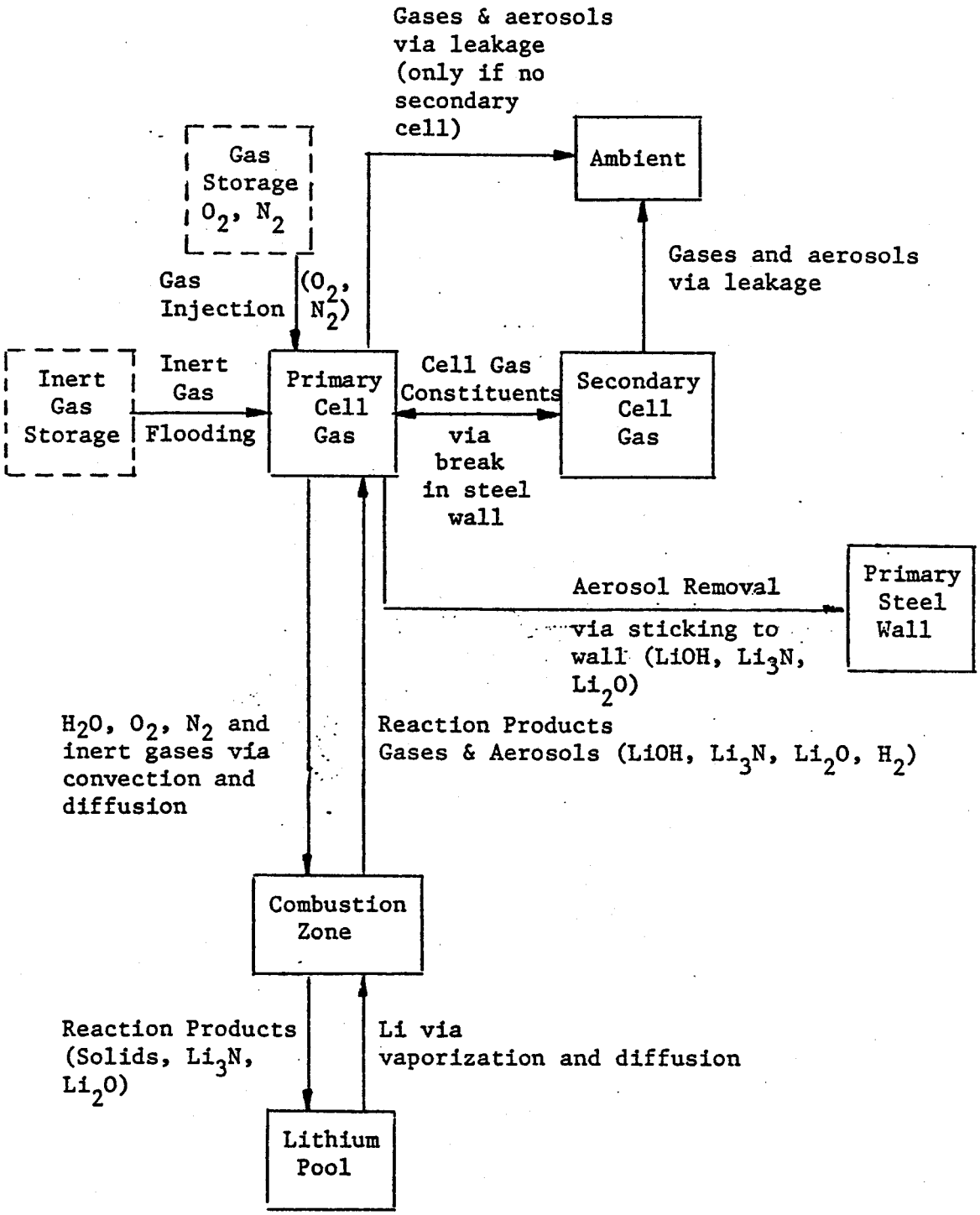

Figure 1.3: Mass flows in LITFIRE

1.4. Scope of Present Work

The purpose of the present work is three-fold. First, to compare predictions from the most recent version of LITFIRE with the latest experimental data available. There are several significant differences between the present modeling in LITFIRE and the modeling in the version that was used for the earlier comparison with the HEDL experiments. [12] In Chapter 2, these differences are discussed and analyzed and the comparison between LITFIRE and experiment is brought up to date.

Second, to study the effects of pure lithium fires in multi-compartment systems. In this case the system approximates those of a commercial scale tokamak torus and containment building. This application of LITFIRE uses the two cell formalism and is described in detail in chapter 3.

The third part of this thesis is to incorporate LiPb-air reactions into the present structure of LITFIRE so that safety comparisons between alternate coolants and/or breeders may be made. This extension of the model required several important changes in the treatment of the pool node and transport of Lithium to the combustion zone. These changes are documented in Chapter 4 as are the results from preliminary comparisons of various LiPb compounds.

2. DEVELOPMENT AND APPLICATION OF SINGLE-CELL LITFIRE

LITFIRE has been in various stages of development at MIT over the past five years. Results of LITFIRE calculations using intermediate versions of the code have been published by Dube [1] (1978) and Tillack [10] (1980). The comparison to experiment by Tillack [10] did not use the LITFIRE version that incorporated many of the changes made since Dube's publication. Therefore, it is the purpose of the following section to summarize the important changes made since Tillack [10] and the purpose of the remainder of the chapter to compare the most recent version of LITFIRE with experiment and previous calculations.

2.1. Recent Changes to the LITFIRE Model

The major changes to the LITFIRE single-cell model since it was described by Tillack [10] are summarized below and are also indicated pictorially in Figure 2.1.

- **Radiation from pool to cell wall and cell gas.** Originally, only the combustion zone was radiating to the cell wall and containment gas. At present, the pool surface is also radiating heat to the cell wall and gas. This change is based on the assumption that the combustion zone is too thin to absorb all of the radiation emitted at the pool surface. Incorporating this pathway into the model required the addition of a combustion zone transmissivity that allowed greater flexibility in coupling the radiative interchange between the combustion zone and pool nodes. The changes were made in order to bring the pool temperature closer to the combustion zone temperature and at the same time minimize the effect on the cell gas temperature. Appropriate values for the transmissivity are the subject of Section 2.3.2.

- **Cell gas emissivity.** The correlation for the emissivity of the primary cell gas was altered in order to bring the cell gas temperatures in agreement with experimental observations. The upper limit of the emissivity was reduced from 1.0 to 0.04 in order to reduce the radiation heat absorption by the gas. The emissivity of the secondary cell gas was not altered and may still reach a maximum of unity (although this is very unlikely since there usually is very little aerosol present in the secondary gas). These changes were documented by Tillack [10] but were not used in his comparisons with experiment nor did they appear in previous versions of LITFIRE that are still available.

- **Aerosol removal from primary cell gas.** An optional mechanism for the removal of aerosols from the primary cell gas has been included in the code. This can have

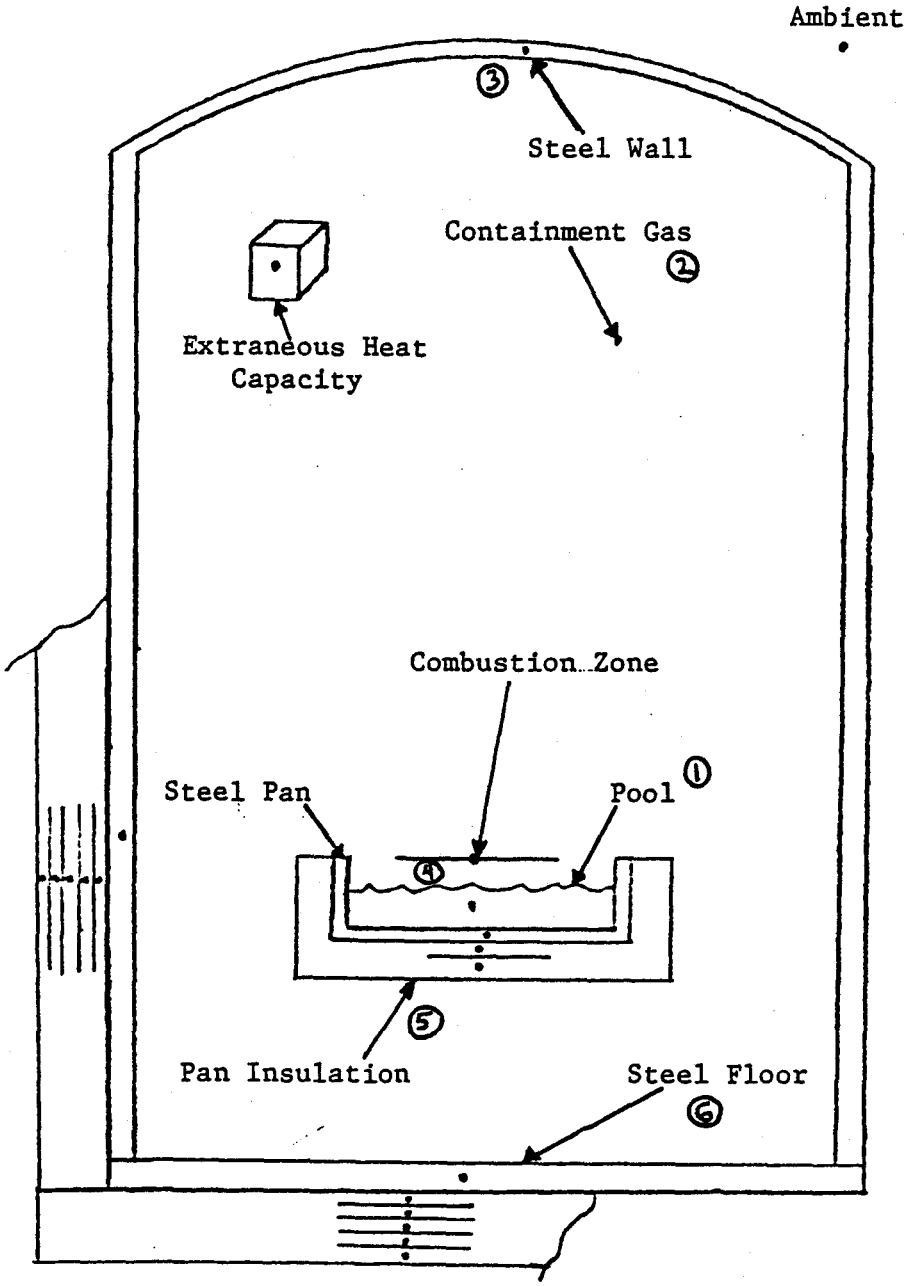

1. Radiation From Pool to Gas and Wall
2. Containment Gas Emissivity
3. Aerosol Removal
4. Film Conductivity
5. Radiation From Pan to Containment Gas
6. Convection from Steel Floor to Containment Gas

Figure 2.1: Diagram of Changes to LITFIRE Single Cell

a significant effect on the cell gas emissivity since

$$\text{gas emissivity} = C_1(1 - \exp(\text{-aerosol} \times C_2)) \qquad (2.1)$$

where C_1 is a user defined constant between zero and one, C_2 is a function of the cell geometry, and 'aerosol' is the combined volume (mass/density) of all aerosols present in the primary gas. The net effect of aerosol removal will be to reduce the cell gas emissivity. The magnitude of this effect as well as its relation to cell gas temperature is discussed in Section 2.3.1.

- **Thermal conductivity between combustion zone and pool.** The region between the combustion zone and lithium pool was originally assumed to be composed only of unreacted nitrogen vapor. This assumption was inconsistent with the assumed transport of Lithium through this region by vapor diffusion. As a result, the conductivity of the film region is now calculated using a pressure weighted mean average of nitrogen and lithium vapors. The partial pressure of lithium is a known function of the pool temperature and the partial pressure of nitrogen is assumed to be equal to the cell gas pressure. The resulting conductivity of the film region is higher (due to lithium's high conductivity) and as a result, more heat is transferred from the combustion zone to heating the pool. Unfortunately, the present modeling does not permit calculation of the diffusion *rate* of lithium through this region. Therefore, the combustion rate of lithium is still assumed to be gas (O_2,N_2) limited and is one of the weakest assumptions in LITFIRE. (This has been changed slightly in the LiPb combustion model and is discussed in detail in chapter 4.)

- **Radiation from pan insulation to cell gas.** This had already been documented as part of LITFIRE but did not appear in the fortran listing. The effect on the cell gas temperature was negligible due to the low emissivity of the insulation.

- **Convection between steel floor liner and primary cell gas.** This is only allowed when the pan geometry is being used since the floor is no longer in direct contact with the lithium pool. This was included because "suspended" position of the pan allowed communication between the steel floor and cell gas. In addition, the size of the steel floor was made independent of the area of the lithium pool or spill pan. Before the change, the floor area was assumed equal to that of the lithium pool area, regardless of geometry, since it was assumed that axial conduction in the floor would be negligible. However, use of the two-cell code emphasized the importance of the floor area in heat transfer to the secondary cell.

2.2. Application of LITFIRE to Experiment

In the past year, additional lithium combustion experiments have been performed at HEDL. [6] These tests include lithium combustion in air, carbon dioxide, and water, and were larger in scale than the tests reported by Tillack [10]. The two most recent air tests (LA-4 :25 kg.-Li,LA-5:100 kg.-Li) were significantly larger than earlier tests (10 kg.-Li) and provide data to check LITFIRE predictions for somewhat larger fires than the present correlations were obtained from. This serves as a partial check on the applicability of using LITFIRE for modeling the large scale lithium fires that are possible in commercial size fusion reactors.

2.2.1. Description of HEDL Experiment

The basic geometry of the test facility described below is shown in Figure 2.2 and a summary of the important test parameters appears is Table 2.1. The lithium pool-air reaction tests were performed in a carbon steel containment vessel measuring 20.4 meters in height and 7.6 meters in diameter with standard dished top and bottom heads. This containment formed the primary pressure and aerosol boundary within which each test was carried out. Inner surfaces were coated with a modified phenolic paint and the interior of the vessel was essentially void. However, a platform and structural supports provided a 50%increase in horizontal surface area for aerosol particle settling.

Lithium supply to the vessel was through a preheated pipeline (2.5 cm. in diameter) from a heated lithium storage tank to the lithium spill pan. The reaction catch pan was made of 316ss. Temperatures (measured in 49 separate locations), pressure, oxygen concentrations, and hydrogen concentrations were monitored continuously. The gas samples from which the average gas concentrations were determined, were taken from six locations within the containment.

The initiating procedures for both experiments were the same, however, the LA-5 reaction was terminated after 65 minutes, while the LA-4 reaction was allowed to go to completion unhindered. A lid was provided in test LA-5 which terminated aerosol generation and the reaction as well, 3900 seconds after the reaction was initiated. LITFIRE is not capable of modeling a reaction termination by such a procedure and (as will be seen in Section 2.2.3) the predictions of LITFIRE after this time are not valid for test LA-5. In test LA-4, a weld in the spill pan corroded 3300 seconds after the reaction began, and the remaining lithium spilled into the steel catch pan where it formed a shallow pool and burned to completion in ten minutes. This change in reaction configuration was not modeled by LITFIRE so again, the predictions by LITFIRE are not valid after leakage from the spill pan begins. (LITFIRE is only capable of modeling a single user specified configuration for each lithium spill, and there is no allowance for changing the spill condition or cell geometry

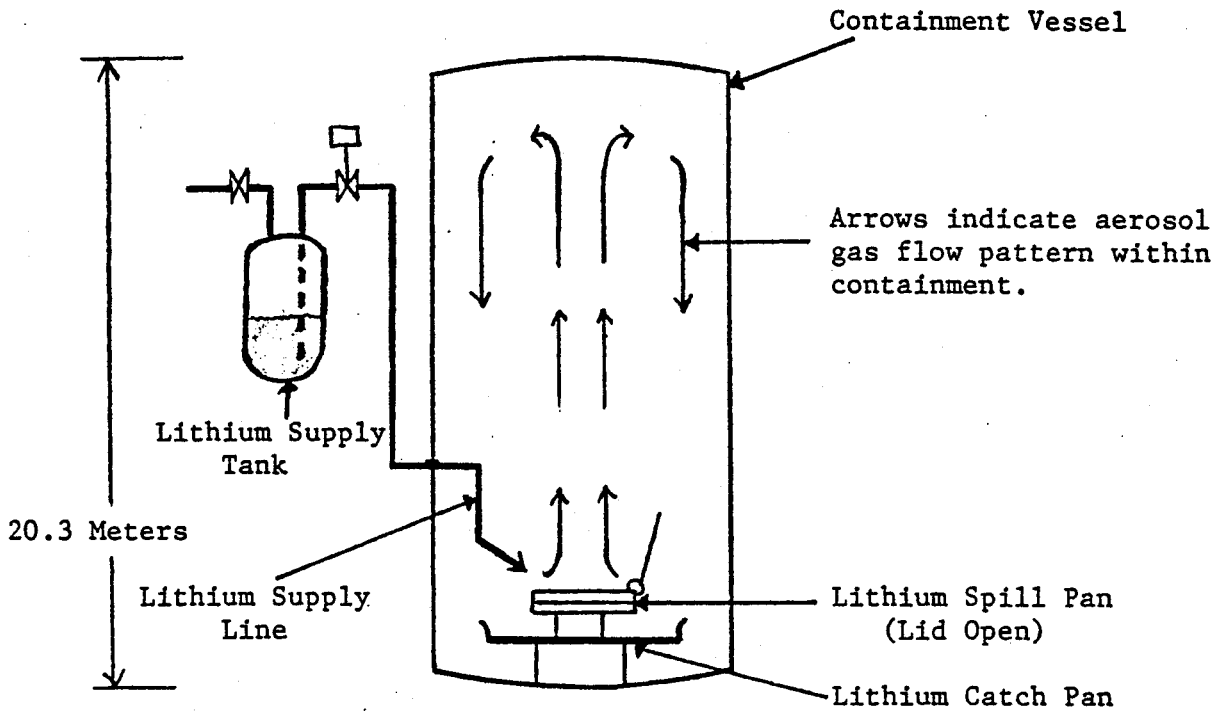

Figure 2.2: HEDL Test Facility

TABLE 2.1

Summary of HEDL Test Conditions

	LA-4	LA-5
Containment Vessel		
Diameter (m)	7.62	7.62
Overall Height (m)	20.3	20.3
Volume (m^3)	850.0	850.0
Total Horizontal Surface (m^2)	88.0	88.0
Wall Surface (m^2)	520.0	520.0
Vessel Mass (Rg)	103,000	103,000
Lithium		
Mass of Lithium Spilled (kg)	26.7	100.0
Lithium Reaction Pan Surface (m^2)	0.124	2.0
Initial Lithium Temperature (°C)	600.0	500.0
Depth of Lithium Pool (m)	0.46	0.10
Containment Atmosphere		
Initial Oxygen (mole %)	20.9	20.8
Initial Gas Temperature (°C)	31.0	31.8
Initial Pressure (MPa, absolute)	0.116	0.113
Maximum Temperature (°C)	68	83
Maximum Pressure (MPa, absolute)	0.127	0.127
Final Oxygen Concentration (mole %)	20.0	19.1

Comments

LA-4 Reaction: As a deep pool for ∿3300 sec when the pan integrity failed and all lithium spilled to the floor and reacted within 10 mins. LA-5 Reaction Terminated after 3900 seconds.

as a function of time or temperature. More detailed descriptions of the test facility along with a description of earlier test procedures appears in [6,10,12] and will not be repeated here.

2.2.2. LITFIRE Geometry Used to Model Experiment

Several of the options available in LITFIRE were used to model the HEDL test. These were the pan geometry, gas injection, and aerosol removal options within a single containment cell. In test LA-5 insulation surrounding the outer cell was modeled by specifying the appropriate properties in the concrete nodes. In test LA-4 the containment was not insulated and the concrete nodes were not used. The geometry used in the LITFIRE calculation is indicated in Figure 2.3 and the input data corresponding to the HEDL test conditions is listed in Appendix A.

Some of the input variables to LITFIRE are the coefficients (C_{ij}) for the convective heat transfer coefficients which are calculated according to

$$h_{ij} = \frac{C_{ij} D_i}{k_i} (Pr\, Gr)^{\frac{1}{3}} \qquad (2.2)$$

Recommended values for the various coefficients (C_{ij}) were obtained by Tillack [10] through trial and error in an attempt to match all the HEDL test data with a consistent set of coefficients. Since the geometry of the earlier tests was very similar to the present experimental setup, the recommended values for the C_{ij}'s will be used. In addition, several new coefficients were required due to the addition of the cell gas convective contact with the steel floor and the insulated pan. Values for these parameters were chosen to be consistent with the values indicated by Tillack [10].

There are three parameters that must be input to the code that have not been precisely determined as yet. These are the aerosol sticking coefficient ("BETA"), the combustion zone emissivity ("EMCZ"), and the combustion zone transmissivity ("TAUCZ"). The importance of these parameters in LITFIRE is discussed in section 2.3 of this report and recommended values determined in that section were used in the present calculation.

The remainder of the input values (geometric and physical properties) for LITFIRE were obtained from a listing of LITFIRE used at HEDL before the tests to predict the consequences of the tests. Data received after the test indicates that these values were properly specified beforehand and no changes were made.

2.2.3. Comparison of LITFIRE Predictions with Experimental Observations

The comparisons between experiment LA-5 and LITFIRE are shown in Figures 2.4a through 2.4d. These comparisons are for the the average cell gas temperature, the lithium pool temperature, and the primary steel wall temperature. In addition, the primary cell gas pressure is plotted since it

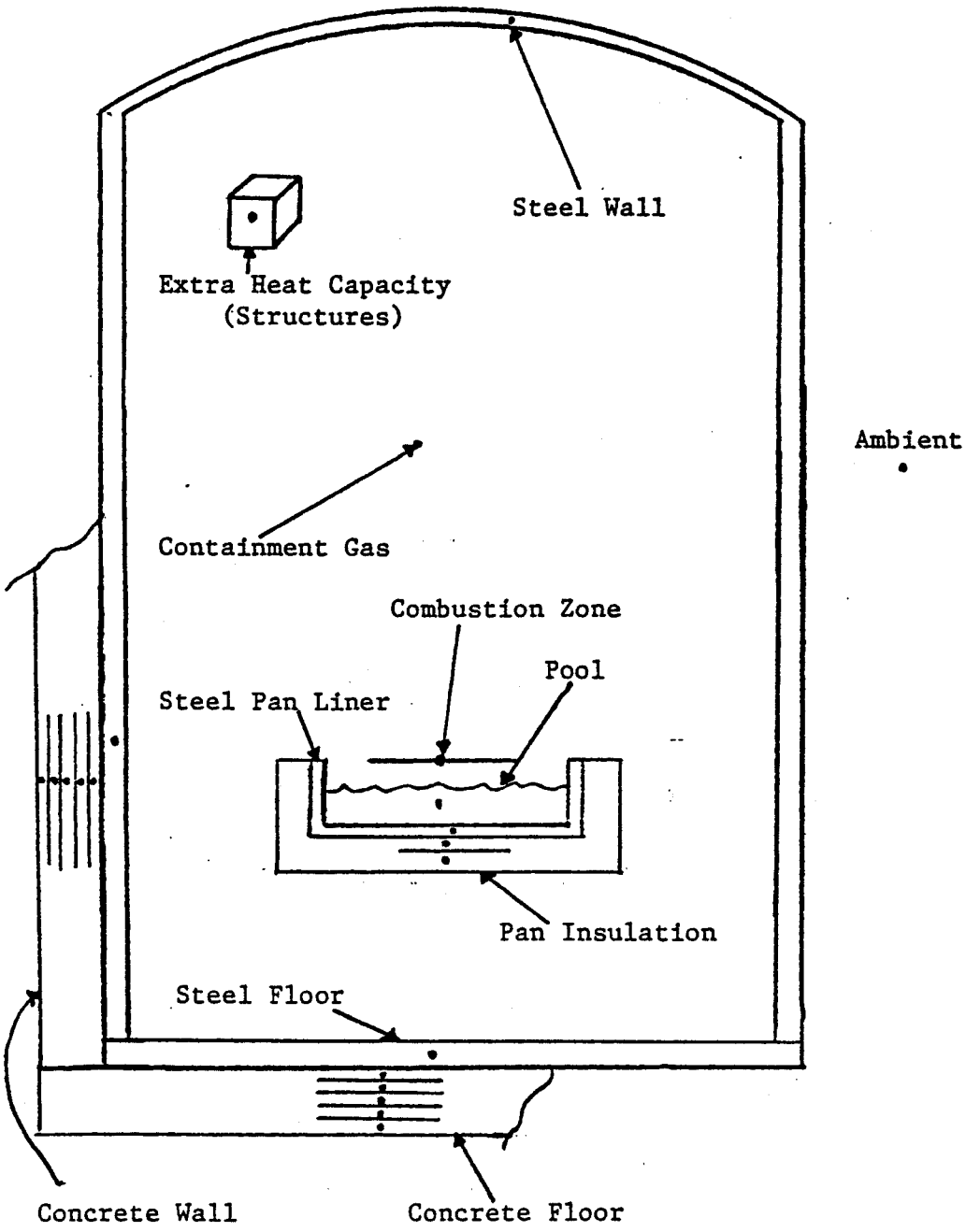

Figure 2.3: LITFIRE Geometry for HEDL Comparison

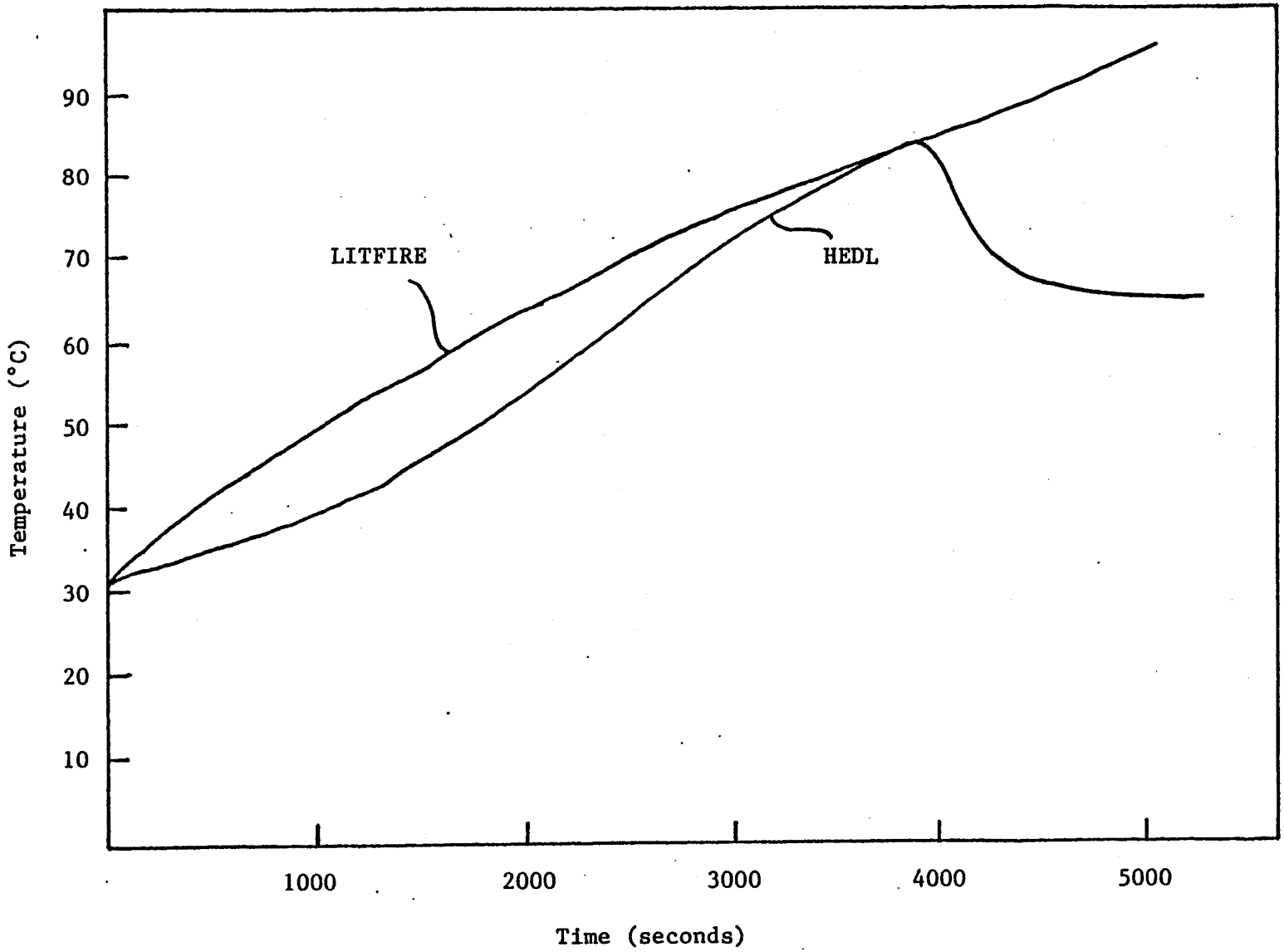

Figure 2.4a: LA-5 Cell Gas Temperature

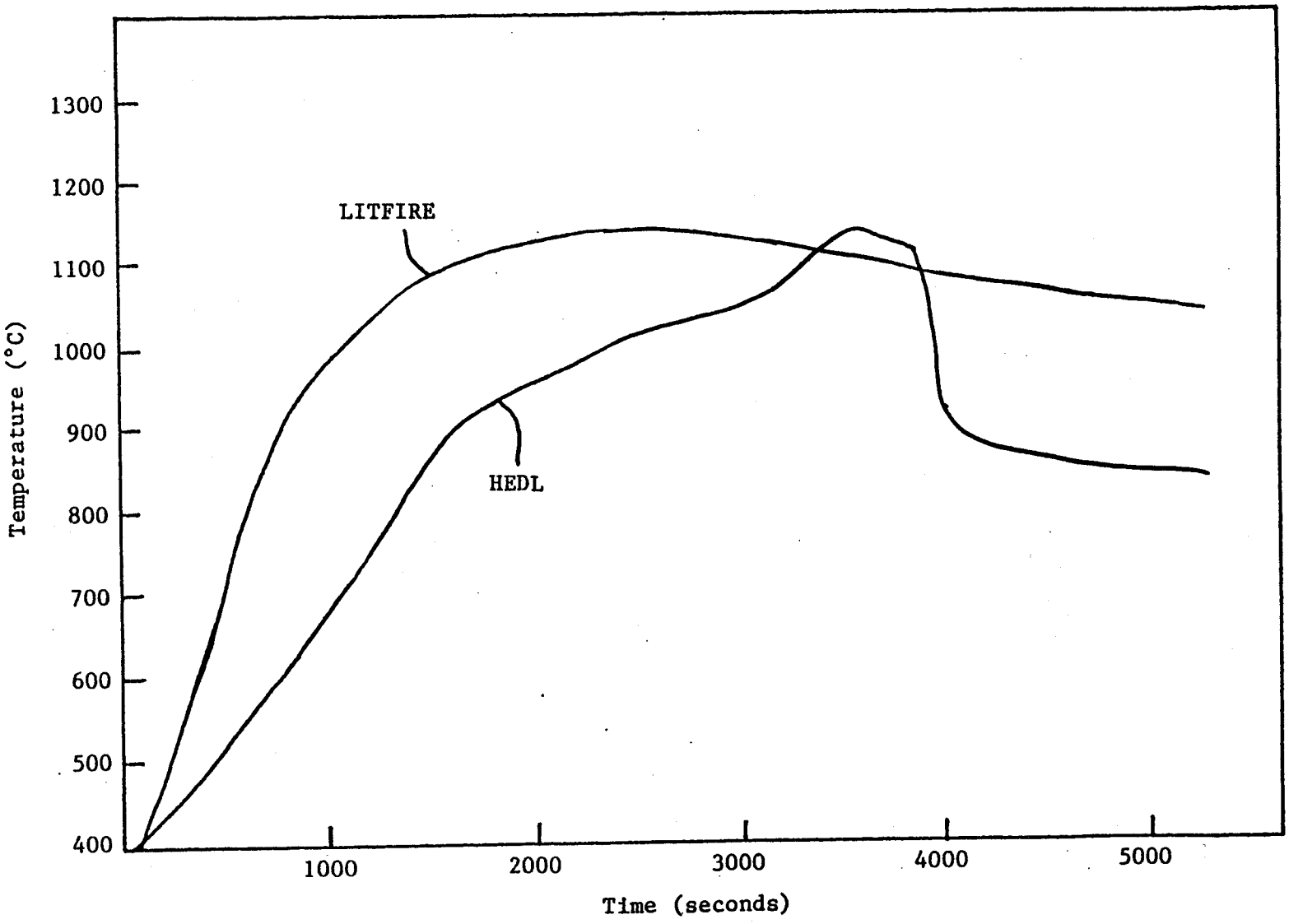

Figure 2.4b: LA-5 Lithium Pool Temperature

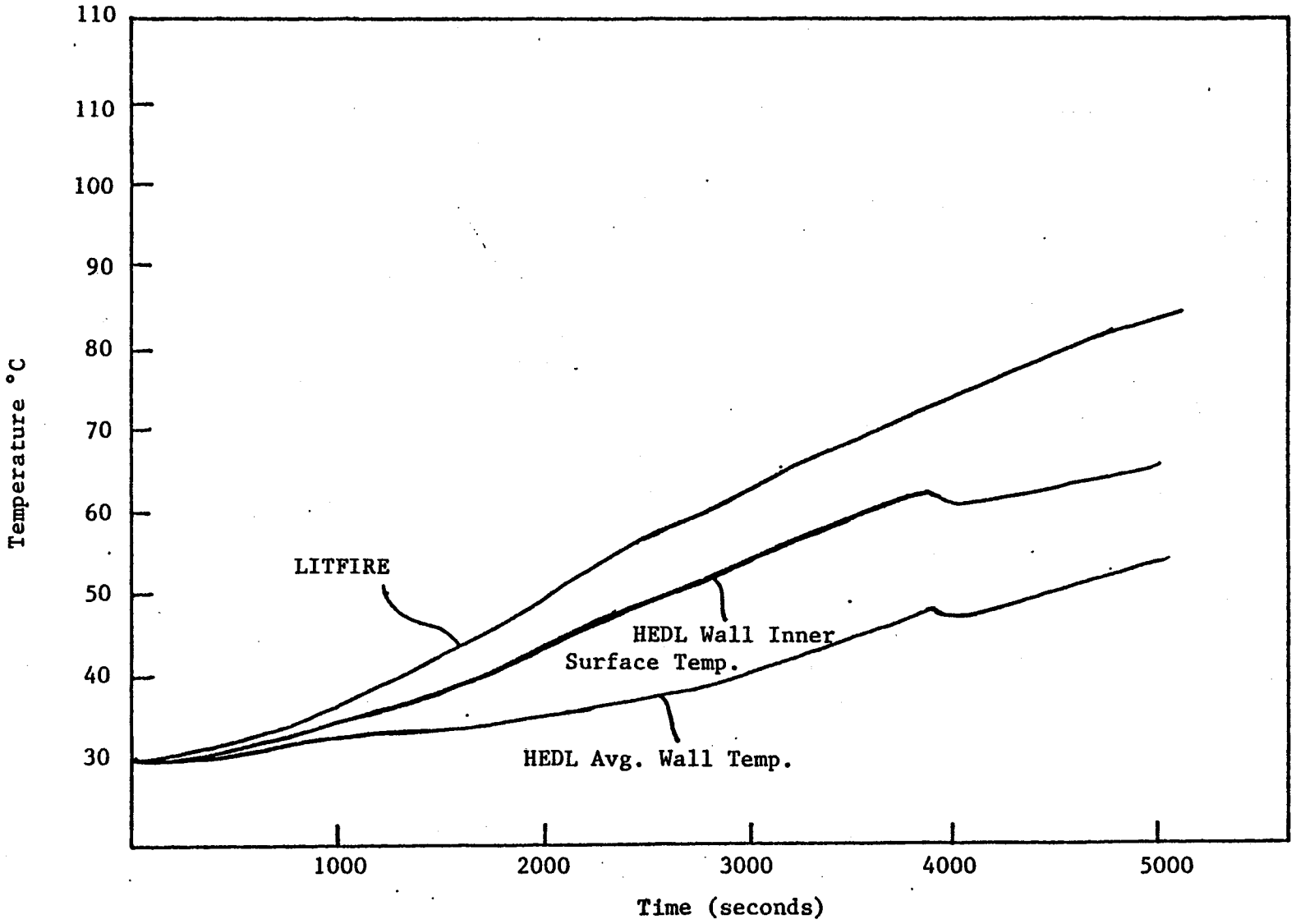

Figure 2.4c: LA-5 Containment Vessel Wall Temperature

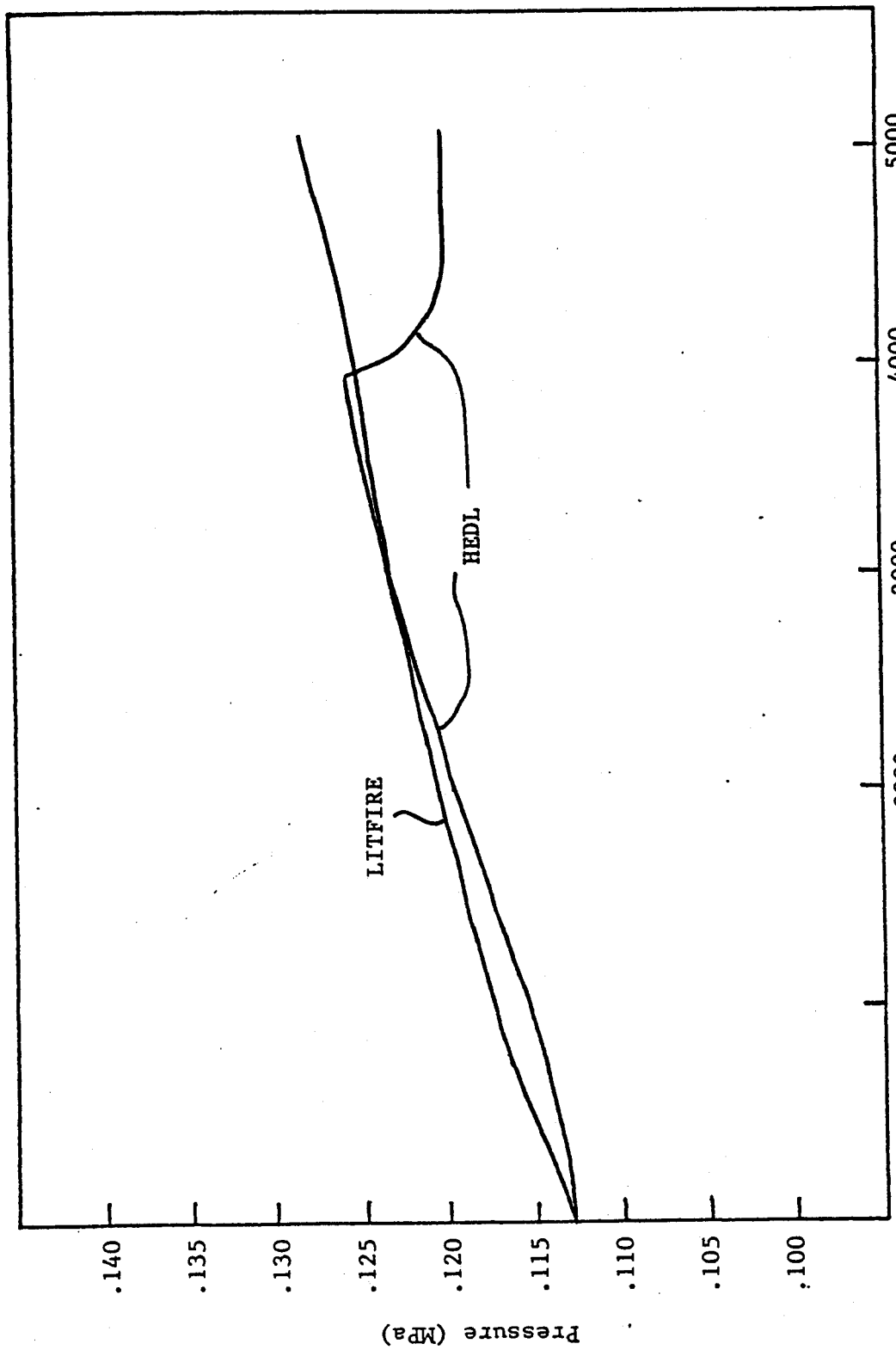

Figure 2.4d: LA-5 Cell Gas Pressure

is dependent on both the cell gas temperature and the mass of the gases present. The temperature and pressure profiles together can provide a check on the combustion rate since this is the dominant pathway for mass transfer from the gas. The reaction at HEDL was terminated after 3900 seconds and this is indicated in the figures by a vertical dashed line.

In the comparisons of the mixed species combustion experiments with LITFIRE by Tillack [10], several areas of importance were recommended for observation. These include: the nitrogen reaction rate as a function of temperature and oxygen concentration; the film conductance between the pool and combustion zone; the thickness of the pool; the cell gas emissivity; and the pool/combustion zone coupling. The experimental data obtained from HEDL indicated that the temperature differential through the lithium pool was a maximum of about 50°C for a pool thickness of 0.46 meters. However, the bottom thermocouple in the pool (which recorded the lowest temperatures) was affected by the buildup of Li_3N and Li_2O solids. These reaction products are formed at the pool surface but tend to fall through the pool and collect at the bottom as the reaction proceeds. The other thermocouples recorded temperature variations of less than 10°C during the time that the lithium was contained in the pan. Therefore, the single node representation of the pool node is probably a reasonable representation and should not add major inaccuracy to the the LITFIRE predictions, even for larger spills.

The reaction rate of lithium with nitrogen and oxygen was not measured directly but must be inferred from the data on gas composition and cell temperature and pressure. This can be done by applying the ideal gas law

$$PV = nRT \tag{2.3}$$

to the experimentally determined profiles of average cell temperature and pressure. The mole percent concentration of oxygen in the cell gas was measured at various points in the cell and an average of these was used in the present calculation. The reaction rate is extrapolated from the change in moles of O_2 and N_2 at specific intervals and is considered constant between those intervals. Table 2.2 lists the results of these calculations and Table 2.3 compares them to the reaction rates calculated by LITFIRE.

The combustion rate of oxygen predicted by LITFIRE is, on average, higher than the experimentally inferred values by a factor of two and a half. However, the actual oxygen consumption rate in the HEDL experiment is probably larger than estimated here since the present analysis used an average oxygen concentration over the entire cell volume, while the actual concentration of oxygen near and in the combustion zone will be much less due to it's uninhibited reaction with lithium. This effect should be larger when the lithium fire is in its early or late stages

TABLE 2.2

Experimental Gas Composition During LA-5

(using $PV = n_M RT$ with $V = 850\ m^3$, $R = 8.314 \times 10^{-6}\ m^3$ MPa/gmole K)

Time (Secs.)	Temp. (°K)	Pressure (MPa)	O_2 (mole fraction)	N_{O_2}	N_{N_2}
0	304.8	.113	.208	7884	29282
200	306	.113(4)	.208	7881	29270
400	308	.114	.208	7871	29233
600	311	.115	.207(5)	7844	29224
1000	316	.116	.207	7769	29024
2000	333	.120	.204	7515	28590
3000	346	.123	.200	7269	28369
3900	356	.126	.196	7092	28356

TABLE 2.3

Comparison of LITFIRE and Experimental Combustion Rates

(Based on Values in Table 2.2)

Time (Secs.)	Lithium Reaction Rate with Nitrogen ($kg-Li/hr-m^2$)		Lithium Reaction Rate with Oxygen ($kg-Li/hr-m^2$)	
	HEDL	LITFIRE	HEDL	LITFIRE
100	4.5	10.9	1.4	16.9
300	13.9	14.05	2.4	23.6
500	3.4	23.56	6.8	26.4
800	37.5	5.22	9.4	27.4
1500	32.5	0.0	12.8	27.0
2500	16.6	0.0	12.4	24.9
3450	1.1	0.0	9.8	22.5
Average During 3900 secs.	17.8	3.6	10.2	25.3

(i.e. when the combustion rate is lower than average) since the combustion zone volume is inversely proportional to combustion rate. Indeed, the discrepancy between LITFIRE and experiment is larger when the expected combustion rates are lower.

The agreement for the nitrogen reaction rate is worse than that for oxygen. LITFIRE predicts no nitrogen combustion will take place above a pool and combustion zone "mean" temperature of 1300 Kelvin or above oxygen concentrations of 0.28 by weight. If the experimental extrapolation is to be believed, and the LITFIRE temperature predictions are accurate, nitrogen is indeed reacting under these conditions. A possible explanation for this may be a difference between the actual combustion zone temperature and the combustion zone temperature predicted by LITFIRE. Unfortunately, direct measurements of an appropriate "combustion zone" were not made during the latest HEDL tests. However, LITFIRE does predict fairly well the cell gas and lithium pool temperature profiles. Since these two nodes bound the combustion zone, the major inaccuracy in the combustion zone temperature would most likely be due to errors in calculating the heat capacity of the combustion zone node itself, and not in the conductivity of the film region or the radiative heat transfer to the pool and cell gas. The present form of the combustion zone heat capacity is based on a quasi-steady state analysis and may not be appropriate for the transients encountered in lithium fires. Further tests are needed to clarify the correct combustion zone temperatures for comparison with LITFIRE.

There is no direct means of checking the predicted film conductance in LITFIRE with the experiment. However, the relative magnitude of the combustion zone and pool temperature coupling provides a check on both the film conductivity and the combustion zone emissivity (and transmissivity as well). In test LA-4 several thermocouples were positioned at various heights above the lithium-air reaction interface, the closest one being 5.08cm above the lithium pool. The temperatures measured at each of these thermocouples was lower than that of the lithium pool, so there is reason to believe that the reaction took place very close to the pool surface. An estimate of the combustion zone temperature might have been made by extrapolating the temperature gradient from these three positions to the pool surface, but the resulting temperatures are very much dependent on the form of the gradient assumed and yield temperatures below that of the lithium pool. However, there is a period during the reaction when the temperatures above the pool have stabilized while the pool temperature continues to rise. This observation is probably due to the leveling off of the combustion zone temperature near its maximum. Previous tests have measured the maximum combustion zone temperature to be in the vicinity of 1260°C [12] and this value is used as the limit in the present comparison. The above approximation is very crude, yet it serves as a partial guide to the degree of heat transfer coupling within the combustion zone-lithium pool system. The results of this estimation are listed in Table 2.4 and a graph of

the combustion zone/pool temperature difference for both the HEDL experiment and LITFIRE prediction is presented in Figure 2.5.

The temperature differences predicted by LITFIRE using a combustion zone emissivity of 0.9 are higher than those estimated from the HEDL experiments. After the reaction rate has peaked (approximately 200 seconds from ignition) the temperature difference begins to decrease, with the predicted and measured slopes of this decrease nearly the same. In order to reduce LITFIRE's temperature difference, the film conductivity should be increased. However, the uncertainty associated with this estimation is quite large and no firm conclusions about conductivity can be drawn. Comparisons using LITFIRE with a combustion zone emissivity of 0.5 or less resulted in very high combustion zone temperatures and temperature differences in excess of 1200°C for the duration of combustion, and eventually lead to bulk pool temperatures above vaporization. The lithium pool emissivity can also have a large effect on the degree of pool and combustion zone coupling, but this parameter is calculated within LITFIRE and is based in part on the buildup of reaction products at the pool surface. The temperature difference between the pool and combustion zone was fairly insensitive to changes in the cell gas emissivity which was already limited to a maximum value of 0.04 as previously indicated. Therefore this comparison is another indication that the combustion zone emissivity should be higher than values recommended earlier.

An additional area of concern is the generation and removal of aerosols in the test containment. The generation of aerosols is determined by the reaction rate and by the fraction of reaction products formed that become suspended in the containment atmosphere. Measurements at HEDL indicate that a maximum aerosol concentration of ~8 grams per cubic meter was achieved 65 minutes after combustion began. An estimate for the fraction of suspended particles may be made using the predicted combustion rate and knowledge of the containment volume, if aerosol removal is neglected. These estimated values range from one to six percent of reaction products evolved into the containment atmosphere. The removal rate of aerosols from the gas is a strong function of the internal geometry of the containment structure. A value for the HEDL test condition may be inferred from the observation that the aerosol concentration decreased to less than 0.001 grams per cubic meter after four days. This yields values of "BETA" that lie between 10^2 and 10^3 seconds. A sensitivity analysis of aerosol removal appears in the next section.

2.3. Sensitivity of LITFIRE to New Modeling

2.3.1. Sensitivity to Aerosol Removal

In LITFIRE, the mechanism for aerosol removal from the primary containment is an optional, highly idealized model and is a function of a single parameter for a given geometry. This parameter,

TABLE 2.4

Estimation of LA-4 "Combustion Zone" Temperatures

(Temperatures are approximate)

Time (Seconds)	Lithium Pool Aug. Temp. (°C)	Air Reaction Interface @5.08 cm (above Pool)(°C)	15.24 cm	30.48 cm	Estimated "C.Z." Temperature (°C)
0	(200 - 600)	165	150	125	∿
600	650	400	350	200	> 800
1200	750	745	600	300	> 900
1800	900	780	630	315	∿1200 - 1300
2400	975	780	620	310	∿1200 - 1300
3000	1020	770	610	310	∿1200 - 1300

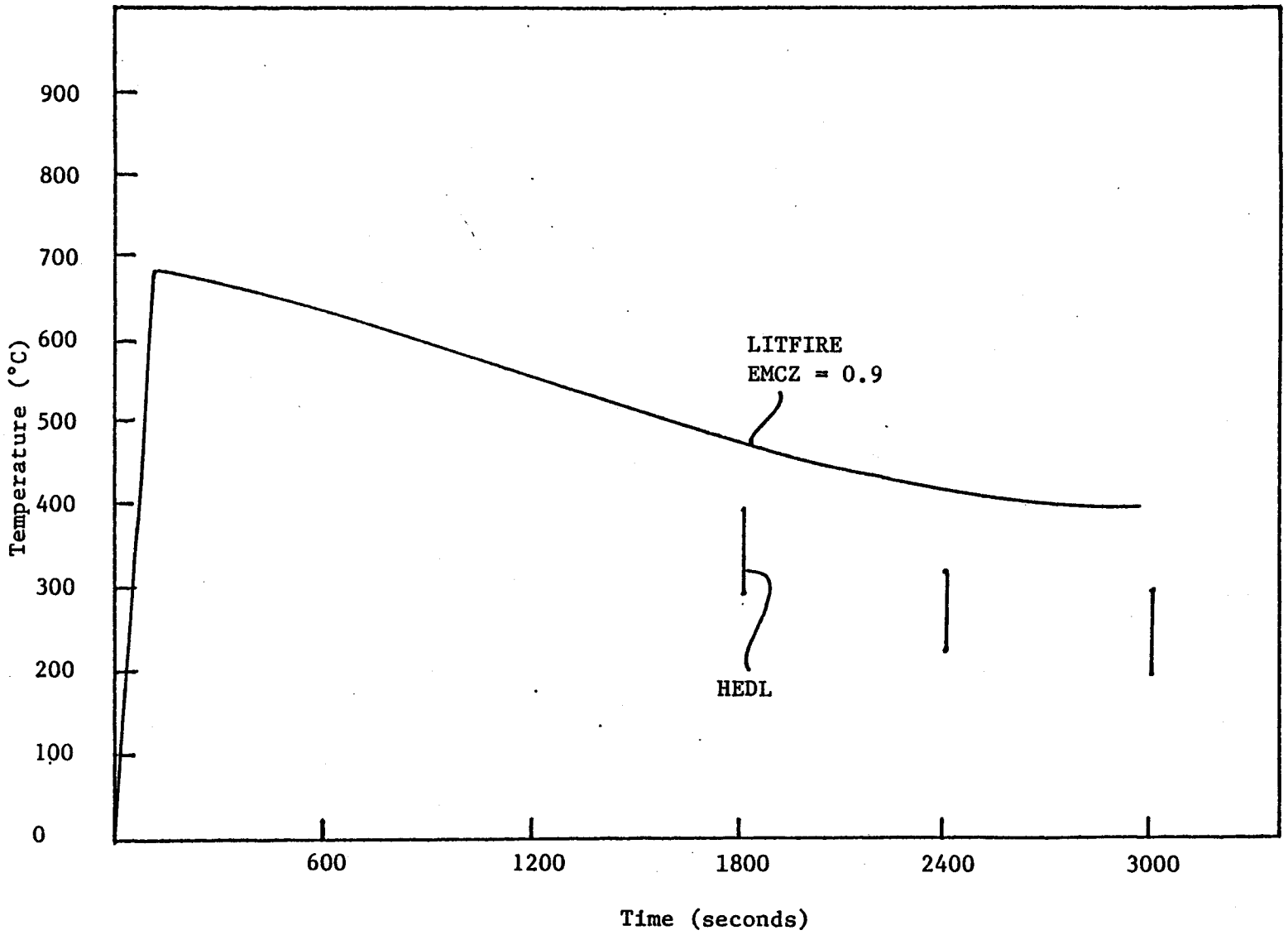

Figure 2.5: LA-4 "Combustion Zone" - Lithium Pool Temperature Difference

(BETA), is an input variable that represents the "sticking time" of the aerosol in containment. The sticking time is defined as the average time it takes for an aerosol particle near a wall to be removed from the cell gas. In LITFIRE, "near the wall" is assumed to be one inch. Therefore, the fraction of aerosols removed per second is equal to the fraction of aerosols within one inch of the wall divided by the sticking time. The removal of aerosols is assumed to take place in the primary cell only, since the concentration of aerosols in the secondary cell should be very small.

The major effect of aerosol removal is in the calculation of the primary cell gas emissivity, since

$$\text{gas emissivity} = C_1(1 - \exp(-C_2\,\text{aerosol})) \qquad (2.4)$$

where C_1 is a user defined constant, and C_2 is a function of geometry, particle size, and path length.

It is possible that for sufficiently low values of BETA, a large fraction (or even all) of the aerosol in containment would be removed in a single time step. LITFIRE checks for this condition and reduces the time step accordingly, in order to insure numerical stability. In addition, program execution is terminated if the aerosol removal fraction is greater than unity.

Figures 2.6 and 2.7 show the sensitivity of the cell gas temperature and emissivity respectively, as a function of BETA. In these tests the maximum emissivity allowed was 0.04, a value recommended by Tillack [10] as best fitting the experimental data. The minimum value of the cell gas emissivity is 0.005 in order to insure numerical stability as well as allow some amount of radiative heat transfer to the cell gas. Although variations in BETA have a pronounced effect on the cell gas emissivity, the calculated effect on the cell gas temperature was negligible. This is due to the restricted maximum value that the cell gas emissivity was allowed to reach. To first order the heat transfer to the gas through the radiation channel is proportional to the cell gas emissivity. Therefore, it is possible that in cases where radiative heat transfer to the gas is the dominating heat transfer mechanism the temperature of the cell gas might be substantially more sensitive to changes in the aerosol removal rate.

2.3.2. Sensitivity to Combustion Zone Transmissivity

LITFIRE currently allows for the selection of combustion zone emissivity (EMCZ) and transmissivity (TAUCZ) separately. In allowing finite transmission through the combustion zone, Tillack [10] rederived the radiative interchange factors for the pool to the wall, cell gas, and combustion zone. In that work the value of EMCZ$\leq$ 0.1 was recommended as best fitting the experimental data then available. Previously, Dube [1] indicated that the probable values for

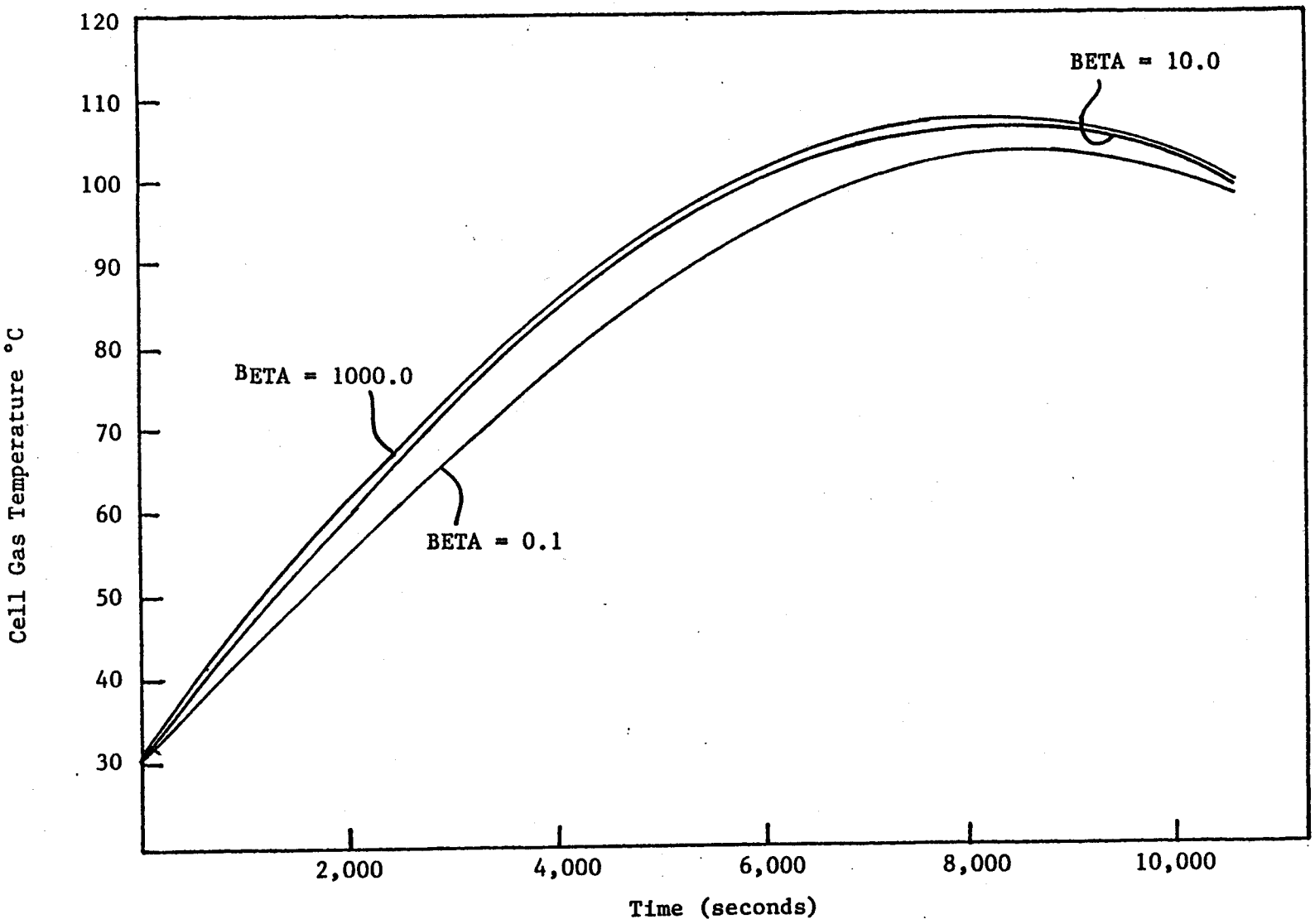

Figure 2.6: Cell Gas Temperature Sensitivity to Aerosol Removal

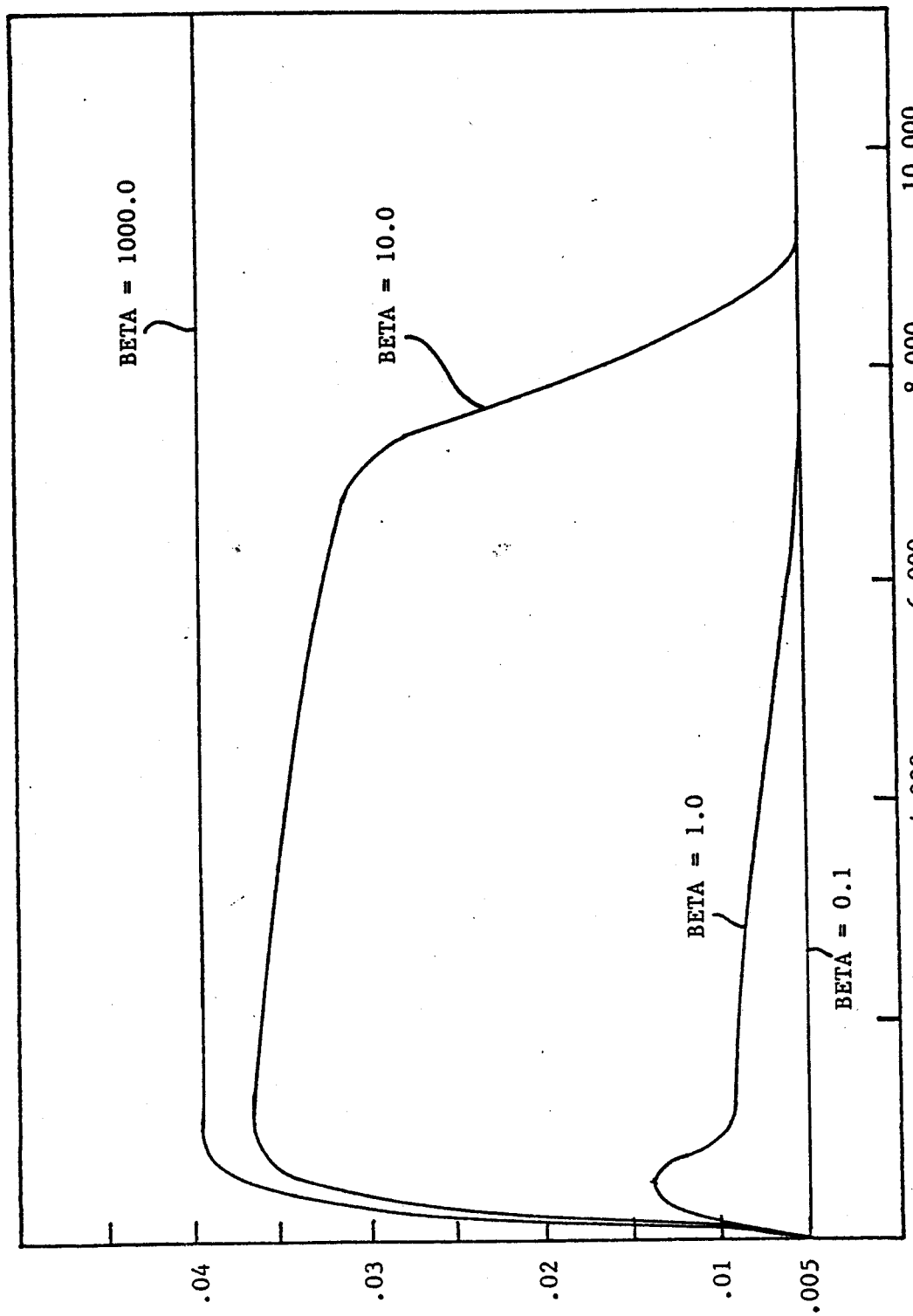

Figure 2.7: Cell Gas Emissivity Sensitivity to Aerosol Removal

EMCZ would lie in the range of 0.5 to 0.9. No mention was made of the appropriate value for TAUCZ except for the condition that, in general, TAUCZ$\leq$1-EMCZ.

The bases for the comparison are the lithium pool and cell gas temperature profiles, since theses are the two nodes that are most sensitive to a change in combustion zone transmissivity and emissivity. (Actually, the combustion zone itself is the most sensitive, but accurate temperature profiles for this node were not made during the HEDL tests.) Since the temperature profiles are more sensitive to changes in the emissivity than changes in transmissivity, the accompanying Figures (2.8 and 2.9) are given for the complete range of emissivities and only the maximum and minimum transmissivity that corresponds to each emissivity. At a given emissivity, the effect of increasing the transmissivity is to decrease the lithium pool temperature. This is due to the larger radiative interchange that is allowed between the pool surface and the gas and steel wall. This trend is seen to be valid at any value of the combustion zone emissivity. However, since the maximum allowed change in the transmissivity decreases as the emissivity is increased, the sensitivity to transmissivity at the higher emissivities is necessarily reduced. Increasing the transmissivity tends to increase the cell gas temperature at lower emissivities, and slightly reduced the cell gas temperature at higher emissivities. Since increasing the transmissivity always increases the radiative interchange between the pool and cell gas regardless of the combustion zone emissivity, the reduction in cell gas temperature must be a second order effect and is probably associated with lower radiative heat transfer from a slightly cooler combustion zone.

The figures indicate that higher emissivities fit the experimental data best. Therefore, the effect of variations in transmissivity are relatively small. The "best guess" values chosen for the present study are an emissivity of 0.9 and a transmissivity of 0.1. Several combinations of values brought the LITFIRE predictions within close agreement to experiment. An additional criterion in choosing the present set was an upper limit applied to the maximum combustion zone temperature. This had been measured in earlier experiments to be about 1260°C.

The results of these comparisons are in disagreement with the recommendations put forth by Tillack [10], and more in agreement with the original indications made by Dube [1]. Tillack's suggestion was based on the expected increased coupling between the pool and combustion zone temperatures after the combustion zone transmissivity model was incorporated into LITFIRE. In point of fact, this coupling did not occur in the LITFIRE calculations because the net effect of reducing the emissivity was to reduce the radiative heat transfer between the pool and combustion zone. This heat transfer pathway is proportional to the temperature difference to the fourth power while that of conduction varies linearly with temperature difference. Even with the higher conductance to the pool, the net effect of lowering the emissivity of the combustion zone is

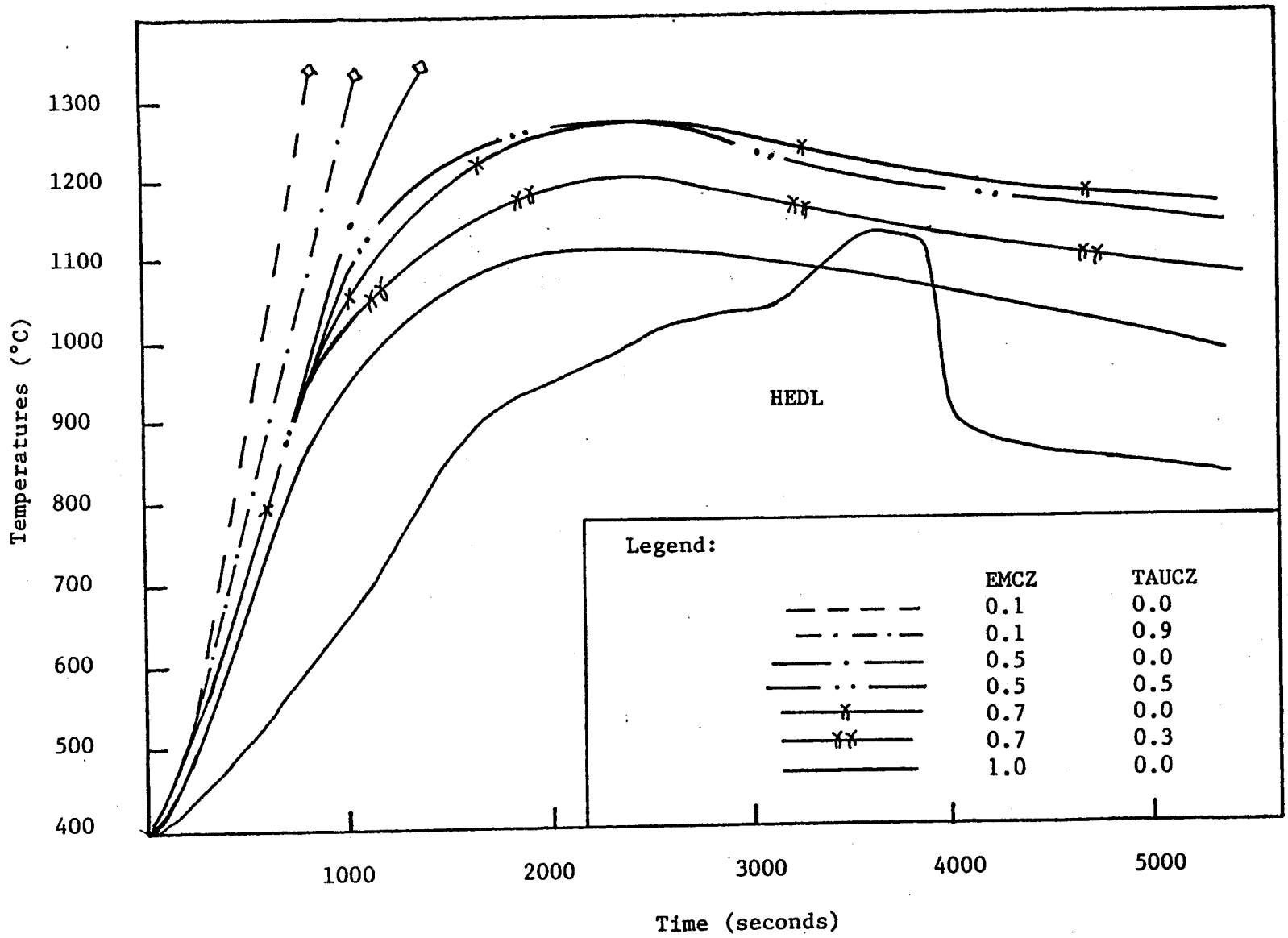

Figure 2.8: Lithium Pool Temperatures LA-5 for Various EMCZs

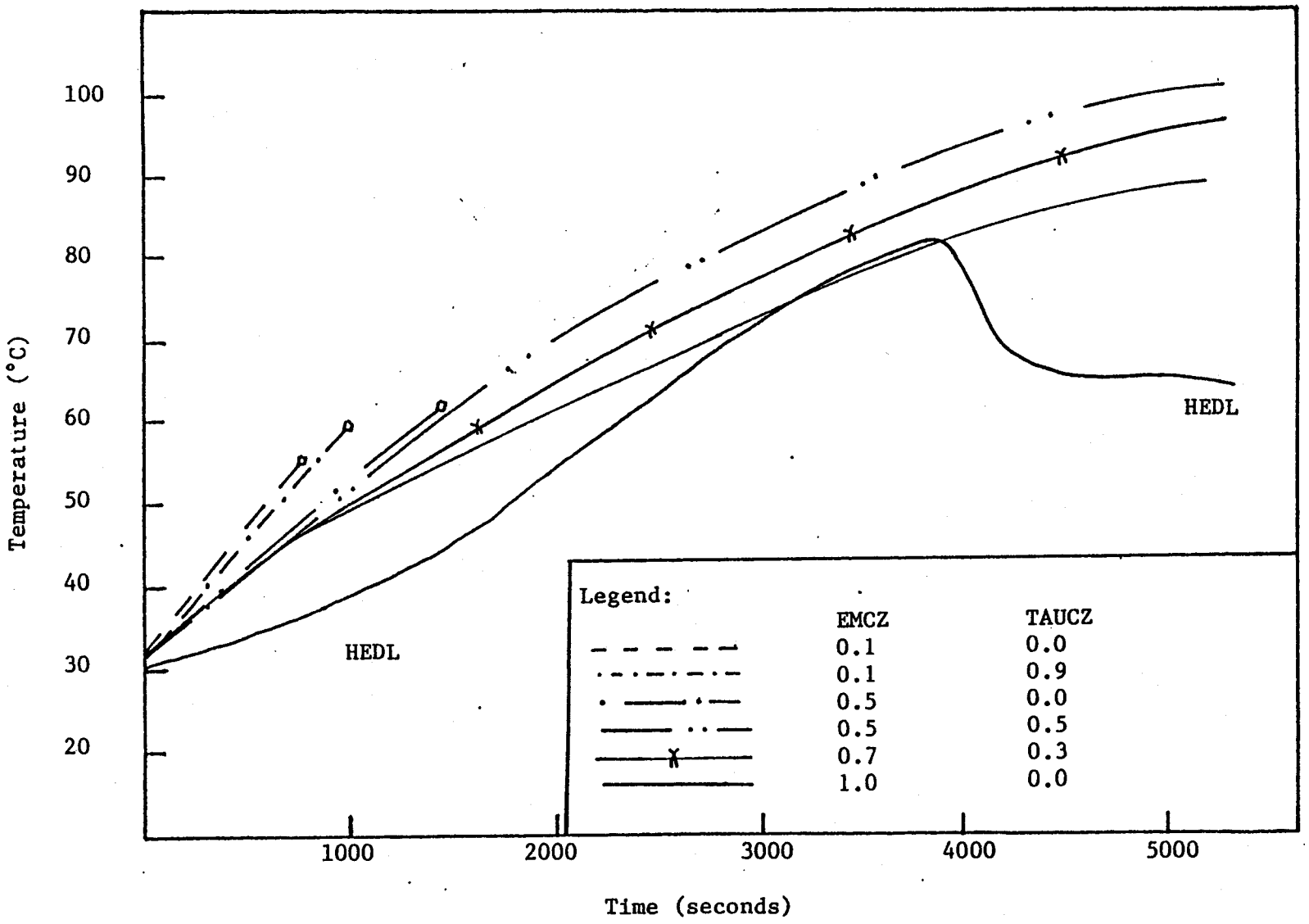

Figure 2.9: LA-5 Cell Gas Temperature Sensitivity to EMCZ

to dramatically increase the combustion zone temperature. Figure 2.10 shows the maximum temperature difference between the pool and combustion zone generated by LITFIRE, for various values of the combustion zone emissivity.

The recommendations of Tillack [10] were also based on fitting LITFIRE predictions to experimentally obtained data so a comparison between that data and the present predictions of LITFIRE might indicate the magnitude of the discrepancy. This comparison is shown in Figures 2.11 and 2.12 and includes data from HEDL test LA-2 which is described in detail by Tillack [10]. Also included are the predictions by LITFIRE using values for emissivities and transmissivities recommended above and also those suggested by Tillack [10].

2.4. Analysis of a Lithium Spill in UWMAK-III

The original purpose of LITFIRE was to predict the consequences of lithium fires in commercial size reactor containments. The agreement between LITFIRE and small scale experiments is encouraging but should not be used as concrete evidence that larger spills and fires will be accurately modeled.

2.4.1. Description of UWMAK and LITFIRE Geometries

The prototypical fusion reactor chosen by Dube [1] for his analysis was the UWMAK- III design of which the containment building is shown in Figure 2.13. Dube [1] published a sensitivity analysis of the relevant parameters for modeling large fires and proposed a base set of parameters as a best guess at predicting the consequences of large fires. This base case is retained for the present modeling with notable exceptions being the concrete nodal distribution and the presence of an extraneous heat capacity. In addition, the coefficients for convective heat transfer were obtained from Tillack's [10] recommendations. The value of the combustion zone emissivity (EMCZ) is 0.9, representing the best guess of the present study. The aerosol removal option (including BETA) was not used in these test cases. None of the options for mitigating the effects of lithium fires were employed in order to make a conservative best estimate. These safety features were found to have significant affects and are discussed in detail in reference [1].

2.4.2. Prediction of Lithium Fire Consequences

The results of this calculation are plotted in Figure 2.14. The reaction stopped ~3850 seconds after ignition because the lithium pool was depleted. Although there should not be any lithium left after this time, LITFIRE requires that a certain amount of lithium exist in the pool node in order to have a finite thickness and insure numerical stability. Thus, LITFIRE artificially constructs a pool node after this time but "knows" that there is no combustible lithium remaining. Therefore, the primary steel floor is still "covered" by the lithium pool and does not interact thermally with

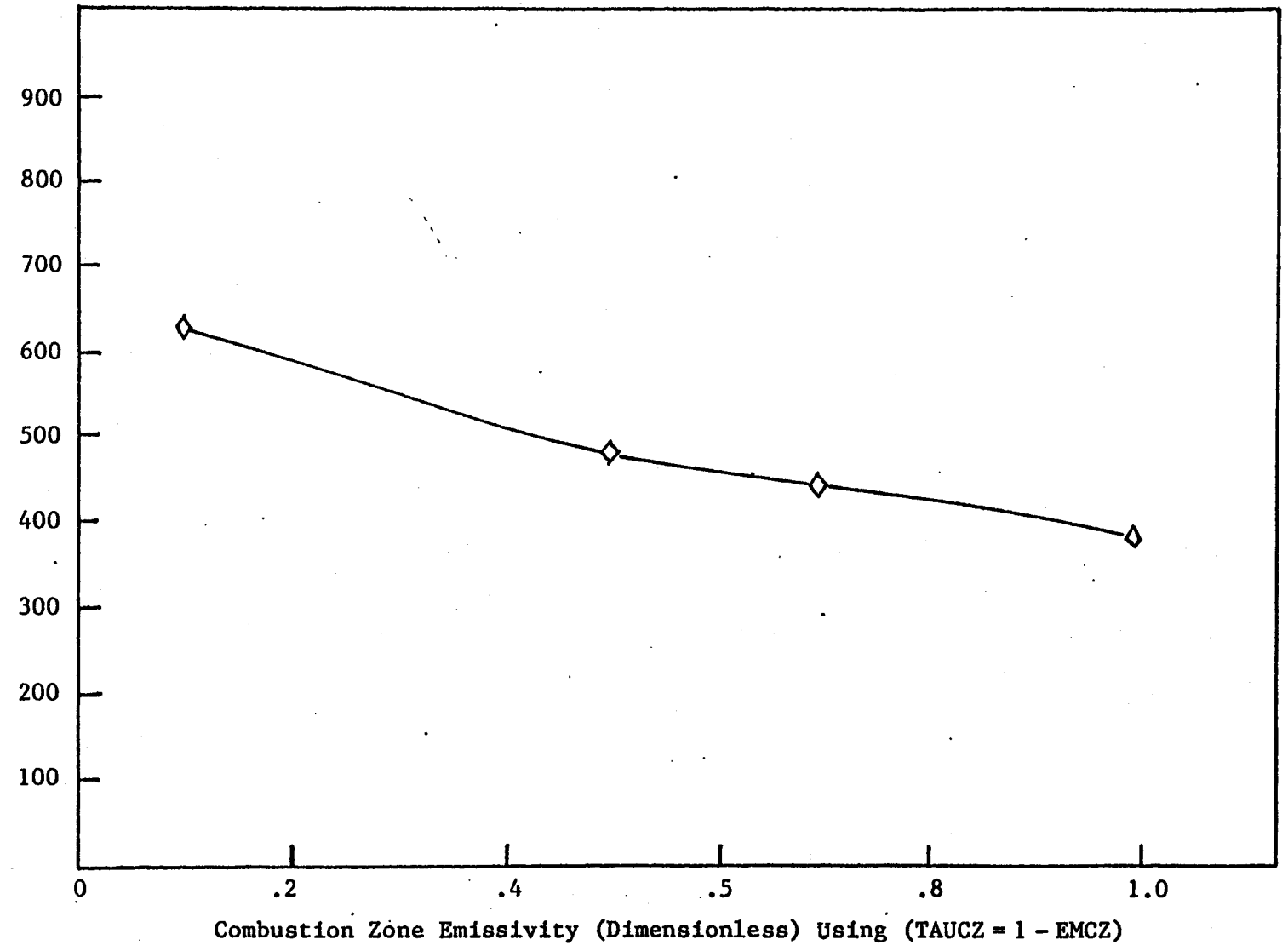

Figure 2.10: LA-5 Maximum Pool-Combustion Zone Temperature Difference

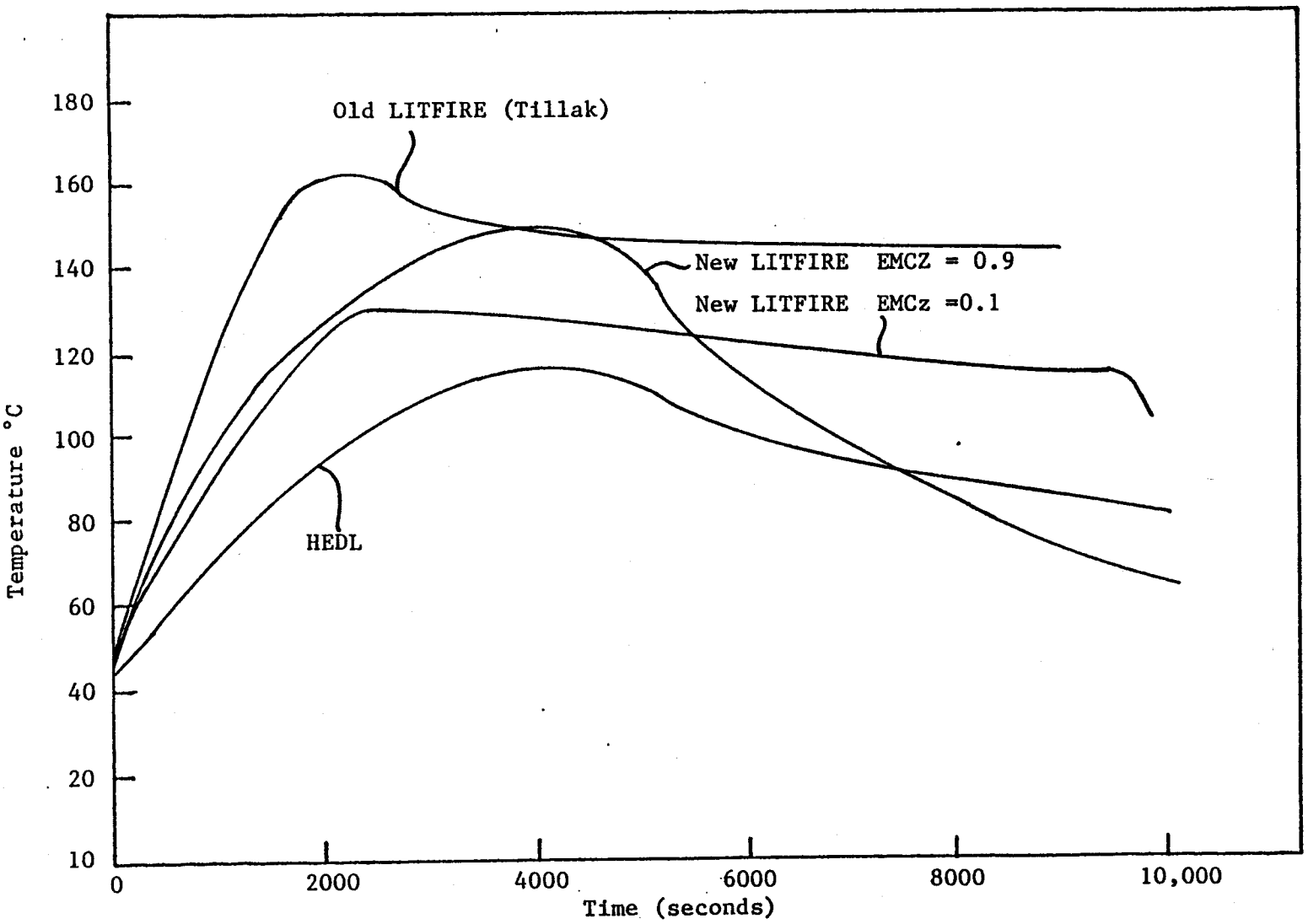

Figure 2.11: LA-2 Comparison between Present and Tillack Cell Gas Temperature

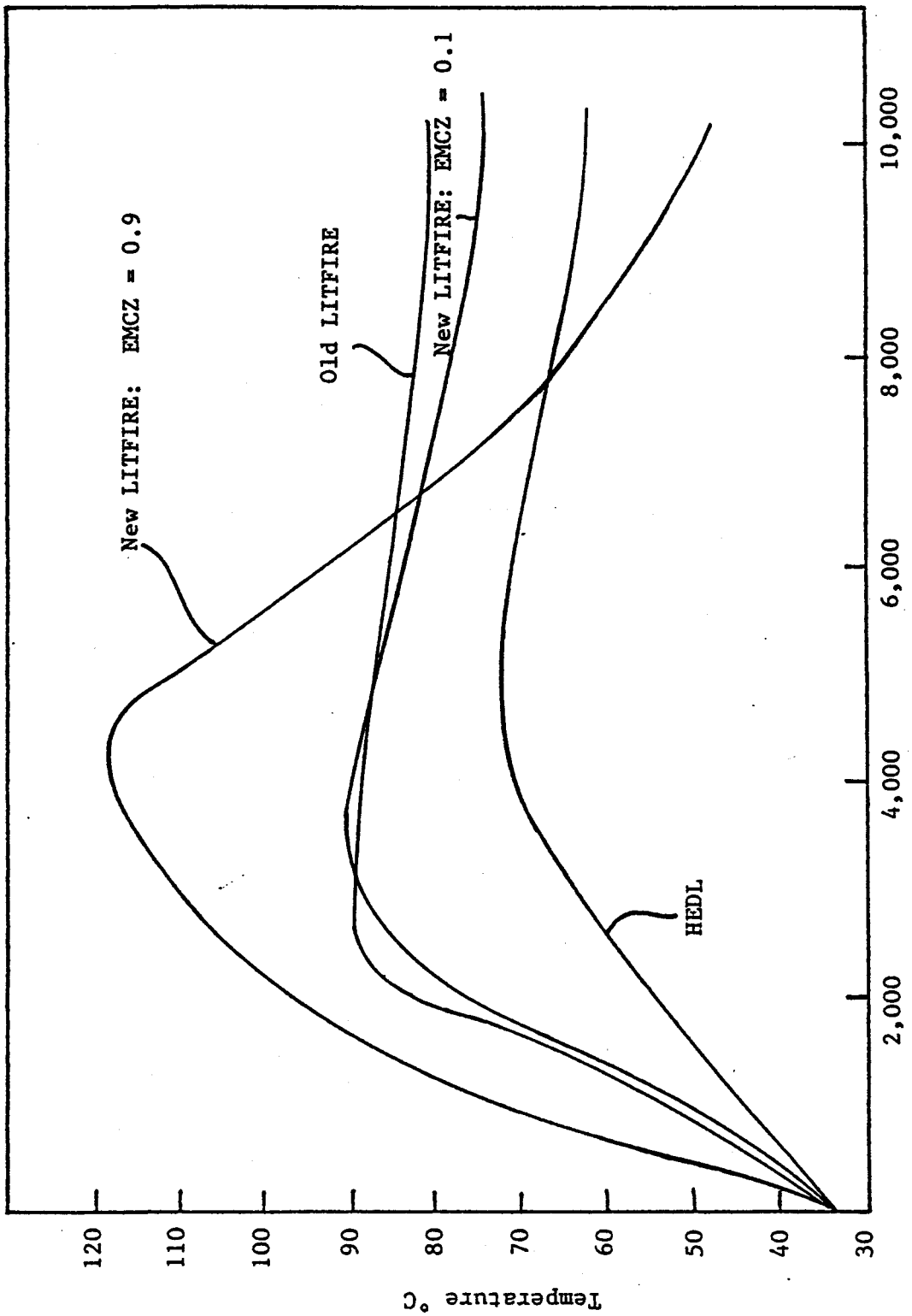

Figure 2.12: LA-2 Steel Vessel Temperature

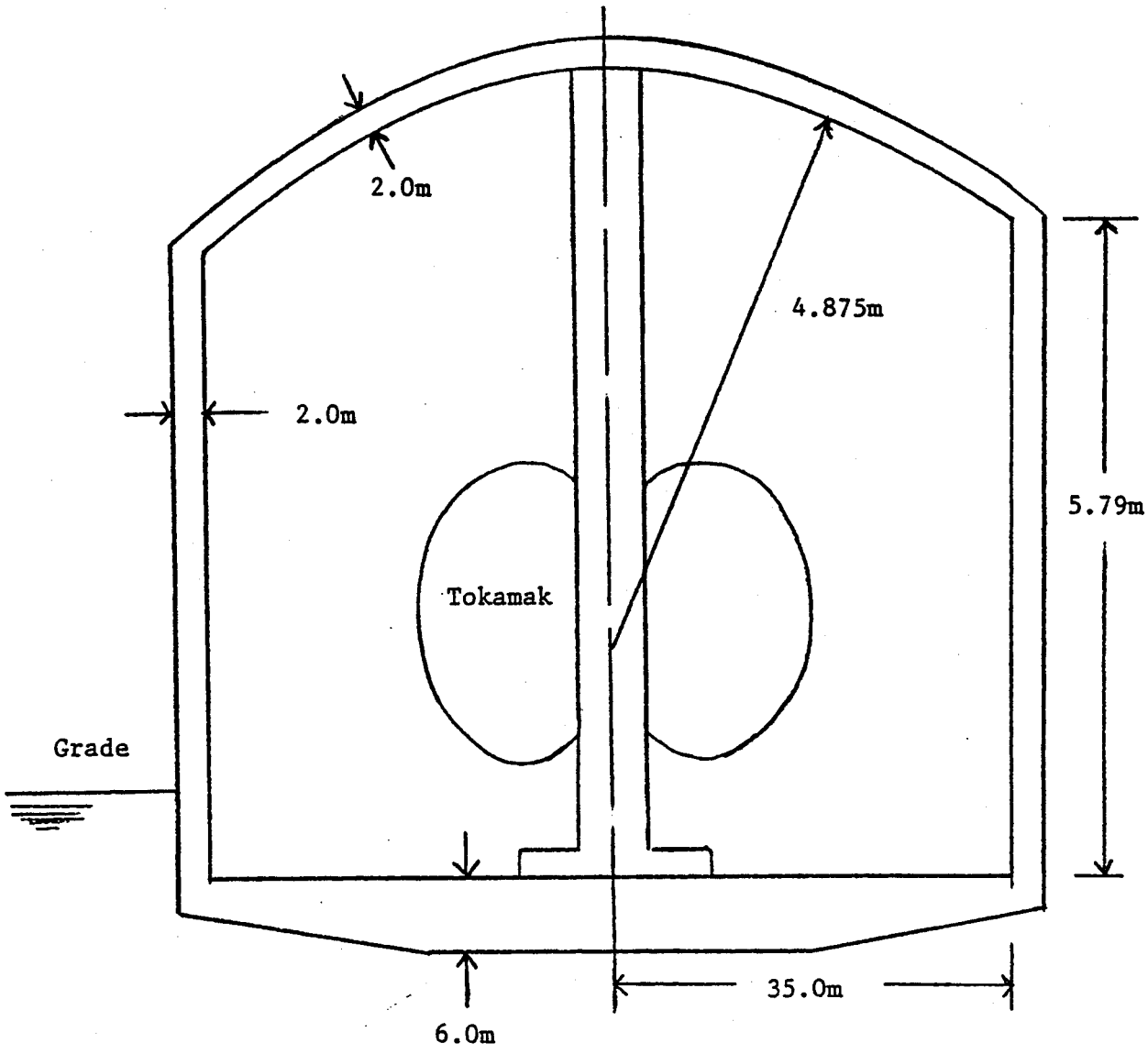

Total Floor Area	$3860m^2$
Total Volume	$250725m^3$
Wall Area	$17050m^2$
Total Lithium Mass	396000kg
Lithium Spilled	22000kg
Ambient Temperature	25.9 °C
Initial Pressure	.101 MPa

Figure 2.13: Cross Section of UWMAK-III Primary Containment Building

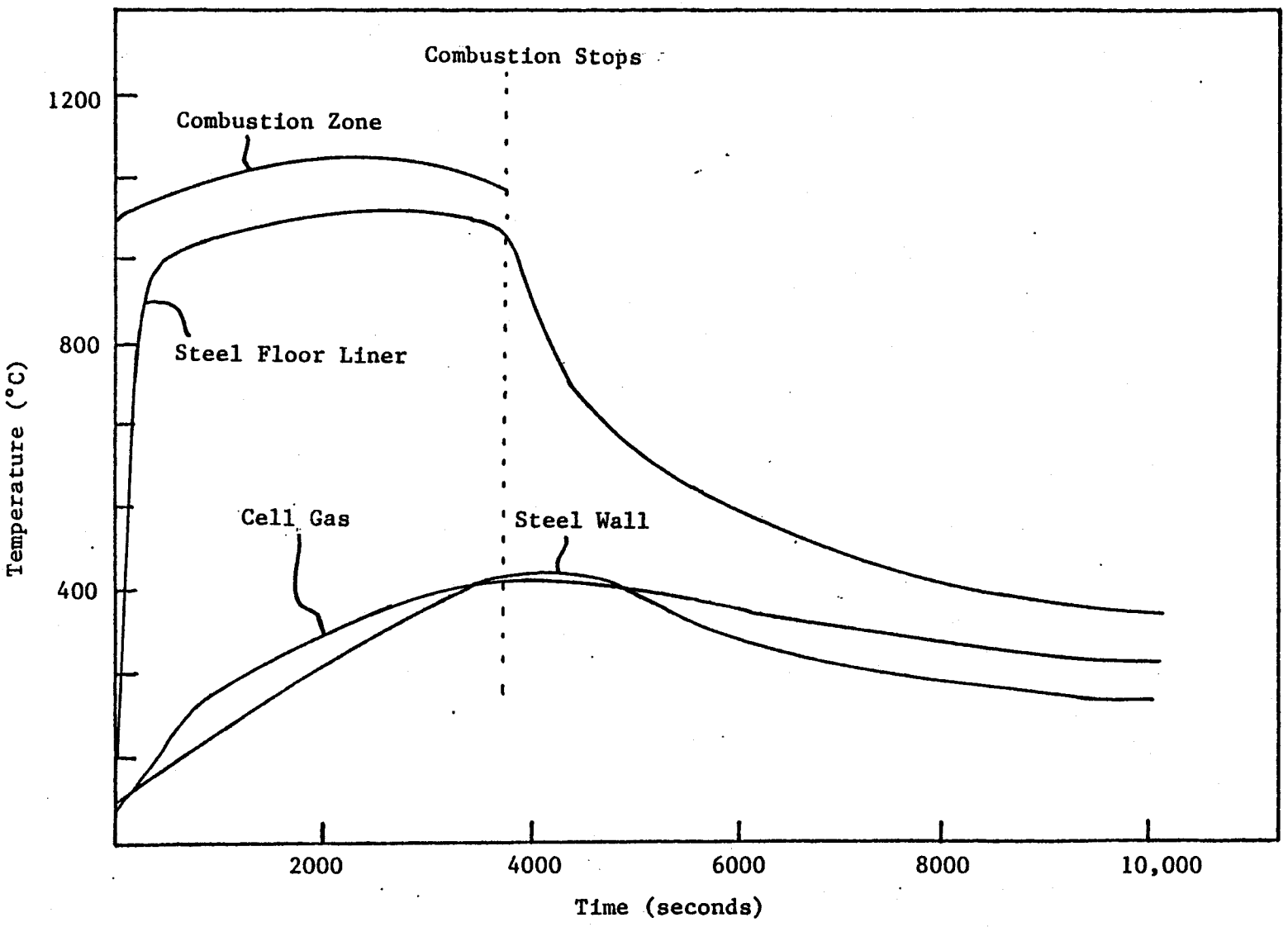

Figure 2.14: UWMAK-III Containment Thermal History Using Present Version

the primary cell gas directly. This should not radically alter the primary cell gas since the thermal conductivity of the lithium is very high and the thickness of the phantom pool node is small.

Even though the containment atmosphere and structures are much larger than in the HEDL experiments, the predicted consequences are much more severe. This is primarily due to the large surface area of the lithium pool in the UWMAK prediction. Since the reaction rate is proportional to surface area, the reaction burned to completion in about one hour, during which time very little heat was transferred to ambient. Lithium fires with smaller surface areas (and smaller primary containment volumes as well) are discussed in the next chapter.

2.4.3. Comparison with Previous Predictions

The consequences of large scale lithium fires were predicted by Dube using a version of LITFIRE that is different than the one used here. Figures 2.15 and 2.16 give the current LITFIRE prediction using the parameters suggested by Dube. The dashed lines are the combustion zone and cell gas temperature profiles that were published in 1978. This has been included to show the direction that the "improved" model has taken with respect to consequences as well as to gain a feel for the sensitivity of LITFIRE to all of the recent changes simultaneously. There is a discrepancy between the heat of vaporization of lithium that was used by Dube and the known value. The one used in the present LITFIRE calculation is correct. One important observation from these comparisons is that the severity of the predicted consequences is not a strong function of the combustion zone emissivity. The range in combustion zone emissivity was from 0.1 to 0.9 while the maximum combustion zone temperature varied from 1120°C to 1265°C. This indicates that very large spills are less sensitive to this parameter than the predicted sensitivity for the smaller tests at HEDL (see Section 2.3.2).

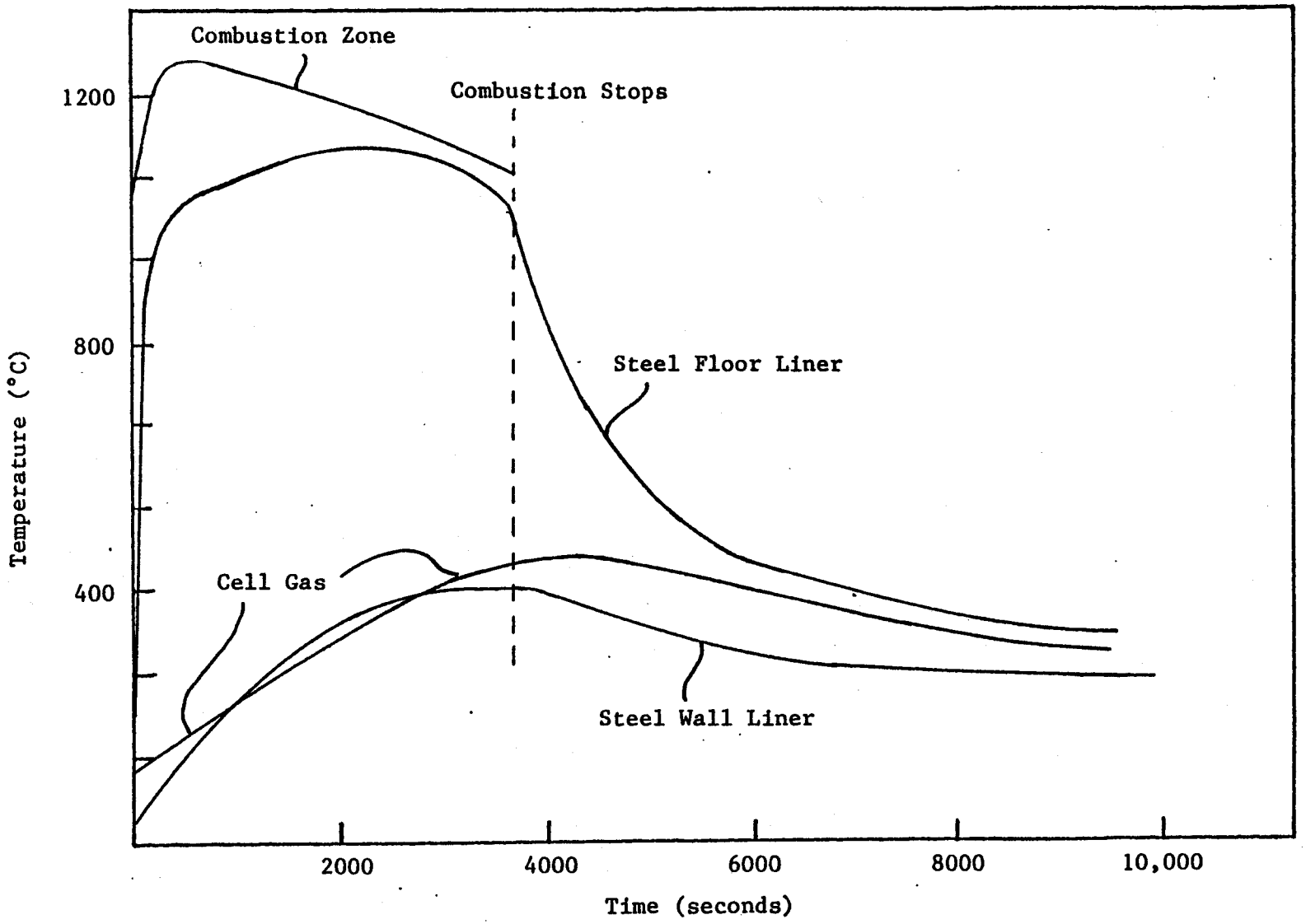

Figure 2.15: UWMAK-III Predictions Based on Dube's Parameters

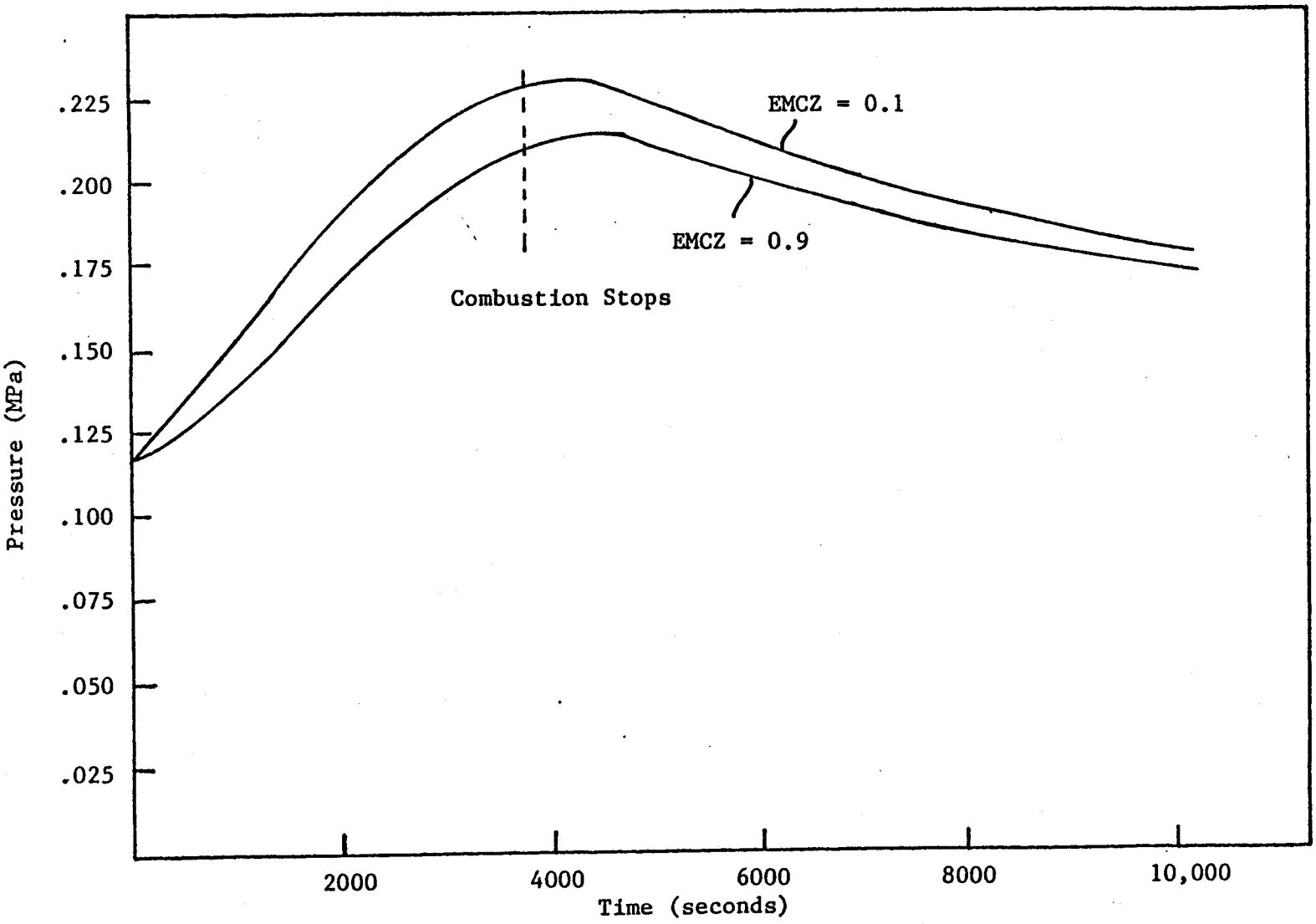

Figure 2.16: UWMAK-III Cell Gas Pressurization History

3. DEVELOPMENT AND APPLICATION OF TWO-CELL LITFIRE

3.1. Motivation for Development of Two-Cell LITFIRE

The optional two cell formalism in LITFIRE was developed in order to more accurately model fusion related components and geometries. Typically the code could be used to model lithium fires contained in one cell, with mass and heat transfer allowed between the two cells. Such configurations could represent a fire in a torus (of a tokamak), in a coolant pipe, or in the inner cell of a double containment. Limiting the combustion to a smaller cell might reduce the consequences of lithium combustion because less combustible gas would be immediately available for reaction with the lithium. However, significant changes in the combustion time history might occur if a breach of the primary containment occurred.

The two-cell LITFIRE geometry was designed to be compatible with the existing one-cell model and is shown in Figure 3.1. No new heat transfer mechanisms within the primary containment were added and the only new mass transfer mechanism is the allowance for the breach of the primary steel liner (herein referred to as "crack") permitting exchange of the cell gases.

It should be noted that several changes to the LITFIRE program that are especially important in two cell applications have been made since the two cell formalism was introduced by Tillack [10]. Principally these are:

- Incorporation of separate floor nodes for the primary and secondary cells.
- Removal of the concrete nodes attached to the primary steel floor.
- Allowance for different properties in each wall and floor node of inner and outer cells.
- Allowance for different emissivities for each wall and floor node.
- Inclusion of radiative and convective heat transfer from primary containment to secondary as well as separate gas convection coefficients for the wall and floor nodes.
- Allowance of gas flow through crack to cease during run if pressures equate in order to reduce computation time.

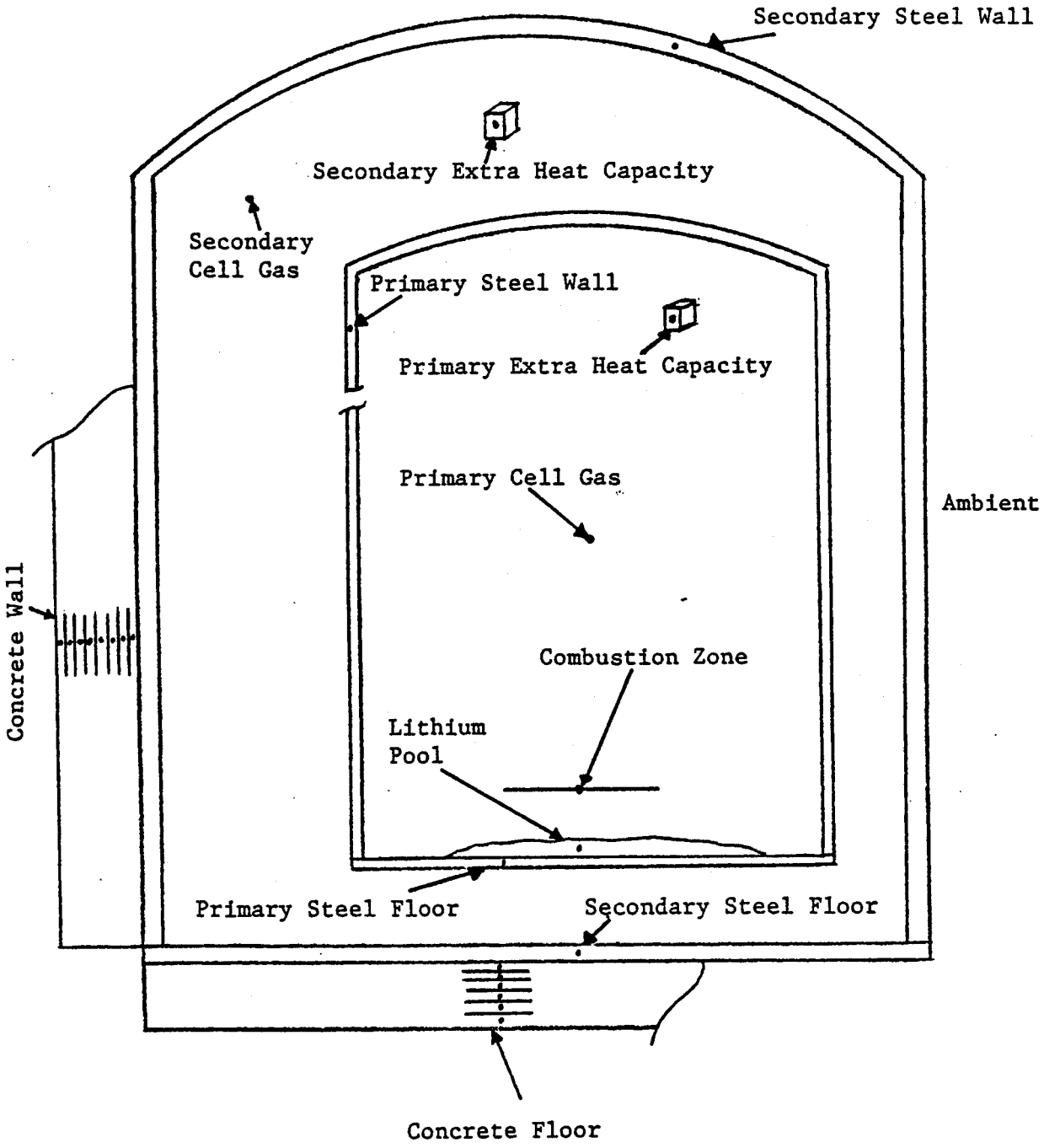

Figure 3.1: Litfire Two Cell Geometry and Nodal Structure

3.2. Model Description

3.2.1. Two-Cell Geometry

The geometry of the two cell LITFIRE model is an extension of the one cell model. All options and nodes present in the one cell version of LITFIRE are incorporated in the two cell formalism. In the idealized description of the two cell geometry (Figure 3.1) it can be seen that the combustion zone and pool are not directly affected by the presence of an outer containment cell. There are new radiative and convective heat transfer pathways between the primary wall and floor nodes to the secondary gas, floor, and wall nodes. The concrete is only permitted around the outer cell steel wall and floor. No allowance was made for concrete around the primary cell wall since the conductivity of concrete is relatively low. Therefore heat transfer between the concrete and ambient or a secondary cell gas would be expected to be very much the same and this setup can be adequately modeled by the existing one cell version of LITFIRE. An important consequence of this exclusion is that there is only a single structural node between the primary and secondary cell gases which can be an important limitation in modeling real systems.

In order to increase the flexibility of the two cell calculation without adding nodes to the present structure, each of the existing structural nodes is allowed to have unique physical properties, thicknesses, emissivities, and convection coefficients. (This is not true for the concrete nodes which are only allowed to vary in their relative thickness.) Since these are all user defined parameters, LITFIRE can mock simple heat flows with various sinks and/or obstructions. For example, the primary steel floor can be "insulated" from the secondary cell (but not the primary) by choosing appropriately low emissivity and convective coefficients.

Another interesting feature allowed by the addition of the secondary cell is the ability to have different atmospheres (and pressures) in the primary and secondary cells. One application of this would be an inert inner cell enclosed in a larger containment of air (or any gas mixture of nitrogen, oxygen, water vapor, and inert gases) at a higher pressure. Such a setup has been proposed for the main containment of the STARFIRE reactor. Another obvious application is the modeling of two cells at different pressures, e.g., a vacuum torus enclosed by a pressurized containment. This application of LITFIRE is discussed in Section 3.4.

The simplicity of LITFIRE is characterized by the single node allotted to each of the secondary cell components. The secondary cell gas, like the primary gas, is assumed well mixed and uniform in temperature. All the internal temperature gradients of the secondary cell structural materials are neglected. This can be a rather crude set of assumptions but the actual temperature gradients that might be generated in the secondary cell will most likely be much smaller than those in the primary cell, which is already characterized by a single, one-dimensional nodal structure.

3.2.2. Explanation of Two-Cell Gas Exchange

The geometry of LITFIRE includes an idealized orifice in the sense that the crack between the two cells has no length and there are no associated pressure and friction losses due to the flow. The inertia of any gas that would be inside a real orifice is neglected and as a result the flow can change directions instantaneously. The flow rate is obtained by using the relation for simple orifices,

$$\frac{dm}{dt} = C_d A \sqrt{2\, g_c \rho \Delta P} \tag{3.1}$$

where

$\frac{dm}{dt}$ = mass flow rate

C_d = coefficient of discharge (unity in LITFIRE)

A = area of orifice .

g_c = dimensional constant $(32.2 \frac{lb_m\, ft}{lb_f\, sec^2})$

ρ = gas density

ΔP = pressure drop between cells

The validity of Eq. (3.1) is subject to the following restriction,

$$\frac{P_{high}}{P_{low}} \leq \left(\frac{\gamma+1}{2}\right)^{\frac{\gamma}{\gamma-1}} \tag{3.2}$$

$$\leq 1.89 \text{ for air,}$$

where the constant γ is the ratio of specific heats C_p/C_v. For larger pressure drops the flow becomes sonic, and the flow rate is calculated according to

$$\frac{dm}{dt} = C_d A \sqrt{0.94\, g_c \rho P} \tag{3.3}$$

where P is the higher of the two cell pressures. Therefore, LITFIRE can track sonic or subsonic flow, into or out of, the primary cell.

The mass that is transferred between the cells represents the same homogeneous mixture (if more than one constituent is present) of gases that characterizes the cell of the higher pressure. It is therefore possible, given high enough exchange rates, to have a significant alteration of the cell gas compositions if they were initially different. This also permits aerosols generated by the combustion of lithium to appear in the outer cell gas. Since these aerosols are corrosive, structural damage to the outer containment cell may occur if they appear in sufficient quantities. LITFIRE

monitors the individual aerosol species in both cell gases. A major assumption implicit in the flow calculation is that mass transfer by diffusion due to a concentration gradient is negligible and is ignored. This assumption may not be valid for large crack sizes when the cell pressures are nearly equal and are of significantly different composition. As a result, the mass transfer through large cracks may not be accurately modeled by LITFIRE. Although there is no correlation indicating what may constitute a "large" crack, Section (3.2.3) describes a limit to the usable crack size due to numerical considerations.

The temperatures of both cell gases will change as a result of the flow due to the convection of the gases at different temperatures. In addition, the associated expansion (or compression) of the cell gas due to the flow will give rise to a temperature change. Using the method of forward differencing, Tillack [10] performed an energy balance on the system shown in Figure 3.2 which is reproduced below:

$$\text{Let } \frac{dT}{dt} = \frac{T_{n+1} - T_n}{\Delta t} \tag{3.4}$$

Applying conservation of energy yields

$$\text{final energy} = \text{initial energy} + \text{energy added} \tag{3.5}$$

$$m_{n+1}U_{n+1} = m_nU_n + (\chi\Delta t)h_n \tag{3.6}$$

where the variables are as indicated in Figure 3.2. Applying this condition to each cell,

$$(m_n^{(1)} - \chi\Delta t)C_vT_{n+1}^{(1)} = m_n^{(1)}C_vT_n^{(1)} - (\chi\Delta t)C_pT_n^{(1)} \tag{3.7}$$

$$(m_n^{(2)} + \chi\Delta t)C_vT_{n+1}^{(2)} = m_n^{(2)}C_vT_n^{(2)} + (\chi\Delta t)C_pT_n^{(1)} \tag{3.8}$$

using $\gamma = C_p/C_v$ (assumed independent of temperature) and some algebraic manipulation, the following expressions for the temperature change result

$$\frac{dT^{(1)}}{dt} = \frac{\chi(1-\gamma)T_n^{(1)}}{m_n^{(1)} - \chi\Delta t} \tag{3.9}$$

$$\frac{dT^{(2)}}{dt} = \frac{\chi(\gamma T_n^{(1)} - T_n^{(2)})}{m_n^{(2)} + \chi\Delta t} \tag{3.10}$$

These expressions are compatible with the LITFIRE integration method since they refer only to the values for the temperature ($T_n^{(i)}$), and mass ($m_n^{(i)}$) at the previous time step.

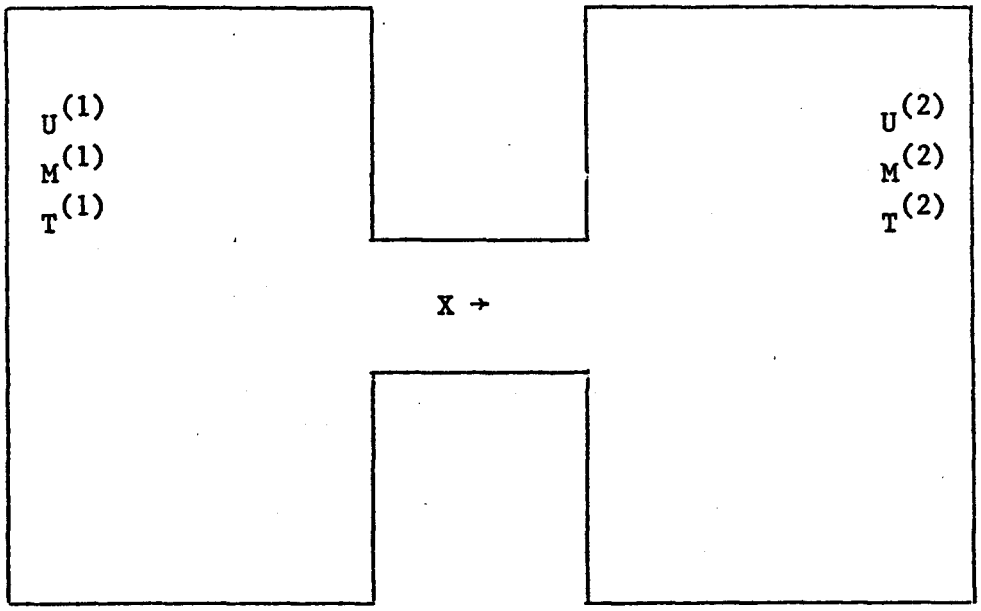

$U_n^{(i)}$ = internal energy of cell i at time t_n.

$M_n^{(i)}$ = Mass of all gases and aerosols in cell i at time t_n.

$T_n^{(i)}$ = Temperature of gas in cell i at time t_n.

X = Mass flow rate

Δt = integration time step.

(Note: mass flow rate is assumed constant during a single time step.)

$h_n = T_n c_p$

Figure 3.2: Two Cell Energy and Mass Balance Diagram

3.2.3. Coding Changes Required for Numerical Stability

In order to insure numerical stability in the calculation of mass exchange between the primary and secondary cells, several checks have been incorporated into LITFIRE. One numerical instability is due to the possibility of an oscillatory solution to the flow rate calculation having a period of the same magnitude as the integration time step. This can cause a discrepancy between the indicated flow direction and the mass buildup of the cell gases. For example, a test case was run where the flow was continually out of the primary yet the mass of nitrogen in the primary cell was increasing in time. The inconsistency is due to the fact that within the integration looping itself, the flow is changing directions with each integration time step. Since there are an even number of integration time steps per "real" time step the flow always appears in the same direction. For such a mechanism to occur the change in pressure drop ΔP in a single time step must be equal to the pressure drop. Applying the equations developed in Section 3.2.2 above, as well as the ideal gas relations

$$P^{(1)}V^{(1)} = m^{(1)}RT^{(1)}, \quad P^{(2)}V^{(2)} = m^{(2)}RT^{(2)} \tag{3.11}$$

results in the following restriction on the integration time step (Δt),

$$\Delta t \leq \frac{C_1 V^{(1)}\sqrt{\Delta P}}{A\sqrt{P^{(1)}}} \tag{3.12}$$

by requiring that the change in the pressure difference $\Delta(\Delta P)$ across a single integration time step must be equal to the pressure difference (ΔP) itself.

$$\frac{\Delta(\Delta P)}{\Delta t} = \Delta P \tag{3.13}$$

C_1 is a constant for a given geometry and small variation in the temperature over a single time step and A is the area of the orifice.

There are two regimes of interest for Δt. The first is when the cell pressures are nearly equal requiring Δt to be small in order to insure stability. The second regime is in the presence of a "large" orifice, A, which also requires that Δt be small. In principle Δt can be made arbitrarily small, but in practical terms a lower limit on Δt is necessary in order consume finite computational time. Fortunately both these regimes are not critical for modeling flow calculations in the sense that cell gas dynamics will be relatively unaffected at low pressure differentials and large cracks almost imply that a single cell calculation would be just as applicable. As a result, LITFIRE now has the user specified option of closing the orifice after a predetermined amount of "real" time if the cell pressures equilibrate to within one part in ten thousand.

3.3. Comparison of One and Two Cell Results for HEDL Test LA-4

Figure 3.3 shows the predicted steel wall temperature for HEDL test LA-4, for both a one cell and two cell geometry. No orifice existed between the cells and the secondary volume was very large to approximate the infinite ambient environment implicit in the LITFIRE code. This node was found to be the most sensitive to this change in geometry due to its direct contact with ambient in the one cell version. The agreement between the two versions is within four percent (up to about 10,000 seconds after ignition). The discrepancy is probably due to a small amount of heating of the secondary cell gas, thus reducing slightly the convective heat transfer to that node from the steel wall.

3.4. Effect of Crack Size on Lithium Fires in a Two-Cell Geometry

A study was performed on the sensitivity of lithium fire consequences in a full scale reactor to the crack size in the steel wall separating the two cells. Since UWMAK-III had been the basis for earlier studies (see Section 2.4) it was retained as the reactor of interest in the present calculation. The major change for this comparison is that the lithium fire is contained in the torus of the reactor (inner cell of LITFIRE) and the secondary containment in UWMAK has become the outer cell for LITFIRE. The spill sizes are approximately the same (~22,000 kg. Li) though the thickness of the pool in the torus is much greater due to the smaller surface area available.

Both cells were initially at atmospheric pressure and contained identical concentrations of oxygen and nitrogen. The volume of the inner cell was approximately three percent of the volume of the outer containment cell. The crack size was varied between 0.0 and 100.0 square centimeters. Above 100 square centimeters the two cells act as one large cell since the communication between the cells limits the maximum pressure difference to less than a few percent. Table 3.1 lists the main combustion characteristics for various crack sizes. Figures 3.4 and 3.5 show the temperature and pressure history for a typical two cell calculation (crack size = 1.0 cm^2) and give an idea of the dynamic effect of a breach of containment. Figure 3.6 gives the temperature profiles for structural components in the inner cell and the lithium pool. The first and second maxima in the temperature and pressure plots (Figures 3.7 and 3.8) were taken at the points indicated by the arrows in Figures 3.4 and 3.5. In this application the outer cell was large enough that the maximum change in pressure was less than eight per cent regardless of the crack size. However, the temperature rise in the outer cell was substantial (up to 90°C) for the larger crack sizes. The maximum outer cell temperature as a function of crack size is plotted in Figure 3.9.

For crack sizes below 1.0 cm^2 the flow was almost always into the inner cell due to the underpressure from gas consumption in combustion. Therefore there was no buildup of reaction

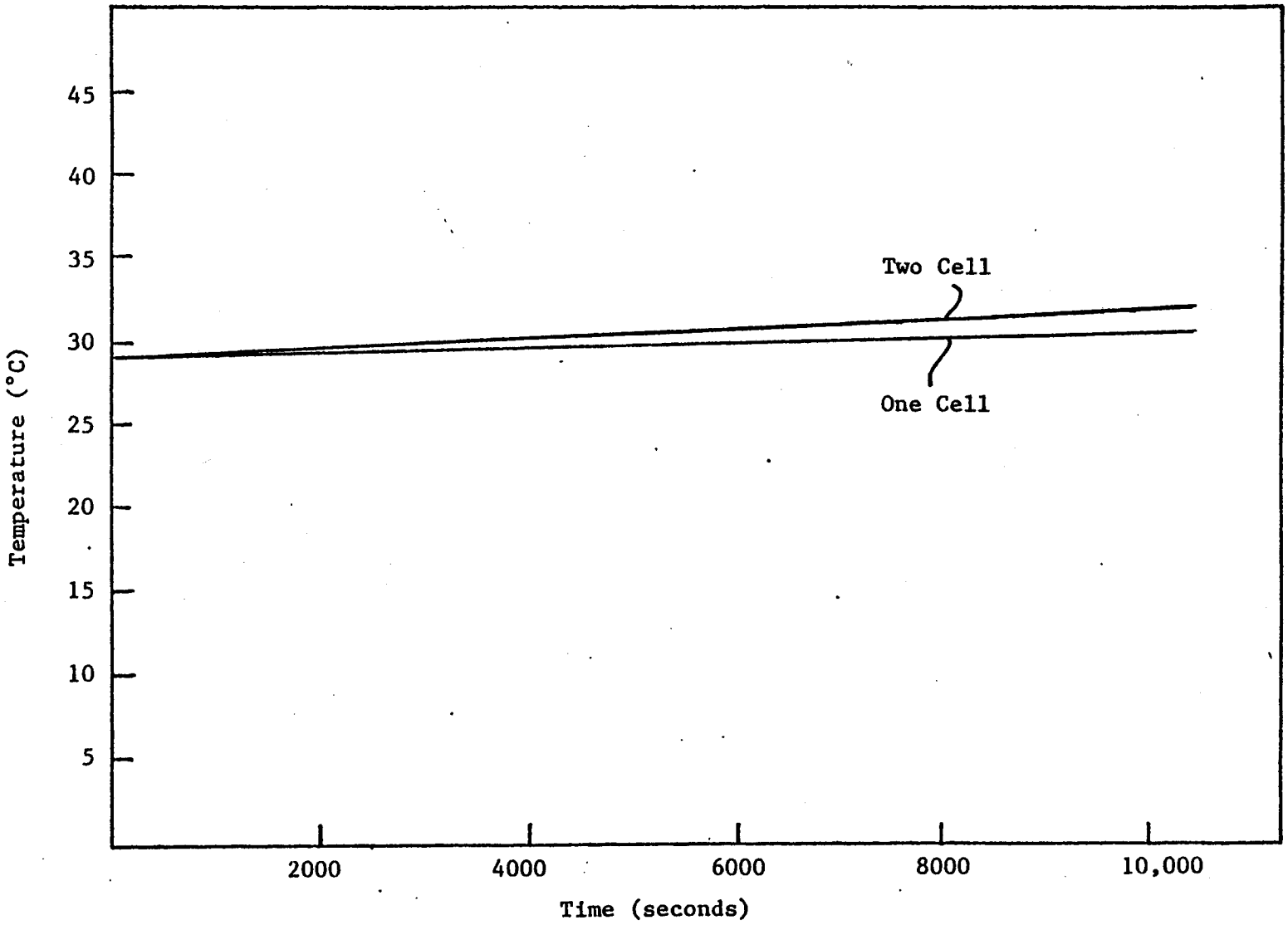

Figure 3.3: Comparison of One Cell and Two Cell Predictions for LA-4 Steel Wall LIner

TABLE 3.1

Combustion Characteristics for Various Crack Sizes

Crack Size (cm^2)	Lithium Consumed in Fire (kg)	Duration of Fire (secs.)	Peak Structural Temperature (°C)
.0000	487.6	3750[t]	318
.0001	487.7	3750[t]	318
.0100	488.9	3800[t]	318
1.0000	930.5	11,000[t]	576
10.0000	22,000.	41,000[i]	576
100.0000	22,000.	19,400[i]	716

t - Temperature of lithium pool dropped to lithium's melting point.

i - Reaction was limited by amount of lithium spilled (22,000 kg.)

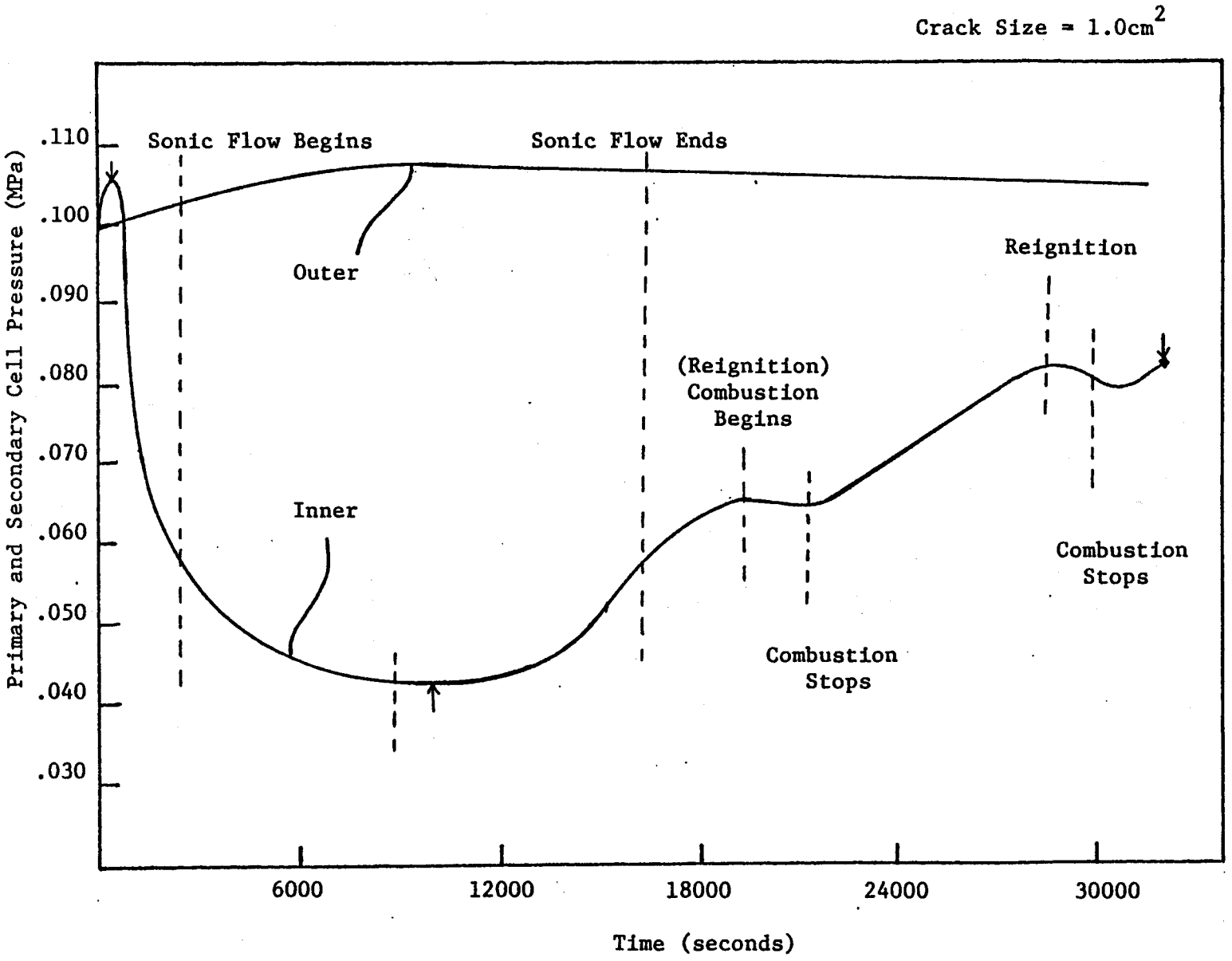

Figure 3.4: Typical Pressurization History for UWMAK-III Two Cell Geometry

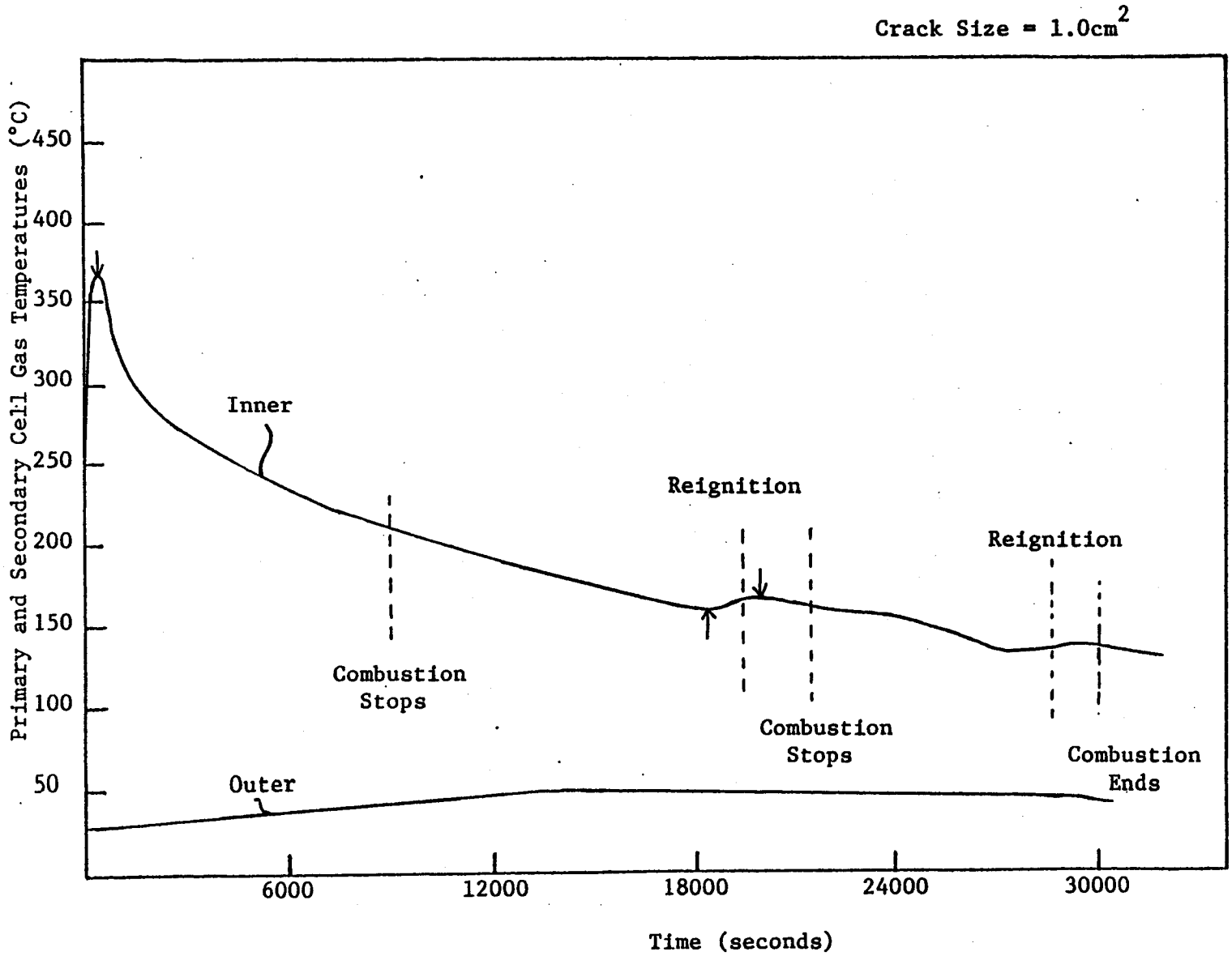

Figure 3.5: Typical Temperature History for UWMAK-III Two Cell Geometry

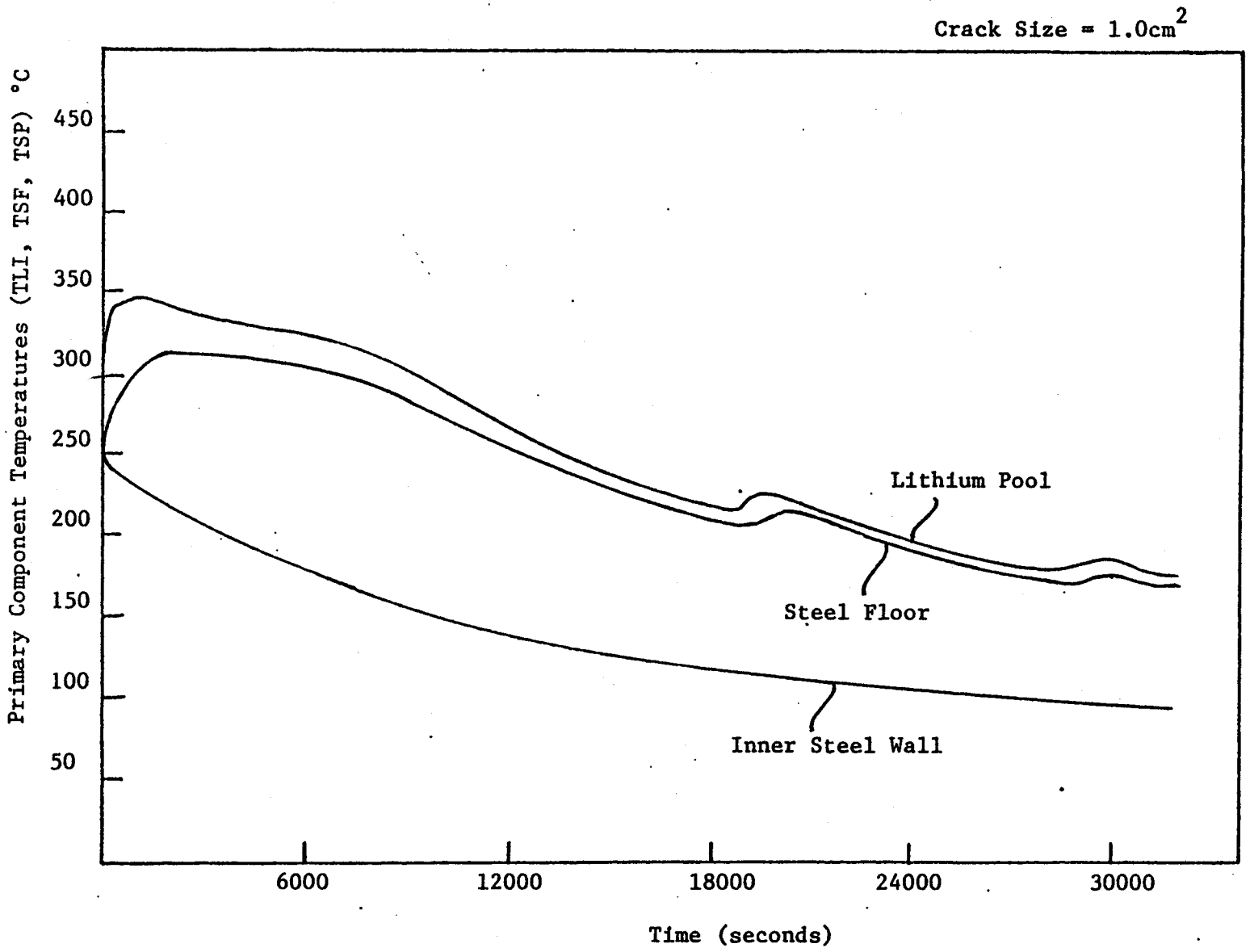

Figure 3.6: Typical Component Temperatures for UWMAK-III Two Cell Geometry

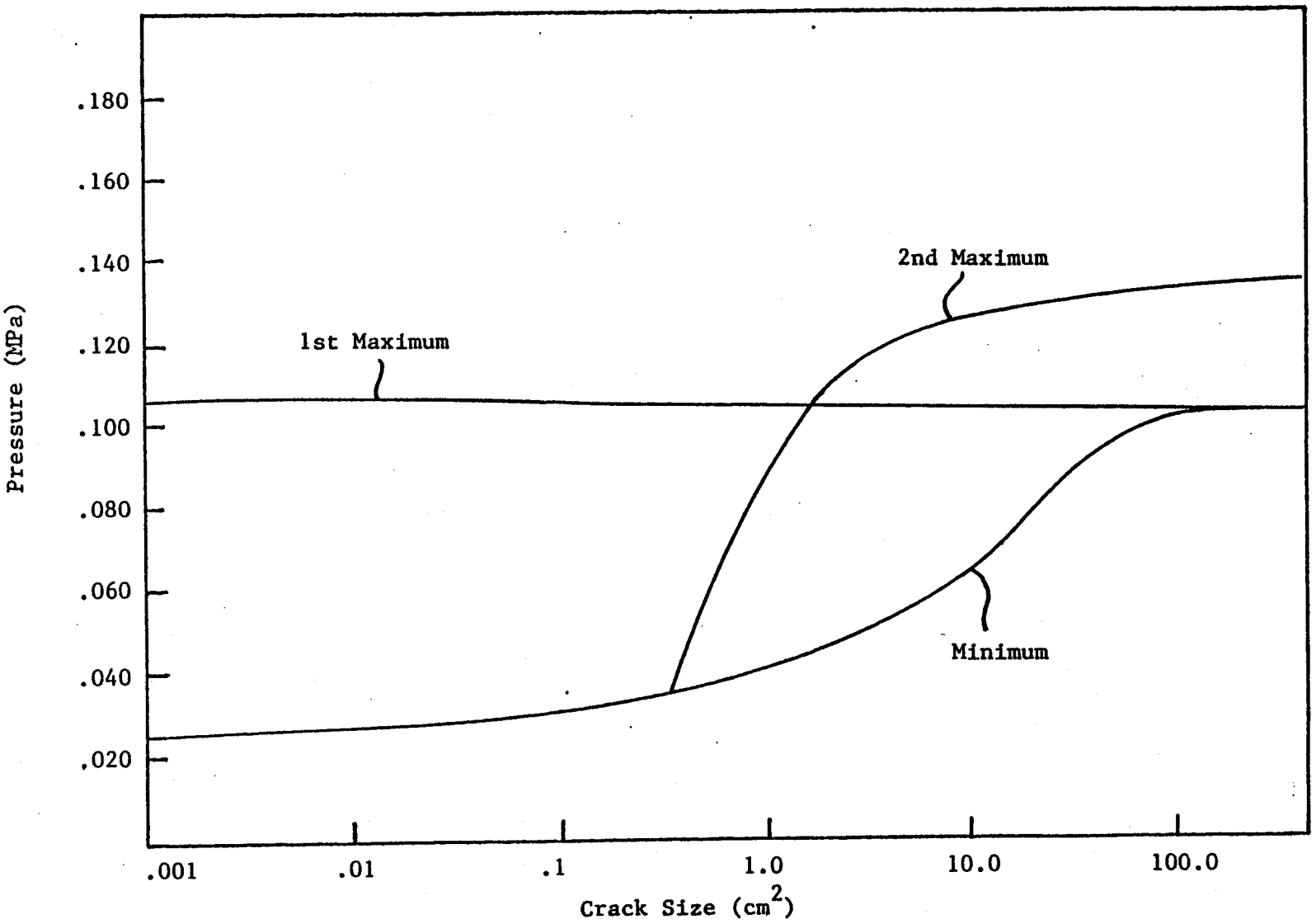

Figure 3.7: Minimum and Maximum Cell Pressure in UWMAK-III Two Cell Geometry (Smoothed)

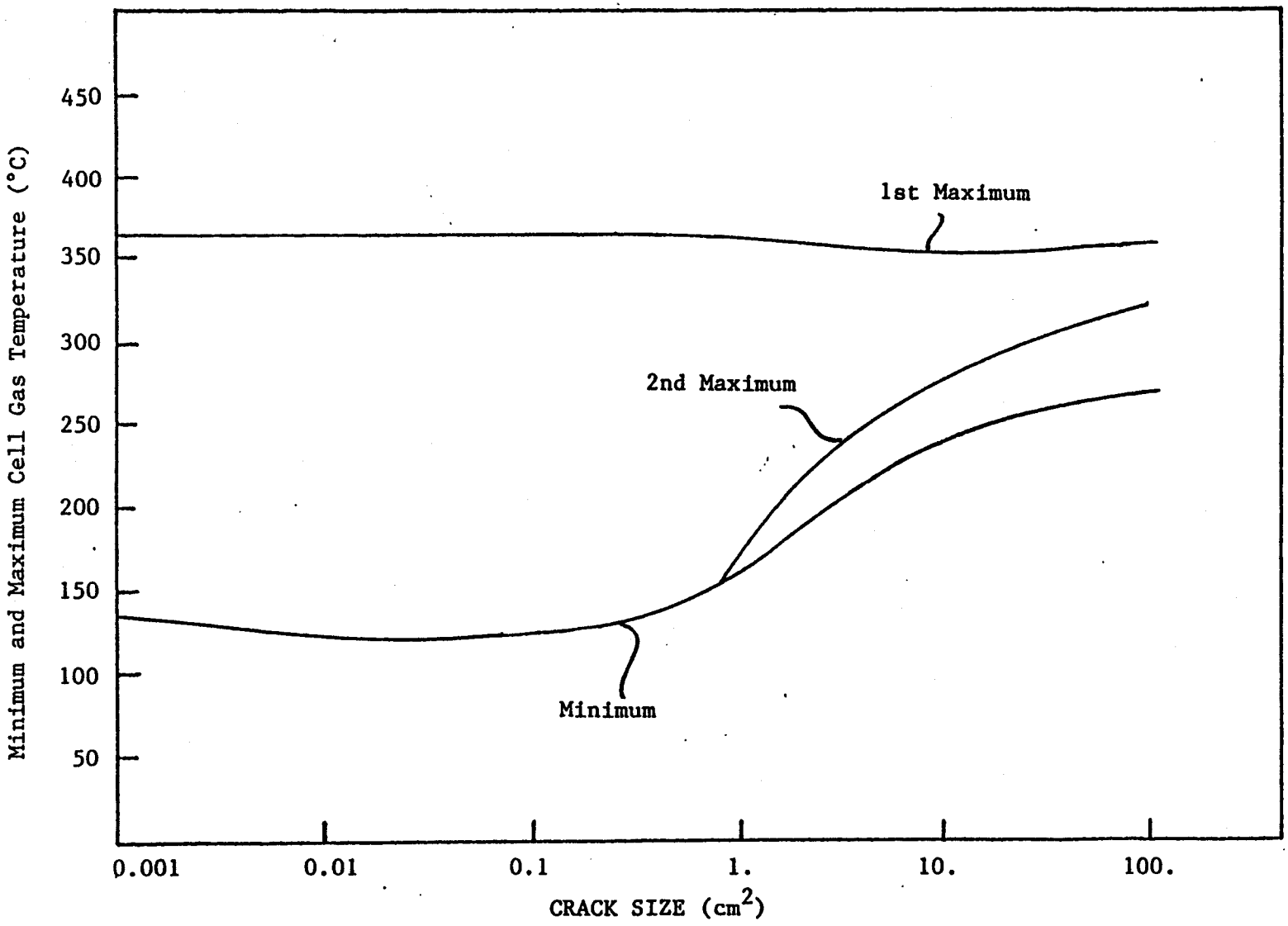

Figure 3.8: Minimum and Maximum Cell Gas Temperature for UWMAK-III Two Cell Geometry.

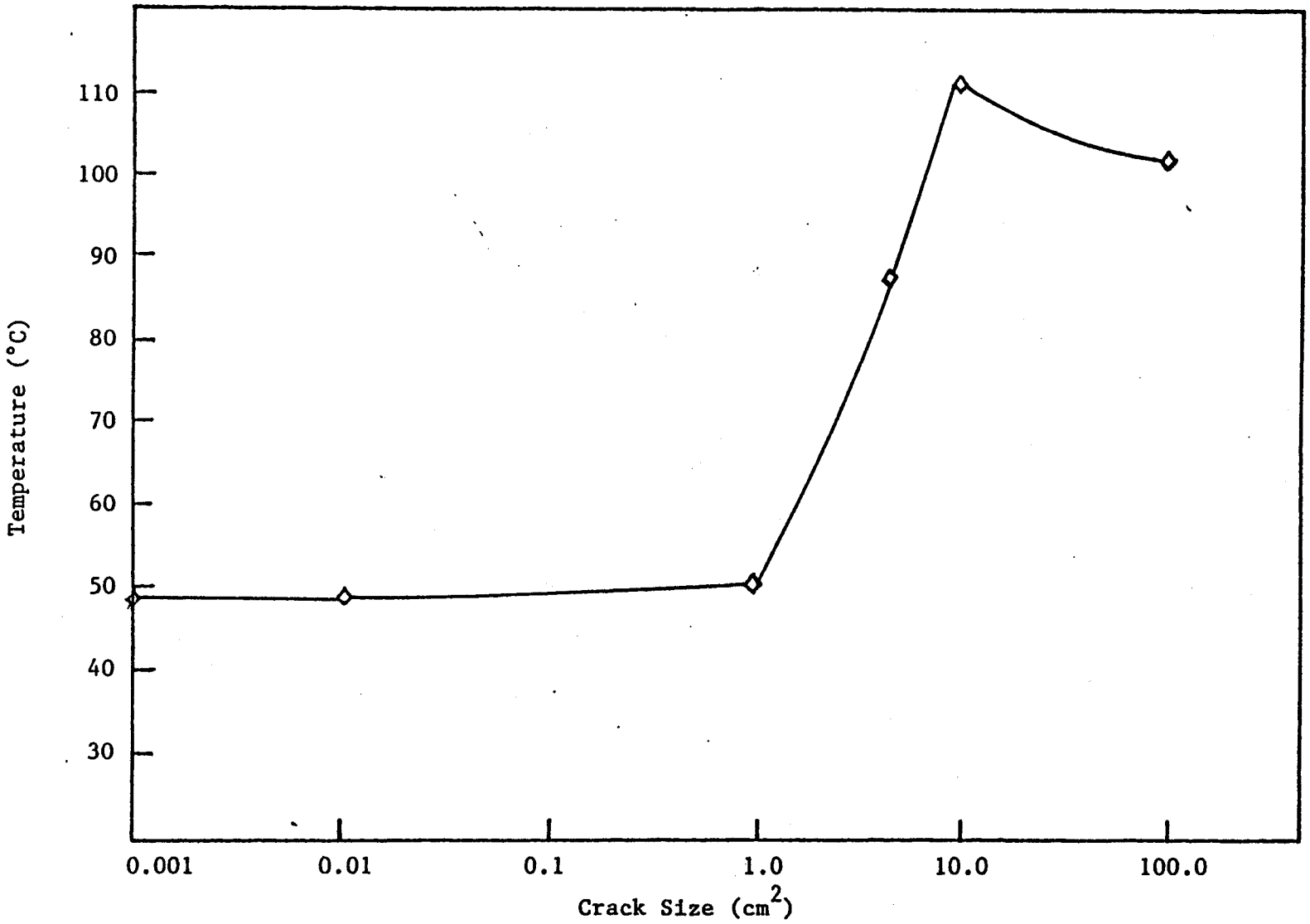

Figure 3.9: Maximum Secondary Cell Temperature (Initial Temperature = 27 °C)

products in the outer cell. However, lithium fires with larger crack sizes did generate inner cell pressures greater than those in the outer cell, causing the flow to go from the inner into the outer cell. For the maximum crack size used (100 cm^2) the maximum reaction product concentration in the outer cell was 4.5×10^{-3} kg/m^3. The maximum concentration of Li_2O and Li_3N in the inner cell was 66.7 kg/m^3. Aerosol removal by particle settling was not allowed in these tests (when permitted removal is assumed to be effective in the inner cell only).

3.5. Application of LITFIRE to a Lithium Spill in a Vacuum Torus

In this section a test case using the UWMAK-III geometry described above was run, but with the inner cell initially at a pressure of 0.001 megapascals. This was done in order to test the ability of LITFIRE to model high velocity flows as well as to see the effect lithium fires might have on the rapid pressurization of the torus and vice versa. Since the reaction rate is determined by the convection of gas to the combustion zone, low pressures can limit and even fail to ignite, the lithium reaction.

The results from this calculation are shown in Figures 3.10 and 3.11 indicate that there is indeed a limitation on the reaction rate due to low pressures, with ignition taking place a little under a thousand seconds after the transient was initiated. In addition, the maximum inner cell pressure attained was limited by the consumption rate of the gases due to combustion. To first order, pressurization is a linear function of crack size, so that larger cracks will reduce the time to ignition and increase the maximum pressure in the inner cell. In these predictions, the intial temperature in the torus components are assumed to be 250°C which is approximately the operating temperature near the first wall of proposed fusion reactors. Also, no spray fire was included in the model since the initial pressure inside the torus was assumed to be negligible.

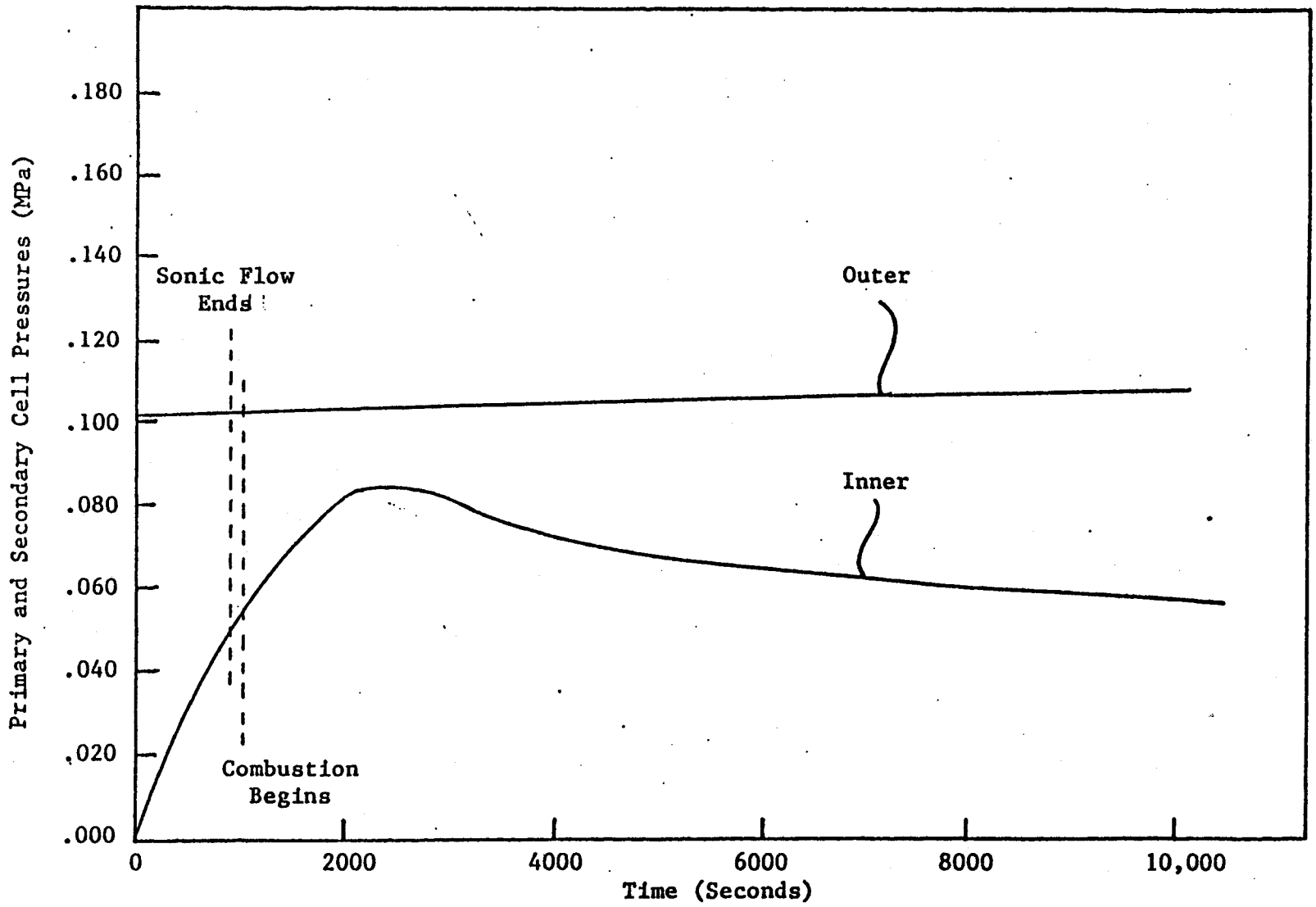

Figure 3.10: Torus Pressurization History, Crack = 10.0 cm^2

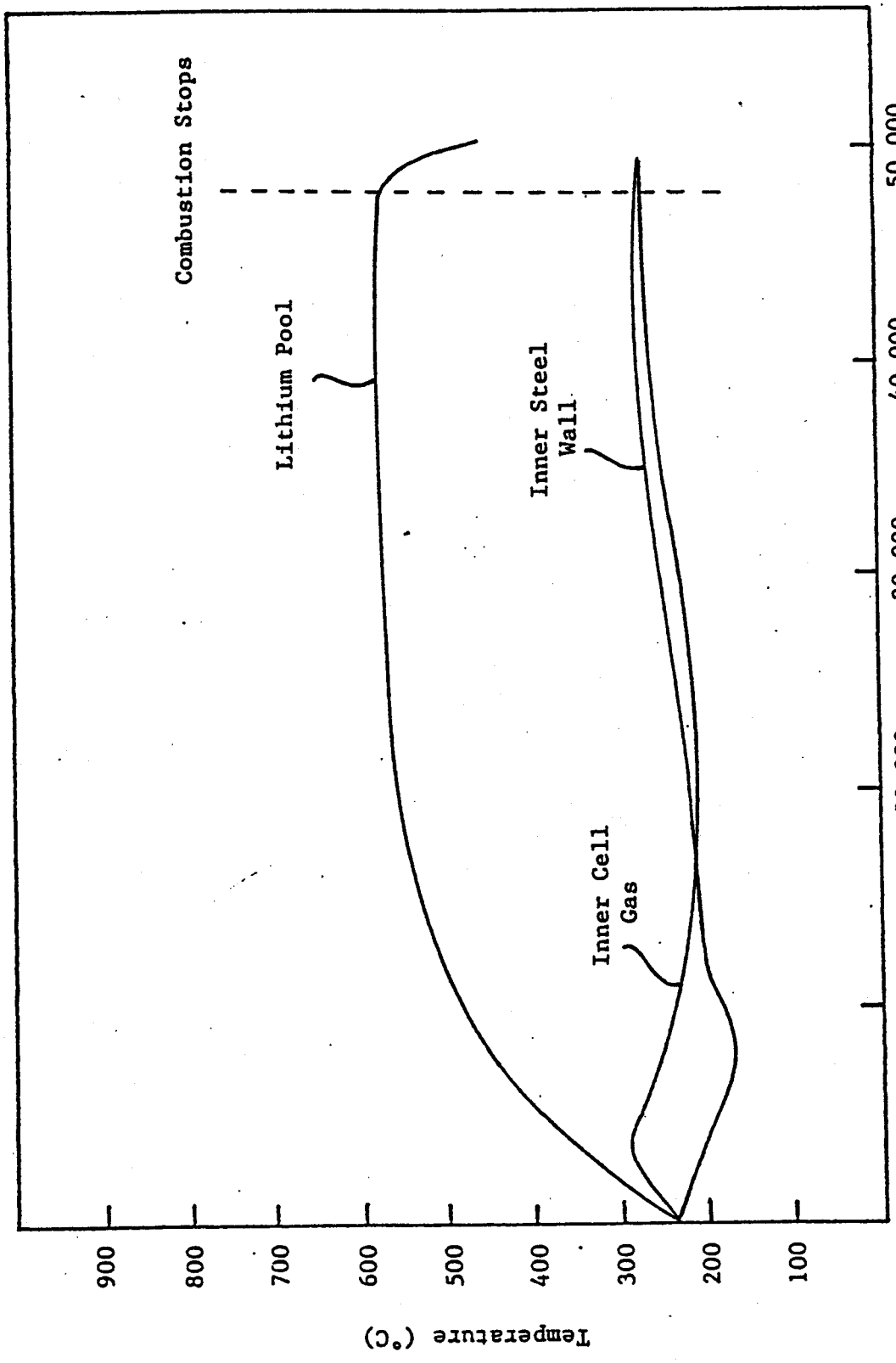

Figure 3.11: Torus Component Temperature History, Crack = 10.0 cm^2

4. LITHIUM-LEAD COMBUSTION IN AIR

4.1. Lithium-Lead Use in Fusion Related Systems

Various compositions of lithium-lead (LiPb) alloy have been proposed as a tritium breeder for fusion reactors using the deuterium-tritium fuel cycle. The form of LiPb is unique in that the lithium acts as a tritium breeder and the lead acts as a neutron multiplier. Thus, the lithium inventory in the blanket can be minimized, limiting the total amount of lithium that is available for combustion in the event of an accident. In addition, LiPb compounds with a low melting point may also function as a coolant as well as breeder, further simplifying the reactor blanket design. The potential problems of using lithium lead alloys are associated with proper tritium confinement, structural material compatibility, and chemical reactions with air and water. The last of these concerns is the focus of this chapter, which presents models for lithium-lead pool combustion in an air atmosphere that is allowed to contain some moisture. Lithium-lead reactions with water in a prototypical fusion blanket assembly have been modeled by Krane [2] and are already incorporated in another version of LITFIRE (see Table 1.3).

4.2. Properties of Lithium-Lead

A recent literature search indicates that there is little data available with regard to physical, chemical, and thermodynamic properties for the temperature range of interest in fire modeling. This section summarizes the available data that is important in the present calculations.

4.2.1. Physical Properties

The density as a function of composition is known as is the phase diagram of the lithium-lead system. These are shown in Figures 4.1 and 4.2. The thermal conductivity of lithium-lead is estimated using the correlation

$$k_{LiPb} = k_1 w_1 + k_2 w_2 - 0.72 \times |k_2 - k_1|(w_1 w_2) \qquad (4.1)$$

which is appropriate for a binary liquid mixture and where the k's are the thermal conductivities of the element and the w's are the weight fraction of each species in the alloy. [13]

The specific heat of the alloy is estimated by using an extrapolation of the specific heats of the pure elements

$$(C_p)_{LiPb} = \chi_{Li}(C_p)_{Li} + \chi_{Pb}(C_p)_{Pb} \qquad (4.2)$$

where χ is the atom percent of each species in the alloy, and the C_p's are the specific heat of each element. [3]

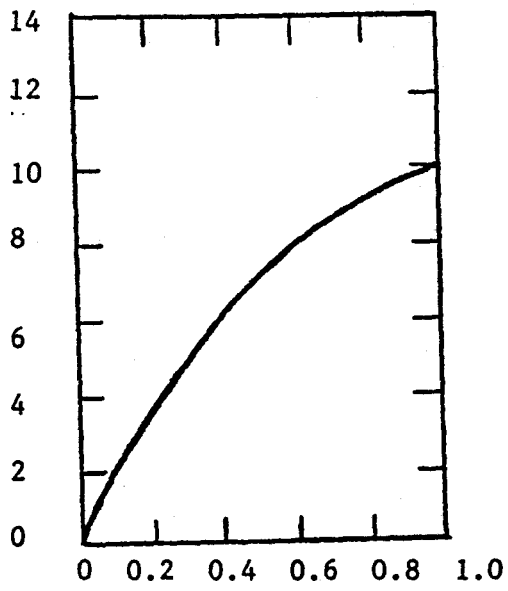

Figure 4.1 Density of LiPb

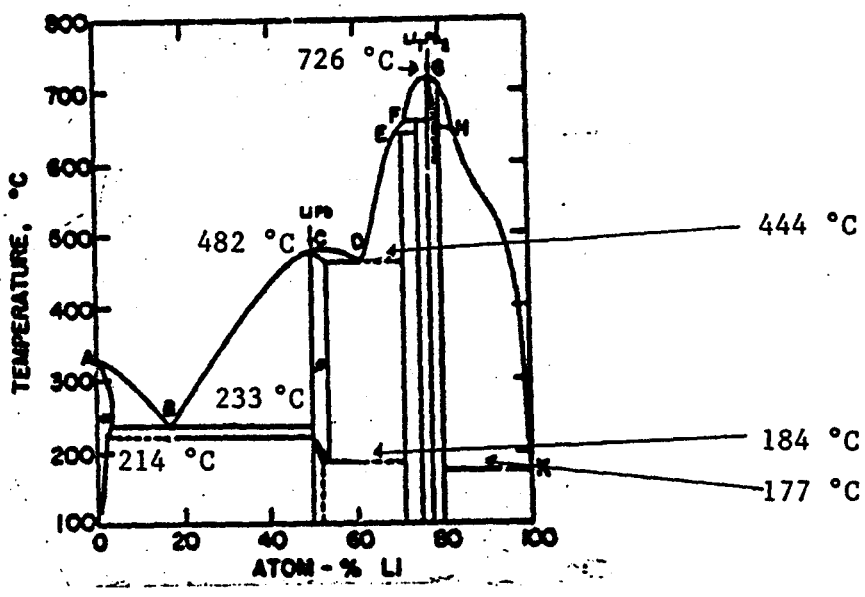

Figure 4.2: LiPb Phase Diagram

The latent heat of melting for a metallic alloy is determined by the correlation

$$\frac{H_{melt}}{T_{melt}} \sim 2.2 \qquad \begin{matrix}(H:\ cal/gm\ mole)\\(T:\ ^\circ Kelvin)\end{matrix} \qquad (4.3)$$

where T_{melt} is the melting temperature of the alloy. [13]

All of the above correlations are approximations at best and are calculated using lithium properties that vary with temperature and lead properties that are fixed for all temperatures.

4.2.2. Thermodynamic and Chemical Properties

The activity of lithium in the lithium-lead system has been measured at a temperature of 750 Kelvin. It decreases continuously from 4.0×10^{-3} at 61 atom percent lithium to 2.0×10^{-5} at five percent lithium. Figure 4.3 shows the lithium activity over the entire range of lithium concentration in lithium-lead. In addition, the activity of $Li_{17}Pb_{83}$ has been measured as a function of temperature [7] and found to follow

$$\ln a_{Li} = \frac{-6960}{T} + 0.0245 \qquad (4.4)$$

where a_{Li} is the activity and T is the alloy temperature in Kelvin. Although the values of activity are quite low for the temperature range of interest, it is expected that the chemical reactivity of LiPb will be dominated by the lithium chemistry, due to the large thermodynamic stability of lithium with oxygen, nitrogen, and hydrogen. A thermodynamic analysis of lithium in lithium-lead performed by Piet [3] indicated that the energetics of a lithium-nitrogen reaction (with lithium from LiPb) is slightly unfavorable from a free energy standpoint at low temperatures ($25^\circ C$) but is favored at higher temperatures. It is expected that the lithium-oxygen reaction at the lower temperatures would catalyze the reaction with nitrogen. In the present analysis, lithium nitrogen reactions will be allowed at all temperatures of interest even if there are no lithium-oxygen reactions taking place.

The dissociation reaction,

$$Li_aPb_b \rightarrow aLi + bPb \qquad (4.5)$$

is assumed to precede all lithium chemical reactions, so that the lithium that is reacting is effectively pure lithium and could just as well have come from a pure lithium pool. This simplifies the coding changes required to model LiPb pool fires and is a credible assumption based on the inert behavior of lead. The estimated heat of dissociation is shown in Figure 4.4 for the full range of lithium concentrations.

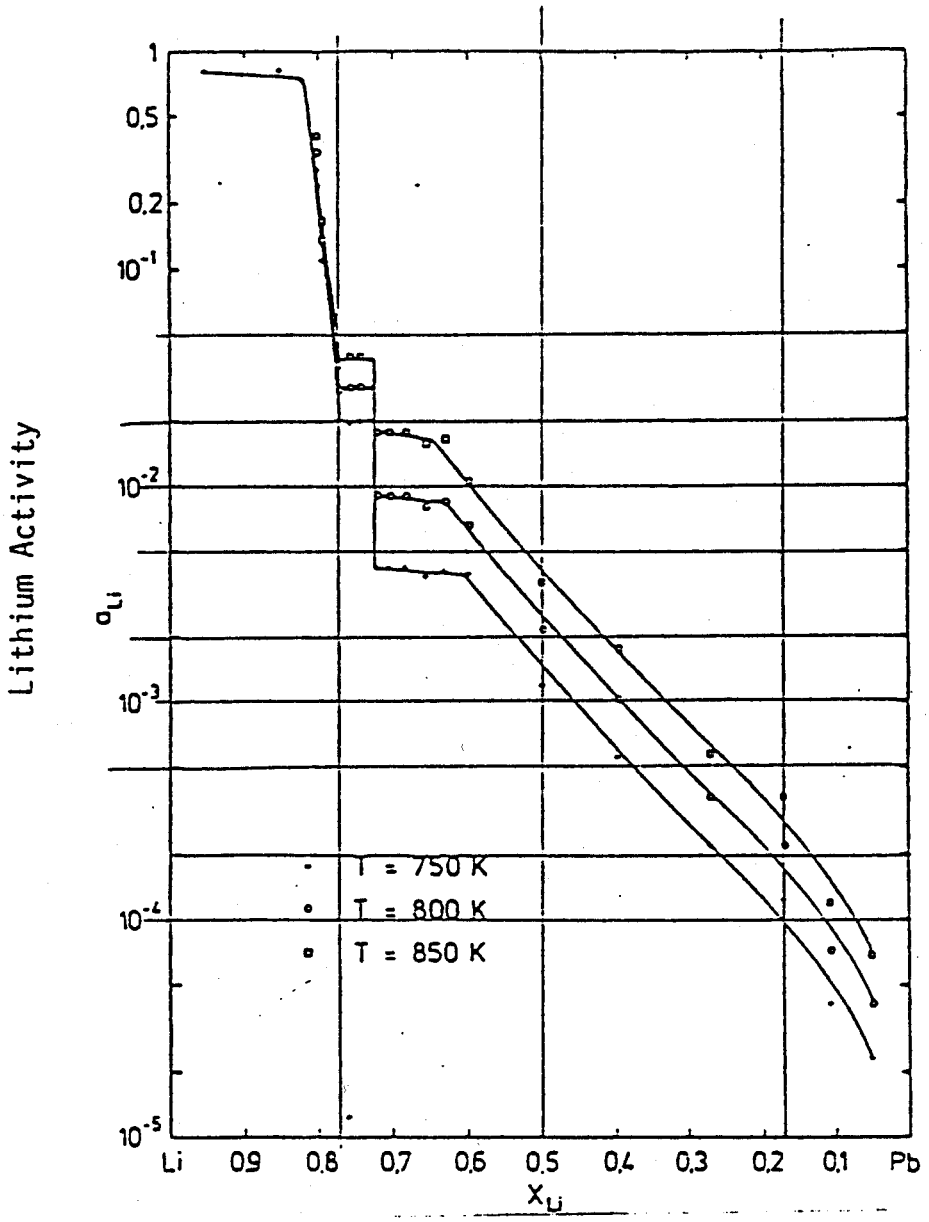

Figure 4.3: Lithium Activity in the LiPb System As a Function of Lithium Concentration [14]

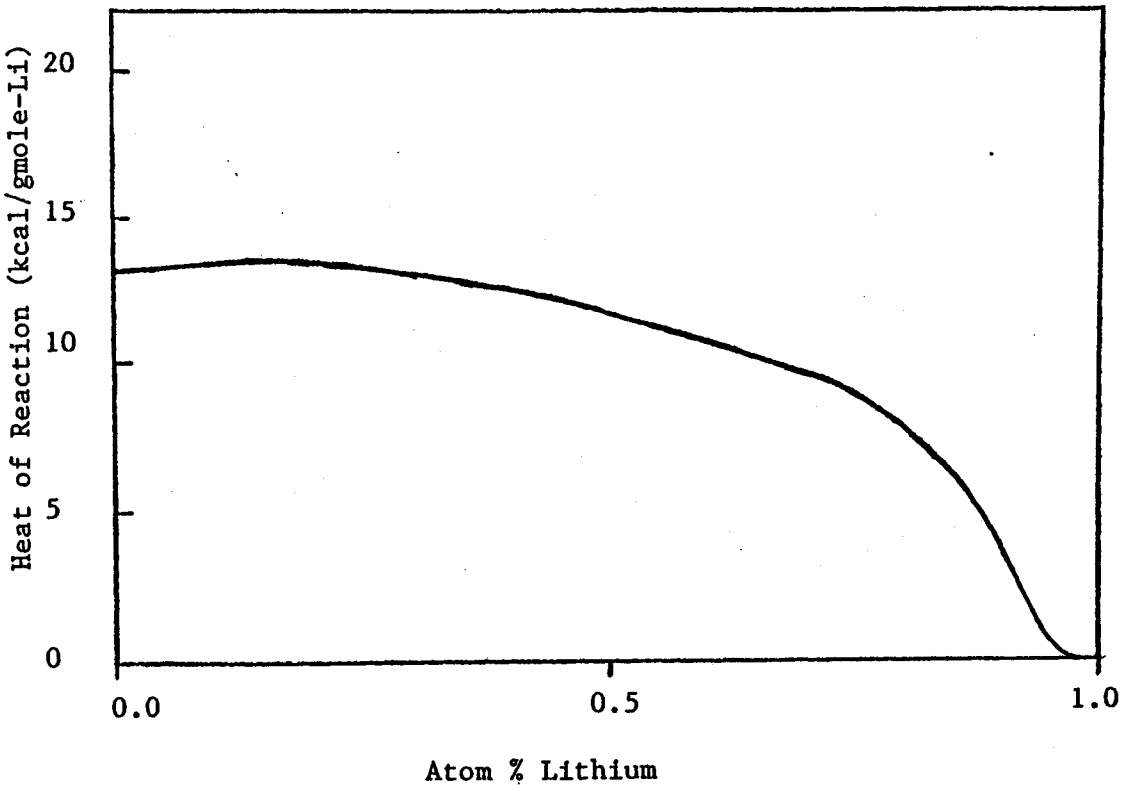

Figure 4.4 Heat of Dissociation for Li From Lithium Lead

The inertness of lead has been demonstrated by one experiment that immersed LiPb in air at 500°C:

> "The material melted and smoked vigorously until all of the lithium had escaped as Li_2O or Li_3N and only molten lead was left."[5]

However, in another test it was found that pure lead will ignite in an atmosphere of pure oxygen at temperatures greater than 850°C. It is conceivable that a LiPb pool fire will have two components: the first, a lithium fire with lead inert, and the second, a surface burning reaction of lead and oxygen once the lithium has been depleted. Due to lack of data on lead combustion, no lead reactions are allowed by LITFIRE.

4.3. Models of Lithium Lead Air Reactions

Since the underlying assumption is that once the lithium leaves the LiPb pool its behavior is not influenced by the presence of lead, the lead can only influence lithium transport within the pool itself, in addition to changes in the physical properties of the pool. Data from tests being performed at HEDL reacting LiPb in air are not yet available so there are no quantitative results on which to base a model of LiPb-air combustion. In light of this, the present study proposes two models of LiPb pool dynamics in order to "bound" the problem from conservative and optimistic views.

The first model is conservative in the sense that no inhibition of the lithium reaction takes place. The reaction rate is still limited by the transport of the cell gases to the combustion zone, and the pool uses the physical properties of LiPb. The pool is assumed well mixed and turbulent and of homogeneous concentration, hence it is called the "turbulent pool model", and is represented by a single pool node. The heat and mass transfer pathways important in this modeling are shown in Figures 4.5 and 4.6.

The second model is probably not conservative since it assumes a large inhibition of the reaction due to the presence of a lead layer above the LiPb pool, through which the lithium must diffuse through before it can reach the combustion zone. The thickness of the lead layer increases with the depletion of lithium and is considered semi-stable in that no mixing between the lead layer and the LiPb pool takes place. This model required the addition of one node in the pool to model the two layers and is called the "layered pool model". The important heat and mass transfer pathways for this modeling are indicated in Figures 4.7 and 4.8.

4.3.1. Turbulent Pool Model

The major assumption in this model is that the pool is well mixed and homogeneous. All

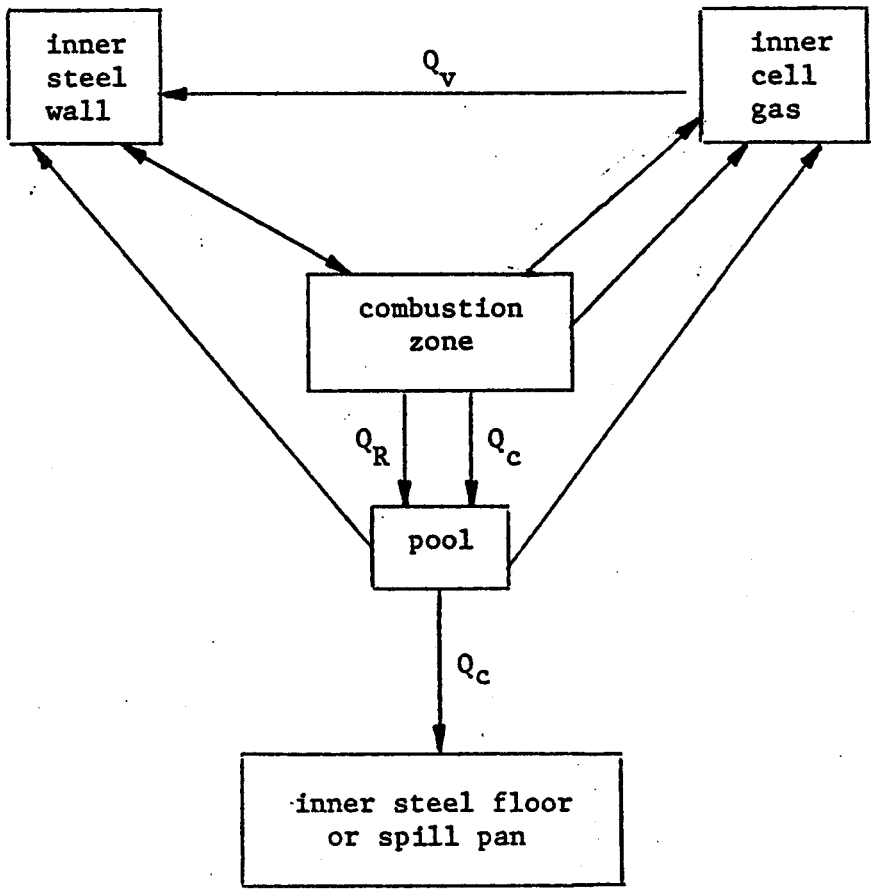

Figure 4.5: Heat Flow in Turbulent Pool Model

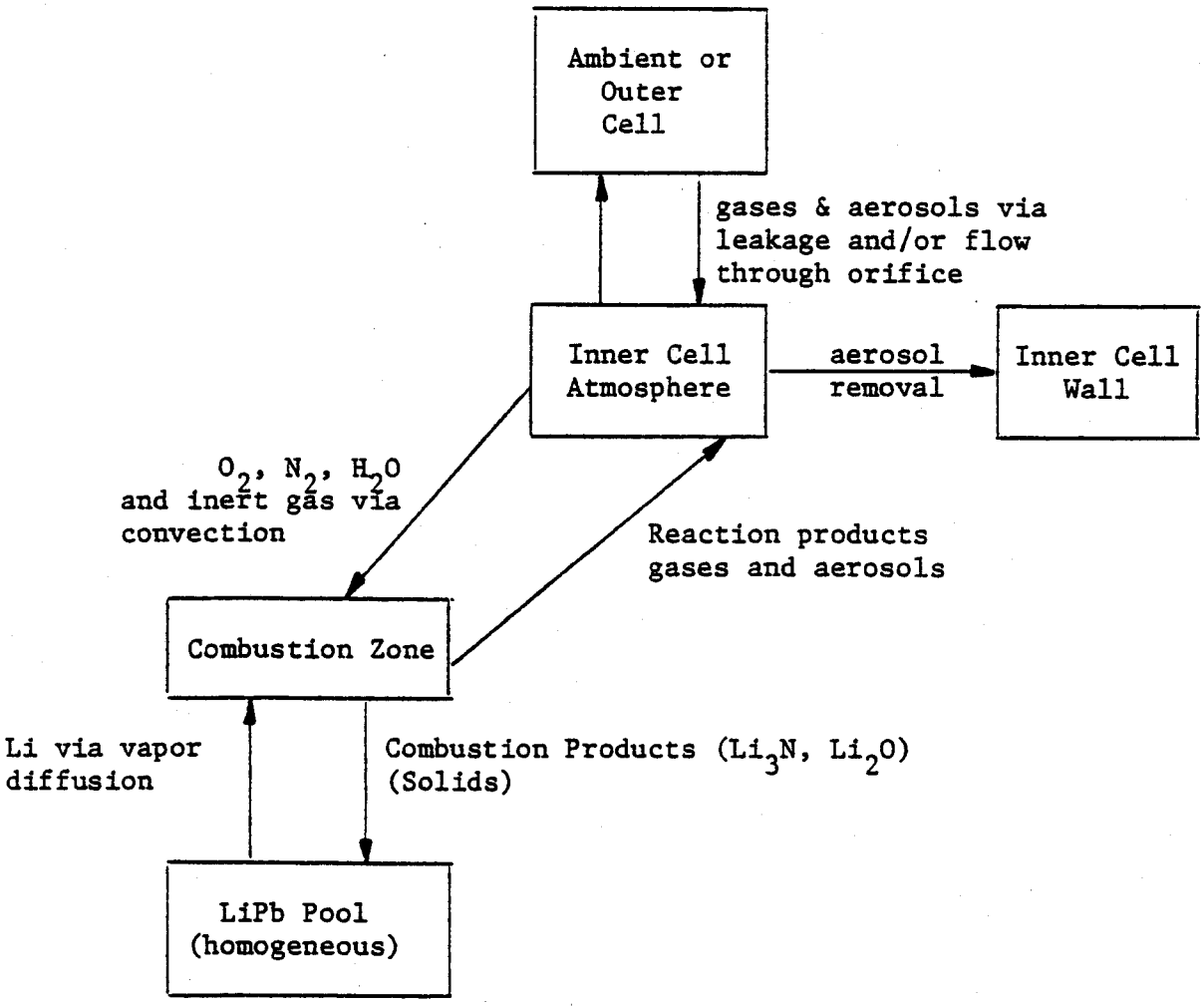

Figure 4.6: Mass Flow in Turbulent Pool Model

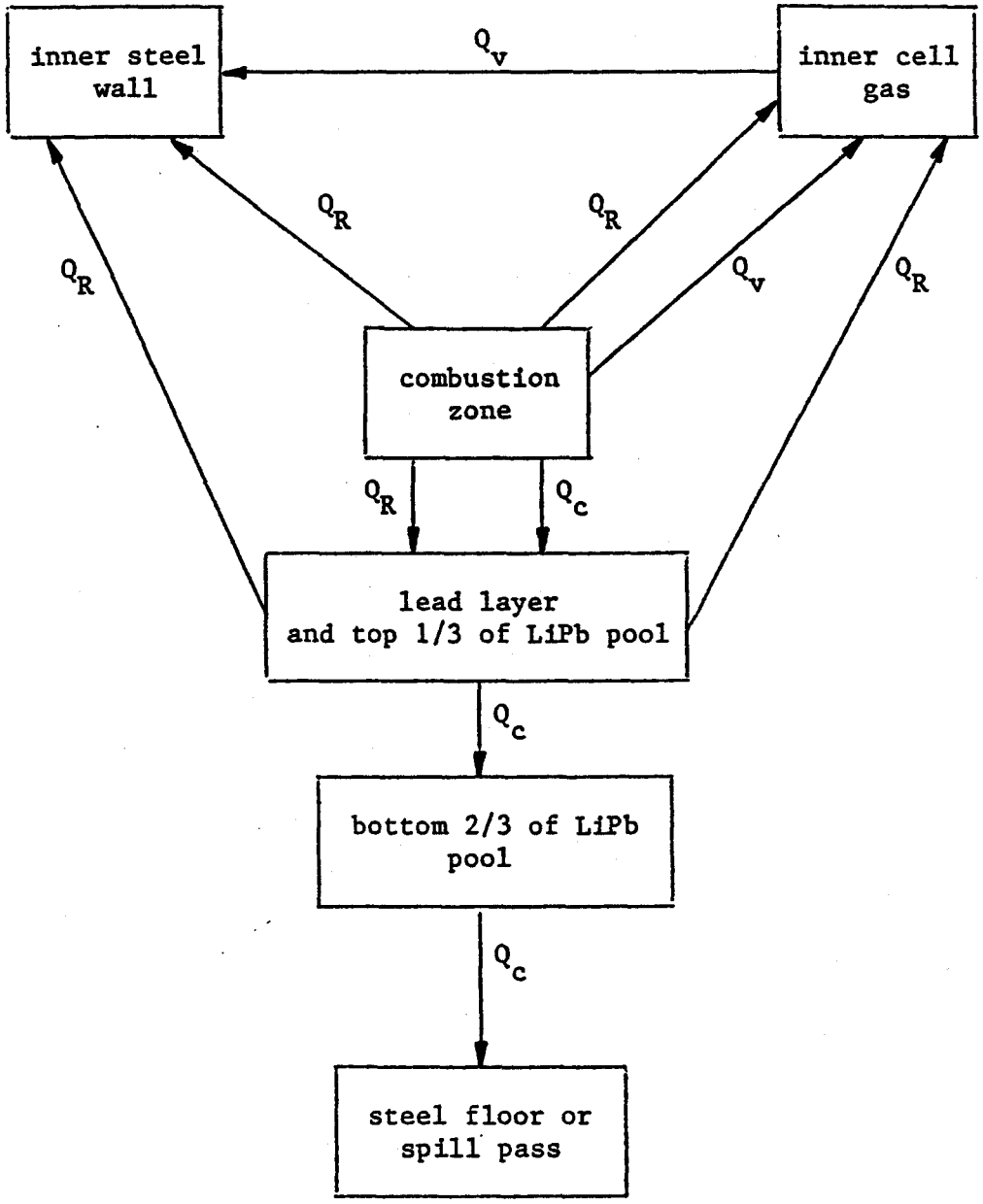

Figure 4.7: Heat Transfer in Layered Pool Model

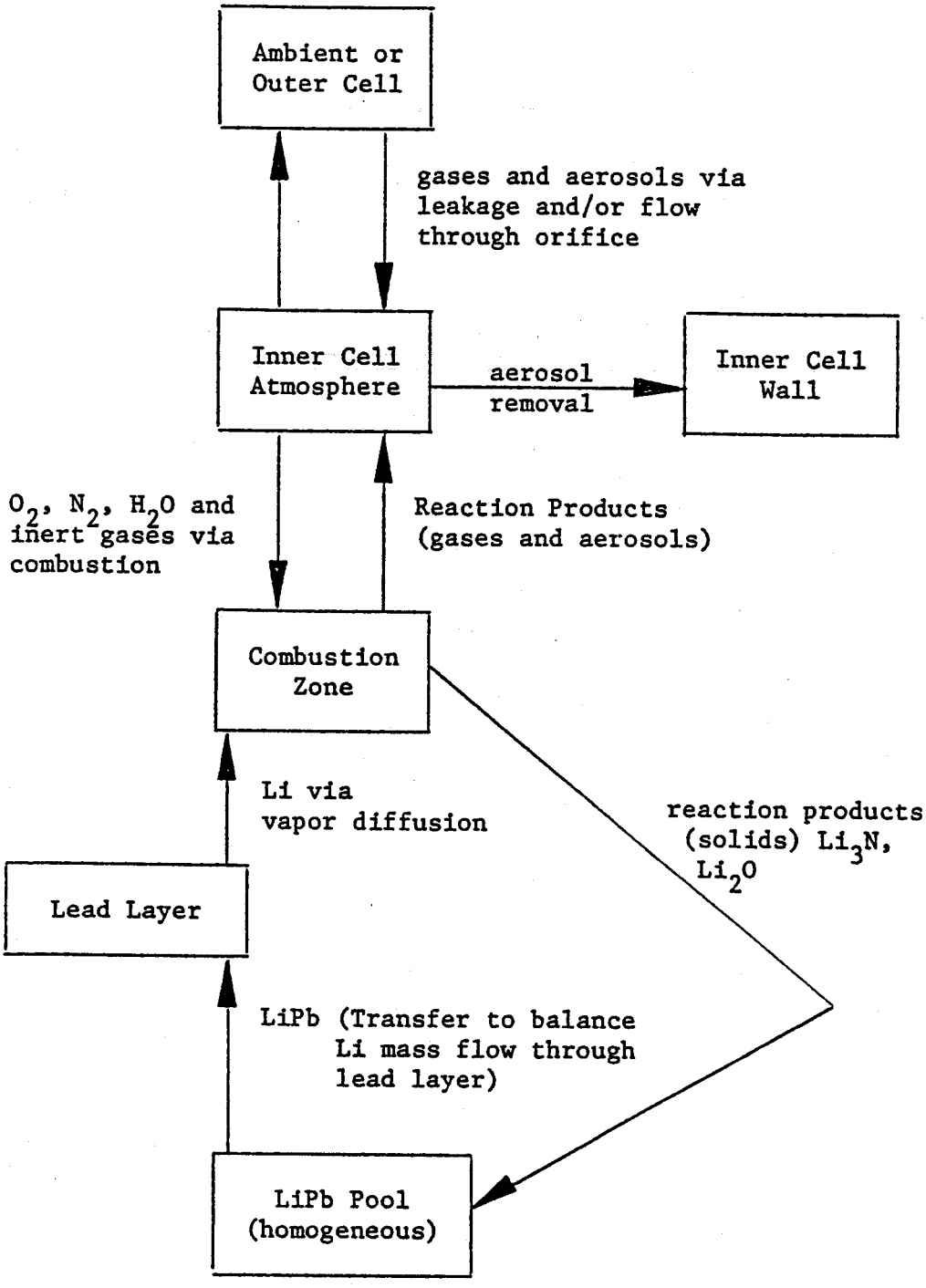

Figure 4.8: Mass Flow in Layered Pool Modeling

the combustion zone and pool modeling remains the same as that of pure lithium pools except for the following changes.

- **Lithium pool properties.** The conductivity, density, and specific heat of the pool are calculated using the correlations presented in section 4.2.1. Since lithium is being depleted by the lithium fire, the concentration of lithium in the pool is decreasing in time. Combustion stops when all the lithium in the pool is depleted or when the pool drops to the pool's melting temperature (which is also a function of concentration).

- **Heat addition to the pool.** The effect of the dissociation reaction is to absorb some of the heat transferred to the pool. The assumption that the dissociation takes place before vaporization and transport to the combustion zone implies that this effect is limited to the pool and does not affect the combustion zone heat balance.

- **Lithium-nitrogen film thickness.** The thickness of the film region between the combustion zone and pool is determined from the diffusion rate of lithium through the region according to the relation

$$d = -D_{Li}\left(\frac{\rho_{cz} - \rho_{Li}}{\left(\frac{dM}{dt}\right)_{Li}}\right) \qquad (4.6)$$

  where D_{Li} is the diffusion coefficient for lithium in air; $(\frac{dM}{dt})_{Li}$ is the mass flow rate of lithium (assumed equal to the combustion rate of lithium); ρ_{cz} is the lithium density in the combustion zone (assumed to be zero); and ρ_{Li} is the density of lithium at the pool surface. This last parameter is affected by the presence of lead in the pool, which reduces the lithium atom density and as a result will reduce the thickness of the film. The net effect is an increase in heat conduction from the combustion zone to the pool due to the smaller thermal resistance of a thinner pool.

The heat of solution (mixing) and "kinetic" energy of the pool are ignored since the latter would reduce the temperature rise by an amount equal to (kinetic energy/$M_{LiPb}C_{pLiPb}$) and the former is an order of magnitude smaller than the heat of dissociation [15].

4.3.2. Layered Pool Model

The basic assumption of this model is that the LiPb pool is covered by a separate layer of pure lead that inhibits the transport of lithium to the combustion zone. Evidence of layered species within pool mixtures during and after combustion was indicated by [16] when investigating petrochemical fires. Since the density of lead is greater than that of LiPb, the top layer in this

model is unstable and would tend to fall into the pool. However, since lithium is continually being depleted at the pool surface it is expected that there should be some finite layer that is lithium poor with respect to the rest of the pool. The stability of this layer would be a function of the turbulence of the fire as well as the lithium depletion rate. Lithium dissociation from lead would also be higher in this region since it is at a higher temperature than the rest of the pool although this effect should be secondary because of the high thermal conductivity of the pool.

The simplest (and least conservative) model incorporating the important effects is to allow lithium diffusion through a pure lead layer since this top layer is no longer a mixture and its properties are not functions of the lithium concentration. This model incorporates the same property changes for the LiPb layer as that of the turbulent pool model above with one major difference. In this model the LiPb layer is assumed constant in concentration. Since lithium is being depleted by combustion, the excess lead is added to the pure lead layer which grows in thickness as the fire progresses. Eventually, the lead layer may retard the mass flow rate of lithium through the pool enough to be the limiting factor in the combustion rate. Therefore, the following two items represent the major difference to the LiPb turbulent pool model.

- **Lithium diffusion rate through lead layer.** The thickness of the lead layer is determined by the amount of excess lead in the pool due to removal of lithium by combustion. The mass of excess lead grows with time according to

$$M_{Pb} = \int_{t=0}^{t} \frac{(1-\chi)}{\chi} \times ASLI \times CMBR \, dt' \tag{4.7}$$

where $ASLI$ is the surface area of the pool, $CMBR$ is the lithium combustion rate in kg/sec, and χ is the weight fraction of lithium in the alloy. The thickness of the lead layer can then be calculated using

$$d_{Pb} = \frac{M_{Pb}}{\rho_{Pb} \times ASLI} \tag{4.8}$$

where the density of lead (ρ_{Pb}) is a known function of temperature.

The lithium that dissociates from the lead in the LiPb pool node is heated by conduction as it passes through the lead layer. The free lithium is assumed to travel through the lead layer according to a Fick's law diffusion of the form

$$\left(\frac{dM}{dt}\right)_{Li} = -D_{Li}\left(\frac{\rho_0 - \rho_{LiPb}}{d_{Pb}}\right) \tag{4.9}$$

where d is the thickness of the lead layer, ρ_0 is the lithium density at the pool surface (assumed to be zero for this calculation only), ρ_{LiPb} is the lithium atom density in the LiPb layer and D is the diffusion coefficient of lithium in lead. The assumption of zero lithium density at the pool surface is reasonable since this value will yield the highest diffusion rate of lithium for a given alloy. The diffusion coefficient, D is evaluated according to the estimate presented by Castleman and Conti [17] for liquid metal diffusion through liquid metals:

$$D = \frac{0.655 T^{\frac{1}{2}} \sigma_{ij}}{M^{\frac{1}{2}} (\frac{\epsilon_{ij}}{k} \times 10^{-3}) \Sigma} \qquad (4.10)$$

where M is the molecular weight of the solvent, T is the absolute diffusion temperature, Σ is a dimensionless force constant, σ_{ij} is the intermolecular separation where the Lennard-Jones potential is zero between unlike molecules, k is the boltzman constant and ϵ_{ij} is the well depth for the Lennard-Jones potential. Hovingh [18] gives an evaluation of these parameters for lead diffusion in lithium. Since all the factors in Eq. (4.10) are symmetric with respect to solute and solvent (except for the molecular weight) Hovingh's analysis can readily be transferred to lithium diffusion through lead. The resulting expression for the diffusion coefficient,

$$D = 6.0 \times 10^{9} \exp(\frac{-680}{T}) \quad \frac{meter^2}{sec} \qquad (4.11)$$

for T in kelvin, is accurate to within 10% of the Eq. (4.10) value for temperatures between 500 and 1800 kelvin.

- Limitations on combustion rate. The thickness of the lead layer increases with the amount of lithium consumed, thereby decreasing the mass flow of the lithium through the pool to the combustion zone. Eventually the the mass diffusion rate may be sufficiently low enough to limit the combustion rate of lithium. LITFIRE models the combustion zone using a quasi-steady state analysis, especially for the mass balance. The mass of the combustion zone is based on the instantaneous combustion rate and does not include any mass buildup of unreacted gases or lithium vapor. This assumption may not be accurate when the combustion is lithium diffusion limited, but no change to the mass balance has been made at this time because of lack of experimental data on which to base a new model.

4.4. Major Changes to Litfire Encompassing Lithium-Lead Combustion in Air

The inclusion of lithium-lead combustion in LITFIRE was simplified by using the existing structure as much as possible. Two subroutines were added to the code that modified the pool

properties and heat transfer parameters in such a way as to make the pool "appear" to be a LiPb alloy. Many variable names were not changed, however, so that the same name may represent a single parameter for either pure lithium or lithium-lead depending on what stage of the calculation is being used.

The addition of one pool node required the addition of two more integrals into the main program. When all options are in effect, the number of integrals now approaches the stated limit (100 simultaneous integrations) of the integrator subroutines, however no decrease in accuracy because of this condition has yet been observed. The new integrals follow the mass and temperature of the top pool node which is a mass weighted average of all the excess lead and one third of the lithium-lead that remains in the pool. This average was necessary in order to increase the thickness of the top node of the pool so that computation time would stay within reasonable limits. Consistent with assumption, the thickness of the pure lead layer never exceeded a small fraction (less than 1/100th) of the total pool thickness. Yet this thickness was sufficient to retard the lithium mass flow rate enough to limit combustion. Therefore, the mass flow calculation is based on the "true" lead layer thickness while the heat transfer calculation is based on the lumped lead and lithium-lead thickness.

The surface pressure of lithium is assumed to be a function of the activity of the lithium-lead alloy according to

$$P_{Li} = a_{Li} P_o \tag{4.12}$$

where a_{Li} is the activity of lithium in the alloy (see section 4.2) and P_o is the vapor pressure of pure lithium which is a known function of temperature. The net effect of the reduced partial pressure is in a reduction of the film thickness between the combustion zone and pool but this effect tends to be very small due to the nitrogen pressure domination in this region.

4.5. LITFIRE Results

The comparison made in this section is again for the UWMAK-III reactor described earlier. However, the amount of alloy spilled was altered in each case so that the total volume of alloy spilled was the same. This was felt to be a more realistic comparison because of the lower lithium atom density in the lithium-lead alloys requiring a larger mass of breeder than pure lithium. However, lead acts as a neutron multiplier, enhancing the breeding ratio of the fewer lithium atoms, so that roughly equal volumes of the alternate breeders will most likely be required. It should be emphasized that the following analysis is not an indication of the consequences from a specific accident scenario but should be taken as an indication of the relative consequences of

pool fires for different alloys. Table 4.1 summarizes the important parameters governing the spills studied in this section.

4.5.1. Comparison of Turbulent Pool and Layered Pool Models

A comparison of the results from the layered pool model and the well mixed pool model are shown in Figures 4.9 and 4.10 where the cell gas and pool temperatures are plotted. In the case of the layered pool the top pool node is indicated by the dashed line. A more interesting comparison appears in Figure 4.11 where the effect of the lead layer on the combustion rate is shown. In both cases the alloy of interest was LiPb. The combustion rate is limited rather early in the fire due to the buildup of the lead layer on the surface. At the point were the combustion was lithium limited, the thickness of the lead layer was 0.15 mm., approximately one thousandth of the thickness of the entire pool. This indicates that LITFIRE's predictions will be very sensitive to the calculated diffusion rate and the lead layer thickness. As was expected, the diffusion model is less conservative than the turbulent pool model, but no evaluation of either model can be made at this time. Figure 4.12 shows the effect of a lithium-lead spill in the HEDL test facility used for LA-5. The models indicate that tests of this size will be much less severe than for the tests using pure lithium.

4.5.2. Comparison of LiPb Combustion to Pure Lithium Combustion

The comparison among the alternate coolants and breeders is shown in Figures 4.13 and 4.14 using the turbulent pool and layered pool models respectively. The temperature profiles are for the pool node since this is where the greatest variation occurred (except for the combustion zone). Comparison of the maximum temperatures predicted indicates that the turbulent pool model closely matches the predictions for a pure lithium fire. The layered pool model predictions show a substantial reduction in the peak temperatures but give higher temperatures after combustion has ceased. The major reason for this is due to the nodal structure of the layered pool model. The top node is made up of the lead layer in addition to one third of the LiPb pool layer, so that it's conductivity is substantially reduced over that of pure lithium or LiPb. Since conduction from the pool is the principal heat transfer mechanism after combustion has stopped, the net effect is to reduce the rate of heat loss from the top pool node. This in turn reduces the heat loss of the lower pool node so that the average pool temperatures are higher than those predicted by the turbulent pool model. A trend that was consistent among the two models was that the lower the lithium atom concentration in the alloy, the lower the consequences of fires using that alloy. The variation in maximum cell gas temperature was ~400°C among the various alloys and models used in the calculation. The cell gas temperature time history is plotted in Figure 4.15.

TABLE 4.1

Summary of Lithium-Lead Calculations

Alloy	Atom % Li	Volume Spilled (m^3)	Mass Spilled (kg)	Initial Temp. (°C)	Maximum Temp. (°C)
Li	1.00	475	22,000	980	1103 *
Li_7Pb_2	0.78	475	202,900	980	1103
LiPb	0.50	475	346,630	980	1105
$LiPb_4$	0.20	475	459,900	980	1125
LiPb	0.50	7.6	1,575	360	890
LiPb	0.50	0.49	100	360	710

* Maximum temperatures are from LiPb turbulent pool model.

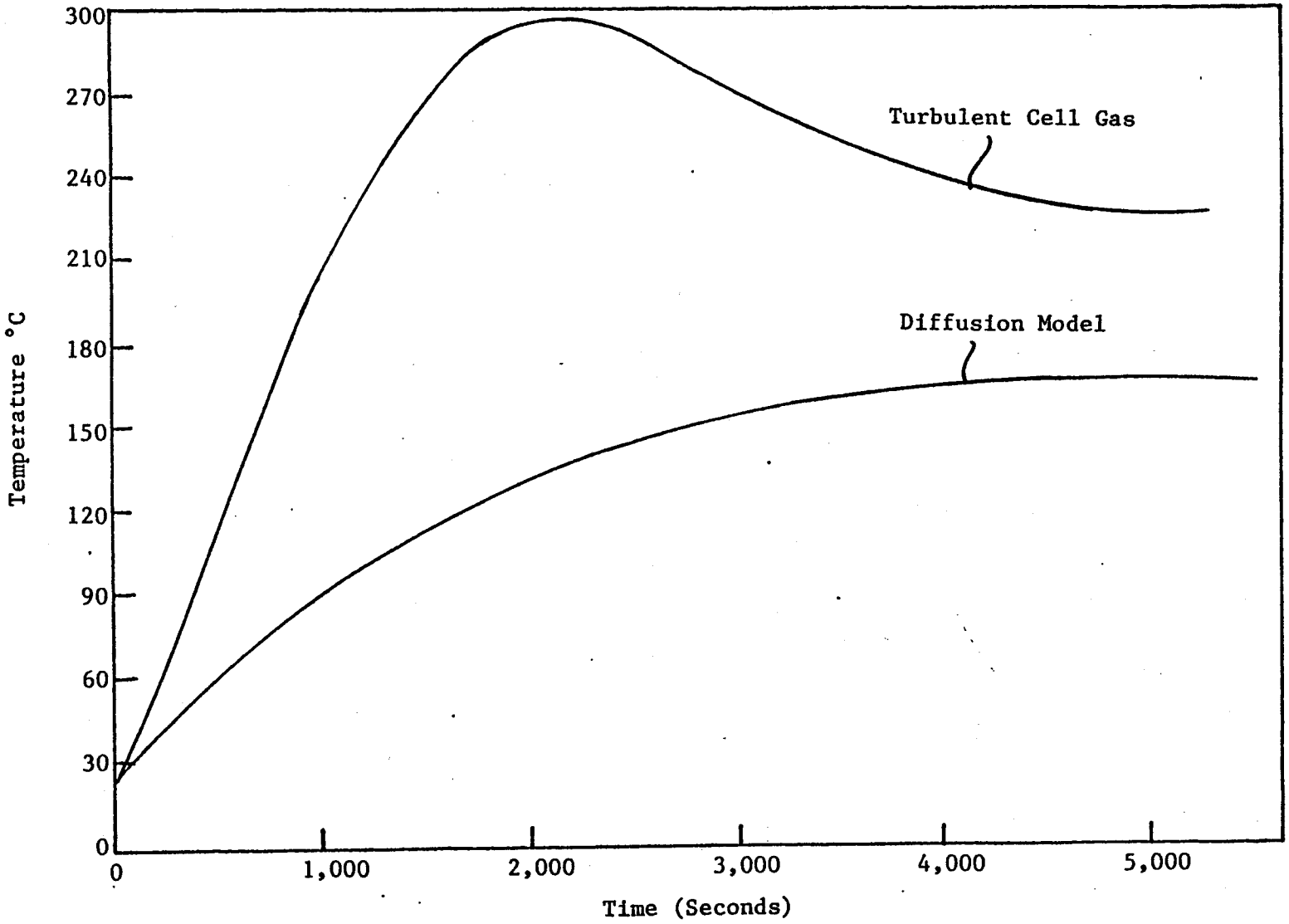

Figure 4.9: Cell Gas Temperatures for LiPb Alloy Using Layered and Turbulent Pool Models

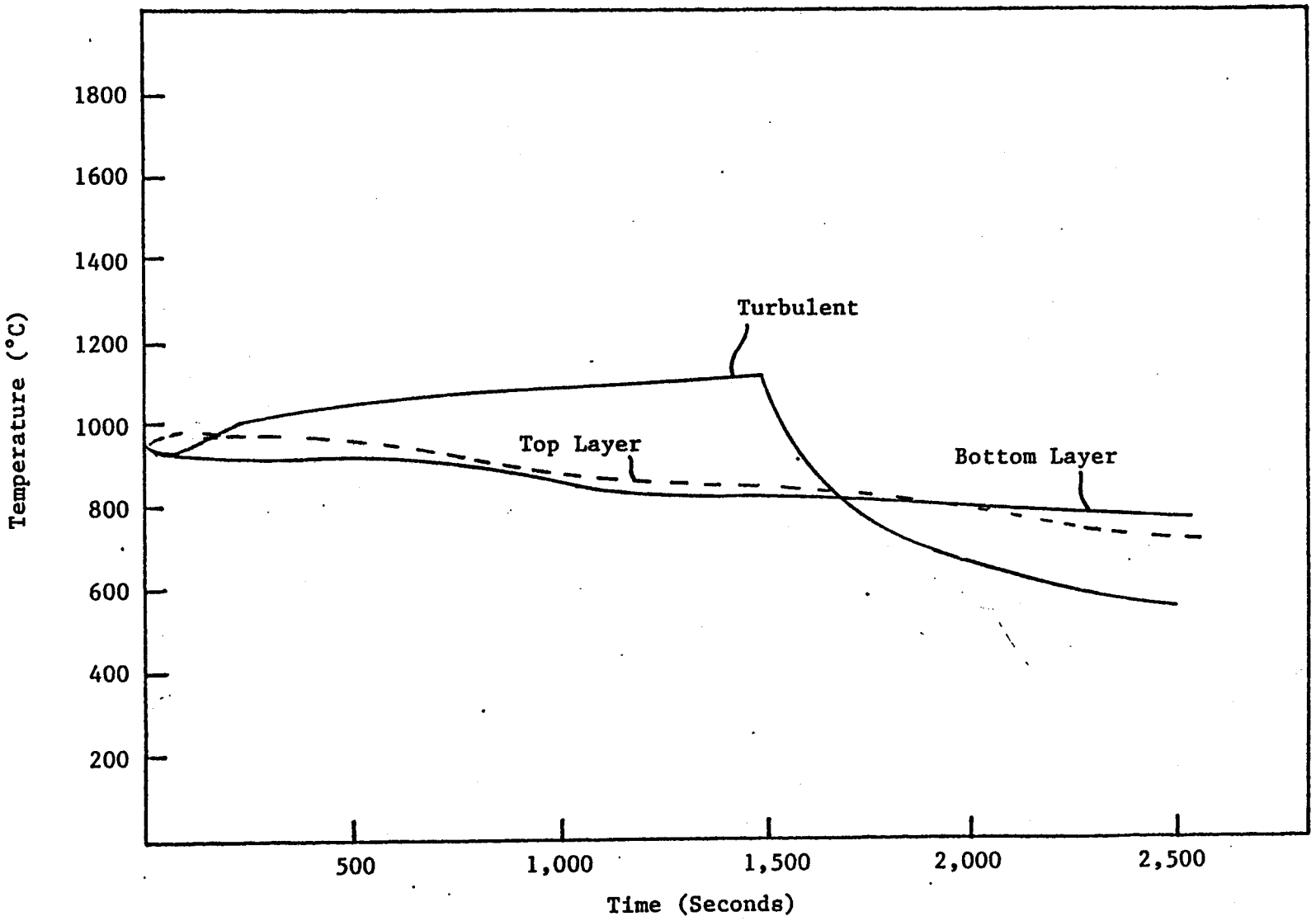

Figure 4.10: Pool Temperatures for LiPb using Layered and Turbulent Pool Models

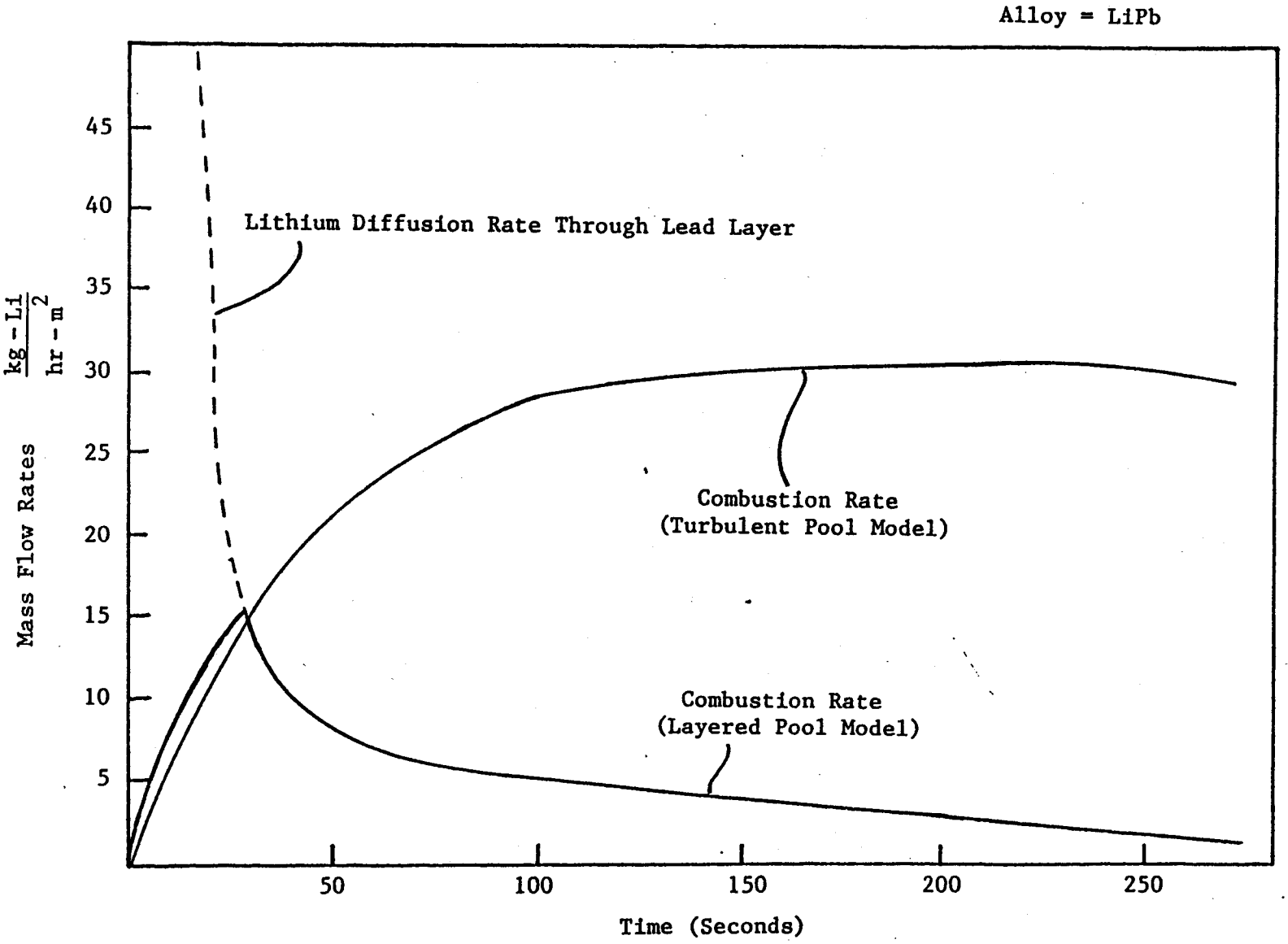

Figure 4.11: Effect of Lithium Diffusion Through Lithium-Lead on Combustion Rate

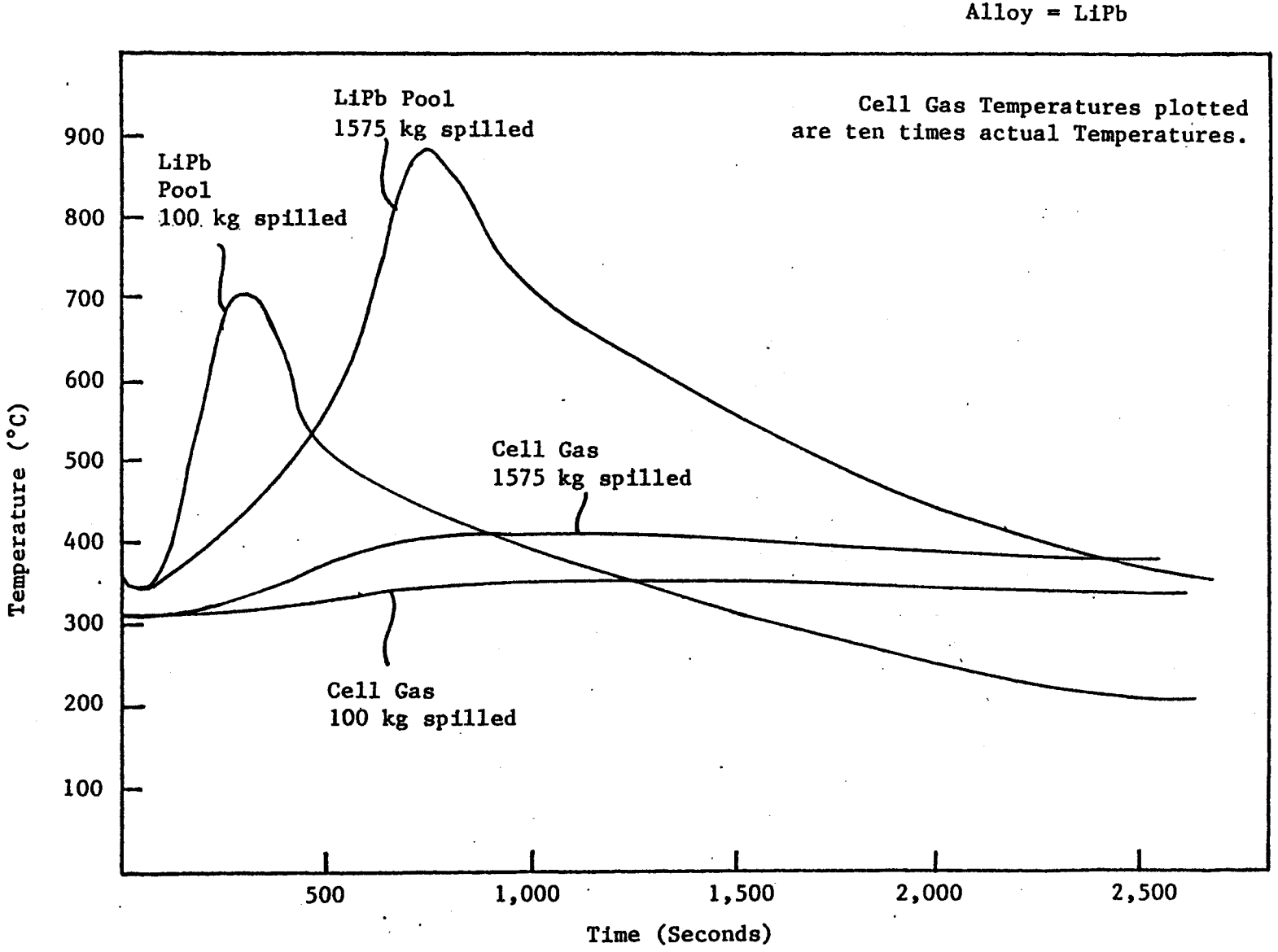

Figure 4.12: Predictions for Lithium-Lead Spill in HEDL Test Facility

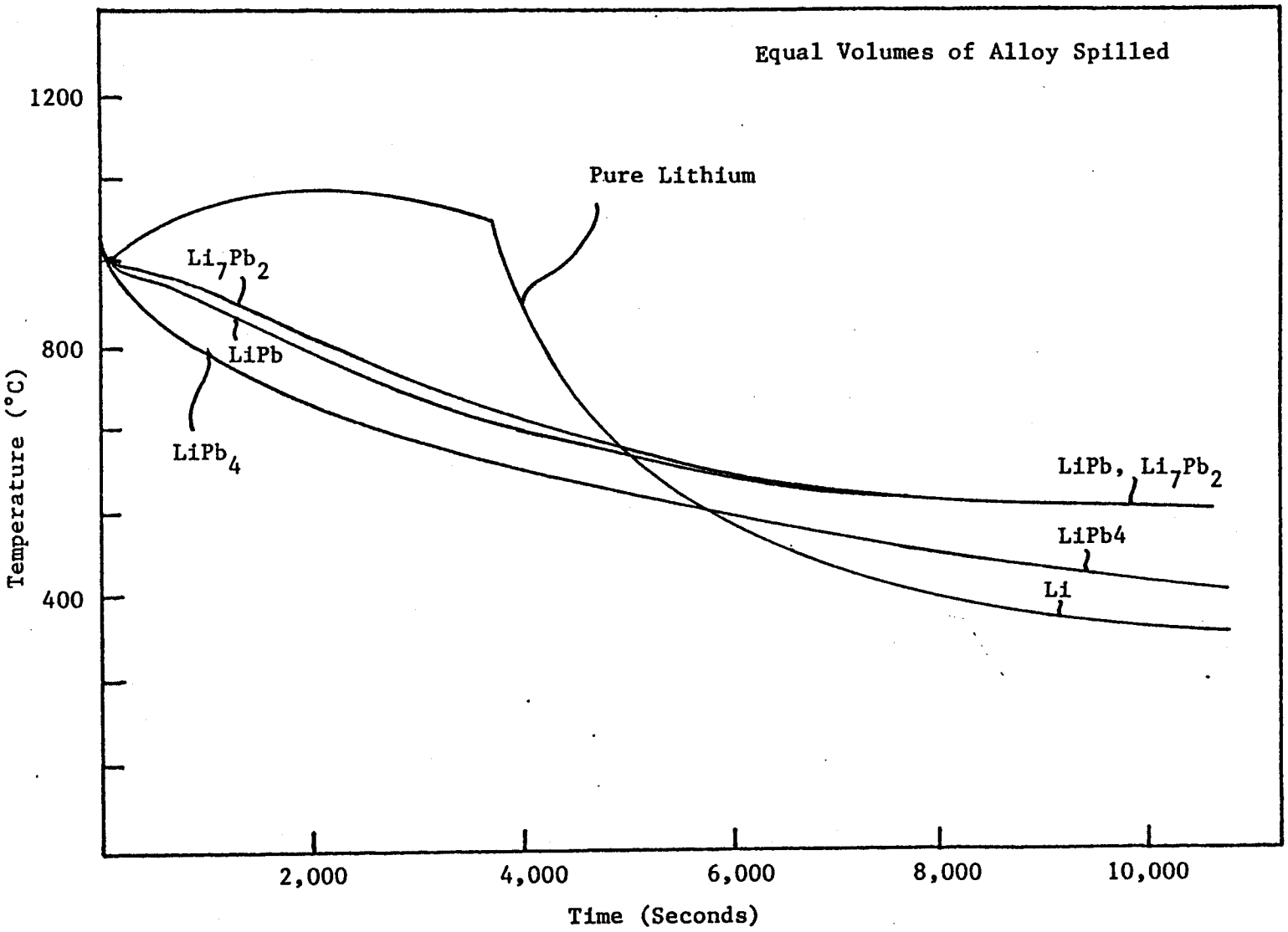

Figure 4.13: UWMAK-III Average Pool Temperature History for Various LiPb Alloys Using Layered Pool Model

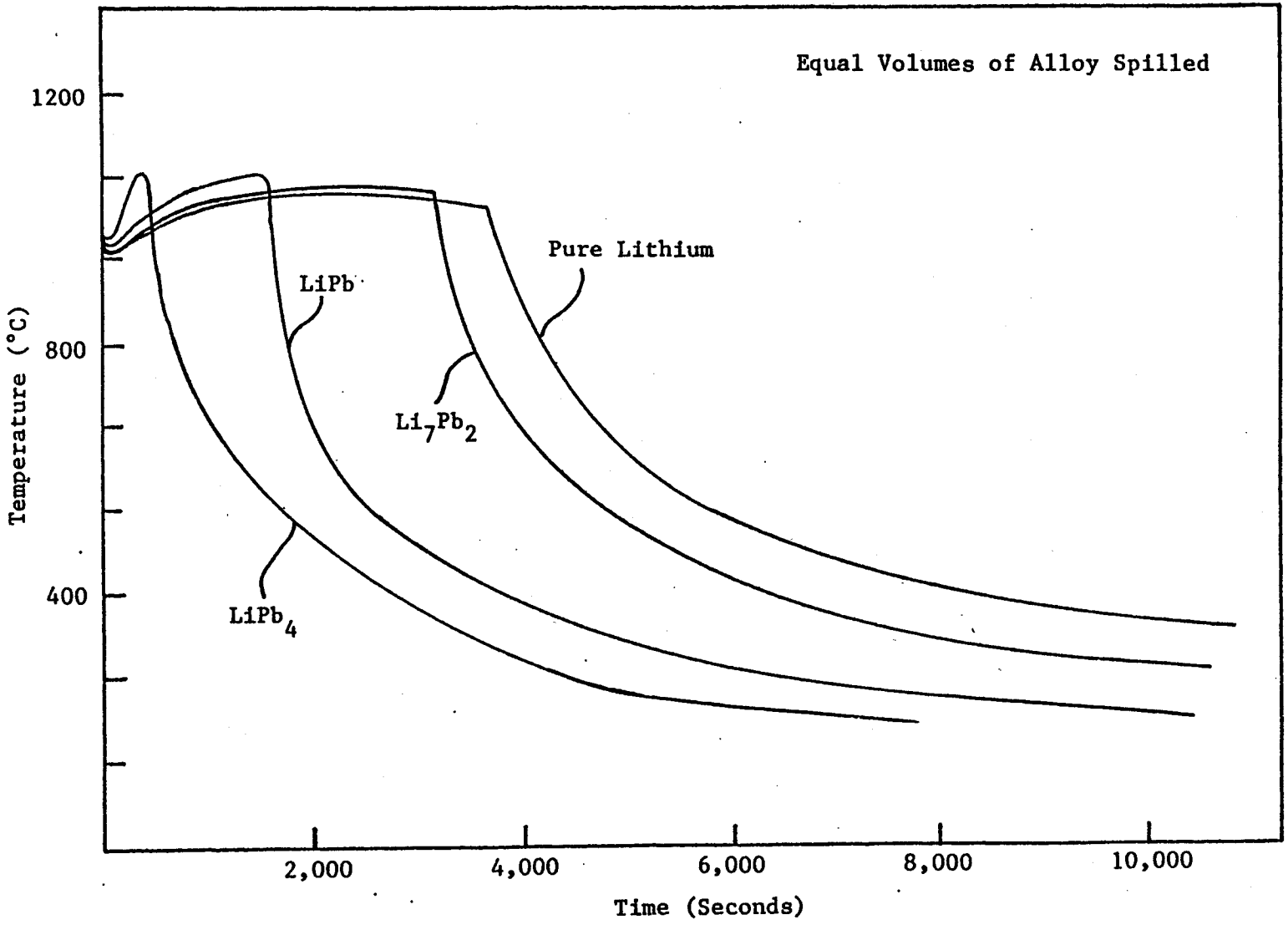

Figure 4.14: UWMAK-III Average Pool Temperature History for Various LiPb Alloys Using Turbulent Pool Model

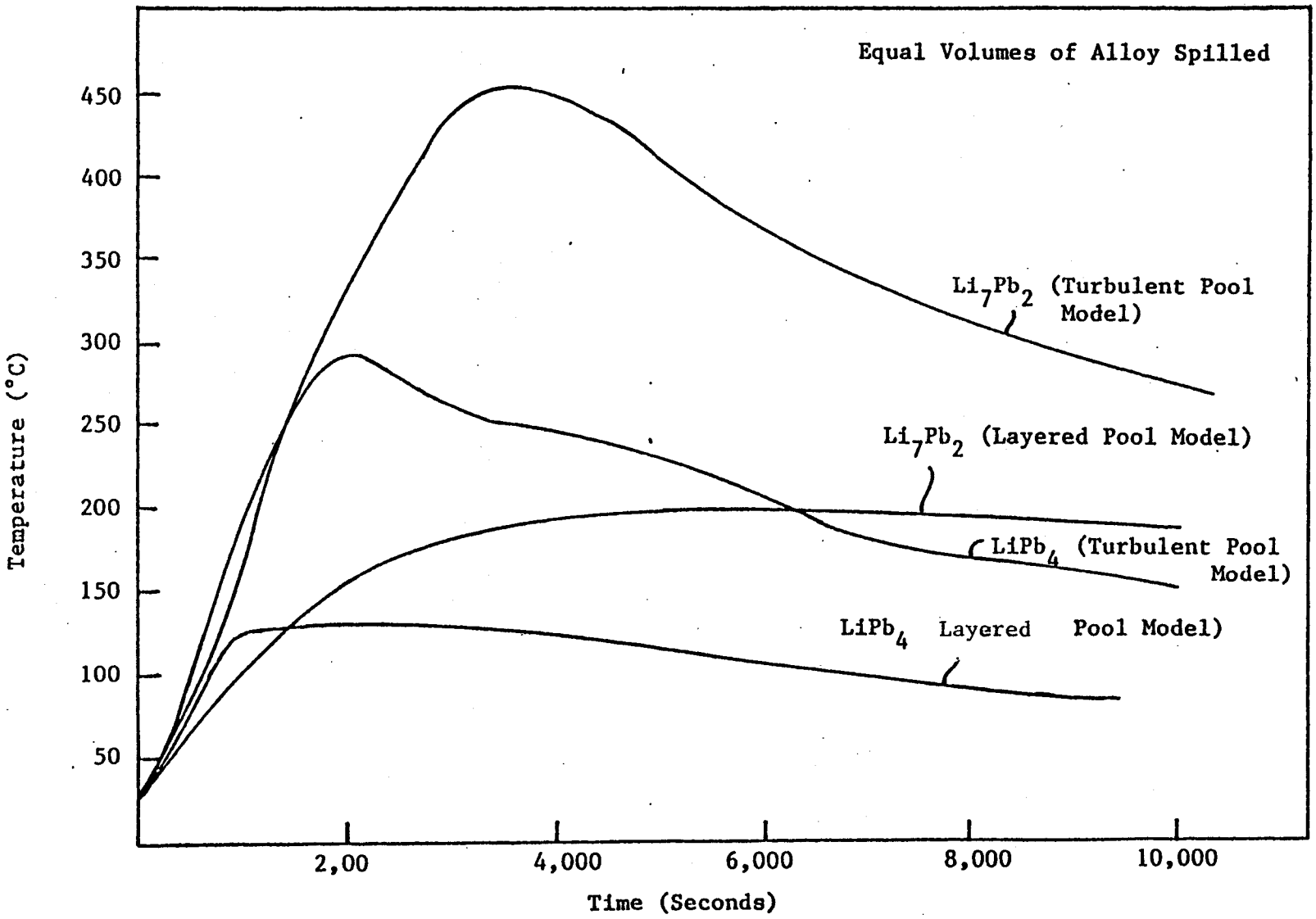

Figure 4.15: UWMAK-III Cell Gas Temperature Profiles for Various Alloys

5. SUMMARY AND CONCLUSIONS

5.1. Code Development and Verification

The underlying purpose of this work was to continue the development of the LITFIRE computer code in order to more accurately asses the consequences of lithium spills and fires in fusion related systems. In order to evaluate the accuracy of the code, many comparisons with experiments have been performed. The most recent comparisons have been discussed in Chapter 2 and indicate that there is fairly close agreement for these particular test cases. However, this agreement was achieved at the expense of some discrepancy with earlier calculations, especially with respect to the combustion zone emissivity values. The present comparison indicates that high emissivities should be used (~.9 or greater) while the work of Tillack indicated that very low emissivities (0.1 or less) would generate the closest agreement with experiment.

Results of the comparison for multiple species combustion indicate that LITFIRE tends to overpredict the combustion rate by more than a factor of three (on average) for both oxygen and nitrogen combustion. While this may be too conservative an estimate, no firm conclusions can be drawn from the present analysis because of the large inaccuracy in determining the actual experimental combustion rates. However, the temperatures and pressure predicted by LITFIRE for the HEDL test case LA-5 are in close agreement with the experimental results. This agreement would tend to validate the overall combustion rate prediction since the cell gas pressure and temperature are primarily dependent on the gas consumption rate and energy generation rate. The comparison of combustion zone and pool temperature coupling is presently limited in accuracy, since the relevant temperature profiles were not measured directly during the latest experiments.

The temperature and pressure profiles in the single containment scheme were found to be very sensitive to the combustion zone emissivity value chosen, less sensitive to the transmissivity of radiation through the combustion zone, and fairly insensitive to the removal of aerosols from the cell gas.

5.2. LITFIRE Applications

The applications of LITFIRE in the present work include use of both the single compartment and multi-compartment geometries. The single cell calculation was for a lithium spill in the containment building of UWMAK-III and updates predictions made by Tillack [10] and Dube [1] using earlier versions of the code. The most recent predictions indicate that the combustion zone and pool node's peak temperatures are lower by more than 100°C but the remaining nodes have temperature profiles quite similar in slope and magnitude to the earlier predictions.

The incorporation of an outer cell in the LITFIRE geometry, described in detail in Chapter 3, allowed much greater flexibility in modeling fusion related systems. The structural components associated with the vacuum torus within a reactor containment were modeled and the effect of cell gas communication on lithium fires was studied. The calculation presented is not indicative of any particular accident scenario but was chosen to compare the effects of a lithium fire within the torus to lithium fires within the larger reactor containment building. The results of this comparison indicate that the reduced amount of gas available inside the torus can significantly reduce the consequences of a large lithium spill. The effect is less pronounced when the lithium spill is smaller or when the orifice between the inner and outer cells is large enough to allow significant transport of gas to the reaction cell. In addition, the ignition time (time when fire begins after lithium is spilled) for a lithium fire in an initially evacuated cell (such as a torus) can be twenty minutes or longer, and is linearly dependent on the size of the orifice through which pressurization occurs.

5.3. Lithium-Lead Combustion

Experimental data on lithium-lead combustion is practically non-existent so two models were developed to sufficiently bound the problem from conservative and non-conservative viewpoints.

The inclusion of lithium-lead combustion in air greatly enhances the utility of LITFIRE in comparing safety aspects of alternate coolants and breeders in fusion reactors. In both of the models presented and discussed in Chapter 4 the geometry of LITFIRE is unchanged but the pool node properties and kinetics are significantly altered to include the effect of lead. The assessment of alternate coolants and breeders is by no means conclusive but should be taken as a preliminary indication as to which alloy may be less hazardous relative to the others considered.

Results of the comparison indicate that in both the conservative and non-conservative models the higher the concentration of lead in the alloy the lower the resulting temperatures will be. This effect is more pronounced in the layered pool model, due to the more rapid buildup of the lead layer with increasing lead concentration.

5.4. Recommendations for Further Development

LITFIRE now has the basic framework to perform many analyses of interest in lithium fire modeling. Among these are pure lithium reactions with air, water vapor, and concrete; lithium-lead reactions with air and water; in various containment schemes. However, all but the lithium-air reactions have not been compared with experimental data. It is expected in the near future that small scale experimental data will be available for all the remaining reactions modeled by LITFIRE.

Data is greatly needed to clarify the following parameters:

- **Combustion rate.** LITFIRE overpredicts the reaction rate for multiple species combustion. This may due to incorrect modeling any combination of the following: mass diffusion rate of gases to the combustion zone by convection; the transport rate of lithium to the combustion zone by vapor diffusion; effect of product accumulation on either of the above; and the nitrogen hindrance factors for a given temperature and O_2 concentration. Accurate measurement of the gas consumption rates, temperatures, and O_2 concentration near the flames of the lithium fire would indicate which of the above effects are causing the discrepancy.

- **Pool and combustion zone coupling.** Values for the emissivity and transmissivity of the combustion zone have been inferred from various experiments. Recommended values for the emissivity vary widely depending on the size of the spill modeled, which may indicate that the emissivity is a strong function of combustion rate. Direct measurement of the radiative properties of flames in lithium fires is required to pinpoint the correct emissivity. In addition, the conductivity of the film region between the combustion zone and the pool may have a significant effect on the coupling of the two nodes but no measurements have yet been made to check the composition of this region. The effect of film conductivity would be greatly enhanced in LITFIRE if the pool region was divided into more than one node. The validity of using a single node for the pool is based on the high conductivity of lithium, but this assumption may incorrect when lithium-lead is used due to the lower conductivity of lead.

- **Lithium-lead combustion.** Accurate measurement of the combustion rate of the lithium in lithium-lead alloys is needed before any evaluation of the two models presented in chapter 4 can be made. If possible, experiments should be designed to observe the pool kinetics as much as possible since this is the region that will be most effected by the presence of lead. If the experimental data that becomes available indicates that the present modeling in LITFIRE correctly bounds the reaction rate, then the next improvement in modeling might incorporate a diffusion model based on some degree of turbulence. This can be done using a lead layer whose thickness depends on the degree of turbulence and the magnitude of the combustion rate. In addition, direct measurement of the diffusion rate of lithium in lead would significantly improve the accuracy of the layered pool model.

The program itself has been extensively modified, modularized, and tested and now includes many options suggested by earlier developers. The following two suggestions are for improvements that would greatly increase the utility of LITFIRE use by the general fusion community, but at the expense of a fair amount of developmental effort. First, the addition of several nodes surrounding the inner steel wall and floor, with each node having unique physical properties. This would increase the flexibility of modeling a real tokamak, coolant piping system, or blanket module for example.

This change would be especially important for modeling the first wall and surrounding blanket and structural material. Second, to make LITFIRE compatible with other fusion related codes so that a comprehensive fusion safety code could be designed. This last suggestion is necessarily vague at this time but should be kept in mind whenever new developmental work is done on LITFIRE. A final suggestion is related to quality assurance but should not be underestimated in future efforts: each and every correlation in LITFIRE should be checked for coding accuracy and the source of the correlation well documented. The documentation is important since property data for lithium and other materials is continuously being updated and would indicate how contemporary the existing coding is.

REFERENCES

1. D. A. Dube and M. S. Kazimi, "Analysis of Design Strategies for Mitigating the Consequences of Lithium Fire Within Containment of Controlled Thermonuclear Reactors," MITNE-219, July 1978.

2. P. J. Krane, "Safety Aspects of Thermonuclear Reactor Designs Employing Use of Lithium-Lead Alloys," Master's Thesis, MIT, June 1980.

3. S. J. Piet, M. S. Kazimi, and L. M. Lidsky, "Potential Consequences of Tokamak Fusion Reactor Accidents: The Materials Impact," MIT, Plasma Fusion Center, Report No. PFC-44-19, May 1982.

4. The University of Wisconsin Fusion Feasibility Study Group, "UWMAK-III, A Non-Circular Tokamak Power Reactor Design," UWFDM-68, March 1974.

5. W.A. Frigerio and L.L. Lavoy, "The Preparation and Properties of LiPb: A Novel Material for Shields and Collimators," Nuclear Technology, (10), March 1971.

6. HEDL Progress Report, personal communication to M. S. Kazimi (MIT) from D. W. Jeppson (HEDL), June 1982.

7. D.K. Sze, R. Clemmer, E. T. Cheng, "LiPb: A Novel Material for Fusion Applications," UWFDM-378, October 1980.

8. P. Gierszewski, et. al., "Property Correlations for Lithium, Sodium, Helium, Flibe, and Water in Fusion Reactor Applications," MIT PFC-RR-80-12, August 1980.

9. I. Charak and L. W. Person, "SPOOL-FIRE: Analyxis of Spray and Pool Sodium Fire," Argonne National Laboratory, October 1976 (presented at the ANS International Meeting on Fast Reactor Safety and Related Physics, Chicago, IL).

10. M.S. Tillack and M. S. Kazimi, "Development and Verification of the LITFIRE Code for Predicting the Effects of Lithium Spills in Fusion Reactor Containments," MIT PFC-RR-80-11, July 1980.

11. V. Gilberti, "LITFIRE User's Guide," in progress at MIT Department of Nuclear Engineering.

12. L. D. Muhlestein, D. W. Jeppson, J. R. Barreca, "Summary of HEDL Fusion Reactor Safety Support Studies," HEDL-SA-2360, Richland, WA 1981.

13. John. H. Perry, et. al., Chemical Engineers Handbook, McGraw Hill Book Co., Inc., 1963.

14. H. R. Ihle, et. al., "The Activity of Lithium, and the Solubility of Deuterium in Lithium-Lead Alloys," Fusion Technology, Proceedings of the Eleventh Symposium on Fusion Technology, Euratom, (EUR-7035-EN), 1980.

15. J. M. Smith and H. C. Van Ness, Introduction to Chemical Engineering Thermodynamics, 2nd Edition, McGraw-Hill, 1959.

16. C. C. Feng, S. H. Lam, and I. Glassman, "Flame Propogation Through Layered Fuel-Air Mixtures," Combustion Science and Technology, (10), No. 2, 1975.

17. A. W. Castleman, Jr. and J. J. Conti, "Consideration of the Mass Effect on Diffusion in the Liquid State," Physical Review A, Vol. 2 No. 5, 1975.

18 J. Hovingh, "An Estimate of the Diffusion Coefficient of Lead in Molten Lithium," Transactions of the American Nuclear Society, 30, 1978.

APPENDIX A

LITFIRE Data: HEDL Experiments LA-4 and LA-5

LA-4 HEDL TEST
USING VERSION OF LITFIRE: "LITFIR"
DATE: 17 AUGUST, 1982

OPTIONS IN EFFECT

IBLOW =	1	IESC =	0	ISFLC =	0	ISWICH =	0
IAROSL =	0	FLAGPN =	T	FLAG2 =	F	FLAGSI =	T
FLAGAS =	F	FLAGC =	F	FLAGW =	F	FLAGF =	F

PHYSICAL PROPERTIES

EMCONC =	0.9000	CPCON =	0.1560	KCON =	1.0000
RHCON =	144.0000	EMLI =	0.2000	CPLI =	0.9960
AKLI =	33.8000	RHLI =	30.0000	RHOLIO =	124.0000
RHOLIN =	86.9400	RHOLIH =	160.0000	EMGPF =	0.0400
EMCZ =	0.9000	TAUCZ =	0.1000		

INNER CONTAINMENT DIMENSIONS

VP =	30086.0000	CHP =	66.7000	CPAP =	0.1247
XMOLA =	39.9000	FRA =	0.0250	RA =	3.0000

EXTRANEOUS HEAT CAPACITY NODE DATA

TEHCZP =	643.0000	XMEHCP =	12300.0000	AEHCP =	5100.0000
CPEHCP =	0.1200	HINECP =	0.0900		

SPILL PARAMETERS

ASLI =	1.3300	SPILL =	59.0000	SPRAY =	0.0000
ZLI =	1.4787				

WALL AND FLOOR NODE DATA

NL =	6	NL1 =	6

THICKNESS OF CONCRETE WALL NODES

.200 .200 .200 .200 .200

THICKNESS OF CONCRETE FLOOR NODES

.200 .200 .200 .200 .200

PARAMETERS ASSOCIATED WITH OUTERMOST CONTAINMENT

THWC =	0.0000	THFC =	0.0000	GAP =	0.0000
KGAP =	0.0150	KLEAK =	0.0000		

PRIMARY STEEL WALL DATA

ESTLWP =	0.8500	CPSWP =	0.1200	KSTLWP =	30.0000
RHSWP =	497.5498	AWP =	5600.0000	THWP =	0.0580

PRIAMRY STEEL FLOOR DATA

ESTLFP =	0.8500	CPSFP =	0.1200	KSTLFP =	30.0000
RHSFP =	497.5498	AFP =	4000.0000	THFP =	0.0580

HEAT TRANSFER CORRELATION COEFFICIENTS

HIN =	0.1200	HINSAM =	0.0700	HINGSP =	0.1200
HINGSS =	0.1200	HINPS =	0.0700	HINFAM =	0.0700
HINFGS =	0.0700	HINFSG =	0.0700		

COMBUSTION PARAMETERS

QCO =	18510.0000	RCMBO =	0.8764	TVAP =	2456.0000
RCMBH2 =	6.9300	PERCEN =	0.0000	QCO1 =	18510.0000
QCO2 =	0.0000	RCMBO1 =	0.8764	RCMBO2 =	0.0000
QCN =	4080.0000	RCMBN =	1.4870	TMELT =	353.0000
QCW =	13784.0000	RCMBW =	0.3830	QVAP =	8431.0000

INITIAL CONDITIONS

PRIMARY

TGPZER =	548.0000	TSPZER =	543.0000	TCZI =	1560.0000
TLII =	1560.0000	TSFPI =	541.0000	TA =	535.0000
WO2P =	0.2316	WAP =	0.0094	WWAP =	0.0062
PAPZER =	16.8700				

INTEGRATION CONTROL PARAMETERS

IMETH =	3	DTMIN =	0.2000	TIMEF =	12000.0000
RELERR =	0.0060	DELOUT =	2000.0000		

MISCELLANEOUS INPUT ASSOCIATED WITH VARIOUS OPTIONS

INERT GAS FLOODING

WO2B =	0.0000	BLOWV =	24.0000	CPAP =	0.1247
WWAB =	0.0000	TBLOUT =	325.0000	CPAB =	0.1247
WN2B =	0.0000	TBLIN =	310.0000	EXHSTV =	0.0000
TBLOW =	535.0000	XMOLAB =	4.0000		

STEEL FLOOR COOLING

SFLTIN =	0.0000	SFLCR =	0.0000	SFLEND =	0.0000

EMERGENCY SPACE COOLING

ESCTIN =	0.0000	ESCR =	0.0000	ESCEND =	0.0000

DATA FOR SUSPENDED PAN OPTIONAL GEOMETRY:

TPANZO =	1560.0000	APAN =	9.7000	CPPAN =	0.1100
THKPAN =	0.0157	BREDTH =	4.1900		
KPAN =	13.0000	RHPAN =	488.0000		
THKIN1 =	0.2080	THKIN2 =	0.0416	AINS =	14.1500
RHINS =	8.0000	CPINS =	0.2550	EMINS =	0.9000
HINGPF =	0.0000				

SPRAY FIRE RESULTS

TGPZER = 548.0 PZEROP = 16.870

LA-5 HEDL TEST THESIS RUN
USING VERSION OF LITFIRE: "LITFIR"
DATE: 17 AUGUST, 1982

OPTIONS IN EFFECT

IBLOW =	0	IESC =	0	ISFLC =	0	ISWICH =	0
IAROSL =	1	FLAGPN =	T	FLAG2 =	F	FLAGSI =	T
FLAGAS =	F	FLAGC =	F	FLAGW =	T	FLAGF =	T

PHYSICAL PROPERTIES

EMCONC =	0.9000	CPCON =	0.2650	KCON =	0.0227
RHCON =	144.0000	EMLI =	0.2000	CPLI =	0.9960
AKLI =	33.8000	RHLI =	30.0000	RHOLIO =	124.0000
RHOLIN =	86.9400	RHOLIH =	160.0000	EMGPF =	0.0400
EMCZ =	0.9000	TAUCZ =	0.1000		

INNER CONTAINMENT DIMENSIONS

VP =	30086.0000	CHP =	66.7000	CPAP =	0.1247
XMOLA =	39.9000	FRA =	0.0500	RA =	5.0000

EXTRANEOUS HEAT CAPACITY NODE DATA

TEMCZP =	543.0000	XMEMCP =	12300.0000	AEMCP =	5100.0000
CPEMCP =	0.1200	HINECP =	0.0900		

SPILL PARAMETERS

ASLI =	21.6500	SPILL =	220.0000	SPRAY =	0.0000
ZLI =	0.3387				

WALL AND FLOOR NODE DATA

NL =	5	NL1 =	5

THICKNESS OF CONCRETE WALL NODES

.200 .200 .200 .200 .200

THICKNESS OF CONCRETE FLOOR NODES

.200 .200 .200 .200 .200

PARAMETERS ASSOCIATED WITH OUTERMOST CONTAINMENT

THWC =	0.0840	THFC =	0.0840	GAP =	0.0000
KGAP =	0.0160	KLEAK =	0.0000		

PRIMARY STEEL WALL DATA

ESTLWP =	0.8500	CPSWP =	0.1200	KSTLWP =	30.0000
RHSWP =	497.6498	AWP =	5600.0000	THWP =	0.0580

PRIAMRY STEEL FLOOR DATA

ESTLFP =	0.8500	CPSFP =	0.1200	KSTLFP =	30.0000
RHSFP =	497.6498	AFP =	4000.0000	THFP =	0.0580

HEAT TRANSFER CORRELATION COEFFICIENTS

HIN =	0.1200	HINSAM =	0.0700	HINGSP =	0.1200
HINGSS =	0.1200	HINPS =	0.0700	HINFAM =	0.0700
HINFGS =	0.0700	HINFSG =	0.0700		

COMBUSTION PARAMETERS

QCO =	18510.0000	RCMBO =	0.8764	TVAP =	2916.0000
RCMBH2 =	6.9300	PERCEN =	0.0000	QCO1 =	18510.0000
QCO2 =	0.0000	RCMBO1 =	0.8764	RCMBO2 =	0.0000
QCN =	4080.0000	RCMBN =	1.4870	TMELT =	353.0000
QCW =	13784.0000	RCMBW =	0.3830	QVAP =	8431.0000

INITIAL CONDITIONS

PRIMARY

TGPZER =	549.1750	TSPZER =	546.9600	TCZI =	1140.0000
TLII =	1140.0000	TSFPI =	546.0000	TA =	540.5300
WO2P =	0.2316	WAP =	0.0094	WWAP =	0.0062
PAPZER =	16.4330				

INTEGRATION CONTROL PARAMETERS

IMETH =	3	DTMIN =	0.2000	TIMEF =	12000.0000
RELERR =	0.0060	DELOUT =	2000.0000		

AEROSOL REMOVAL FROM PRIMARY CONTAINMENT

BETA = 100.0000

DATA FOR SUSPENDED PAN OPTIONAL GEOMETRY:

TPANZO =	535.0000	APAN =	35.2900	CPPAN =	0.1200
THKPAN =	0.0157	BREDTH =	16.5000		
KPAN =	13.0000	RHPAN =	490.0000		
THKIN1 =	0.1667	THKIN2 =	0.0833	AINS =	14.1500
RHINS =	10.0000	CPINS =	0.2000	EMINS =	0.9000
HINGPF =	0.0000				

SPRAY FIRE RESULTS

TGPZER = 549.2 PZEROP = 16.433

APPENDIX B

LITFIRE Data: Two-Cell Calculation

UWMAK-III TWO CELL TEST CASES WITH CRACK=0.0 CM**2
USING VERSION OF LITFIRE: "LITFIR" IN SI UNITS
DATE: 23 august, 1982

OPTIONS IN EFFECT

IBLOW =	0	IESC =	0	ISFLC =	0	ISWICH =	0
IAROSL =	0	FLAGPN =	F	FLAG2 =	T	FLAGSI =	T
FLAGAS =	F	FLAGC =	F	FLAGW =	T	FLAGF =	T

PHYSICAL PROPERTIES

EMCONC =	0.9000	CPCON =	653.0000	KCON =	1.7300
RHCON =	2306.6600	EMLI =	0.2000	CPLI =	4170.0000
AKLI =	48.4400	RHLI =	480.5500	RHOLIO =	1986.2900
RHOLIN =	1392.6400	RHOLIH =	2562.9500	EMGPF =	0.0400
EMCZ =	0.1000	TAUCZ =	0.5000		

INNER CONTAINMENT DIMENSIONS

VP =	950.0000	CHP =	6.2000	CPAP =	622.0000
XMOLA =	40.0000	FRA =	0.7600	RA =	300.0000

EXTRANEOUS HEAT CAPACITY NODE DATA

TEHCZP =	643.0000	XMEHCP =	12300.0000	AEHCP =	0.0000
CPEHCP =	502.0000	HINECP =	0.0000		

SPILL PARAMETERS

ASLI =	150.0000	SPILL =	22000.0000	SPRAY =	0.0000
ZLI =	0.3052				

WALL AND FLOOR NODE DATA

NL =	8	NL1 =	8

THICKNESS OF CONCRETE WALL NODES

.100 .100 .100 .150 .150 .150 .150 .100

THICKNESS OF CONCRETE FLOOR NODES

.100 .100 .100 .150 .150 .150 .150 .100

PARAMETERS ASSOCIATED WITH OUTERMOST CONTAINMENT

THWC =	0.2540	THFC =	0.6350	GAP =	0.0076
KGAP =	0.0260	KLEAK =	0.0000		

PRIMARY STEEL WALL DATA

ESTLWP =	0.8500	CPSWP =	502.0000	KSTLWP =	51.9000
RHSWP =	7970.0000	AWP =	650.0000	THWP =	0.0500

PRIAMRY STEEL FLOOR DATA

ESTLFP =	0.8500	CPSFP =	502.0000	KSTLFP =	51.9000
RHSFP =	7970.0000	AFP =	160.0000	THFP =	0.0500

HEAT TRANSFER CORRELATION COEFFICIENTS

HIN =	0.1200	HINSAM =	0.0700	HINGSP =	0.1200
HINGSS =	0.1200	HINPS =	0.0700	HINFAM =	0.0700
HINFGS =	0.0700	HINFSG =	0.0700		

COMBUSTION PARAMETERS

QCO =	42936.7002	RCMBO =	0.8764	TVAP =	1615.0000
RCMBH2 =	6.9300	PERCEN =	0.0000	QCO1 =	42936.7002
QCO2 =	0.0000	RCMBO1 =	0.8764	RCMBO2 =	0.0000
QCN =	9464.1600	RCMBN =	1.4870	TMELT =	453.7000
QCW =	31974.0000	RCMBW =	0.3830	QVAP =	19370.0000

INITIAL CONDITIONS

PRIMARY

TGPZER =	523.0000	TSPZER =	523.0000	TCZI =	593.0000
TLII =	593.0000	TSFPI =	523.0000	TA =	300.0000
WO2P =	0.2316	WAP =	0.0000	WWAP =	0.0000
PAPZER =	1.0000				

INTEGRATION CONTROL PARAMETERS

IMETH =	3	DTMIN =	0.0300	TIMEF =	50222.0000
RELERR =	0.0060	DELOUT =	2000.0000		

SECONDARY CONTAINMENT DIMENSIONS

CHS =	45.0000	VS =	255000.0000	WO2S =	0.2320
WWAS =	0.0000	WAS =	0.0000	CPAS =	522.0000
CRACK =	10.0000				

EXTRANEOUS HEAT CAPACITY NODE DATA

TEHCZS =	300.0000	XMEHCS =	11500.0000	AEHCS =	50.0000
CPEHCS =	502.0000	HINECS =	0.0900		

SECONDARY INITIAL CONDITIONS

TGSZER =	300.0000	TSSZER =	300.0000	TFSZER =	300.0000
PASZER =	101.4000				

SECONDARY STEEL WALL DATA

ESTLWS =	0.8500	CPSWS =	502.0000	KSTLWS =	51.9000
RHSWS =	7970.0000	AWS =	17000.0000	THWS =	0.0060

SECONDARY STEEL FLOOR DATA

ESTLFS =	0.8500	CPSFS =	502.0000	KSTLFS =	51.9000
RHSFS =	7970.0000	AFS =	6000.0000	THFS =	0.0060

SPRAY FIRE RESULTS

TGPZER =	941.4	PZEROP =	0.145

APPENDIX C

LITFIRE Data: LiPb Combustion

UWMAK-III GEOMETRY LARGE SPILL COMPARISON.
USING VERSION OF LITFIRE: DIFSI
DATE: 13 SEPTEMBER 1982 RUN NUMBER: ONE

OPTIONS IN EFFECT

IBLOW =	0	IESC =	0	ISFLC =	0	ISWICH =	0
IAROSL =	0	FLAGPN =	F	FLAG2 =	F	FLAGSI =	T
FLAGAS =	F	FLAGC =	F	FLAGW =	T	FLAGF =	T
		FLAGPB =	T	FLAGDF =	T		

PHYSICAL PROPERTIES

EMCONC =	0.9000	CPCON =	0.1560	KCON =	1.0000
RHCON =	144.0000	EMLI =	0.2000	CPLI =	0.9960
AKLI =	28.0000	RHLI =	30.0000	RHOLIO =	124.0000
RHOLIN =	86.9400	RHOLIH =	160.0000	EMGPF =	0.0400
EMCZ =	0.1000	TAUCZ =	0.9000		

INNER CONTAINMENT DIMENSIONS

VP =	8855700.0000	CHP =	150.0000	CPAP =	0.1247
XMOLA =	39.9000	FRA =	0.7500	RA =	300.0000

EXTRANEOUS HEAT CAPACITY NODE DATA

TEHCZP =	538.0000	XMEHCP =	6.0000	AEHCP =	10.0000
CPEHCP =	0.1200	HIHECP =	0.0900		

SPILL PARAMETERS

ASLI =	10386.0000	SPILL =	763418.0000	SPRAY =	0.0000
ZLI =	2.4502				

WALL AND FLOOR NODE DATA

NL =	8	NL1 =	8

THICKNESS OF CONCRETE WALL NODES

.100 .100 .100 .150 .150 .150 .150 .100

THICKNESS OF CONCRETE FLOOR NODES

.100 .100 .100 .150 .150 .150 .150 .100

PARAMETERS ASSOCIATED WITH OUTERMOST CONTAINMENT

THWC =	0.8333	THFC =	2.0833	GAP =	0.0021
KGAP =	0.0150	KLEAK =	0.0000		

PRIMARY STEEL WALL DATA

ESTLWP =	0.8500	CPSWP =	0.1200	KSTLWP =	30.0000
RHSWP =	497.6498	AWP =	183532.0000	THWP =	0.0210

PRIAMRY STEEL FLOOR DATA

ESTLFP =	0.8500	CPSFP =	0.1200	KSTLFP =	30.0000
RHSFP =	497.6498	AFP =	10386.0000	THFP =	0.0210

HEAT TRANSFER CORRELATION COEFFICIENTS

HIN =	0.1200	HINSAM =	0.0700	HINGSP =	0.1200
HINGSS =	0.0700	HINPS =	0.0700	HINFAM =	0.0700
HINFGS =	0.0700	HINFSG =	0.0700		

COMBUSTION PARAMETERS

QCO =	18510.0000	RCMBO =	0.8764	TVAP =	2916.0000
RCMBH2 =	6.9300	PERCEN =	0.0000	QCO1 =	18510.0000
QCO2 =	0.0000	RCMBO1 =	0.8764	RCMBO2 =	0.0000
QCN =	4080.0000	RCMBN =	1.4870	TMELT =	813.0000
QCW =	13784.0000	RCMBW =	0.3830	QVAP =	8350.0000

INITIAL CONDITIONS

PRIMARY

TGPZER =	538.0000	TSPZER =	538.0000	TCZI =	2300.0000
TLII =	2266.0000	TSFPI =	538.0000	TA =	538.0000
WO2P =	0.2310	WAP =	0.0000	WWAP =	0.0000
PAPZER =	14.7000				

INTEGRATION CONTROL PARAMETERS

IMETH =	3	DTMIN =	1.0000	TIMEF =	12121.1000
RELERR =	0.0060	DELOUT =	2000.0000		

DATA FOR LITHIUM LEAD COMBUSTION OPTION:

CPLEAD =	0.0350	KLEAD =	9.3000	RHLEAD =	708.0000
ALLOYI =	0.6000	QDISS =	3316.0000		

MODIFIED PARAMETERS FOR LITHIUM IN LITHIUM LEAD POOL

AMOUNT OF LITHIUM AVAILABLE FOR COMBUSTION = 24744.8379

THICKNESS OF LIPB POOL IS LESS THAN ZLI ABOVE AND
IS CALCULATED IN PROGRAM

SPRAY FIRE RESULTS

TGPZER = 538.0 PZEROP = 14.700

APPENDIX D

Listing of the LITFIRE Computer Code

```
C -*- fortran -*-
C
C               LIBP COMBUSTION MODELING INCLUDED
C
C               AKEXX SUBROUTINE INCLUDED
C
C   MODELED WITH: TAUCZ,EMGP=1.0ETC.,EMGF IS INCLUDED,KNIT/KLIT.
C                 BETA AND STICK
C                 SEPERATE EMISSIVIITES AND STEEL PROPERTIES.
C                 NEW FLOOR NODE IN SECODARY.
C
C
      IMPLICIT REAL (K,L,N)
      LOGICAL FLAGW,FLAGF,FLAGL,FLAGPN,FLAGAS,FLAGM,FLAG2,FLAGSI,FLAGN,
     .        FLAGC,FLAGPB
      REAL INTGRL
      COMMON // NAME(320),FLAG2,FLAGAS,FLAGC,FLAGF,FLAGN,
     .          FLAGPN,FLAGW,IPAGE,ISWICH,IAROSL,FLAGDF,ICZ
      COMMON /LITH/ AKLI,ASLI,CPLI,CSBLI,HB,LIBP,LIL,LILP,LIT,
     .              RHLI,SPILL,TLI,TLII,ZLI
      COMMON /LEAD/ CPLEAD,KLEAD,RHLEAD,MLIPB,XALLOY,ATML,ATMPB,CMBR
      COMMON /PBPOOL/ DMPBDT,ZZPB,MLEAD,TLEADI,XWLI,DFLIPB,XLIDOT,
     .                THPB,TLEADF
      COMMON /STEEL/ CPSFP,CPSFS,CPSWP,CPSWS,ESTLFP,ESTLWP,KSTLFP,
     .               KSTLFS,KSTLWP,KSTLWS,RHSFP,RHSFS,RHSWP,RHSWS
      COMMON /MISC/ AFP,AFS,AWP,AWS,C7,C21,GIN,
     .              HA,HINFAM,HINSAM,HTCPGP,QRADC,RADC,RCZW,
     .              RHOAP,RLIW,RWPWS,SIGMA,TA,TC(20),TFS,
     .              TFSZER,TGP,TGS,TGPZER,TSFP,TSP,TSS,
     .              TSSZER,THFP,THFS,THWP,THWS,ZZES,ZZS,ZZ1,ZZ7
      COMMON /INTGL/ IMETH,ICOUNT,ISTORE,INOIN,IPASS,DELT,
     .               XIC(101),ZZZ(501)
      COMMON /INJOP/ DP1,DP2,DP3,MNIINJ,MOXINJ,TIME,VP
      COMMON /PANOP/ AINS,APAN,BREDTH,CLIST,CPINS,CPPAN,EMGP,FPG,FPW,
     .               KPAN,RHINS,RHPAN,THKIN1,THKIN2,THKPAN,
     .               TINS1,TINS1F,TINS1I,TINS2,TINS2F,TINS2I,
     .               TPAN,TPANF,TPANZO,ZZ2,ZZ4,ZZ8,ZZ9
      COMMON /CONOP/ C8,CPCON,DTBDT(20),DTCDT(20),GAP,KCON,KGAP,
     .               L(20),L1(20),NL,NL1,QRADB,RADB,RHCON,
     .               SFLCR,TB(20),TBF(20),TBIC(20),TCF(20),
     .               TCIC(20),THFC,THWC,TSFPI,TSPZER,XSFL
      COMMON /CCOP/ CMBRO,CRACON,DCOCZ,H2LEFT,QCCONC,RCMBO,RCMBW,
     .              RELESE,TCIGNI,TCON,TCONF,XMH2OI,ZZC,ZZD,ZZDIN
      COMMON /SECOP/ AEHCS,C11,C20,CHS,CPEHCS,CPH2,CPLIH,CPWA,CRACK,
     .               FOUTP,FOUTS,FOUTT,HINFGS,HINFSG,HINGSS,HINPS,KLEAK,
     .               LEAK,MAIRP,MAIRS,MAIS,MAS,MH2S,MLIHS,MLIHIS,MLINS,
     .               MLIOIS,MLIOS,MNIIS,MNIS,MOXIS,MOXS,MWAIS,
     .               MWAS,PAP,PAS,PASZER,RA,RBREAK,RHOLIH,
     .               RHOLIN,RHOLIO,RWPGAS,TEHCS,TEHCSF,TEHCZS,TGSF,
     .          TFSF,TGSZER,TSSF,VS,XMDOT,XMEHCS,XMOLA,ZZ3,ZZFS
      COMMON /UNITS/ AEHCP,BETA,CHP,CMBRH,CPAP,CPEHCP,MAP,MNIP,
     .               MOXP,MWAP,PAPZER,QCW,QCO,QCO1,QCO2,QCW,QVAP,
     .               TCZ,TCZF,TCZI,TEHCP,TEHCPF,TEHCZP,TGPF,
     .               TLIF,TMELT,TSFPF,TSPF,TVAP,XMEHCP
      COMMON /PBDIF/ CCZP,CGLI,CLIG,CPCZ,CPMCZ,DFILM,KFILM,PYUP,
     .               QRADP,RCZP,RGLI,RIFCZP,RIFPG,RIFPW,RLIG,RWLI,
     .               TLEAD,YAPCZ,ZZ6
C
      open(unit=1,device='dsk',access='seqin',
     .   file='indat1',mode='ascii')
      open(unit=2,device='dsk',access='seqin',
     .   file='indat2',mode='ascii')
      open(unit=3,device='dsk',access='seqin',
     .   file='indat3',mode='ascii')
      open(unit=4,device='dsk',access='seqin',
     .   file='indat4',mode='ascii')
      open(unit=10,device='dsk',access='seqout',
     .   file='outd1',mode='ascii')
      open(unit=11,device='dsk',access='seqout',
     .   file='outd2',mode='ascii')
      open(unit=12,device='dsk',access='seqout',
     .   file='outd3',mode='ascii')
```

```
      open(unit=13,device='dsk',access='seqout',
     .   file='outd4',mode='ascii')
      open(unit=14,device='dsk',access='seqout',
     .   file='outd5',mode='ascii')
C
C*****************************************************************************
C                    INPUT SECTION                                             *
C*****************************************************************************
C   SEE LITFIRE USERS GUIDE FOR DEFINITIONS AND DIMENSIONS OF INPUT VARIABLES  *
C
C**********      READ IN TITLE AND HEADINGS      **********
C
      READ (1,700)  (NAME(I),I=1,80)
      READ (2,700)  (NAME(I),I=81,160)
      READ (3,700)  (NAME(I),I=161,240)
      READ (4,700)  (NAME(I),I=241,320)
  700 FORMAT(20A4)
C
C**********      READ IN FLAGS AND OPTIONS      **********
C
C THE NEXT BUNCH OF STATEMENTS ARE HERE BECAUSE OF COMPILE TROUBLE AT
C  LIVERMORE. HOPEFULLY THIS WILL BE CORRECTED SOON. (1/26/82).
C
      READ (1,701) IFLAGW,IFLAGF,IFLAGP,IFLAG2,IFLAGS,IFLAGC,
     .             IFLAGU,IFLAGB,IBLOW,IESC,ISFLC,ISWICH,IAROSL,IFLAGD
  701 FORMAT(1X,14(I1,1X))
      FLAGW=.FALSE.
      FLAGF=.FALSE.
      FLAGPN=.FALSE.
      FLAG2=.FALSE.
      FLAGAS=.FALSE.
      FLAGC=.FALSE.
      FLAGSI=.FALSE.
      FLAGPB=.FALSE.
      FLAGDF=.FALSE.
      IF (IFLAGW .EQ. 1) FLAGW=.TRUE.
      IF (IFLAGF .EQ. 1) FLAGF=.TRUE.
      IF (IFLAGP .EQ. 1) FLAGPN=.TRUE.
      IF (IFLAG2 .EQ. 1) FLAG2=.TRUE.
      IF (IFLAGS .EQ. 1) FLAGAS=.TRUE.
      IF (IFLAGC .EQ. 1) FLAGC=.TRUE.
      IF (IFLAGU .EQ. 1) FLAGSI=.TRUE.
      IF (IFLAGB .EQ. 1) FLAGPB=.TRUE.
      IF (IFLAGD .EQ. 1) FLAGDF=.TRUE.
C
C**********      READ IN PRIMARY CONTAINMENT SPECIFICATIONS      **********
C
      READ (1,703) NL,NL1
      READ (1,704) (L(I),I=1,NL)
      READ (1,704) (L1(I),I=1,NL1)
      READ (1,702) VP,CHP,CPAP,XMOLA
      READ (1,702) TEHCZP,XMEHCP,AEHCP,CPEHCP,HINECP
  702 FORMAT (6F12.4)
  703 FORMAT (I4,I4)
  704 FORMAT (10F5.3/10F6.3)
C
C**********      READ IN PARAMETERS ASSOCIATED WITH     *********
C          OUTERMOST CONTAINMENT SHELL AND CONCRETE
C
      READ (1,702) THWC,THFC,GAP,KGAP,KLEAK
      IF (THWC .LT. 0.001) FLAGW=.FALSE.
      IF (THFC .LT. 0.001) FLAGF=.FALSE.
C
C**********      READ IN PHYSICAL CONSTANTS      **********
C                  AND EMISSIVITIES
C
      READ (1,702) ESTLWP,CPSWP,KSTLWP,RHSWP,AWP,THWP
      READ (1,702) ESTLFP,CPSFP,KSTLFP,RHSFP,AFP,THFP
      READ (1,702) EMLI,CPLI,AKLI,RHLI
      READ (1,702) EMCONC,CPCON,KCON,RHCON
      READ (1,702) RHOLIO,RHOLIN,RHOLIH,EMGPF,EMCI,TAUCI
C
```

```
C**********     READ IN REACTION CONSTANTS     **********
C
      READ (1,702) QCO1,QCO2,QCN,QCW
      READ (1,702) RCMBO1,RCMBO2,RCMBN,RCMBW,RCMBH2
      READ (1,702) TMELT,TVAP,QVAP,PERCEN
      RCMBO=((100.-PERCEN)*RCMBO1+PERCEN*RCMBO2)/100.
      QCO=((100.-PERCEN)*RCMBO1*QCO1+PERCEN*RCMBO2*QCO2)/(RCMBO*100.)
C
C**********     READ IN HEAT TRANSFER CORRELATION COEFFICIENTS       *********
C
      READ (1,702) HIN,HINGSP,HINGSS,HINPS,HINSAM,HINFAN
      READ (1,702) HINFGS,HINFSG
C
C**********     READ IN SPILL PARAMETERS     **********
C
      READ (1,702) ASLI,SPILL,SPRAY,FRA,RA
      ZLI=SPILL/RHLI/ASLI
C
C**********     READ IN INITIAL CONDITIONS     **********
C
      READ (1,702) TCZI,TGPZER,TSPZER,TSFPI,TA,TLII
      READ (1,702) PAPZER,WO2P,WWAP,WAP
C
C**********     READ IN INTEGRATION CONTROL PARAMETERS     **********
C
      READ (1,705) IMETH,DTMIN,TIMEF,RELERR,DELOUT
  705 FORMAT(I4,5F12.4)
C
C         **********************************
C**********              OPTIONS           **********
C         **********************************
C
C
C**********     CONTAINMENT FLOODING WITH INERT GAS OPTION     **********
C
      DATA TBLIN,TBLOUT,BLOWV,EXHSTV,XBLOW,WO2B,WN2B,WWAB,XMOLAB,CPAB,
     .     TBLOW/8*0.0,3*1.0/
C
C**             READ IN GAS FLOODING PARAMETERS IF USING OPTION        **
C
      IF (IBLOW.NE.1) GO TO 900
      READ (4,702) WO2B,WWAB,WN2B,XMOLAB,CPAB,TBLOW
      READ (4,702) BLOWV,EXHSTV,TBLIN,TBLOUT
C
  900 CONTINUE
      WAB=1.-WO2B-WN2B-WWAB
C
C**********     EMERGENCY SPACE COOLING OF CONTAINMENT OPTION     **********
C
      DATA XESC,ESCR,ESCTIN,ESCEND/4*0.0/
      IF (IESC.EQ.1) READ (4,702) ESCR,ESCTIN,ESCEND
C
C**********     EMERGENCY STEEL FLOOR LINER COOLING OPTION     *********
C
      DATA XSFL,SFLCR,SFLTIN,SFLEND/4*0.0/
      IF (ISFLC.EQ.1) READ (4,702) SFLCR,SFLTIN,SFLEND
C
C**********     AEROSOL REMOVAL FROM PRIMARY CONTAINMENT      **********
C
      IF (IAROSL .EQ. 1) READ (4,702) BETA
C
C**********     CLOSURE OF CRACK BETWEEN PRIMARY AND SECONDARY   *******
C
C
C*************************************************************************
C    PRINT OUT THE INPUT          **********
C*************************************************************************
C
C
      WRITE (10,800) (NAME(I),I=1,60)
      WRITE (10,801) IBLOW,IESC,ISFLC,ISWICH,IAROSL,FLAGPN,FLAG2,
                     FLAGSI,FLAGAS,FLAGC,FLAGW,FLAGF,FLAGPB,FLAGDF
```

```
      WRITE (10,802) EMCONC,CPCON,KCON,RHCON,EMLI,CPLI,AKLI,RHLI,
     .               RHOLIO,RHOLIN,RHOLIH,EMGPF,EMCZ,TAUCZ
      WRITE (10,803) VP,CHP,CPAP,XMOLA,FRA,RA
      WRITE (10,804) TEHCZP,XMEHCP,AEHCP,CPEHCP,HINECP
      WRITE (10,805) ASLI,SPILL,SPRAY,ZLI
      WRITE (10,806) NL,NL1
      WRITE (10,807) (L(I),I=1,NL)
      WRITE (10,808) (L1(I),I=1,NL1)
      WRITE (10,809) THWC,THFC,GAP,KGAP,KLEAK
      WRITE (10,810) ESTLWP,CPSWP,KSTLWP,RHSWP,AWP,THWP
      WRITE (10,811) ESTLFP,CPSFP,KSTLFP,RHSFP,AFP,THFP
      WRITE (10,812) HIN,HINSAM,HINGSP,HINGSS,HINPS,HINFAM,HINFGS,HINFSG
      WRITE (10,813) QCO,RCMBO,TVAP,RCMBH2,PERCEN,QCO1,QCO2,RCMBO1,
     .               RCMBO2,QCN,RCMBN,TMELT,QCW,RCMBW,QVAP
      WRITE (10,814) TGPZER,TSPZER,1CZI,TLII,TSFPI,
     .               TA,WO2P,WAP,WWAP,PAPZER
      WRITE (10,815) IMETH,DTMIN,TIMEF,RELERR,DELOUT
C
C*********      THE FOLLOWING PARAMETERS ARE ASSOCIATED WITH THE   *******
C              DIFFERENT OPTIONS AND ARE WRITTEN ONLY WHEN USED
C
      IF (IBLOW.EQ.1.OR.ISFLC.EQ.1.OR.IESC.EQ.1) WRITE (10,819) WO2B,
     .        BLOWV,CPAP,WWAB,TBLOUT,CPAB,WN2B,TBLIN,EXHSTV,TBLOW,
     .        XMOLAB,SFLTIN,SFLCR,SFLEND,ESCTIN,ESCR,ESCEND
C
      IF (IAROSL .EQ. 1) WRITE (10,820) BETA
C
  800 FORMAT (' ',3(20A4,/),/)
  801 FORMAT(' OPTIONS IN EFFECT'/1X,17(1H-)//T10,'IBLOW = ',I4,T25,
     .'IESC =  ',I4,T40,'ISFLC = ',I4,T55,'ISWICH =',I4//T10,'IAROSL =',
     .,I4,T25,'FLAGPN =',L4,T40,'FLAG2 = ',L4,T55,'FLAGSI =',L4//T10,
     .'FLAGAS =',L4,T25,'FLAGC = ',L4,T40,'FLAGW = ',L4,T55,'FLAGF = ',
     .L4//T25,'FLAGPB =',L4,T40,'FLAGDF =',L4//)
  802 FORMAT(' PHYSICAL PROPERTIES'/1X,19(1H-)//T10,'EMCONC =',F12.4,
     .T35,'CPCON = ',F12.4,T60,'KCON =  ',F12.4//T10,'RHCON = ',F12.4,
     .T35,'EMLI =  ',F12.4,T60,'CPLI =  ',F12.4//T10,'AKLI =  ',F12.4,
     .T35,'RHLI =  ',F12.4,T60,'RHOLIO =',F12.4//T10,'RHOLIN =',F12.4,
     .T35,'RHOLIH =',F12.4,T60,'EMGPF = ',F12.4//T10,'EMCZ =  ',F12.4,
     .T35,'TAUCZ = ',F12.4//)
  803 FORMAT(' INNER CONTAINMENT DIMENSIONS'/1X,28(1H-)//T10,'VP =    ',
     .F12.4,T35,'CHP =   ',F12.4,T60,'CPAP =  ',F12.4//T10,'XMOLA = ',
     .F12.4,T35,'FRA =   ',F12.4,T60,'RA =    ',F12.4//)
  804 FORMAT(//' EXTRANEOUS HEAT CAPACITY NODE DATA'/1X,33(1H-)//T10,
     .'TEHCZP =',F12.4,T35,'XMEHCP =',F12.4,T60,'AEHCP = ',F12.4//
     .T10,'CPEHCP =',F12.4,T35,'HINECP =',F12.4//)
  805 FORMAT(' SPILL PARAMETERS'/1X,16(1H-)//T10,'ASLI =  ',F12.4,T35,
     .'SPILL = ',F12.4,T60,'SPRAY = ',F12.4//T10,'ZLI =   ',F12.4//)
  806 FORMAT(/,' WALL AND FLOOR NODE DATA'/1X,24(1H-)//T10,'NL =    ',
     .I2,T35,'NL1 =   ',I2//)
  807 FORMAT(' THICKNESS OF CONCRETE WALL NODES'/1X,31(1H-)//T10,
     .10(F5.3),//T10,10(F5.3)//)
  808 FORMAT(/,' THICKNESS OF CONCRETE FLOOR NODES'/1X,32(1H-)//T10,
     .10(F5.3),//T10,10(F5.3))
  809 FORMAT(//,' PARAMETERS ASSOCIATED WITH OUTERMOST CONTAINMENT'/1X,
     .48(1H-)//T10,'THWC =  ',F12.4,T35,'THFC =  ',F12.4,T60,
     .'GAP =   ',F12.4//T10,'KGAP =  ',F12.4,T35,'KLEAK = ',F12.4//)
  810 FORMAT (' PRIMARY STEEL WALL DATA'/1X,23(1H-)//T10,
     .'ESTLWP =',F12.4,T35,'CPSWP = ',F12.4,T60,'KSTLWP =',F12.4//T10,
     .'RHSWP = ',F12.4,T35,'AWP =   ',F12.4,T60,'THWP =  ',F12.4//)
  811 FORMAT (' PRIAMRY STEEL FLOOR DATA'/1X,24(1H-)//T10,
     .'ESTLFP =',F12.4,T35,'CPSFP = ',F12.4,T60,'KSTLFP =',F12.4//T10,
     .'RHSFP = ',F12.4,T35,'AFP =   ',F12.4,T60,'THFP =  ',F12.4//)
  812 FORMAT(' HEAT TRANSFER CORRELATION COEFFICIENTS'/1X,38(1H-)//
     .T10,'HIN =   ',F12.4,T35,'HINSAM =',F12.4,T60,'HINGSP =',F12.4//
     .T10,'HINGSS =',F12.4,T35,'HINPS = ',F12.4,T60,'HINFAM =',F12.4//
     .T10,'HINFGS =',F12.4,T35,'HINFSG =',F12.4//)
  813 FORMAT(' COMBUSTION PARAMETERS'/1X,21(1H-)//T10,'QCO =   ',F12.4,
     .T35,'RCMBO = ',F12.4,T60,'TVAP =  ',F12.4//T10,'RCMBH2 =',F12.4,
     .T35,'PERCEN =',F12.4,T60,'QCO1 =  ',F12.4//T10,'QCO2 =  ',F12.4,
     .T35,'RCMBO1 =',F12.4,T60,'RCMBO2 =',F12.4//T10,'QCN =   ',F12.4,
     .T35,'RCMBN = ',F12.4,T60,'TMELT = ',F12.4//T10,'QCW =   ',F12.4,
     .T35,'RCMBW = ',F12.4,T60,'QVAP =  ',F12.4//)
```

```
  814 FORMAT (' INITIAL CONDITIONS'/1X,18(1H-)/5X,'PRIMARY'//
     .T10,'TGPZER =',F12.4,T35,'TSPZER =',F12.4,T60,'TCZI =  ',F12.4//
     .T10,'TLII =  ',F12.4,T35,'TSFPI = ',F12.4,T60,'TA =    ',F12.4//
     .T10,'WO2P =  ',F12.4,T35,'WAP =   ',F12.4,T60,'WWAP =  ',F12.4//
     .T10,'PAPZER =',F12.4//)
  815 FORMAT(' INTEGRATION CONTROL PARAMETERS'/1X,30(1H-)//T10,
     .'IMETH = ',I4,T35,'DTMIN = ',F12.4,T60,'TIMEF = ',F12.4//T10,
     .'RELERR =',F12.4,T35,'DELOUT =',F12.4//)
  819 FORMAT(' MISCELLANEOUS INPUT ASSOCIATED WITH VARIOUS OPTIONS'/1X
     .51(1H-)/5X,'INERT GAS FLOODING'//T10,'WO2B =  ',F12.4,T35,
     .'BLOWV = ',F12.4,T60,
     .'CPAP =  ',F12.4//T10,'WWAB =  ',F12.4,T35,'TBLOUT =',F12.4,T60,
     .'CPAB =  ',F12.4//T10,
     .'WN2B =  ',F12.4,T35,'TBLIN = ',F12.4,T60,'EXHSTV =',F12.4//T10,
     .'TBLOW = ',F12.4,T35,'XMOLAB =',F12.4//5X,
     .'STEEL FLOOR COOLING'//T10,'SFLTIN =',F12.4,T35,'SFLCR = ',F12.4,
     .T60,'SFLEND =',F12.4//5X,'EMERGENCY SPACE COOLING'//T10,
     .'ESCTIN =',F12.4,T35,'ESCR =  ',F12.4,T60,'ESCEND =',F12.4//)
  820 FORMAT (' AEROSOL REMOVAL FROM PRIMARY CONTAINMENT'/1X,41(1H-)//
     .T10,'BETA =  ',F12.4//)
C*********************************************************************
C                      ********************                          *
C**********************     OPTIONS        ******************         *
C                      ********************                          *
C    SEE LITFIRE USERS GUIDE FOR DIMENSIONS OF OPTION VARIABLES      *
C                                                                    *
C    IN THIS STEP THE SECONDARY CELL, PAN GEOMETRY, AND CONCRETE WALL *
C        AND FLOOR VARIABLES ARE READ IN  AND WRITTEN                *
C*********************************************************************
      IF (FLAGPB .AND. SPRAY .GT. 0.) GO TO 984
      IF (FLAGC .AND.FLAGPN) GO TO 980
      FLAGN=.TRUE.
      IF (FLAG2) CALL CELL2
      IF (FLAGPN) CALL PAN
      IF (FLAGAS) CALL INJEC
      IF (FLAGC) CALL CONCC
      IF (FLAGPB) CALL LIPB
      IF (FLAGDF) CALL LIDIFF
      IF (FLAGSI) CALL SI
      FLAGN=.FALSE.
C
C*********************************************************************
C    INITIALIZE PROGRAM VARIABLES           **********
C*********************************************************************
C
      FLAGL=.FALSE.
C
      ICZ=1
      ICMB=1
      ILIT=1
      ICNI=1
C
      TIMEO=-.001
      TAU=120.
C  tau should be time dependent see note by mst.
      SIGMA=4.7619E-13
      GIN=32.2
      IPAGE=40
      DELT=DTMIN
C
C**********   INITIALIZE PRIMARY CONTAINMENT VARIABLES   **********
C
      DATA CMBRO,CMBRN,CMBRW,CMBRHI,DFILM,HF,HB,LIBP,LILOX,LILNI,LEAKO,
     .     MLINIP,MLINP,MLIHP,MH2P,OXLB,OXLBI,OUTINT,ROXLB,RNILB,RWALB,
     .     TIME,ZZ1,ZZ2,ZZ4,ZZ5,ZZ6,ZZ7,ZZ8,ZZ9,ZZEP,FPG,
     .     FPW/31*0.0,2*1.0/
C
      FMLEFT=1.0
      LIS=SPILL*SPRAY
      LIT=SPILL-LIS
      LILP=LIT
      LIL=LILP
```

```
      WN2P=1.-WO2P-WWAP-WAP
      XMOLP=1./(WO2P/32.+WN2P/28.+WWAP/18.+WAP/XMOLA)
      RINP=1545./XMOLP
      TEHCP=TEHCZP
      TLI=TLII
      TCZ=TCZI
      TSP=TSPZER
      TSFP=TSFPI
      RHOAIP=PAPZER*144./RINP/TGPZER
      RHOAP=RHOAIP
      MNIIP=WN2P*RHOAIP*VP
      MOXIP=WO2P*RHOAIP*VP
      MNIP=MNIIP
      MLIOIP=LIS*(1.+RCMBO)/RCMBO
      MWAIP=WWAP*RHOAIP*VP
      MWAP=MWAIP
      MAIP=WAP*RHOAIP*VP
      MAP=MAIP
C
C**********   INITIALIZE OPTION VARIABLES  ********
C
      IF (FLAG2) CALL CELL2
      IF (.NOT. FLAG2) RBREAK=0.0
      IF (FLAGPN) CALL PAN
      IF (FLAGC) CALL CONCC
      FLAGN=.TRUE.
      IF (FLAGW) CALL CONCW
      IF (FLAGF) CALL CONCF
      FLAGN=.FALSE.
      BLOWR=1.35E-03*BLOWV
      EXHSTR=1.35E-03*EXHSTV
      STICK=0.0
      IF (IAROSL .EQ. 1) STICK=AWP/(VP*BETA)/12.
      IF (STICK .GE. 1.0) GO TO 986
      IF (STICK .GT. .25) WRITE (11,823)
  823 FORMAT (' AEROSOL REMOVAL FRACTION IS GREATER THAN ONE QUARTER
     .  OF AEROSOL'/'INVENTORY.  TIME STEP HAS BEEN DECREASED TO INSURE
     .  STABILITY.')
      IF (STICK .GT. .25) IPAGE=IPAGE+2
C
C**********     CONVERSION TO FT. - LB. - SEC.     **********
C
      AKLI=AKLI/3600.
      KSTLWP=KSTLWP/3600.
      KSTLFP=KSTLFP/3600.
      KCON=KCON/3600.
      KGAP=KGAP/3600.
C
C
C*************************************
C*   SPRAY FIRE COMPUTATION STARTED    *
C*************************************
C
C
C******  CHECK THAT ENOUGH OXYGEN IS LEFT FOR POOL FIRE AFTER SPRAY FIRE  ***
C
      OXLFS=WO2P*RHOAP*VP-LIS/RCMBO
      IF (OXLFS .LT. 0.0) LIS=RCMBO*WO2P*RHOAIP*VP
      IF (OXLFS .LT. 0.0) OXLFS=0.0
C
      IF (LIS.LE.0.0) GO TO 902
      TO=TGPZER
      QIN= LIS*(QCO+CPLI*(TLI-TO))
      FF2=QIN
      TE=TGPZER+1.
  901 CONTINUE
C**********     SPECIFIC HEAT FOR DILITHIUM OXIDE     **********
C    CP = .0602*T**.326  T = DEG. R                          *
C    IF A DIFFERENT REACTION PRODUCT IS DESIRED, THE INTEGRAL OF THE *
C    DESIRED PRODUCT MUST BE SUBSTITUTED IN QOUT1.           *
C*****************************************************************
      QOUT1=(1.+RCMBO)/RCMBO*LIS*(0.0602/1.326)*(TE**1.326-TO**1.326)
```

```
      QOUT2=WN2P*RHOAP*VP*(.172*(TE-TO)+8.57E-06/2.*(TE*TE-TO*TO)+
     .   1.02E-09/3.*(TE**3.-TO**3.))
      QOUT3=OXLFS*(.184*(TE-TO)+3.2E-6/2.*(TE**2.-TO**2.)+1.36E04*
     .         (1./TE-1./TO))
      QOUT4=WWAP*RHOAP*VP*(0.44*(TE-TO))+WAP*RHOAP*VP*CPAP*(TE-TO)
      FF1=QIN-QOUT1-QOUT2-QOUT3-QOUT4
      IF (FF1*FF2.LT.0.) GO TO 903
      TE=TE+1.
      IF (TE.GT.1.0E06) GO TO 979
      FF2=FF1
      GO TO 901
C*****   PORTION OF PROGRAM FOR GETTING INITIAL GAS TEMP. AND PRESS. ***
  902 CONTINUE
      TE=TGPZER
  903 CONTINUE
      TGP=TE
      MOXP=MOXIP-LIS/RCMBO
      MOXIP=MOXP
      MLIOP=MLIOIP
      XMAIRP=MNIP/28.+MOXP/32.+MAP/XMOLA+MWAP/18.
      PZEROP=1545.*XMAIRP*TGP/144./VP
      PAP=PZEROP
      TGPZER=TGP
      WRITE (10.825) TGP,PZEROP
  825 FORMAT (//' SPRAY FIRE RESULTS'/1X,18(1H-)//5X,'TGPZER = ',F6.1,
     .'    PZEROP = ',F8.3///)
C**********     SPRAY FIRE COMPUTATION CONCLUDED     **********
C
      CALL INIT
C
C**************************************
C*   START OF DYNAMIC CYCLE           *
C*   ----------------------           *
C*   START OF INTEGRATION CYCLE       *
C**************************************
C
  200 CONTINUE
C*****   INJECTION OF GASES TO MODEL HEDL EXPERIMENT  *****
      MOXINJ=0.0
      MNIINJ=0.0
      IF (FLAGAS) CALL INJEC
C
C*****     COMPUTE PHYSICAL PROPERTIES DEPENDENT ON TEMPERATURE   *****
C*****  CALCULATE AIR COMPOSITION AND SPECIFIC HEAT AT CONST. VOLUME   ******
C
      MAIRP=MOXP+MNIP+MWAP+MH2P+MAP
      RHOAP=MAIRP/VP
      FOXP=MOXP/MAIRP
      FWAP=MWAP/MAIRP
      FNIP=MNIP/MAIRP
      CPO2P=(0.184+3.2E-06*TGP-1.36E04/(TGP*TGP))
      CPMOXP=CPO2P*MOXP
      CPN2P=(0.172+8.57E-06*TGP+1.02E-09*TGP*TGP)
      CPMNIP=CPN2P*MNIP
      CPWA=0.44
      CPH2=3.78
      CPLIH=0.67
      CPLIOP=0.0602*TGP**.326
      CPLINP=0.3368+3.67E-04*TGP
      CPMLOP=CPLIOP*MLIOP
C
C
      RHLI=33.49-.0035*(TLI-460.)
      AKLI=(10.48+2.767E-03*(TLI-817.)-0.322E-06*(TLI-817.)**2)/1488.
      CPFAC=0.004938*TLI-6.20741
      CPLI=1.0037-.01063*CPFAC+.00564*CPFAC**2-.001279*CPFAC**3
      CPLI=((LIT-LIBP)*CPLI+LILOX*CPLIOP+LILNI*CPLINP)/LILP
C
      IF (FLAGPB) CALL LIPB
C
C*****  TWO MILLIMETERS ARE ASSUMED TO COVER THE POOL OPTICALLY  *****
      ZP=(LILOX/RHOLIO+LILNI/RHOLIN)/ASLI
```

```
      EMF=0.9
      IF (EMLI.LT.EMF)EMLI=0.2+(EMF-0.2)*ZP/0.00656
C
      HTCPGP=CPMOXP+CPMNIP+CPMLOP+CPAP*MAP+CPLINP*MLINP+CPLIH*MLIHP+
     .   CPH2*MH2P+CPWA*MWAP
C
      EMGP=1.-EXP(-(MLIOP/RHOLIO+MLINP/RHOLIN+MLIHP/RHOLIH)*
     .   2.27E05*CHP/VP/RA)
      EMGP=EMGP*EMGPF
      IF (EMGP .LE. 0.005) EMGP=0.005
C
C***** CALCULATING RADIATIVE INTERCHANGE FACTORS   *****
C   FPG AND FPW REPRESENT VIEW FACTORS FROM THE POOL. THEY ARE
C   INITIALIZED AS UNITY IF PAN IS NOT PRESEN. INITIALIZED IN
C   PAN OPTION IF IT IS USED.   TAUCZ IS USED INSTEAD OF (1.-EMCZ)
C   TO MORE FLEXIBLY MODEL COMBUSTION ZONE-POOL COUPLING.
C
      RIFPW=1./((1.-EMLI)/EMLI+(1.-ESTLWP)*ASLI/ESTLWP/AWP+1./
     .   ((1.-EMGP)*(ICZ*(TAUCZ-1.)+1.)*FPW+EMGP/(ASLI/AWP+1./
     .   FPG/(ICZ*(TAUCZ-1.)+1.))))
      RIFCZW=1./((1.-EMCZ)/EMCZ+(1.-ESTLWP)*ASLI/ESTLWP/AWP+1./
     .   ((1.-EMGP)+EMGP/(1.+ASLI/AWP)))
      RIFPG=(EMLI*EMGP)/((1.-EMLI)*EMGP+EMLI/FPG/(ICZ*(TAUCZ-1.)+1.))
      RIFCZG=(EMCZ*EMGP)/((1.-EMCZ)*EMGP+EMCZ)
      RIFSCW=(ESTLWP*EMCONC)/(ESTLWP+EMCONC-ESTLWP*EMCONC)
      RIFSCF=(ESTLFP*EMCONC)/(ESTLFP+EMCONC-ESTLFP*EMCONC)
      RIFCZP=(EMLI*EMCZ)/(EMCZ+EMLI-EMCZ*EMLI)
C
C**********     CALCULATING GAS CONVECTION COEFFICIENT     **********
C
c the following calculation invokes Reynold's analogy between
c heat and mass transfer by assuming that
c
c                          1/3
c                Sh=c(GrSc)
c
c The Sherwood number, (h  L / D), is defined by the relation:
c                        m
c
c           j = h  rho (w  -w )
c                m     1   2
c
c Reynold's analogy, together with the Lewis relation, gives us:
c
c                    h  = h  /rho C
c                     m    c       p
c
c In LITFIRE, w  is assumed to be zero.
c             2
C
C  POOL OR COMBUSTION ZONE TO PRIMARY GAS
      IF (ICZ .EQ. 1)  T1=0.5*(TGP+TCZ)
      IF (ICZ .EQ. 0) T1=0.5*(TGP+TLI)
      B1= 1.0/T1
      D1=((4.94E-05*T1+0.0188)/(RHOAP*3600.))**2
      AK1=(0.014+1.92E-05*(T1-460.))/3600.
      IF (ICZ .EQ. 1) EXX=(GIN*B1*ABS(TCZ-TGP)/D1)
      IF (ICZ .EQ. 0) EXX=(GIN*B1*ABS(TLI-TGP)/D1)
      IF   (EXX .LE. 0.0) GO TO 985
      EX1 = (EXX)**0.3333
      DIFF=241.57/(132.0+T1/1.8)*(T1/493.2)**2.5/3600.
      HFINF=HIN*DIFF*EX1
      HBINF=HIN*AK1*EX1
      IF (TAU .LT. DELT) TAU=DELT
      HF=HF+(HFINF-HF)*DELT/TAU
      HB=HB+(HBINF-HB)*DELT/TAU
C
C**********     CALCULATING GAS HEAT TRANSFER COEFFICIENTS     **********
C  PRIMARY GAS TO PRIMARY STEEL LINER
      HGWP=HINGSP*AKEXX(TGP,TSP,RHOAP)
C  PRIMARY GAS TO PRIMARY EXTRANEOUS HEAT CAPACITY
      HEHCP=HINECP*AKEXX(TGP,TEHCP,RHOAP)
```

```
C  PRIMARY STEEL LINER TO AMBIENT IF NOT TWO CELL OR CONCRETE OPTION
      IF (.NOT. (FLAG2 .OR. FLAGW)) HA=HINSAM*AKEXX(TSP,TA,.074)
C  PRIMARY STEEL FLOOR TO AMBIENT (IF NOT TWO CELL OR CONCRETE)
      IF (.NOT. (FLAG2 .OR. FLAGF)) HAMF=HINFAM*AKEXX(TSFP,TA,.074)
C    *****    CALCULATING THERMAL DIFFUSIVITIES BETWEEN NODES     *****
      IF (FLAGW) CALL CONCW
      IF (FLAGF) CALL CONCF
      CEHCGP=HEHCP*AEHCP/HTCPGP
      CGPEHC=HEHCP*AEHCP/XMEHCP/CPEHCP
      C1=KSTLWP*HGWP*AWP/HTCPGP/(THWP*HGWP/2.+KSTLWP)
      C6=KSTLWP*HGWP/(RHSWP*CPSWP*THWP*(THWP*HGWP/2.+KSTLWP))
C  THE NEXT THERMAL DIFFUSIVITY IS VALID ONLY IF NO WALL CONCRETE AND
C  NO SECONDARY CONTAINMENT CELL, AND IS BETWEEN STEEL LINER AND AMBIENT
      IF (.NOT. (FLAGW.OR.FLAG2)) C11=KSTLWP*HA/(RHSWP*CPSWP*THWP*
     .   (KSTLWP+THWP*HA/2.))
      IF (.NOT. (FLAGW.OR.FLAG2)) C12=KSTLFP*HAMF/(RHSFP*CPSFP*THFP*
     .   (KSTLFP+THFP*HAMF/2.))
C
C
C**********************************************************************
C   REPEAT ABOVE CALCULATIONS DEPENDENT ON TEMPERATURE FOR SECONDARY   *
C                    CONTAINMENT                                       *
      IF (FLAG2) CALL CELL2
C**********************************************************************
C
C***** TESTING TO SEE IF EMERGENCY SPACE COOLING OR STEEL COOLING IN EFFECT
      IF (TIME .GT. ESCTIN) XESC=1.
      IF (TIME .GT. ESCEND) XESC=0.
      IF (TIME .GT. SFLTIN) XSFL=1.
      IF (TIME .GT. SFLEND) XSFL=0.
C
C*****     LITHIUM LEAD DIFFUSION CALCULATION IN PREPERATION     *****
C              FOR COMBUSTION RATE CALCULATION
      IF (FLAGDF) CALL LIDIFF
C***************       TESTING FOR COMBUSTION     ******************
      ICNI=0
      TEZ=(TCZ+TLI)/2.
      IF (TEZ .LE. 2340. .AND.FOXP.LE.0.28 .AND. MNIP.GT.0.0) ICNI=1
      IF (.NOT.(ILIT.EQ.0 .OR.(ICMB.EQ.0 .AND. ICNI.EQ.0) .OR. TLI.LT.
     .    TMELT)) GO TO 909
      IF (ICZ.EQ.1)WRITE (11,827)ICZ,ICNI,ILIT,ICMB,TCZ,FOXP,TLI,TIME
  827 FORMAT(' COMBUSTION HAS JUST STOPPED.  PARAMETERS ARE  ICZ=',I1,
     .' ICNI=',I1/' ILIT=',I1,'  ICMB=',I1,'  TCZ= ',F8.2,'  FOXP= ',
     .   F7.3,'  TLI= ',F8.2,'   AT TIME= ',F9.2)
      IF (ICZ.EQ.1) IPAGE=IPAGE+2
      GO TO 910
C
C
C**********************************************************************
C      COMPUTATIONS USING COMBUSTION ZONE MODEL       **********
C**********************************************************************
C
C**********     COMPUTING RATE OF LITHIUM COMBUSTION     **********
  909 RN2=0.
      ICZ=1
      IF (TEZ.LT.1900. .AND. FOXP .LE. 0.28)   RN2=
     .    (1.0-FOXP/0.28)/EXP(((1900.-TEZ)/665.)**2.76)
      IF (TEZ.GE.1900. .AND. TEZ.LE. 2340. .AND.FOXP.LE.0.28)   RN2=
     .    (1.0-FOXP/0.28)*(1.-((TEZ-1900.)/440.)**2)
      CMBRO=HF*FOXP*RHOAP*RCMBO
      CMBRN=HF*FNIP*RHOAP*RCMBN*RN2
      CMBRW=HF*FWAP*RHOAP*RCMBW
      CMBR = CMBRO + CMBRN + CMBRW
      IF (.NOT. FLAGDF) GO TO 1909
      IF (CMBR .LT. XLIDOT) GO TO 1909
      CMBRO=CMBRO*XLIDOT/CMBR
      CMBRN=CMBRN*XLIDOT/CMBR
      CMBRW=CMBRW*XLIDOT/CMBR
      CMBR=CMBRO+CMBRN+CMBRW
 1909 CONTINUE
      IF (CMBR*3600. .LT. 0.2) GO TO 910
      RNIL8=CMBRN*ASLI/RCMBN
```

```
      ROXLB=CMBRO*ASLI/RCMBO
      RWALB=CMBRW*ASLI/RCMBW
C
C**********     COMPUTATION OF LITHIUM VAPOR DIFFUSION     **********
      TFEFF=0.002*(TCZ+TLI)/2.-3.92
      PLIV=(10.**(4.8631-14180.2/TLI))*14.
      IF (FLAGPB) PLIV=ACTVTY(XALLOY)*PLIV
      RHOLIV=PLIV*144./RINP/TLI
      DIFFLI=3.56E-03*((TLI/460.)**1.81)/PAP
      DFILM=DIFFLI*RHOLIV/CMBR
      EFILM=DFILM*12.
C
      KNIT=.0432+TFEFF*(.0078-TFEFF*(8.2E-04+TFEFF*2.08E-04))
      KLIT=0.55+TFEFF*(-4.99E-04+TFEFF*1.206E-07)
      KFILM=(PLIV*(KLIT-KNIT)+PAP*KNIT)/14.7
C**********     COMPUTATION OF HEAT TRANSFER COEFFICIENTS     **********
      YAPCZ=KFILM*AKLI*ASLI/(DFILM*AKLI+KFILM*ZLI/2.)
C***** THIS HEAT CAPACITY IS SHEER GUESS WORK THE 0.1 IS FOR LOW COMB. RATES
      CPMCZ=ASLI*((1.+RCMBO)/RCMBO*CMBRO*CPLIOP+(1.+RCMBN)/RCMBN*CMBRN*
     .   CPLINP+((1.+RCMBW)/RCMBW-(1./RCMBH2))*CMBRW*CPWA+(1.+RCMBH2)/
     .    RCMBH2*CMBRW*CPH2+RN2*HF*FNIP*RHOAP*CPN2P)*300.+1.
      IF (CPMCZ/ASLI .LE. 0.001) CPMCZ=0.001*ASLI
      CGCZ=HB*ASLI/CPMCZ
      CCZG=HB*ASLI/HTCPGP
      CPCZ=YAPCZ/CPMCZ
      CCZP=YAPCZ/(CPLI*LIL)
      CCZ=(CMBRO*QCO+CMBRN*QCN+CMBRW*QCW)*ASLI
      CLIST=2.*ASLI*AKLI*KSTLFP/(LIL*CPLI*(ZLI*KSTLFP+THFP*AKLI))
      CSBLI=2.*AKLI*KSTLFP/(RHSFP*THFP*CPSFP*(ZLI*KSTLFP+THFP*AKLI))
      QRADP=SIGMA*ASLI*(TCZ**4-TLI**4)*RIFCZP
      QRADW=SIGMA*ASLI*(TCZ**4-TSP**4)*RIFCZW
      QRADG=SIGMA*ASLI*(TCZ**4-TGP**4)*RIFCZG
      RCZW=QRADW/(THWP*AWP*RHSWP*CPSWP)
      RCZP=QRADP/(LIL*CPLI)
      RCZG=QRADG/HTCPGP
      QRADY=SIGMA*ASLI*(TLI**4-TSP**4)*RIFPW
      QRADZ=SIGMA*ASLI*(TLI**4-TGP**4)*RIFPG
      RLIW=QRADY/(THWP*AWP*RHSWP*CPSWP)
      RWLI=QRADY/CPLI/LIL
      RGLI=QRADZ/CPLI/LIL
      RLIG=QRADZ/HTCPGP
C
C
C*************************************************************
C*   CALCULATING TEMPERATURE RATES OF CHANGE  WITH COMBUSTION  *
C*************************************************************
C
C**********     CALCULATE COMB. ZONE TEMP. RATE OF CHANGE  DEG.R/SEC.     ******
      ZZ6=(CCZ-(QRADP+QRADW+QRADG))/CPMCZ+QVAP*CMBR*ASLI/CPMCZ
     .       -CPCZ*(TCZ-TLI)-CGCZ*(TCZ-TGP)
C
C**********     CALC. LITHIUM TEMP. RATE OF CHANGE  DEG. R/SEC.     **********
      ZZ1=CCZP*(TCZ-TLI)+RCZP-CLIST*(TLI-TSFP)-QVAP*CMBR*ASLI*CCZP/YAPCZ
     .      -RWLI-RGLI
C
C**********     CALC. CELL GAS TEMP. RATE OF CHANGE  DEG. R/SEC.     **********
      ZZ4=C1*(TSP-TGP)+CCZG*(TCZ-TGP)+RCZG+RBREAK+XBLOW*BLOWR*CPAB*
     .   (TBLOW-TGP)/HTCPGP-ESCR*XESC/HTCPGP+CEHCGP*(TEHCP-TGP)+RLIG
C
C**********     CALC. WALL STEEL TEMP. RATE OF CHANGE  DEG. R/SEC.     *********
      ZZ5=C6*(TGP-TSP)+RCZW+RLIW
      GO TO 911
C
C
C*****************************************************
C*   COMPUTATIONS WITHOUT COMBUSTION ZONE MODEL     *
C*****************************************************
C
  910 CONTINUE
      ICZ=0
      CMBR=0.0
      RN2=0.0
```

```
      YALIG=AKLI*HB*ASLI/(AKLI+HB*ZLI/2.)
      CLIG=YALIG/HTCPGP
      QRADW=SIGMA*ASLI*(TLI**4-TSP**4)*RIFPW
      QRADG=SIGMA*ASLI*(TLI**4-TGP**4)*RIFPG
      RLIW=QRADW/(THWP*AWP*RHSWP*CPSWP)
      RWLI=QRADW/CPLI/LIL
      RGLI=QRADG/CPLI/LIL
      RLIG=QRADG/HTCPGP
      CGLI=YALIG/(LIL*CPLI)
      CLIST=2.*ASLI*AKLI*KSTLFP/(LIL*CPLI*(ZLI*KSTLFP+THFP*AKLI))
      CSBLI=2.*AKLI*KSTLFP/(RHSFP*THFP*CPSFP*(ZLI*KSTLFP+THFP*AKLI))
C
C**********************************************
C*   CALCULATING TEMPERATURE RATES OF CHANGE   *
C**********************************************
C
C**********     CALC. LITHIUM TEMP. RATE OF CHANGE  DEG. R/SEC.     **********
      ZZ1=CGLI*(TGP-TLI)-CLIST*(TLI-TSFP)-RWLI-RGLI
C  LET COMBUSTION FOLLOW POOL TEMPERATURE FOR POSSIBLE REIGNITION
      ZZ6=(TLI-TCZ)/DELT
C
C  ******* CALC. CELL GAS TEMP. RATE OF CHANGE DEG . R/SEC.    ********
      ZZ4=C1*(TSP-TGP)+CLIG*(TLI-TGP)+RLIG+RBREAK+XBLOW*BLOWR*CPAB*
     .   (TBLOW-TGP)/HTCPGP-ESCR*XESC/HTCPGP+CEHCGP*(TEHCP-TGP)
C
C**********     CALC. WALL STEEL TEMP. RATE OF CHANGE  DEG. R/SEC.     *********
      ZZ5=C6*(TGP-TSP)+RLIW
  911 CONTINUE
C
C**********************************************
C*   COMPUTATIONS VALID WITH EITHER MODEL      *
C**********************************************
C
      ZZEP=CGPEHC*(TGP-TEHCP)
C**********     CALC. FLOOR STEEL TEMP. RATE OF CHANGE  DEG. R/SEC.  ********
      ZZ7=-XSFL*SFLCR*12./(THFP*AFP*RHSFP*CPSFP)
C
      IF (FLAG2) GO TO 915
      IF (.NOT. FLAGW) QRADC=SIGMA*AWP*(TSP**4-TA**4)*ESTLWP
      IF (FLAGW) QRADC=SIGMA*AWP*(TSP**4-TC(1)**4)*RIFSCW
      RADC=QRADC/(THWP*AWP*RHSWP*CPSWP)
      IF (.NOT. FLAGW) ZZ5=ZZ5-C11*(TSP-TA)-RADC
      IF (FLAGW) ZZ5=ZZ5-C7*(TSP-TC(1))-RADC
      IF (.NOT. FLAGF) QRADB=SIGMA*AFP*(TSFP**4-TA**4)*ESTLFP
      IF (FLAGF) QRADB=SIGMA*AFP*(TSFP**4-TB(1)**4)*RIFSCF
      RADB=QRADB/(THFP*AFP*RHSFP*CPSFP)
      IF (.NOT. FLAGF)  ZZ7=ZZ7+CSBLI*(TLI-TSFP)-C12*(TSFP-TA)-RADB
      IF (FLAGF) ZZ7=ZZ7+CSBLI*(TLI-TSFP)-C8*(TSFP-TB(1))-RADB
  915 CONTINUE
      IF (FLAG2) CALL CELL2
      IF (FLAGF) CALL CONCF
      IF (FLAGW) CALL CONCW
      IF (FLAGPB) CALL LIPB
      IF (FLAGDF) CALL LIDIFF
C
C
C**********CALCULATIONS WITH SUSPENDED PAN GEOMETRY*********
C
      IF (FLAGPN) CALL PAN
C
C******* CALCULATIONS USING COMBUSTION OF CONCRETE (BREACH OF STEEL LINER)****
C
      IF (FLAGC) CALL CONCC
C
C**********************************
C**    CALCULATING OVERPRESSURE   **
C**********************************
      XMAIRP=MOXP/32.+MNIP/28.+MWAP/18.+MAP/XMOLA
      PAP=1545.*XMAIRP*TGP/144./VP
      OVERPP=PAP-PAPZER
      IF (TIME.GT.TBLIN) XBLOW=1.
      IF (TIME.GT.TBLOUT) XBLOW=0.
```

```
C
C**********************************
C**    CALCU. TOTAL  LEAKAGE     ***
C**********************************
C
      LEAK=0.0
      IF (FLAG2) CALL CELL2
      IF (FLAG2) GO TO 932
      IF (PAP .GT. 14.7) LEAK=KLEAK*(PAP-14.7)**0.5
      XMDOT=0.0
      FOUTS=0.0
      FOUTP=EXHSTR/MAIRP*XBLOW+LEAK
  932 CONTINUE
      FMLEFT= EXP(-OUTINT)
      FMLEAK=1.-FMLEFT
C
C************************
C*   DO INTEGRATIONS     *
C************************
C
      LIBP=INTGRL(0..CMBR*ASLI)
      LILOX=INTGRL(0.,(1.+RCMBO)/RCMBO*CMBRO*ASLI*(1.-FRA))
      LILNI=INTGRL(0.,(1.+RCMBN)/RCMBN*CMBRN*ASLI*(1.-FRA))
      OXLB=INTGRL(OXLBI,ROXLB)
      TCZ=INTGRL(TCZI,ZZ6)
      TLI=INTGRL(TLII,ZZ1)
      TGP=INTGRL(TGPZER,ZZ4)
      TSP=INTGRL(TSPZER,ZZ5)
      TEHCP=INTGRL(TEHCZP,ZZEP)
      TSFP=INTGRL(TSFPI,ZZ7)
      MOXP=INTGRL(MOXIP,WOZB*BLOWR*XBLOW+MOXS*FOUTS-MOXP*FOUTP-
     .            ROXLB+MOXINJ)
      MNIP=INTGRL(MNIIP,WNZB*BLOWR*XBLOW+MNIS*FOUTS-MNIP*FOUTP
     .            -RNILB+MNIINJ)
      MAP=INTGRL(MAIP,WAB*BLOWR*XBLOW+MAS*FOUTS-MAP*FOUTP)
      MWAP=INTGRL(MWAIP,WWAB*BLOWR*XBLOW+MWAS*FOUTS-MWAP*FOUTP-RWALB)
      MLIOP=INTGRL(MLIOIP,-MLIOP*FOUTP+(1.+RCMBO)/RCMBO*CMBRO*ASLI*FRA+
     .      MLIOS*FOUTS-MLIOP*STICK)
      MLINP=INTGRL(MLINIP,-MLINP*FOUTP+(1.+RCMBN)/RCMBN*CMBRN*ASLI*FRA+
     .      MLINS*FOUTS-MLINP*STICK)
      MLIHP=INTGRL(0.,-MLIHP*FOUTP+CMBRW*ASLI*((1.+RCMBW)/RCMBW-
     .      1./RCMBH2)+MLIHS*FOUTS-MLIHP*STICK)
      MH2P=INTGRL(0.,MH2S*FOUTS-MH2P*FOUTP+(1.+RCMBH2)/RCMBH2*
     .      CMBRW*ASLI)
      OUTINT=INTGRL(LEAKO,LEAK)
      IF (.NOT. FLAGPN) GO TO 935
      TPAN=INTGRL(TPANZO,ZZ2)
      TINS1=INTGRL(TINS1I,ZZ8)
      TINS2=INTGRL(TINS2I,ZZ9)
  935 CONTINUE
      IF (.NOT. FLAG2) GO TO 938
      MOXS=INTGRL(MOXIS,MOXP*FOUTP-MOXS*FOUTT)
      MNIS=INTGRL(MNIIS,MNIP*FOUTP-MNIS*FOUTT)
      MAS=INTGRL(MAIS,MAP*FOUTP-MAS*FOUTT)
      MWAS=INTGRL(MWAIS,MWAP*FOUTP-MWAS*FOUTT)
      MLIOS=INTGRL(MLIOIS,MLIOP*FOUTP-MLIOS*FOUTT)
      MLINS=INTGRL(MLINIS,MLINP*FOUTP-MLINS*FOUTT)
      MLIHS=INTGRL(0.,MLIHP*FOUTP-MLIHS*FOUTT)
      MH2S=INTGRL(0.,MH2P*FOUTP-MH2S*FOUTT)
      TGS=INTGRL(TGSZER,ZZ3)
      TSS=INTGRL(TSSZER,ZZS)
      TFS=INTGRL(TFSZER,ZZFS)
      TEHCS=INTGRL(TEHCZS,ZZES)
  938 CONTINUE
      IF (.NOT. FLAGW) GO TO 1008
      DO 1008 I=1,NL
      TC(I)=INTGRL(TCIC(I),DTCDT(I))
 1008 CONTINUE
      IF (.NOT. FLAGF) GO TO 1009
      DO 1009 I=1,NL1
      TB(I)=INTGRL(TBIC(I),DTBDT(I))
 1009 CONTINUE
```

```
      IF (.NOT. FLAGC) GO TO 941
      TCON=INTGRL(TSFPI,ZZC)
      DCOC2=INTGRL(0.01,ZZD)
      H2LEFT=INTGRL(XMH2OI,-RELESE)
  941 CONTINUE
      IF (FLAGDF) MLEAD=INTGRL(0.,DMPBDT)
      IF (FLAGDF) TLEAD=INTGRL(TLEADI,ZZPB)
C
      CALL DYNAMI(TIME,&200)
C
C*************************************************************
C*   POST INTEGRATION SECTION                                *
C    CHECK OVERP AND TLI FOR STOP CONDTION
C    CHECK AND CORRECT FOR LITHIUM AND OXYGEN SUPPLY
C*************************************************************
C
  950 CONTINUE
      IF (THPB .GT. .333*ZLI) GO TO 987
      IF (TLI .GE. TVAP) GO TO 978
      LILP=LIT-LIBP+LILOX+LILNI
      IF (LILP .LE. 0.) LILP=0.0
      IF (.NOT. FLAGPB) ZLI=LILP/RHLI/ASLI
      ALPHA=AKLI/(RHLI*CPLI)
      IF ((LILP .LT. 0.1*LIT) .AND. (ALPHA*DELT .GT. ZLI*ZLI .OR. LILP
     .   .LT. 1.0) .AND. (.NOT. FLAGPB)) FLAGL=.TRUE.
      IF (FLAGL) LIL=LIT/10.
      IF (.NOT. FLAGL .AND. .NOT. FLAGPB) LIL=LILP
      IF (TGP .LT. 500. .AND. OVERPP .LT. 1. .AND. ABS(XMDOT)
     .      .LT. 0.1) GO TO 977
      IF (TLI .LT. TMELT) GO TO 976
      IF (ICMB .EQ. 0 .OR. MOXP .GT. 0.01) GO TO 951
      OXLB=OXLFS
      ICMB=0
      CMBRO=0.0
      ROXLB=0.0
  951 CONTINUE
      IF (ILIT .EQ. 0 .OR. (LIT-LIBP) .GE. 0.01) GO TO 952
      OXLB=LIT/RCMBO
      ILIT=0
      LIT=LIBP
      CMBR=0.0
      CMBRO=0.0
      CMBRN=0.0
      CMBRW=0.0
      ROXLB=0.0
      RNILB=0.0
      RWALB=0.0
  952 CONTINUE
      IF (MNIP .GE. 0.0) GO TO 953
      MNIP=0.0
      ICNI=0
      CMBRN=0.
      RNILB=0.0
  953 CONTINUE
      IF (MWAP .GE. 0.0) GO TO 954
      MWAP=0.0
      CMBRW=0.0
      RWALB=0.0
  954 CONTINUE
      CMBRH=3600.*(CMBRO+CMBRN+CMBRW)
      IF (CMBRH .GE. 0.2 .OR. TIME .LE. 10.) GO TO 955
      ICZ=0
      CMBRO=0.0
      CMBRN=0.0
      CMBRW=0.0
      CMBRH=0.0
      ROXLB=0.0
      RNILB=0.0
      RWALB=0.0
  955 CONTINUE
C
C*********************************
```

```
C*   CONVERT TEMP. TO DEG. F      *
C*********************************
C
      TSFPF=TSFP -460.
      TCZF=TCZ-460.
      TLIF=TLI-460.
      TGPF=TGP-460.
      TSPF=TSP-460.
      TEHCPF=TEHCP-460.
      IF (.NOT. FLAG2) GO TO 960
      TGSF=TGS-460.
      TFSF=TFS-460.
      TSSF=TSS-460.
      TEHCSF=TEHCS-460.
  960 CONTINUE
      IF (.NOT. FLAGPN) GO TO 961
      TPANF=TPAN-460.
      TINS1F=TINS1-460.
      TINS2F=TINS2-460.
  961 CONTINUE
      IF (.NOT. FLAGW) GO TO 1001
      DO 1001 I=1,20
      TCF(I)=TC(I)-460.
 1001 CONTINUE
      IF (.NOT. FLAGF) GO TO 1002
      DO 1002 I=1,20
      TBF(I) =TB(I)-460.
 1002 CONTINUE
      TCONF=TCON-460.
      IF (FLAGDF) TLEADF=TLEAD-460.
C
C*************************
C*   TIME STEP CONTROL     *
C*************************
C
      DT1=ABS(RELERR*TLI/ZZ1)
      DT2=ABS(RELERR*TGP/ZZ4)
      DT3=ABS(RELERR*TSP/ZZ5)
      IF (ILIT.EQ.0 .OR. ICZ.EQ.0) GO TO 965
      DT5=ABS(RELERR*TCZ/ZZ6)
      ZZ99=(CMBRH-CMBRHI)/DELT
      IF (ZZ99.EQ.0.) GO TO 965
      DT4=ABS(RELERR*CMBRH/ZZ99)
      CMBRHI=CMBRH
      IF (IPASS.EQ.1) DT4=1.E06
      GO TO 966
  965 CONTINUE
      DT4=1.0E06
      DT5=1.0E06
  966 CONTINUE
      IF (FLAGDF .AND. ZZPB .LT. 1.0E-15) ZZPB=1.0E-15
      IF (FLAGDF) DT6=ABS(RELERR*TLEAD/ZZPB)
      BILGE=AMIN1(DT1,DT2,DT3,DT4,DT5)
      IF (FLAGDF) BILGE=AMIN1(BILGE,DT6)
      BIL=(BILGE-DELT)/DELT
C   THIS CONDTION IS TO REMOVE INSTABILITY DUE TO STEEP
C    NITROGEN REACTION CURVE
      IF (TCZ .GT. 1900..AND.ABS(BIL).GT.0.1)DELT=DELT+(BILGE-DELT)/10.
      IF (.NOT.(TCZ.GT.1900..AND.ABS(BIL).GT.0.1)) DELT=BILGE
C
      IF (TIME .LT. 8000.) DELOUT=50.
      IF (TIME .LT. 800.) DELOUT=20.
      IF (TIME .LT. 120.) DELOUT=5.0
      IF (TIME .LT. 25.) DELOUT=0.2
      IF (TIME .LE. 3.0) DELOUT=0.1
      IF (TIME .GE. 8000.) DELOUT=600.
C*****  TEST CONDUCTION LIMITS ON TIME STEP   ***
C     LIMITING CONDUCTION RATE IS DETERMINED FROM POOL TO PAN
C     (IF USING PAN OPTION) OTHERWISE FROM POOL TO STEEL LINER
C
      IF (FLAGPN) ALPHA2=((THKPAN+ZLI)/(ZLI/AKLI+THKPAN/KPAN))/
     .   ((RHLI*CPLI*ZLI+RHPAN*CPPAN*THKPAN)/(THKPAN+ZLI))
```

```
      IF (FLAGPN) PYU=0.075*(THKPAN+ZLI)**2/ALPHA2
      IF (.NOT. FLAGPN) ALPHA2=((THFP+ZLI)/(ZLI/AKLI+THFP/KSTLFP))/
     .   ((RHLI*CPLI*ZLI+RHSFP*CPSFP*THFP)/(THFP+ZLI))
      IF (.NOT. FLAGPN) PYU=0.075*(THFP+ZLI)**2/ALPHA2
      IF (DELT .GT. PYU) DELT=PYU
C     CONDUCTION TEST FOR POOL LAYERS IF USING DIFFUSION MODEL
      IF (FLAGDF .AND. DELT .GT. PYUP) DELT=PYUP
C   TESTING TWO CELL EXCHANGE RATE ON TIME STEP
      IF (.NOT. FLAG2 .OR. ABS(XMDOT) .LT. 0.0001) GO TO 959
      IF ((ABS(PAP-PAS)) .LT. .01 .AND. DELT .GT. .04) DELT=.04
      DELMP=MAIRP/ABS(XMDOT)/250.
      DELMS=MAIRS/ABS(XMDOT)/250.
      IF (DELT .GT. DELMP)  DELT=DELMP
      IF (DELT .GT. DELMS) DELT=DELMS
  959 CONTINUE
C    AEROSOL REMOVAL TIME STEP CHECK
      IF (DELT*STICK .GT. .40) DELT=.40/STICK
C
      IF (DELT .GT. 3.0) DELT=3.0
C
      IF (DELT.LT.DTMIN) DELT=DTMIN
      IF (DELT .GT. DELOUT) DELT=DELOUT
C
C**********************
C*   OUTPUT SECTION    *
C**********************
C
      IF (TIME.LT.TIMEO) GO TO 978
      IF (FLAGSI) CALL SI
      TIMEO=TIMEO+DELOUT
      IF (IPAGE.LT.40) GO TO 974
      WRITE (11,830)  (NAME(I),I=1,80)
      WRITE (12,830)  (NAME(I),I=81,160)
      WRITE (13,830)  (NAME(I),I=161,240)
      WRITE (14,830)  (NAME(I),I=241,320)
  830 FORMAT(' ',3(20A4./),//,20A4)
  974 CONTINUE
      IF (IPAGE.GE.40) IPAGE=0
      IPAGE=IPAGE+1
      WRITE (11,826) TIME,DELT,TCZF,TLIF,TGPF,PAP,TSPF,TSFPF
      IF (FLAG2) WRITE (12,832) TIME,TGSF,TFSF,PAP,PAS,XMDOT
      IF (.NOT. FLAG2) WRITE (12,832) TIME,LIBP,CMBRH,MOXP,MNIP,RN2
      IF (FLAGPN) WRITE (13,832) TIME,TLIF,TPANF,TINS1F,TINS2F,PAP
      IF (.NOT. FLAGPN) WRITE (13,832) TIME,MNIP,MOXP,RN2,CMBRH,LIBP
      WRITE (14,832) TIME,XLIDOT,TLEADF,MLEAD,THPB,ZLI
  826 FORMAT(3X,F9.1,F6.2,F10.2,F10.2,4(1X,F7.2),F8.2)
  831 FORMAT(3X,F9.1,5F11.2)
  832 FORMAT(3X,F9.1,5E13.4)
      IF (FLAGSI) CALL SI
  975 CONTINUE
      IF (TIME.GT.TIMEF) GO TO 990
C***** RETURN TO TOP OF DYNAMIC CYCLE *****
      GO TO 200
C
C**********************
C*     ERROR POINTERS   *
C**********************
C
  976 CONTINUE
      WRITE (11,836)
  836 FORMAT(' POOL TEMP. HAS DROPPED TO LITHIUMS MELTING TEMP.')
      GO TO 990
  977 CONTINUE
      WRITE (11,836)
  836 FORMAT(' CELL GAS TEMP. AND PRESS. HAVE RETURNED TO NORMAL')
      GO TO 990
  978 CONTINUE
      WRITE (11,837)
  837 FORMAT(' LITHIUM TEMP. ABOVE BOILING POINT')
  838  FORMAT(1X,E12.4,E12.4)
      GO TO 990
  979 CONTINUE
```

```
      WRITE (11,838)
  838 FORMAT(1X,'NO ROOT FOUND FOR SPRAY FIRE FOR TEMP.S LESS THAN ',
     .       '1 MILLION DEG. R')
      GO TO 990
  980 CONTINUE
      WRITE (11,839)
  839 FORMAT (' SUSPENDED PAN OPTION CANNOT BE SELECTED CONCURRENT'/
     .        ' CONCRETE COMBUSTION OPTION')
      GO TO 990
  984 CONTINUE
      WRITE (11,844)
  844 FORMAT (' SPRAY FIRE AND LITHIUM LEAD COMBUSTION ARE NOT',
     .        ' COMPATIBLE')
      GO TO 990
  985 CONTINUE
      WRITE (11,845)
  845 FORMAT(' EXX IS NEGATIVE--CANNOT TAKE ROOT')
      WRITE (11,846) TCZ,CMBRH,ZZ6,ZZ8,RNZ
  846 FORMAT(' MESSED UP VARIABLES',5E10.3)
      GO TO 990
  986 CONTINUE
      WRITE (11,847) STICK,BETA
  847 FORMAT (' AEROSOL REMOVAL FRACTION IS TOO LARGE'/
     .       'STICK = ',F12.4,'    BETA = ',F12.4/)
      GO TO 990
  987 CONTINUE
  848 FORMAT(' LEAD LAYER THICKNESS IS GREATER THAN ZLI/3. DIFFUSION'/
     .' MODEL IS NO LONGER VALID'/)
  990 CONTINUE
      WRITE (11,867)
  867 FORMAT(' PROGRAM EXECUTION STOPPED BY PROGRAM')
      WRITE (11,868) DT1,DT2,DT3,DT4,DT6
  868 FORMAT(' VALUES', 6E10.3)
      close(unit=1)
      close(unit=2)
      close(unit=3)
      close(unit=4)
      close(unit=10)
      close(unit=11)
      close(unit=12)
      close(unit=13)
      close(unit=14)
      CALL EXIT
      END
```

```
C     THESE 3 SUBROUTINES ARE DESIGNED TO BE USED IN A MAIN PROGRAM WHICH
C     SIMULATES A DYNAMIC SYSTEM EXPRESSED AS A SET OF ODE'S. THESE ODE'S
C     MAY BE REEXPRESSED AS A SET OF INTEGRALS WHICH MUST BE INTEGRATED
C     SIMULTANEOUSLY THROUGH THE DOMAIN OF INTEREST STARTING WITH THE APPROPRIATE
C     INITIAL CONDITIONS.  FOR EXAMPLE, THE FUNCTION Y MAY BE FOUND FROM THE
C     SOLUTION OF  DY/DT = RATE = F(Y,T) AND Y=Y0 AT T=T0. THIS MAY BE
C     REWRITTEN Y = INTGRL(Y0, RATE). THE OPEN INTEGRAL OF RATE OVER T STARTING
C     AT Y0. A SET OF ODE'S MAY BE TREATED IN A SIMILIAR MANNER.
C         THE MAIN PROGRAM SHOULD CONSIST OF TWO MAIN PARTS, THE INITIALIZATION
C     SECTION AND THE DYNAMIC SECTION.  THE DYNAMIC SECTION IS FURTHER DIVIDED
C     INTO INTEGRATION AND POST-INTEGRATION SECTIONS.
C         THE INITIAL SECTION SHOULD BE USED FOR INPUT, CALCULATION OF NECESSARY
C     CONSTANTS, AND FOR CALCULATING AND SETTING OF INITIAL CONDITIONS. IT
C     SHOULD CONTAIN THE REAL INTGRL, COMMON, AND CALL INIT STATEMENTS.
C         THE INTEGRATION SECTION SHOULD START WITH A NUMBERED CONTINUE
C     STATEMENT AND END WITH THE CALL DYNAMI  STATEMENT.  IT SHOULD CONTAIN
C     ALL CALCULATIONS OF PROGRAM VARIABLES AND NON-CONSTANT RATES. ALL INTGRL
C     FUNCTION STATEMENTS SHOULD APPEAR IN A GROUP IMMEDIATELY PRECEDING THE
C     CALL DYNAMI STATEMENT.
C         THE INTEGRATION SECTION WILL BE LOOPED SEVERAL TIMES DURING EACH
C     INTEGRATION STEP (SIMPSON'S RULE USES 4 LOOPS PER STEP, RUNGE-KUTTA USES
```

```
C     5 LOOPS PER STEP).  DYNAMI CONTROLS THE INTEGRATION BY TELLING THE
C     INTGRL FUNCTION WHAT STEP IT SHOULD PERFORM NEXT. THE INTEGRATION
C     VARIABLE TIME IS ALSO CONTROLED BY DYNAMI.  IT MAY OR MAY NOT BE INCREMENT-
C     ED DURING EACH LOOP. TIME SHOULD BE INITIALIZED IN THE INTIAL SECTION.
C     DYNAMI UTILIZES MULTIPLE RETURNS TO CONTROL PROGRAM FLOW.  THE STATEMENT
C     NUMBER PASSED TO DYNAMI SHOULD BE THAT OF THE FIRST STATEMENT IN THE
C     INTEGRATION SECTION. THIS CAUSES THE PROPER INTEGRATION LOOPING. AT THE
C     END OF EACH INTEGRATION STEP A NORMAL RETURN IS EXECUTED AND CONTROL
C     RETURNS TO THE FIRST STATEMENT FOLLOWING CALL DYNAMI. THIS SHOULD BE
C     THE FIRST STATEMENT OF THE POST-INTEGRATION SECTION.
C         BECAUSE VARIABLE VALUES MAY DIFFER FROM THEIR TRUE VALUE DURING THE
C     INTEGRATION LOOPING, ALL PROGRAM LOGIC AND VARIABLE TIME STEP CALCULATIONS
C     EXECUTED ONCE AT THE END OF EACH INTEGRATION STEP. TIME AND ALL VARIABLES
C     CONTAINED WITHIN THE INTEGRATION SECTION WILL BE UPDATED TO THEIR 'TRUE'
C     VALUES BEFORE CONTROL IS TRANSFERED TO THE POST-INTEGRATION SECTION.
C     THIS SECTION SHOULD CONTAIN AT LEAST ONE IF STATEMENT WHICH STOPS PROGRAM
C     EXECUTION. AND THE LAST STATEMENT SHOULD BE A GO TO ST.NO. WHERE ST.NO.
C     IS THE STATEMENT NUMBER OF THE FIRST STATEMENT IN THE INTEGRATION SECTION.
C         APPROXIMATELY 100 INTEGRATIONS MAY BE PERFORMED SIMULTANEOUSLY.
C
C     VARIABLE LIST
C
C       A    MATRIX WHICH STORES THE INTERMIATE VALUES CALCULATED DURING EACH LOOP
C       DELT    INTEGRATION TIME STEP
C       DXDT    RATE BEING INTEGRATED. CALCULATED USING  INTEGRAL VALUE AS
C               RETURNED BY INTGRL DURING THE PREVIOUS LOOP AND TIME SET BY
C               DYNAMI.  USED BY INTGRL AS CALLED FOR BY ICOUNT.
C       ICOUNT   TELLS INTGRL WHICH INTEGRATION LOOP IS PRESENTLY BEING DONE
C       IMETH = 1 USE RUNGE-KUTTA METHOD
C             = 3 USE SIMPSON'S RULE
C       INOIN    TELL DYNAMI HOW MANY INTGRL STATEMENTS THERE ARE IN THE MAIN
C                PROGRAM.
C       IPASS    TELLS INTGRL TO DO TWO SPECIAL FUNCTIONS DURING THE FIRST TWO
C                EXECUTIONS OF THE INTEGRATION SECTION.
C       ISTORE    TELLS INTGRL WHERE TO STORE THE RESULT OF ITS INTERMEDIATE
C                CALCULATION IN MATRIX A.
C       XIC    MATRIX WHICH STORE  INTIAL CONDITIONS AND THEN IS UPDATED TO THE
C              PRESENT INTEGRAL VALUE AT THE END OF EACH INTEGRATION STEP.
C       XXIC    INITIAL CONDITION
C
      SUBROUTINE DYNAMI(TIME,*)
      COMMON /INTGL/ IMETH,ICOUNT,ISTORE,INOIN,IPASS,DELT,
     .               XIC(101),A(501)
      IF (IPASS.EQ.0) GO TO 40
      IF (IMETH.EQ.1) GO TO 10
C
C     SIMPSON'S RULE (DEFAULT) IMETH>2
C
      IF (ICOUNT.EQ.4) GO TO 4
      IF (ICOUNT.EQ.3) GO TO 3
      TIME=TIME+DELT/2.
      ICOUNT=ICOUNT+1
      RETURN 1
    4 CONTINUE
      ISTORE=0
      ICOUNT=1
      IPASS=IPASS+1
      INOIN=0
      RETURN
    3 CONTINUE
      ICOUNT =4
      RETURN 1
C
C     RUNGE-KUTTA METHOD -FIXED STEP-  IMETH=1
C
   10 CONTINUE
      IF (ICOUNT.EQ.5) GO TO 4
      IF (ICOUNT.EQ.4) GO TO 14
      IF (ICOUNT.EQ.2) GO TO 12
      TIME=TIME+DELT/2.
      ICOUNT=ICOUNT+1
      RETURN 1
```

```
   12 CONTINUE
      ICOUNT=3
      RETURN 1
   14 CONTINUE
      ICOUNT= 6
      RETURN 1
   40 CONTINUE
      IPASS=1
      RETURN
      END
C     THIS SUBROUTINE INITIALIZES VARIABLES USED BY THE INTEGRATION ROUTINES.
C     IT SHOULD BE PLACED IN THE INITIALIZATION SECTION OF THE MAIN PROGRAM
C     BEFORE THE FIRST STATEMENT OF THE DYNAMIC SECTION.  SEE DYNAMI FOR VARIABLE
C     LIST AND INTEGRATION DESCRIPTION.
C
      SUBROUTINE INIT
      COMMON /INTGL/ IMETH,ICOUNT,ISTORE,INOIN,IPASS,DELT,
     .               XIC(101),A(501)
      IPASS=0
      ISTORE=0
      ICOUNT=1
      INOIN=0
      RETURN
      END
C       FUNCTION INTGRL PERFORMS THE ACTUAL INTEGRATIONS. IN THE MAIN
C     PROGRAM, ALL INTGRL STATEMENTS SHOULD BE PLACED IN A GROUP AT THE END
C     OF THE INTEGRATION SECTION.  ALL RATE CALCULATIONS SHOULD PRECEDE THIS
C     GROUP AND IT SHOULD BE IMMEDIATELY FOLLOWED BY THE CALL DYNAMI STATEMENT.
C     FOR VARIABLE LIST AND DESCRIPTIONS SEE DYNAMI.
      REAL FUNCTION INTGRL(XXIC,DXDT)
      COMMON /INTGL/ IMETH,ICOUNT,ISTORE,INOIN,IPASS,DELT,
     .               XIC(101),A(501)
      IF (IPASS.EQ.0) GO TO 40
      ISTORE=ISTORE+1
      IF (IMETH.EQ.1) GO TO 10
C
C     SIMPSON'S RULE (DEFAULT) IMETH GREATER THAN 2
C
      IF (ICOUNT.EQ.4) GO TO 4
      IF (ICOUNT.EQ.3) GO TO 3
      IF (ICOUNT.EQ.2) GO TO 2
    1 CONTINUE
      INOIN=INOIN+1
      IF (IPASS.EQ.1) XIC(INOIN)=XXIC
      A(ISTORE)=DXDT
      INTGRL=XIC(INOIN)+DELT*DXDT/2.
      A(500-ISTORE)=INTGRL
      RETURN
    2 CONTINUE
      A(ISTORE)=DXDT
      INTGRL=A(500+INOIN-ISTORE)+DELT*DXDT/2.
      RETURN
    3 CONTINUE
      INTGRL=XIC(ISTORE-2*INOIN)+DELT/6.*(A(ISTORE-2*INOIN)+4.*
     .             A(ISTORE-INOIN)+DXDT)
      XIC(ISTORE-2*INOIN)=INTGRL
      RETURN
    4 CONTINUE
      INTGRL=XIC(ISTORE-3*INOIN)
      RETURN
C
C     RUNGE-KUTTA METHOD -FIXED STEP-  IMETH=1
C
   10 CONTINUE
      IF (ICOUNT.EQ.5) GO TO 15
      IF (ICOUNT.EQ.4) GO TO 14
      IF (ICOUNT.EQ.3) GO TO 13
      IF (ICOUNT.EQ.2) GO TO 12
   11 CONTINUE
      INOIN=INOIN+1
      IF (IPASS.EQ.1) XIC(INOIN)=XXIC
      A(ISTORE)=DELT*DXDT
```

```
      INTGRL=XIC(INOIN)+.5*A(ISTORE)
      RETURN
   12 CONTINUE
      A(ISTORE)=DELT*DXDT
      INTGRL=XIC(ISTORE-INOIN)+.5*A(ISTORE)
      RETURN
   13 CONTINUE
      A(ISTORE)=DELT*DXDT
      INTGRL=XIC(ISTORE-2*INOIN)+A(ISTORE)
      RETURN
   14 CONTINUE
      AA=DELT*DXDT
      INTGRL=XIC(ISTORE-3*INOIN)+1./6.*(A(ISTORE-3*INOIN)+2.*
     .     A(ISTORE-2*INOIN)+2.*A(ISTORE-INOIN)+AA)
      XIC(ISTORE-3*INOIN)=INTGRL
      RETURN
   15 CONTINUE
      INTGRL=XIC(ISTORE-4*INOIN)
      RETURN
   40 CONTINUE
      INTGRL=XXIC
      RETURN
      END
C
C
C
      FUNCTION AKEXX(T01,T02,RHOBAR)
      GINBAR=32.2
      TBAR=0.5*(T01+T02)
      BBAR=1.0/TBAR
      DBAR=((4.94E-05*TBAR+0.0188)/(RHOBAR*3600.))**2
      AKBAR=(0.014+1.92E-05*(TBAR-460.))/3600.
      EXBAR=(GINBAR*BBAR*ABS(T01-T02)/DBAR)**0.3333
      AKEXX=AKBAR*EXBAR
      RETURN
      END
C
C
C     THIS FUNCTION IS FOR CALCULATING THE PARTIAL PRESSURE OF LITHIUM IN
C         LITHIUM-LEAD AS A FUNCTION OF CONCENTRATION
      FUNCTION ACTVTY(XALI)
      ALILN=8.835*(XALI**2.219)-6.0
      IF (ALILN .GT. 0.0) ALILN=0.0
      ACTVTY=XALI*EXP(ALILN)
      RETURN
      END
C
C These subroutines are used to modularize litfire. they include the
C options of two cell geometry and pan geometry as well as floor and
C concrete combustion.
C
C  this is the secondary cell subroutine.
      SUBROUTINE CELL2
      IMPLICIT REAL (K,L,M)
      LOGICAL FLAGN,FLAGM,FLAGW,FLAGF,FLAG2
      COMMON // NAME(320),FLAG2,FLAGAS,FLAGC,FLAGF,FLAGN,
     .          FLAGPN,FLAGW,IPAGE,ISWICH,IAROSL,FLAGDF,ICZ
      COMMON /INTGL/ IMETH,ICOUNT,ISTORE,INOIN,IPASS,DELT,
     .               XIC(101),ZZZ(501)
      COMMON /LITH/ AKLI,ASLI,CPLI,CSBLI,HB,LIBP,LIL,LILP,LIT,
     .              RHLI,SPILL,TLI,TLII,ZLI
      COMMON /STEEL/ CPSFP,CPSFS,CPSWP,CPSWS,ESTLFP,ESTLWP,KSTLFP,
     .               KSTLFS,KSTLWP,KSTLWS,RHSFP,RHSFS,RHSWP,RHSWS
      COMMON /MISC/ AFP,AFS,AWP,AWS,C7,C21,GIN,
     .              HA,HINFAM,HINSAM,HTCPGP,QRADC,RADC,RCZW,
     .              RHOAP,RLIW,RWPWS,SIGMA,TA,TC(20),TFS,
     .              TFSZER,TGP,TGS,TGPZER,TSFP,TSP,TSS,
     .              TSSZER,THFP,THFS,THWP,THWS,ZZES,ZZ5,ZZS,ZZ1,ZZ7
      COMMON /CONOP/ C8,CPCON,DTBDT(20),DTCDT(20),GAP,KCON,KGAP,
     .               L(20),L1(20),NL,NL1,QRADB,RADB,RHCON,
     .               SFLCR,TB(20),TBF(20),TBIC(20),TCF(20),
     .               TCIC(20),THFC,THWC,TSFPI,TSPZER,XSFL
```

```
      COMMON /INJOP/ DP1,DP2,DP3,MNIINJ,MOXINJ,TIME,VP
      COMMON /SECOP/ AEHCS,C11,C20,CHS,CPEHCS,CPH2,CPL1H,CPWA,CRACK,
     .               FOUTP,FOUTS,FOUTT,HINFGS,HINFSG,HINGSS,HINPS,KLEAK,
     .               LEAK,MAIRP,MAIRS,MAIS,MAS,MH2S,MLIHS,MLINIS,MLINS,
     .               MLIOIS,MLIOS,MNIIS,MNIS,MOXIS,MOXS,MWAIS,
     .               MWAS,PAP,PAS,PASZER,RA,RBREAK,RHOLIH,
     .               RHOLIN,RHOLIO,RWPGAS,TEHCS,TEHCSF,TEHCZS,TGSF,
     .          TFSF,TGSZER,TSSF,VS,XMDOT,XMEHCS,XMOLA,ZZ3,ZZFS
C
      IF (FLAGN) N=1
      GO TO (1,2,3,4,5)N
    1 CONTINUE
C
C**********     READ IN SECONDARY CELL PARAMETERS AND      ********
C                    INITIAL CONDITIONS
C
      READ (2,701) VS,CHS,PASZER,TGSZER,TSSZER,TFSZER
      READ (2,701) CRACK,WWAS,WO2S,WAS,CPAS
      READ (2,701) TEHCZS,XMEHCS,AEHCS,CPEHCS,HINECS
      READ (2,701) ESTLWS,CPSWS,KSTLWS,RHSWS,AWS,THWS
      READ (2,701) ESTLFS,CPSFS,KSTLFS,RHSFS,AFS,THFS
      IF (ISWICH .EQ. 1) READ (2,701) TSWICH
C
      WRITE (10,800) CHS,VS,WO2S,WWAS,WAS,CPAS,CRACK
      WRITE (10,801) TEHCZS,XMEHCS,AEHCS,CPEHCS,HINECS
      WRITE (10,802) TGSZER,TSSZER,TFSZER,PASZER
      WRITE (10,803) ESTLWS,CPSWS,KSTLWS,RHSWS,AWS,THWS
      WRITE (10,804) ESTLFS,CPSFS,KSTLFS,RHSFS,AFS,THFS
      IF (ISWICH .EQ. 1) WRITE (10,810) TSWICH
C
  700 FORMAT(20A4)
  701 FORMAT (6F12.4)
  800 FORMAT (' SECONDARY CONTAINMENT DIMENSIONS'/1X,32(1H-)//T10,
     .'CHS =   ',F12.4,T35,'VS =    ',F12.4,T60,'WO2S =   ',F12.4//T10,
     .'WWAS =  ',F12.4,T35,'WAS =   ',F12.4,T60,'CPAS =   ',F12.4//T10,
     .'CRACK = ',F12.4//)
  801 FORMAT(' EXTRANEOUS HEAT CAPACITY NODE DATA'/1X,33(1H-)//T10,
     .'TEHCZS =',F12.4,T35,'XMEHCS =',F12.4,T60,'AEHCS = ',F12.4//
     .T10,'CPEHCS =',F12.4,T35,'HINECS =',F12.4//)
  802 FORMAT (' SECONDARY INITIAL CONDITIONS'/1X,28(1H-)//T10,
     .'TGSZER =',F12.4,T35,'TSSZER =',F12.4,T60,'TFSZER =',F12.4//T10,
     .'PASZER =',F12.4//)
  803 FORMAT (' SECONDARY STEEL WALL DATA'/1X,25(1H-)//T10,
     .'ESTLWS =',F12.4,T35,'CPSWS = ',F12.4,T60,'KSTLWS =',F12.4//T10,
     .'RHSWS = ',F12.4,T35,'AWS =   ',F12.4,T60,'THWS =  ',F12.4//)
  804 FORMAT (' SECONDARY STEEL FLOOR DATA'/1X,26(1H-)//T10,
     .'ESTLFS =',F12.4,T35,'CPSFS = ',F12.4,T60,'KSTLFS =',F12.4//T10,
     .'RHSFS = ',F12.4,T35,'AFS =   ',F12.4,T60,'THFS =  ',F12.4//)
  810 FORMAT (' CLOSING OF CRACK BETWEEN PRIMARY AND SECONDARY CELLS
     . IS'/'ALLOWED WHEN TIME IS GREATER THAN TSWICH =',F11.2//)
C
      N=2
      RETURN
    2 CONTINUE
C*********  INITIALIZE SECONDARY CELL CONTAINMENT VARIABLES   ********
      DATA BREAKS,FOUTP,FOUTS,FOUTT,MH2S,MLIHS,MLINIS,MLINS,MLIOIS,MLIOS
     .     ,RBREAK,XMDOT,ZZ3,ZZES/14*0.0/
C
      FLAGM=.FALSE.
      GAMMA=1.4
      CD=1.
      TEHCS=TEHCZS
      TSS=TSSZER
      THFS=THFP
      TFS=TFSZER
      TGS=TGSZER
      WN2S=1.-WO2S-WWAS-WAS
      XMOLS=1./(WO2S/32.+WN2S/28.+WWAS/18.+WAS/XMOLA)
      RINS=1545./XMOLS
      RHOAIS=PASZER*144./RINS/TGSZER
      RHOAS=RHOAIS
      MNIIS=WN2S*RHOAIS*VS
```

```
      MNIS=MNIIS
      MWAIS=WWAS*RHOAIS*VS
      MWAS=MWAIS
      MOXIS=WO2S*RHOAIS*VS
      MOXS=MOXIS
      MAIS=WAS*RHOAIS*VS
      MAS=MAIS
C**********     CONVERSION TO FT. - LB. - SEC.     **********
C
      CRACK=CRACK/144.
      KSTLWS=KSTLWS/3600.
      KSTLFS=KSTLFS/3600.
      N=3
      RETURN
    3 CONTINUE
C*****     COMPUTE PHYSICAL PROPERTIES DEPENDENT ON TEMPERATURE   *****
C*****  CALCULATE AIR COMPOSITION AND SPECIFIC HEAT AT CONST. VOLUME   ******
      MAIRS=MOXS+MNIS+MWAS+MH2S+MAS
      RHOAS=MAIRS/VS
      FOXS=MOXS/MAIRS
      FWAS=MWAS/MAIRS
      FNIS=MNIS/MAIRS
      CPO2S=(0.184+3.2E-06*TGS-1.36E04/(TGS*TGS))
      CPMOXS=CPO2S*MOXS
      CPN2S=(0.172+8.57E-06*TGS+1.02E-09*TGS*TGS)
      CPMNIS=CPN2S*MNIS
      CPLIOS=0.0602*TGS**.326
      CPLINS=0.3368+3.67E-04*TGS
      CPMLOS=CPLIOS*MLIOS
      HTCPGS=CPMOXS+CPMNIS+CPMLOS+CPAS*MAS+CPLINS*MLINS+CPLIH*MLIHS+
     .   CPH2*MH2S+CPWA*MWAS
C***** CALCULATING RADIATIVE INTERCHANGE FACTORS   *****
      EMGS=1.-EXP(-(MLIOS/RHOLIO+MLINS/RHOLIN+MLIHS/RHOLIH)*2.27E06*CHS/
     .   VS/RA)
      IF (EMGS .LE. 0.006) EMGS=0.006
      RIFPS=1./((1.-ESTLWP)/ESTLWP+(1.-ESTLWS)/ESTLWS*(AWP/AWS)+
     .   (1.+AWP/AWS)/(1.+AWP/AWS*(1.-EMGS)))
      RIFPGA=(ESTLWP*EMGS)/((1.-ESTLWP)*EMGS+ESTLWP)
      RIFFPS=1./((1.-ESTLFP)/ESTLFP+(1.-ESTLFS)/ESTLFS*(AFP/AFS)+
     .   (1.+AFP/AFS)/(1.+AFP/AFS*(1.-EMGS)))
      RIFFGS=(ESTLFP*EMGS)/((1.-ESTLFP)*EMGS+ESTLFP)
      RIFSCW=(ESTLWS*EMCONC)/(ESTLWS+EMCONC-ESTLWS*EMCONC)
      RIFSCF=(ESTLFS*EMCONC)/(ESTLFS+EMCONC-ESTLFS*EMCONC)
C**********     CALCULATING GAS HEAT TRANSFER COEFFICIENTS     **********
C  SECONDARY GAS TO SECONDARY EXTRANEOUS HEAT CAPACITY
      HEHCS=HINECS*AKEXX(TGS,TEHCS,RHOAS)
C  SECONDARY STEEL LINER TO SECONDARY GAS
      HSEC=HINGSS*AKEXX(TGS,TSS,RHOAS)
C  PRIMARY STEEL WALL LINER TO SECONDARY CONTAINMENT GAS
      HWPGAS=HINPS*AKEXX(TSP,TGS,RHOAS)
C  PRIMARY STEEL FLOOR LINER TO SECONDARY CONTAINMENT GAS
      HFPGAS=HINFGS*AKEXX(TSFP,TGS,RHOAS)
C  SECONDARY STEEL FLOOR TO SECONDARY CELL GAS
      HFSGAS=HINFSG*AKEXX(TFS,TGS,RHOAS)
C  SECONDARY STEEL LINER TO AMBIENT (SUPERCEDED BY CONCRETE TO AMBIENT
C       IF CONCRETE OPTION IN USE)
      IF (.NOT. FLAGW) HA=HINSAM*AKEXX(TSS,TA,.074)
C    SECONDARY STEEL FLOOR LINER TO AMBIENT
      IF (.NOT. FLAGF) HAMF=HINFAM*AKEXX(TFS,TA,.074)
  100 CONTINUE
C*****    CALCULATING THERMAL DIFFUSIVITIES BETWEEN NODES    *****
      C11=KSTLWS*HA/(RHSWS*CPSWS*THWS*(KSTLWS+THWS*HA/2.))
      C12=KSTLFS*HAMF/(RHSFS*CPSFS*AFS*(KSTLFS+THFS*HAMF/2.))
      C14=KSTLFS*HFSGAS/(RHSFS*CPSFS*THFS*(THFS*HFSGAS/2.+KSTLFS))
      C15=KSTLFS*HFSGAS*AFS/HTCPGS/(THFS*HFSGAS/2.+KSTLFS)
      C18=KSTLFP*HFPGAS/(RHSFP*CPSFP*THFP*(THFP*HFPGAS/2.+KSTLFP))
      C19=KSTLFP*HFPGAS*AFP/HTCPGS/(THFP*HFPGAS/2.+KSTLFP)
      C20=KSTLWP*HWPGAS/(RHSWP*CPSWP*THWP*(THWP*HWPGAS/2.+KSTLWP))
      C21=KSTLWS*HSEC/(RHSWS*CPSWS*THWS*(THWS*HSEC/2.+KSTLWS))
      C22=KSTLWP*HWPGAS*AWP/HTCPGS/(THWP*HWPGAS/2.+KSTLWP)
      C23=KSTLWS*HSEC*AWS/HTCPGS/(THWS*HSEC/2.+KSTLWS)
      CEHCGS=HEHCS*AEHCS/HTCPGS
```

```
      CGSEHC=HEHCS*AEHCS/XMEHCS/CPEHCS
C*****   CALCULATING RADIATIVE HEAT TRANSFER BETWEEN NODES   *****
      QRADPS=SIGMA*AWP*(TSP**4-TSS**4)*RIFPS
      RWPWS=QRADPS/(THWP*AWP*RHSWP*CPSWP)
      RWSWP=QRADPS/(THWS*AWS*RHSWS*CPSWS)
      QRADFS=SIGMA*AFP*(TSFP**4-TFS**4)*RIFFPS
      RFPFS=QRADFS/(THFP*AFP*RHSFP*CPSFP)
      RFSFP=QRADFS/(THFS*AFS*RHSFS*CPSFS)
      QRADPG=SIGMA*AWP*(TSP**4-TGS**4)*RIFPGA
      RWPGAS=QRADPG/(THWP*AWP*RHSWP*CPSWP)
      RSPGS=QRADPG/HTCPGS
      QRADFG=SIGMA*AFP*(TSFP**4-TGS**4)*RIFFGS
      RFPGAS=QRADFG/(THFP*AFP*RHSFP*CPSFP)
      RGASFP=QRADFG/HTCPGS
      N=4
      RETURN
    4 CONTINUE
C***** CALCULATING RADIATION FROM OUTER STEEL LINERS   *****
      IF (.NOT. FLAGW) QRADC=SIGMA*AWS*(TSS**4-TA**4)*ESTLWS
      IF (FLAGW) QRADC=SIGMA*AWS*(TSS**4-TC(1)**4)*RIFSCW
      RADC=QRADC/(THWS*AWS*RHSWS*CPSWS)
      IF (.NOT. FLAGF) QRADB=SIGMA*AFS*(TFS**4-TA**4)*ESTLFS
      IF (FLAGF) QRADB=SIGMA*AFS*(TFS**4-TB(1)**4)*RIFSCF
      RADB=QRADB/(THFS*AFS*RHSFS*CPSFS)
C* MODIFYING PRIMARY STEEL WALL AND FLOOR TEMPERATURE RATES OF CHANGE
      ZZ5=ZZ5-C20*(TSP-TGS)-RWPWS-RWPGAS
      ZZ7=ZZ7+CSBLI*(TLI-TSFP)-C18*(TSFP-TGS)-RFPFS-RFPGAS
CALCULATE EXTRANEOUS HEAT CAPACITY TEMPERATURE RATE OF CHANGE
      ZZES=CGSEHC*(TGS-TEHCS)
CALCULATE OUTER CELL GAS TEMPERATURE RATE OF CHANGE   DEG R/SEC
      ZZ3=BREAKS+RSPGS+C22*(TSP-TGS)+C23*(TSS-TGS)+CEHCGS*(TEHCS-TGS)
     .    +C19*(TSFP-TGS)+RGASFP+C15*(TFS-TGS)
CALCULATE OUTER WALL STEEL TEMPERATURE RATE OF CHANGE   DEG R/SEC
      IF (.NOT. FLAGW) ZZS=C21*(TGS-TSS)-C11*(TSS-TA)+RWSWP-RADC
      IF (FLAGW) ZZS=C21*(TGS-TSS)-C7*(TSS-TC(1))+RWSWP-RADC
CALCULATE OUTER FLOOR STEEL TEMPERATURE RATE OF CHANGE  DEG R/SEC
      IF (.NOT. FLAGW) ZZFS=C14*(TGS-TFS)-C12*(TFS-TA)+RFSFP-RADB
      IF (FLAGW) ZZFS=C14*(TGS-TFS)-C8*(TFS-TB(1))+RFSFP-RADB
      N=5
      RETURN
    5 CONTINUE
C**********************************
C**    CALCULATING OVERPRESSURE    **
C**********************************
      XMAIRS=MOXS/32.+MNIS/28.+MWAS/18.+MAS/XMOLA
      PAS=1545.*XMAIRS*TGS/144./VS
      OVERPS=PAS-PASZER
C**********************************
C**    CALCU. TOTAL  LEAKAGE     ***
C**********************************
      LEAK=KLEAK*(ABS(PAS-14.7))**0.5
      IF (PAS .LT. 14.7) LEAK=0.
      IF (ABS(PAP-PAS) .LT. 0.0006 .AND. ISWICH .EQ. 1 .AND.
     .    TIME .GT. TSWICH) CRACK=0.0
      IF (CRACK .EQ. 0.0 .AND. ISWICH .EQ. 1) WRITE (11,815) TIME
  815 FORMAT (' CELL PRESSURES HAVE EQUILIZED AT TIME = ',F11.2/
     .  'CRACK SIZE HAS BEEN SET TO ZERO FOR REMAINDER OF CALCULATION')
      IF (CRACK .EQ. 0.0) ISWICH=0
      IF (CRACK .EQ. 0.0) GO TO 112
      IF (ABS(PAP-PAS) .LT. 0.0006) GO TO 106
      IF (PAP-PAS) 101,106,107
C*****  FLOW OUT OF SECONDARY INTO PRIMARY  *****C
  101 FOUTP=0.
      IF (PAP/PAS .GE. 0.53) GO TO 103
C*****  SONIC  *****C
      IF (FLAGM) GO TO 102
C*****  FIRST TIME SONIC  *****C
      WRITE (12,816)
      IPAGE=IPAGE+1
      FLAGM=.TRUE.
  102 XMDOT=CD*CRACK*12.*SQRT(0.94*GIN*PAS*RHOAS)
      GO TO 105
```

```
C*****  SUBSONIC  *****C
  103 IF (.NOT. FLAGM) GO TO 104
C*****  FIRST TIME BACK TO NORMAL SUBSONIC  *****C
      WRITE (12,817)
      IPAGE=IPAGE+1
      FLAGM=.FALSE.
  104 XMDOT=CD*CRACK*SQRT(2.*GIN*(PAS-PAP)*RHOAS)*12.
  105 FOUTS=XMDOT/MAIRS
      RBREAK=XMDOT*(GAMMA*TGS-TGP)/(MAIRP+DELT*XMDOT)
      BREAKS=XMDOT*TGS*(1.-GAMMA)/(MAIRS-DELT*XMDOT)
      GO TO 112
C*****   NO FLOW   *****C
  106 FOUTP=0.
      FOUTS=0.
      XMDOT=0.
      RBREAK=0.
      BREAKS=0.
      GO TO 112
C*****  FLOW OUT OF PRIMARY INTO SECONDARY  *****C
  107 FOUTS=0.
      IF (PAS/PAP .GE. 0.53) GO TO 109
C*****   SONIC   *****C
      IF (FLAGM) GO TO 108
C*****  FIRST TIME SONIC   *****C
      WRITE (12,816)
      IPAGE=IPAGE+1
      FLAGM=.TRUE.
  108 XMDOT=CD*CRACK*12.*SQRT(0.94*GIN*PAP*RHOAP)
      GO TO 111
C*****   SUBSONIC   *****C
  109 IF (.NOT. FLAGM) GO TO 110
C*****  FIRST TIME BACK TO NORMAL SUBSONIC   *****C
      WRITE (12,817)
      IPAGE=IPAGE+1
      FLAGM=.FALSE.
  110 XMDOT=CD*CRACK*SQRT(2.*GIN*(PAP-PAS)*RHOAP)*12.
  111 FOUTP=ABS(XMDOT)/MAIRP
      RBREAK=ABS(XMDOT)*TGP*(1.-GAMMA)/(MAIRP-DELT*ABS(XMDOT))
      BREAKS=ABS(XMDOT)*(GAMMA*TGP-TGS)/(MAIRS+DELT*ABS(XMDOT))
      XMDOT=0.-XMDOT
  816 FORMAT (' FLOW BETWEEN PRIMARY AND SECONDARY HAS BECOME SONIC')
  817 FORMAT(' FLOW BETWEEN PRIMARY AND SECONDARY HAS RETURNED TO SUBSON
     .IC')
  112 CONTINUE
      FOUTT=FOUTS+LEAK
      N=3
      RETURN
      END
C
C
C
C  this is the pan geometry subroutine.
      SUBROUTINE PAN
      IMPLICIT REAL (K,L,M)
      LOGICAL FLAGN
      COMMON // NAME(320),FLAG2,FLAGAS,FLAGC,FLAGF,FLAGN,
     .          FLAGPN,FLAGW,IPAGE,ISWICH,IAROSL,FLAGDF,ICZ
      COMMON /LITH/ AKLI,ASLI,CPLI,CSBLI,HB,LIBP,LIL,LILP,LIT,
     .              RHLI,SPILL,TLI,TLII,ZLI
      COMMON /STEEL/ CPSFP,CPSFS,CPSWP,CPSWS,ESTLFP,ESTLWP,KSTLFP,
     .               KSTLFS,KSTLWP,KSTLWS,RHSFP,RHSFS,RHSWP,RHSWS
      COMMON /MISC/ AFP,AFS,AWP,AWS,C7,C21,GIN,
     .              HA,HINFAM,HINSAM,HTCPGP,QRADC,RADC,RCZW,
     .              RHOAP,RLIW,RWPWS,SIGMA,TA,TC(20),TFS,
     .              TFSZER,TGP,TGS,TGPZER,TSFP,TSP,TSS,
     .              TSSZER,THFP,THFS,THWP,THWS,ZZES,ZZS,ZZS,ZZ1,ZZ7
      COMMON /PANOP/ AINS,APAN,BREDTH,CLIST,CPINS,CPPAN,EMGP,FPG,FPW,
     .               KPAN,RHINS,RHPAN,THKIN1,THKIN2,THKPAN,
     .               TINS1,TINS1F,TINS1I,TINS2,TINS2F,TINS2I,
     .               TPAN,TPANF,TPANZO,ZZ2,ZZ4,ZZ8,ZZ9
C
      IF (FLAGN) N=1
```

```
      GO TO (1,2,3)N
    1 CONTINUE
C
C**********     READ IN PAN GEOMETRY PARAMETERS     **********
C              (ONLY IF USING PAN OPTION)
C
      READ (3,701) KPAN,RHPAN,CPPAN,RHINS,CPINS,EMINS
      READ (3,701) TPANZO,APAN,BREDTH,AINS,HINGPF
      READ (3,701) THKPAN,THKIN1,THKIN2
C
      WRITE (10,800) TPANZO,APAN,CPPAN,THKPAN,BREDTH,KPAN,RHPAN
      WRITE (10,801) THKIN1,THKIN2,AINS,RHINS,CPINS,EMINS,HINGPF
C
  700 FORMAT(20A4)
  701 FORMAT (6F12.4)
  800 FORMAT(///,' DATA FOR SUSPENDED PAN OPTIONAL GEOMETRY:',/,1X,
     .41(1H-),//T10,'TPANZO =',F12.4,T35,'APAN =  ',F12.4,T60,
     .'CPPAN = ',F12.4//T10,'THKPAN =',F12.4,T35,'BREDTH =',F12.4//T10,
     .'KPAN =  ',F12.4,T35,'RHPAN = ',F12.4//)
  801 FORMAT(//T10,'THKIN1 =',F12.4,T35,'THKIN2 =',F12.4,T60,'AINS =  '
     .,F12.4//T10,'RHINS = ',F12.4,T35,'CPINS = ',F12.4,T60,
     .'EMINS = ',F12.4//T10,'HINGPF =',F12.4//)
C
      N=2
      RETURN
    2 CONTINUE
C*********  INITIALIZE PAN GEOMETRY VARIABLES    *********
      FPG=0.23
      FPW=0.384
      TINS1I=0.5*(TPANZO+TGPZER)
      TINS2I=TGPZER
      TINS1=TINS1I
      TINS2=TINS2I
C  CONVERT THERMAL CONDUCTIVITY OF LI PAN TO BTU/SEC-FT-DEG R
      KPAN=KPAN/3600.
      N=3
      RETURN
    3 CONTINUE
C
C*****  COMPUTE PHYSICAL PROPERTIES DEPENDENT ON TEMPERATURE   *****
C
C*****      RADIATIVE INTERCHANGE FACTORS     *****
      RIFPAS=1./((1.-EMINS)/EMINS+(1.-ESTLFP)/ESTLFP*AINS/AFP+
     .   (AINS/AFP+1.)/(1.+AINS/AFP*(1.-EMGP)))
      RIFPAG=EMINS*EMGP/(EMINS+EMGP-EMINS*EMGP)
C
C**********     CALCULATING GAS HEAT TRANSFER COEFFICIENTS    **********
      HFPGP=HINGPF*AKEXX(TGP,TSFP,RHOAP)
C
C*****  CALCULATIONS WITH SUSPENDED LITHIUM SPILL PAN   *****
C
      HPAN=0.714*HB
      AHT=ASLI+ZLI*BREDTH
      TET1=0.0025*(TINS1-460.)-2.5
      KIN1=(.70892+.36584*TET1+.04565*TET1**2-.00791*TET1**3)/43200.
      TET2=0.0025*(TINS2-460.)-2.5
      KIN2=(.70892+.36584*TET2+.04565*TET2**2-.00791*TET2**3)/43200.
      YPAGAS=AINS/(THKIN2/2./KIN2+1./HPAN)
      C2=YPAGAS/HTCPGP
      C13=YPAGAS/(RHINS*AINS*THKIN2*CPINS)
      C16=KSTLFP*HFPGP/(RHSFP*CPSFP*THFP*(THFP*HFPGP/2.+KSTLFP))
      C17=KSTLFP*HFPGP*AFP/HTCPGP/(THFP*HFPGP/2.+KSTLFP)
      QRADS=SIGMA*AINS*(TINS2**4-TSFP**4)*RIFPAS
      QRADCG=SIGMA*AINS*(TINS2**4-TGP**4)*RIFPAG
      RPANST=QRADS/(RHSFP*AFP*THFP*CPSFP)
      RSTPAN=QRADS/(RHINS*AINS*THKIN2*CPINS)
      RGASPA=QRADCG/(RHINS*AINS*THKIN2*CPINS)
      RPAGAS=QRADCG/HTCPGP
      CLIPAN=2.*AHT/(LIL*CPLI)/(ZLI/AKLI+THKPAN/KPAN)
      CPANLI=2.*AHT/(RHPAN*APAN*THKPAN*CPPAN)/(ZLI/AKLI+THKPAN/KPAN)
      CPNIN1=2./(RHPAN*APAN*THKPAN*CPPAN)/(THKPAN/KPAN/APAN+THKIN1/
     .   KIN1/AINS)
```

```
      CIN1PN=2./(RHINS*AINS*THKIN1*CPINS)/(THKPAN/KPAN/APAN+THKIN1/
     .   KIN1/AINS)
      CIN12=2./(RHINS*CPINS*THKIN1)/(THKIN1/KIN1+THKIN2/KIN2)
      CIN21=CIN12*THKIN1/THKIN2
C****MODIFYING PRIMARY CELL TEMPERATURE RATES OF CHANGE DUE TO PAN  ***
      ZZ1=ZZ1+CLIST*(TLI-TSFP)-CLIPAN*(TLI-TPAN)
      ZZ4=ZZ4+C2*(TINS2-TGP)+RPAGAS+C17*(TSFP-TGP)
      ZZ7=ZZ7-CSBLI*(TLI-TSFP)+C16*(TGP-TSFP)+RPANST
C
C *****   CALCULATE LI SPILL PAN TEMP. RATE OF CHANGE  DEG R/SEC  *****
      ZZ2=CPANLI*(TLI-TPAN)+CPNIN1*(TINS1-TPAN)
C        CALCULATE INSULATION TEMPERATURE RATE OF CHANGE
      ZZ8=CIN1PN*(TPAN-TINS1)+CIN12*(TINS2-TINS1)
      ZZ9=CIN21*(TINS1-TINS2)+C13*(TGP-TINS2)-RSTPAN-RGASPA
      RETURN
      END
C  this is the wall concrete subroutine
      SUBROUTINE CONCW
      IMPLICIT REAL (K,L,M)
      DIMENSION  C4(20)
      LOGICAL FLAGN,FLAG2
      COMMON // NAME(320),FLAG2,FLAGAS,FLAGC,FLAGF,FLAGM,
     .          FLAGPN,FLAGW,IPAGE,ISWICH,IAROSL,FLAGDF,ICZ
      COMMON /LITH/ AKLI,ASLI,CPLI,CSBLI,HB,LIBP,LIL,LILP,LIT,
     .              RHLI,SPILL,TLI,TLII,ZLI
      COMMON /STEEL/ CPSFP,CPSFS,CPSWP,CPSWS,ESTLFP,ESTLWP,KSTLFP,
     .               KSTLFS,KSTLWP,KSTLWS,RHSFP,RHSFS,RHSWP,RHSWS
      COMMON /MISC/ AFP,AFS,AWP,AWS,C7,C21,GIN,
     .              HA,HINFAM,HINSAM,HTCPGP,QRADC,RADC,RCZW,
     .              RHOAP,RLIW,RWPWS,SIGMA,TA,TC(20),TFS,
     .              TFSZER,TGP,TGS,TGPZER,TSFP,TSP,TSS,
     .              TSSZER,THFP,THFS,THWP,THWS,ZZ5,ZZ6,ZZS,ZZ1,ZZ7
      COMMON /INTGL/ IMETH,ICOUNT,ISTORE,INOIN,IPASS,DELT,
     .               XIC(101),ZZZ(601)
      COMMON /CONOP/ C8,CPCON,DTBOT(20),DTCDT(20),GAP,KCON,KGAP,
     .               L(20),L1(20),NL,NL1,QRADB,RADB,RHCON,
     .               SFLCR,TB(20),TBF(20),TBIC(20),TCF(20),
     .               TCIC(20),THFC,THWC,TSFPI,TSPZER,XSFL
C
      IF (FLAGN) N=1
      GO TO (1,2,3)N
    1 CONTINUE
      NLM1=NL-1
C*****   INITIALIZE WALL CONCRETE VARIABLES   *****
      DATA C3,C5,C7,RADCC/4*0.0/
      IF (FLAG2) GO TO 100
      AWS=AWP
      CPSWS=CPSWP
      KSTLWS=KSTLWP
      RHSWS=RHSWP
      THWS=THWP
      TSSZER=TSPZER
  100 CONTINUE
      DO 1001 IAM=1,20
      C4(IAM)=0.
 1001 DTCDT(IAM)=0.
      DO 1002 I=1,NL
      TCIC(I)=TSSZER
      TC(I)=TSSZER
 1002 L(I)=THWC*L(I)
      N=2
      RETURN
    2 CONTINUE
C***** CALCULATING GAS HEAT TRANSFER COEFFICIENT FROM OUTERMOST *****
C               CONCRETE NODE TO AMBIENT
      TCNL=TC(NL)
      HA=HINSAM*AKEXX(TCNL,TA,.074)
C   *****     CALCULATING THERMAL DIFFUSIVITIES BETWEEN NODES     *****
      USUBA=KCON*HA/(KCON+HA*L(NL)/2.)
      B=L(1)/(KCON*2.)+GAP/KGAP+THWS/(KSTLWS*2.)
      C3=1./(B*L(1)*RHCON*CPCON)
      DO 1004 I=1,NLM1
```

```
      C4(I)=2.*KCON/(RHCON*CPCON*L(I)*(L(I)+L(I+1)))
 1004 CONTINUE
      C5=USUBA/(RHCON*CPCON*L(NL))
      C7=1./(B*THWS*RHSWS*CPSWS)
      N=3
      RETURN
    3 CONTINUE
      IF (.NOT. FLAG2) TSS=TSP
      RADCC=QRADC/(L(1)*AWS*RHCON*CPCON)
C*****          WALL CONCRETE TEPERATURE CHANGE          **********
      DTCDT(1)=C3*(TSS-TC(1))+C4(1)*(TC(2)-TC(1))+RADCC
      DTCDT(NL)=C4(NLM1)*(TC(NLM1)-TC(NL))-C5*(TC(NL)-TA)
      DO 1006 I=2,NLM1
 1006 DTCDT(I)=C4(I)*(TC(I+1)-TC(I))+C4(I-1)*(TC(I-1)-TC(I))
      N=2
      RETURN
      END
C
C
C  this is the floor concrete subroutine
      SUBROUTINE CONCF
      IMPLICIT REAL (K,L,M)
      DIMENSION  C10(20)
      LOGICAL FLAGN
      COMMON // NAME(320),FLAG2,FLAGAS,FLAGC,FLAGF,FLAGN,
     .          FLAGPN,FLAGW,IPAGE,ISWICH,IAROSL,FLAGDF,ICZ
      COMMON /LITH/ AKLI,ASLI,CPLI,CSBLI,HB,LIBP,LIL,LILP,LIT,
     .              RHLI,SPILL,TLI,TLII,ZLI
      COMMON /STEEL/ CPSFP,CPSFS,CPSWP,CPSWS,ESTLFP,ESTLWP,KSTLFP,
     .               KSTLFS,KSTLWP,KSTLWS,RHSFP,RHSFS,RHSWP,RHSWS
      COMMON /MISC/ AFP,AFS,AWP,AWS,C7,C21,GIN,
     .              HA,HINFAM,HINSAM,HTCPGP,QRADC,RADC,RCZW,
     .              RHOAP,RLIW,RWPWS,SIGMA,TA,TC(20),TFS,
     .              TFSZER,TGP,TGS,TGPZER,TSFP,TSP,TSS,
     .              TSSZER,THFP,THFS,THWP,THWS,ZZES,ZZ6,ZZS,ZZ1,ZZ7
      COMMON /INTGL/ IMETH,ICOUNT,ISTORE,INOIN,IPASS,DELT,
     .               XIC(101),ZZZ(501)
      COMMON /CONOP/ C8,CPCON,DTBDT(20),DTCDT(20),GAP,KCON,KGAP,
     .               L(20),L1(20),NL,NL1,QRADB,RADB,RHCON,
     .               SFLCR,TB(20),TBF(20),TBIC(20),TCF(20),
     .               TC1C(20),THFC,THWC,TSFPI,TSPZER,XSFL
C
      IF (FLAGN) N=1
      GO TO (1,2,3)N
    1 CONTINUE
      IF (FLAG2) GO TO 100
      AFS=AFP
      CPSFS=CPSFP
      KSTLFS=KSTLFP
      RHSFS=RHSFP
      THFS=THFP
      TFSZER=TSFPI
  100 CONTINUE
      NL1M1=NL1-1
C********   INITIALIZE FLOOR CONCRETE VARIABLES   ********
      DATA C8,C9,RADCB/3*0.0/
C
      DO 1001 IAM=1,20
      C10(IAM)=0.
 1001 DTBDT(IAM)=0.
      DO 1003 I=1,NL1
      TBIC(I)=TFSZER
      TB(I)=TFSZER
 1003 L1(I)=THFC*L1(I)
      N=2
      RETURN
C
    2 CONTINUE
C   *****     CALCULATING THERMAL DIFFUSIVITIES BETWEEN NODES     *****
      BB=L1(1)/(KCON*2.)+GAP/KGAP+THFS/(KSTLFS*2.)
      C8=1./(BB*THFS*RHSFS*CPSFS)
      C9=1./(BB*L1(1)*RHCON*CPCON)
```

```
      DO 1005 I=1,NL1M1
      C10(I)=2.*KCON/(RHCON*CPCON*L1(I)*(L1(I)+L1(I+1)))
 1005 CONTINUE
      N=3
      RETURN
    3 CONTINUE
      IF (.NOT. FLAG2) TFS=TSFP
      RADCB=QRADB/(L1(1)*AFS*RHCON*CPCON)
C*****          FLOOR CONCRETE TEMPERATURE CHANGE
      DTBDT(1)=C9*(TFS-TB(1))+C10(1)*(TB(2)-TB(1))+RADCB
      DTBDT(NL1)=C10(NL1M1)*(TB(NL1M1)-TB(NL1))
      DO 1007 IB=2,NL1M1
 1007 DTBDT(IB)=C10(IB)*(TB(IB+1)-TB(IB))+C10(IB-1)*(TB(IB-1)-TB(IB))
      N=2
      RETURN
      END
C
C
Cthis is the gas injection subroutine
      SUBROUTINE INJEC
      IMPLICIT REAL (K,L,M)
      LOGICAL FLAGN,FLAGAS
      COMMON // NAME(320),FLAG2,FLAGAS,FLAGC,FLAGF,FLAGN,
     .          FLAGPN,FLAGW,IPAGE,ISWICH,IAROSL,FLAGDF,ICZ
      COMMON /INJOP/ DP1,DP2,DP3,MNIINJ,MOXINJ,TIME,VP
      COMMON /MISC/ AFP,AFS,AWP,AWS,C7,C21,GIN,
     .              HA,HINFAM,HINSAM,HTCPGP,QRADC,RADC,RCZW,
     .              RHOAP,RLIW,RWPWS,SIGMA,TA,TC(20),TFS,
     .              TFSZER,TGP,TGS,TGPZER,TSFP,TSP,TSS,
     .              TSSZER,THFP,THFS,THWP,THWS,ZZES,ZZ6,ZZS,ZZ1,ZZ7
C
      IF (FLAGN) N=1
      GO TO (1,2)N
    1 CONTINUE
C
C*****   READ IN GAS INJECTION VARIABLES  *****
C.     (ONLY IF USING GAS INJECTION OPTION)
      READ (4,700) TONE,TTWO,TTHREE,DP1,DP2,DP3,FCT1,FCT2,FCT3
  700 FORMAT (3F10.2,6F8.4)
C
      WRITE (10,800) TONE,TTWO,TTHREE,DP1,DP2,DP3,FCT1,FCT2,FCT3
  800 FORMAT (///' DATA FOR GAS INJECTION MODELING:',/,1X,31(1H-),
     .//T10,'TONE =  ',F12.4,T35,'TTWO =  ',F12.4,T60,'TTHREE =',F12.4
     .//T10,'DP1 =   ',F12.4,T35,'DP2 =   ',F12.4,T60,'DP3 =   ',F12.4
     .//T10,'FCT1 =  ',F12.4,T35,'FCT2 =  ',F12.4,T60,'FCT3 =  ',F12.4)
C
      INJEC1=0
      INJEC2=0
      INJEC3=0
      N=2
      RETURN
    2 CONTINUE
C*****  INJECTION OF NITROGEN AND OXYGEN TO MODEL HEDL EXPERIMENT  ***
      IF (TIME .LT. TONE .OR. TIME .GT. (TONE+60.)) GO TO 100
      IF (INJEC1 .EQ. 0 .AND. DP1 .GT. 0.0) WRITE (11,801) TONE,DP1
  801 FORMAT (/,' INJECTION OF GAS AT TIME = ',F8.0,' TO RAISE
     .      PRESSURE BY',F8.4,'  PSI.')
      INJEC1=1
      MOINJ1=2.9822*VP/TGP*DP1*(1.0-FCT1)
      MNINJ1=2.6094*VP/TGP*DP1*FCT1
      MOXINJ=MOINJ1/60.
      MNIINJ=MNINJ1/60.
  100 CONTINUE
      IF (TIME .LT. TTWO .OR. TIME .GT. (TTWO+60.)) GO TO 101
      IF (INJEC2 .EQ. 0 .AND. DP2 .GT. 0.0) WRITE (11,801) TTWO,DP2
      INJEC2=1
      MOINJ2=2.9822*VP/TGP*DP2*(1.0-FCT2)
      MNINJ2=2.6094*VP/TGP*DP2*FCT2
      MOXINJ=MOINJ2/60.
      MNIINJ=MNINJ2/60.
  101 CONTINUE
      IF (TIME .LT. TTHREE .OR. TIME .GT. (TTHREE+60.)) GO TO 102
```

```
      IF (INJEC3 .EQ. 0 .AND. DP3 .GT. 0.0) WRITE (11,801) TTHREE,DP3
      INJEC3=1
      MOINJ3=2.9822*VP/TGP*DP3*(1.0-FCT3)
      MNINJ3=2.6094*VP/TGP*DP3*FCT3
      MOXINJ=MOINJ3/60.
      MNIINJ=MNINJ3/60.
  102 CONTINUE
      IF (TIME .GT. (TTHREE+60.)) FLAGAS=.FALSE.
      RETURN
      END
C
C
C
Cthis is the concrete combustion subroutine
      SUBROUTINE CONCC
      IMPLICIT REAL (K,L,M)
      LOGICAL FLAGN,FLAGD
      COMMON // NAME(320),FLAG2,FLAGAS,FLAGC,FLAGF,FLAGN,
     .          FLAGPN,FLAGW,IPAGE,ISWICH,IAROSL,FLAGDF,ICZ
      COMMON /LITH/ AKLI,ASLI,CPLI,CSBLI,HB,LIBP,LIL,LILP,LIT,
     .              RHLI,SPILL,TLI,TLII,ZLI
      COMMON /MISC/ AFP,AFS,AWP,AWS,C7,C21,GIN,
     .              HA,HINFAM,HINSAM,HTCPGP,QRADC,RADC,RCZW,
     .              RHOAP,RLIW,RWPWS,SIGMA,TA,TC(20),TFS,
     .              TFSZER,TGP,TGS,TGPZER,TSFP,TSP,TSS,
     .              TSSZER,THFP,THFS,THWP,THWS,ZZES,ZZS,ZZS,ZZ1,ZZ7
      COMMON /CONOP/ C8,CPCON,DT8DT(20),DTCDT(20),GAP,KCON,KGAP,
     .               L(20),L1(20),NL,NL1,QRADB,RADB,RHCON,
     .               SFLCR,TB(20),TBF(20),TBIC(20),TCF(20),
     .               TCIC(20),THFC,THWC,TSFPI,TSPZER,XSFL
      COMMON /CCOP/ CMBRO,CRACON,DCOCZ,H2LEFT,QCCONC,RCMBO,RCMBW,
     .              RELESE,TCIGNI,TCON,TCONF,XMH2OI,ZZC,ZZD,ZZDIN
C
      IF (FLAGN) N=1
      GO TO (1,2,3)N
    1 CONTINUE
C***** READ IN CONCRETE COMBUSTION PARAMETERS *******
      READ (3,700) ZZDIN,QCCONC,CRACON,XMH2OI,TCIGNI,RCMBC
  700 FORMAT (6F12.4)
C
      WRITE (10,800) ZZDIN,QCCONC,CRACON,XMH2OI,TCIGNI,RCMBC
  800 FORMAT (///' CONCRETE COMBUSTION INPUT DATA'/1X,30(1H-)//T10,
     .'ZZDIN = ',F12.4,T35,'QCCONC =',F12.4,T60,'CRACON =',F12.4//
     .T10,'XMH2OI =',F12.4,T35,'TCIGNI =',F12.4,T60,'RCMBC = ',F12.4//)
C
      N=2
      RETURN
    2 CONTINUE
      DATA CCOCOZ,CCOCZP,CCOZCO,CPCOCZ,RELESE,ZZC/6*0.0/
      ZZD=ZZDIN
      TCON=TSFPI
      DCOCZ=0.01
      XMCOCZ=1.0
      FLAGD=.FALSE.
      H2LEFT=XMH2OI
      VCONC=AFP*L1(1)
      N=3
      RETURN
    3 CONTINUE
C  WATER RELEASE FROM CONCRETE  --- CORRELATION BASED ON DRYING TESTS
C  OF MAGNITITE.  SEE R.D. PEAK "CACECO  A CONTAINMENT ANALYSIS CODE-
C  USERS GUIDE"
      RELESE=0.
      IF (TB(1) .GE. 658.6 .AND. TB(1) .LT. 1960.)  WATER=(1.-EXP(26.207
     .  +TB(1)*(-0.0721+TB(1)*(6.96E-05-TB(1)*2.26E-08)))/11.7)*XMH2OI
C  "WATER" IS THE AMOUNT THAT SHOULD BE LEFT AT TB(1) IN UNITS OF LBS./FT**3
      IF (TB(1) .GE. 658.6 .AND. (H2LEFT-WATER) .GT. 0. .AND. TB(1)
     .    .LT. 1960.) RELESE=(H2LEFT-WATER)*VCONC/30.
      IF (TB(1) .GE. 1960. .AND. H2LEFT .GT. 0.) RELESE=H2LEFT*VCONC/30.
C  IN OTHER WORDS THE RELEASE RATE OF WATER IS SUCH THAT THE DIFFERENCE
C  BETWEEN THE ACTUAL AMOUNT AND THE CORRECT AMOUNT ( ACCORDING TO THE
C  CORRELATION USED) IS GIVEN OFF IN THIRTY SECONDS.
```

```
C*****     CALCULATE THERMAL DIFFUSIVITIES     *****
      XMCOCZ=DCOCZ*CRACON*RHCON
      CPCOCZ=2.*CRACON*KCON*AKLI/(KCON*ZLI+AKLI*DCOCZ)/XMCOCZ
      CCOCZP=2.*CRACON*KCON*AKLI/(KCON*ZLI+AKLI*DCOCZ)/LIL
      CCOCOZ=2.*CRACON*KCON/(DCOCZ+L1(1))/XMCOCZ
      CCOZCO=2.*CRACON*KCON/(DCOCZ+L1(1))/(RHCON*CPCON*L1(1)*AFP)
C  FLAGD IS TRUE WHEN CONCRETE COMBUSTION STOPS
      FLAGD=.FALSE.
      IF (LILP .LT. 0.1 .OR. TCON .LT. TCIGNI) FLAGD=.TRUE.
      ZZD=ZZDIN
      IF (FLAGD) ZZD=0.0
      ZZC=CPCOCZ*(TLI-TCON)+CCOCOZ*(TB(1)-TCON)+ZZD*CRACON*QCCONC*RHCON
     .    /XMCOCZ/CPCON+RELESE*QCW*RCMBW/XMCOCZ/CPCON
      ZZ1=ZZ1+CCOCZP*(TCON-TLI)
      DTBDT(1)=DTBDT(1)+CCOCZO*(TCON-TB(1))
      CMBRO=RELESE*RCMBO+ZZD*CRACON*RHCON*RCMBC
      N=3
      RETURN
      END
C
C
C     THIS IS THE LITHIUM LEAD COMBUSTION SUBROUTINE
C
C
      SUBROUTINE LIPB
      IMPLICIT REAL (K,L,N)
      LOGICAL FLAGN,FLAGL
      COMMON /LITH/ AKLI,ASLI,CPLI,CSBLI,HB,LIBP,LIL,LILP,LIT,
     .              RHLI,SPILL,TLI,TLII,ZLI
      COMMON // NAME(320),FLAG2,FLAGAS,FLAGC,FLAGF,FLAGN,
     .          FLAGPN,FLAGW,IPAGE,ISWICH,IAROSL,FLAGDF,ICZ
      COMMON /LEAD/ CPLEAD,KLEAD,RHLEAD,MLIPB,XALLOY,ATML,ATMPB,CMBR
      COMMON /PBPOOL/ DMPBDT,ZZPB,MLEAD,TLEADI,XWLI,DFLIPB,XLIDOT,
     .                THPB,TLEADF
C
      IF (FLAGN) N=1
      GO TO (1,2,3)N
    1 CONTINUE
C
C*****    READ IN LEAD PARAMETERS     *****
C
      READ (3,701) CPLEAD,KLEAD,RHLEAD,ALLOYI,QDISS
C
      WRITE (10,800) CPLEAD,KLEAD,RHLEAD,ALLOYI,QDISS
C
  701 FORMAT (6F12.4)
  800 FORMAT(//,' DATA FOR LITHIUM LEAD COMBUSTION OPTION:',/,1X,40(1H-)
     .,//T10,'CPLEAD =',F12.4,T35,'KLEAD =',F12.4,T60,'RHLEAD =',F12.4//
     .T10,'ALLOYI =',F12.4,T35,'QDISS = ',F12.4//)
C
      KLEAD=KLEAD/3600.
      DFLIPB=DFLIPB/1.0E08
      ATMLPB=SPILL/(6.941*ALLOYI+(1.-ALLOYI)*207.2)
      ATMPB=(1.-ALLOYI)*ATMLPB
      ATMLI=ALLOYI*ATMLPB
      MLIPBI=SPILL
      SPILL=ATMLPB*6.941*ALLOYI
C
      WRITE (10,801) SPILL
  801 FORMAT(' MODIFIED PARAMETERS FOR LITHIUM IN LITHIUM LEAD POOL',/,
     .1X,52(1H-),//T10,' AMOUNT OF LITHIUM AVAILABLE FOR COMBUSTION =',
     .F12.4//T10,' THICKNESS OF LIPB POOL IS LESS THAN ZLI ABOVE AND',/
     .T35,' IS CALCULATED IN PROGRAM')
      N=2
      RETURN
C
    2 CONTINUE
C*****     MODIFYING LITHIUM POOL PROPERTIES TO INCLUDE LEAD     *****
C
      IF (FLAGDF) GO TO 100
      MLIPB=MLIPBI-LIBP
      XMLIPB=MLIPBI-LIT+LILP
```

```
      ATML=ATMLI-LIBP/6.941
      IF (ATML .LE. 0.0) ATML=0.0
      XALLOY=ATML/(ATML+ATMPB)
      GO TO 110
  100 CONTINUE
      MLIPB=MLIPBI-LIBP-MLEAD
      IF (MLIPB .LT. 0.0) MLIPB=0.0
      XMLIPB=MLIPB
      ATML=ATMLI*MLIPB/MLIPBI
      XALLOY=ALLOYI
  110 CONTINUE
      XWLI=XALLOY*6.941/(XALLOY*6.941+(1.-XALLOY)*207.2)
      AKLI=XWLI*AKLI+(1.-XWLI)*KLEAD-0.72*ABS(AKLI-KLEAD)*XWLI*(1.-XWLI)
      CPLI=XALLOY*CPLI+(1.-XALLOY)*CPLEAD
      RHLI=XALLOY*RHLI+(1.-XALLOY)*RHLEAD+332.6*XALLOY*(1.-XALLOY)**0.84
      ZLI=XMLIPB/RHLI/ASLI
      IF ((MLIPB .LT. 0.1*MLIPBI) .AND. (ALPHA*DELT .GT. ZLI*ZLI .OR.
     .   XMLIPB .LT. 1.0)) FLAGL=.TRUE.
      IF (FLAGL) LIL=MLIPBI/10.
      IF (.NOT. FLAGL) LIL=XMLIPB
      N=3
      RETURN
C
    3 CONTINUE
C*****     MODIFYING POOL TEMP RATE OF CHANGE TO INCLUDE HEAT OF LITHIUM    *****
C             DISSOCIATION FROM LEAD
      ZZ1=ZZ1-QDISS*CMBR*ASLI/(LIL*CPLI)
      N=2
      RETURN
      END
C
C
C     THIS IS THE LITHIUM LEAD DIFFUSION MODEL SUBROUTINE.
C
      SUBROUTINE LIDIFF
      IMPLICIT REAL (K,L,M)
      LOGICAL FLAGN,FLAGPB
      COMMON // NAME(320),FLAG2,FLAGAS,FLAGC,FLAGF,FLAGN,
     .          FLAGPN,FLAGW,IPAGE,ISWICH,IAROSL,FLAGDF,ICZ
      COMMON /LITH/ AKLI,ASLI,CPLI,CSBLI,HB,LIBP,LIL,LILP,LIT,
     .              RHLI,SPILL,TLI,TLII,ZLI
      COMMON /LEAD/ CPLEAD,KLEAD,RHLEAD,MLIPB,XALLOY,ATML,ATMPB,CMBR
      COMMON /INJOP/ DP1,DP2,DP3,MNIINJ,MOXINJ,TIME,VP
      COMMON /PBPCOL/ DMPBDT,ZZPB,MLEAD,TLEADI,XWLI,DFLIPB,XLIDOT,
     .                THPB,TLEADF
      COMMON /STEEL/ CPSFP,CPSFS,CPSWP,CPSWS,ESTLFP,ESTLWP,KSTLFP,
     .               KSTLFS,KSTLWP,KSTLWS,RHSFP,RHSFS,RHSWP,RHSWS
      COMMON /MISC/ AFP,AFS,AWP,AWS,C7,C21,GIN,
     .              HA,HINFAM,HINSAM,HTCPGP,QRADC,RADC,RCZW,
     .              RHOAP,RLIW,RWPWS,SIGMA,TA,TC(20),TFS,
     .              TFSZER,TGP,TGS,TGPZER,TSFP,TSP,TSS,
     .              TSSZER,THFP,THFS,THWP,THWS,ZZES,ZZS,ZZS,ZZ1,ZZ7
      COMMON /PANOP/ AINS,APAN,BREDTH,CLIST,CPINS,CPPAN,EMGP,FPG,FPW,
     .               KPAN,RHINS,RHPAN,THKIN1,THKIN2,THKPAN,
     .               TINS1,TINS1F,TINS1I,TINS2,TINS2F,TINS2I,
     .               TPAN,TPANF,TPANZO,ZZ2,ZZ4,ZZ8,ZZ9
      COMMON /UNITS/ AEHCP,BETA,CHP,CMBRH,CPAP,CPEHCP,MAP,MNIP,
     .               MOXP,MWAP,PAPZER,QCN,QCO,QCO1,QCO2,QCW,QVAP,
     .               TCZ,TCZF,TCZI,TEHCP,TEHCPF,TEHCZP,TGPF,
     .               TLIF,TMELT,TSFPF,TSPF,TVAP,XMEHCP
      COMMON /INTGL/ IMETH,ICOUNT,ISTORE,INOIN,IPASS,DELT,
     .               XIC(101),ZZZ(501)
      COMMON /PBDIF/ CCZP,CGLI,CLIG,CPCZ,CPMCZ,DFILM,KFILM,PYUP,
     .               QRADP,RCZP,RGLI,RIFCZP,RIFPG,RIFPW,RLIG,RWLI,
     .               TLEAD,YAPCZ,ZZ6
C
      IF (FLAGN) N=1
      GO TO (1,2,3)N
    1 CONTINUE
      TLEADI=TLII
      ZZPB=0.
      N=2
```

```
      RETURN
C
    2 CONTINUE
      THPB=MLEAD/RHLEAD/ASLI
      IF (THPB .LT. 1.0E-16) THPB=1.0E-16
      DFLIPB=6.5E-08*EXP(-1224./TLI)
      XLIDOT=DFLIPB*RHLI*XWLI/THPB
      DMPBDT=(1.-XALLOY)/XALLOY*CMBR*ASLI*207.2/6.941
      N=3
      RETURN
    3 CONTINUE
C
      ZLI1=.667*ZLI
      ZLI2=.333*ZLI
      KLIPB1=(MLEAD*KLEAD+.333*LIL*AKLI)/(MLEAD+.223*LIL)
      CPLPB1=(MLEAD*CPLEAD+.333*LIL*CPLI)
      THPB1=ZLI2+THPB
C
C*****     MODIFY POOL, COMBUSTION ZONE AND PRIMARY CELL TEMP RATES OF CHANGE
  100 CONTINUE
      IF (ICZ .EQ. 0) GO TO 110
      ZZ1=ZZ1-CCZP*(TCZ-TLI)-RCZP+QVAP*CMBR*ASLI*CCZP/YAPCZ+RWLI+RGLI
      ZZ4=ZZ4-RLIG
      ZZ5=ZZ5-RLIW
      ZZ6=ZZ6+CPCZ*(TCZ-TLI)+QRADP/CPMCZ
C
      CCLIPB=2.*ASLI*KLIPB1*AKLI/
     .       (.667*LIL*CPLI*(ZLI1*KLIPB1+THPB1*AKLI))
      CCPBLI=2.*KLIPB1*AKLI*ASLI/(CPLPB1*(2LI1*KLIPB1+THPB1*AKLI))
      YAPCZ=KFILM*KLIPB1*ASLI/(DFILM*KLIPB1+KFILM*THPB1/2.)
      CPCZ=YAPCZ/CPMCZ
      CCZP=YAPCZ/CPLPB1
      QRADP=SIGMA*ASLI*(TCZ**4-TLEAD**4)*RIFCZP
      RCZP=QRADP/CPLPB1
      QRADY=SIGMA*ASLI*(TLEAD**4-TSP**4)*RIFPW
      QRADZ=SIGMA*ASLI*(TLEAD**4-TGP**4)*RIFPG
      RLIW=QRADY/(THWP*AWP*RHSWP*CPSWP)
      RWLI=QRADY/CPLPB1
      RGLI=QRADZ/CPLPB1
      RLIG=QRADZ/HTCPGP
C
      ZZPB=CCZP*(TCZ-TLEAD)+RCZP-QVAP*CMBR*ASLI/CPLPB1
     .     -RWLI-RGLI-CCPBLI*(TLEAD-TLI)
      ZZ1=ZZ1+CCLIPB*(TLEAD-TLI)
      ZZ4=ZZ4+RLIG
      ZZ5=ZZ5+RLIW
      ZZ6=ZZ6-QRADP/CPMCZ-CPCZ*(TCZ-TLEAD)
      GO TO 120
  110 CONTINUE
C***** MODIFY TEMPS WITHOUT COMBUSTION ZONE MODELING *****
      ZZ1=ZZ1-CGLI*(TGP-TLI)+RWLI+RGLI
      ZZ4=ZZ4-CLIG*(TLI-TGP)-RLIG
      ZZ5=ZZ5-RLIW
C
      YALIG=KLIPB1*HB*ASLI/(KLIPB1+HB*THPB1/2.)
      CLIG=YALIG/HTCPGP
      QRADW=SIGMA*ASLI*(TLEAD**4-TSP**4)*RIFPW
      QRADG=SIGMA*ASLI*(TLEAD**4-TGP**4)*RIFPG
      RLIW=QRADW/(THWP*AWP*RHSWP*CPSWP)
      RWLI=QRADW/CPLPB1
      RGLI=QRADG/CPLPB1
      RLIG=QRADG/HTCPGP
      CGLI=YALIG/CPLPB1
      CCLIPB=2.*ASLI*KLIPB1*AKLI/
     .       (.667*LIL*CPLI*(ZLI1*KLIPB1+THPB1*AKLI))
      CCPBLI=2.*KLIPB1*ASLI*AKLI/(CPLPB1*(ZLI1*KLIPB1+THPB1*AKLI))
C
      ZZPB=CGLI*(TGP-TLEAD)-RWLI-RGLI-CCPBLI*(TLEAD-TLI)
      ZZ1=ZZ1+CCLIPB*(TLEAD-TLI)
      ZZ4=ZZ4+CLIG*(TLEAD-TGP)+RLIG
      ZZ5=ZZ5+RLIW
      ZZ6=(TLI-TCZ)/DELT
```

```
  120 CONTINUE
      ALPHAP=((THPB1+ZLI1)/(ZLI1/AKLI+THPB1/KLIPB1))/
     .   (((RHLI*CPLI*ZLI1)+(CPLPB1/ASLI))/(THPB1+ZLI1))
      PYUP=0.075*(THPB1+ZLI1)**2/ALPHAP
      N=2
      RETURN
      END
C
C this is the System International unit conversion subroutine allowing
C the input and output to be prepeared and written in SI units.
      SUBROUTINE SI
      IMPLICIT REAL (K,L,M)
      LOGICAL FLAGW,FLAGF,FLAG2,FLAGPN,FLAGC,FLAGAS,FLAGN
      COMMON // NAME(320),FLAG2,FLAGAS,FLAGC,FLAGF,FLAGN,
     .          FLAGPN,FLAGW,IPAGE,ISWICH,IAROSL,FLAGDF,ICZ
      COMMON /LITH/ AKLI,ASLI,CPLI,CS8LI,HB,LIBP,LIL,LILP,LIT,
     .              RHLI,SPILL,TLI,TLII,ZLI
      COMMON /STEEL/ CPSFP,CPSFS,CPSWP,CPSWS,ESTLFP,ESTLWP,KSTLFP,
     .               KSTLFS,KSTLWP,KSTLWS,RHSFP,RHSFS,RHSWP,RHSWS
      COMMON /MISC/ AFP,AFS,AWP,AWS,C7,C21,GIN,
     .              HA,HINFAM,HINSAM,HTCPGP,QRADC,RADC,RCZW,
     .              RHOAP,RLIW,RWPWS,SIGMA,TA,TC(20),TFS,
     .              TFSZER,TGP,TGS,TGPZER,TSFP,TSP,TSS,
     .              TSSZER,THFP,THFS,THWP,THWS,ZZES,ZZ5,ZZS,ZZ1,ZZ7
      COMMON /INJOP/ DP1,DP2,DP3,MNIINJ,MOXINJ,TIME,VP
      COMMON /PANOP/ AINS,APAN,BREDTH,CLIST,CPINS,CPPAN,EMGP,FPG,FPW,
     .               KPAN,RHINS,RHPAN,THKIN1,THKIN2,THKPAN,
     .               TINS1,TINS1F,TINS1I,TINS2,TINS2F,TINS2I,
     .               TPAN,TPANF,TPANZO,ZZ2,ZZ4,ZZ8,ZZ9
      COMMON /CONOP/ C8,CPCON,DTBOT(20),DTCOT(20),GAP,KCON,KGAP,
     .               L(20),L1(20),NL,NL1,QRADB,RADB,RHCON,
     .               SFLCR,TB(20),TBf(20),TBIC(20),TCF(20),
     .               TCIC(20),THFC,THWC,TSFPI,TSPZER,XSFL
      COMMON /CCOP/ CMBRG,CRACON,DCOC2,H2LEFT,QCCONC,RCMBO,RCMBW,
     .              RELESE,TCIGNI,TCON,TCONF,XMH2OI,ZZC,ZZD,ZZDIN
      COMMON /PBPOOL/ DMPBDT,ZZPB,MLEAD,TLEADI,XWLI,DFLIPB,XLIDOT,
     .                THPB,TLEADF
      COMMON /PBDIF/ CCZP,CGLI,CLIG,CPCZ,CPMCZ,DFILM,KFILM,PYUP,
     .               QRADP,RCZP,RGLI,RIFCZP,RIFPG,RIFPW,RLIG,RWLI,
     .               TLEAD,YAPCZ,ZZ6
      COMMON /SECOP/ AEHCS,C11,C20,CHS,CPEHCS,CPH2,CPLIH,CPWA,CRACK,
     .               FOUTP,FOUTS,FOUTT,HINFGS,HINFSG,HINGSS,HINPS,KLEAK,
     .               LEAK,MAIRP,MAIRS,MAIS,MAS,MH2S,MLIHS,MLINIS,MLINS,
     .               MLIOIS,MLIOS,MNIIS,MNIS,MOXIS,MOXS,MWAIS,
     .               MWAS,PAP,PAS,PASZER,RA,RBREAK,RHOLIH,
     .               RHOLIN,RHOLIO,RWPGAS,TEHCS,TEHCSF,TEHCZS,TGSF,
     .          TFSF,TGSZER,TSSF,VS,XMDOT,XMEHCS,XMOLA,ZZ3,ZZFS
      COMMON /UNITS/ AEHCP,BETA,CHP,CMBRH,CPAP,CPEHCP,MAP,MNIP,
     .               MOXP,MWAP,PAPZER,QCN,QCO,QCO1,QCO2,QCW,QVAP,
     .               TCZ,TCZF,TCZI,TEHCP,TEHCPF,TEHCZP,TGPF,
     .               TLIF,TMELT,TSFPF,TSPF,TVAP,XMEHCP
C
      IF (FLAGN) N=2
      GO TO (1,2,3)N
    1 CONTINUE
      AEHCP=AEHCP*10.766
      AFP=AFP*10.766
      AKLI=AKLI*0.57803
      ASLI=ASLI*10.766
      AWP=AWP*10.766
      CHP=CHP*3.281
      CPAP=CPAP*2.389E-04
      CPCON=CPCON*2.389E-04
      CPEHCP=CPEHCP*2.389E-04
      CPLI=CPLI*2.389E-04
      CPSFP=CPSFP*2.389E-04
      CPSWP=CPSWP*2.389E-04
      GAP=GAP*3.281
      KLEAK=KLEAK*0.03771
      KCON=KCON*0.57803
      KGAP=KGAP*0.57803
      KSTLFP=KSTLFP*0.57803
```

```
      KSTLWP=KSTLWP*0.57803
      PAPZER=PAPZER*1.450E-01
      QCN=QCN*4.311E-01
      QCO=QCO*4.311E-01
      QCO1=QCO1*4.311E-01
      QCO2=QCO2*4.311E-01
      QCW=QCW*4.311E-01
      QVAP=QVAP*4.311E-01
      RHCON=RHCON*0.062428
      RHLI=RHLI*0.062428
      RHOLIH=RHOLIH*0.062428
      RHOLIN=RHOLIN*0.062428
      RHOLIO=RHOLIO*0.062428
      RHSFP=RHSFP*0.062428
      RHSWP=RHSWP*0.062428
      SPILL=SPILL*2.2046
      TA=TA*1.8
      TCZI=TCZI*1.8
      TEHCZP=TEHCZP*1.8
      TGPZER=TGPZER*1.8
      THFC=THFC*3.281
      THWC=THWC*3.281
      THFP=THFP*3.281
      THWP=THWP*3.281
      TLII=TLII*1.8
      TMELT=TMELT*1.8
      TSFPI=TSFPI*1.8
      TSPZER=TSPZER*1.8
      TVAP=TVAP*1.8
      VP=VP*35.32
      XMEHCP=XMEHCP*2.2046
      ZLI=ZLI*3.281
C
      IF (.NOT. FLAG2) GO TO 100
      AEHCS=AEHCS*10.765
      AFS=AFS*10.765
      AWS=AWS*10.765
      CHS=CHS*3.281
      CPAS=CPAS*2.389E-04
      CPEHCS=CPEHCS*2.389E-04
      CPSFS=CPSFS*2.389E-04
      CPSWS=CPSWS*2.389E-04
      CRACK=CRACK*0.1550
      KSTLFS=KSTLFS*0.57803
      KSTLWS=KSTLWS*0.57803
      PASZER=PASZER*1.450E-01
      RHSFS=RHSFS*0.062428
      RHSWS=RHSWS*0.062428
      TEHCZS=TEHCZS*1.8
      TFSZER=TFSZER*1.8
      TGSZER=TGSZER*1.8
      THFS=THFS*3.281
      THWS=THWS*3.281
      TSSZER=TSSZER*1.8
      VS=VS*35.32
      XMEHCS=XMEHCS*2.2046
  100 CONTINUE
C
      IF (.NOT. FLAGPN) GO TO 101
      AINS=AINS*10.765
      APAN=APAN*10.765
      BREDTH=BREDTH*3.281
      CPINS=CPINS*2.389E-04
      CPPAN=CPPAN*2.389E-04
      KPAN=KPAN*0.57803
      RHINS=RHINS*0.062428
      RHPAN=RHPAN*0.062428
      THKIN1=THKIN1*3.281
      THKIN2=THKIN2*3.281
      THKPAN=THKPAN*3.281
      TPANZO=TPANZO*1.8
  101 CONTINUE
```

```
C
      IF (IBLOW .NE. 1) GO TO 102
      BLOWV=BLOWV*2119.2
      CPAB=CPAB*2.389E-04
      EXHSTV=EXHSTV*2119.2
      TBLOW=TBLOW*1.8
  102 CONTINUE
      IF (ISFLC .EQ. 1) SFLCR=SFLCR*9.475E-04
      IF (IESC .EQ. 1) ESCR=ESCR*9.475E-04
C
      IF (IAROSL .EQ. 1) BETA=BETA/3.281
C
      IF (.NOT. FLAGC) GO TO 103
      CRACON=CRACON*10.766
      QCCONC=QCCONC*4.311E-01
      TCIGNI=TCIGNI*1.8
      XMH2OI=XMH2OI*2.2046
      ZZDIN=ZZDIN*3.281
  103 CONTINUE
C
      IF (.NOT. FLAGAS) GO TO 104
      DP1=DP1*1.450E-01
      DP2=DP2*1.450E-01
      DP3=DP3*1.450E-01
  104 CONTINUE
C
      N=2
      RETURN
    2 CONTINUE
C
C***  THIS STEP CONVERTS OUTPUT VARIABLES TO SI  ***
C
      CMBRH=CMBRH*4.8824
      LIBP=LIBP/2.2046
      MAP=MAP/2.2046
      MNIP=MNIP/2.2046
      MOXP=MOXP/2.2046
      MWAP=MWAP/2.2046
      PAP=PAP/1.450E-01
      TCZF=TCZ/1.8-273.
      TEHCPF=TEHCP/1.8-273.
      TGPF=TGP/1.8-273.
      TLIF=TLI/1.8-273.
      TSFPF=TSFP/1.8-273.
      TSPF=TSP/1.8-273.
      ZLI=ZLI/3.281
      IF (.NOT. FLAG2) GO TO 106
      PAS=PAS/1.450E-01
      TEHCSF=TEHCS/1.8-273.
      TGSF=TGS/1.8-273.
      TFSF=TFS/1.8-273.
      TSSF=TSS/1.8-273.
      XMDOT=XMDOT/2.2046
  105 CONTINUE
      IF (FLAGPN) TPANF=TPAN/1.8-273.
      IF (FLAGPN) TINS1F=TINS1/1.8-273.
      IF (FLAGPN) TINS2F=TINS2/1.8-273.
      IF (FLAGC) TCONF=TCON/1.8-273.
      IF (.NOT. FLAGDF) GO TO 110
      MLEAD=MLEAD/2.2046
      THPB=THPB/3.281
      TLEADF=TLEAD/1.8-273.
      XLIDOT=XLIDOT*4.8824*3600.
  110 CONTINUE
      IF (.NOT. FLAGW) GO TO 1001
      DO 1001 I=1,20
      TCF(I)=TC(I)/1.8-273.
 1001 CONTINUE
      IF (.NOT. FLAGF) GO TO 1002
      DO 1002 I=1,20
      TBF(I)=TB(I)/1.8-273.
 1002 CONTINUE
```

```
      N=3
      RETURN
    3 CONTINUE
C
C****  THIS STEP CONVERTS OUTPUT FROM SI TO ENGLISH AFTER  ****
C       OUTPUT IS PRINTED SO THAT PROGRAM CAN CALCULATE
C      THINGS IN ENGLISH AGAIN. NOT NEEDED FOR OUTPUT TEMPS.
C
      CMBRH=CMBRH/4.8824
      LIBP=LIBP*2.2046
      MAP=MAP*2.2046
      MNIP=MNIP*2.2046
      MOXP=MOXP*2.2046
      MWAP=MWAP*2.2046
      PAP=PAP*1.450E-01
      ZLI=ZLI*3.281
      IF (FLAG2) PAS=PAS*1.450E-01
      IF (FLAG2) XMDOT=XMDOT*2.2046
      IF (FLAGDF) XLIDOT=XLIDOT/3600./4.8824
      IF (FLAGDF) MLEAD=MLEAD*2.2046
      IF (FLAGDF) THPB=THPB*3.281
      N=2
      RETURN
      END
```

APPENDIX E

Sample Input/Output for LITFIRE

```
   LA-5 HEDL TEST      LI-1;PB-4  THESIS RUNS
   USING VERSION OF LITFIRE: "LITFIR"
   DATE: 28 AUGUST, 1982
       TIME  DELT     TCZF      TLIF     TGPF      PAP    TSPF     TSFPF
 1 1 1 0 0 0 1 0 0 0 0 0 1 0
   5   5
  .20  .20  .20  .20  .20
  .20  .20  .20  .20  .20
  30086.00       66.70        0.1247     39.90
    543.0     12300.000     5100.0        0.120       0.09
     00.0840      00.0840       0.0000     0.015       0.00
      0.85         0.1200      30.00      497.5498   5600.00        0.0580
      0.85         0.1200      30.00      497.5498   4000.00        0.0580
      0.2          0.9960      33.80       30.00
      0.9          0.2550       0.0227    144.00
    124.00        86.9400     160.00        0.04        0.90        0.100
  18510.0          0.0        4080.0     13784.0
     0.8764        0.0           1.487       0.383       6.93
    815.0        2916.0        8431.0        0.0
      0.12         0.12          0.120       0.070       0.07        0.07
      0.07         0.07
     21.650      220.00          0.0000      0.050       5.0
   1140.0        549.175       546.96      546.0       540.53      1140.0
     16.433        0.2316        0.0062      0.0094
00030000000.20000009935.0000000000.00600002000.0000


  THIS OUTPUT CORRESPONDS TO ONE CELL GEOMETRY
   HEDL TEST CASE: LA-5
    DATE: 17 AUGUST 1982
     TIME        TGSF       TFSF        PAP         PAS         XMDOT
250000.00        44.00       14.7       534.00      534.00      534.00
    00.00        00.000       0.232      00.0000       0.1247
   534.1          1.0         00.00       1.00        0.0
     0.85         0.1200      30.00      497.5498  20960.10        0.0260
     0.85         0.1200      30.00      497.5498     88.00        0.0260
   350.00


   THIS IS THE PAN OUTPUT FILE      TESTING LIPB CODE
    HEDL TEST CASE: LA-5
    DATE: 24 AUGUST 1982
        TIME       TLIF       TPANF      TIWS1F      TIWS2F       PAP
0000013.00000000490.00000000000.12000000010.00000000000.20000000000.9000
    535.00        35.20        16.50        14.15          .000
      0.0157       0.1667       0.0833
      0.0350       9.30       708.00         0.2000   3315.0        10.7600



   CONCRETE NODAL TEMPERATURE PROFILES.

          TIME      TBF(1)      TBF(2)      TBF(3)      TBF(4)      TBF(5)
0000100.0000
```

UWMAK-III TWO CELL TEST CASES WITH CRACK=0.01 CM**2
USING VERSION OF LITFIRE: "AKEXX" IN SI UNITS
DATE: 12 august, 1982

TIME	DELT	TCZF	TLIF	TGPF	PAP	TSPF	TSBF
0.0	0.10	320.00	320.00	250.00	101.40	250.00	250.00
0.1	0.10	320.00	320.00	250.00	101.40	250.00	250.01
0.2	0.10	320.00	319.99	250.00	101.40	250.00	250.01
0.3	0.10	319.99	319.99	250.00	101.40	249.99	250.02
0.4	0.10	319.99	319.99	250.00	101.40	249.99	250.03
0.5	0.10	319.99	319.98	250.00	101.40	249.99	250.04
0.6	0.10	319.98	319.98	250.00	101.40	249.98	250.04
0.7	0.10	319.98	319.98	250.00	101.40	249.98	250.05
0.8	0.10	319.98	319.97	250.00	101.40	249.98	250.06
0.9	0.10	319.97	319.97	250.01	101.40	249.98	250.07
1.0	0.10	319.97	319.97	250.01	101.40	249.98	250.07
1.1	0.10	319.97	319.96	250.01	101.40	249.98	250.08
1.2	0.10	319.96	319.96	250.01	101.40	249.97	250.09
1.3	0.10	319.96	319.96	250.01	101.40	249.97	250.10
1.4	0.10	319.96	319.96	250.01	101.40	249.97	250.10
1.5	0.10	319.96	319.95	250.01	101.40	249.97	250.11
1.6	0.10	319.95	319.95	250.01	101.40	249.97	250.12
1.7	0.10	319.95	319.95	250.01	101.40	249.96	250.13
1.8	0.10	319.95	319.94	250.01	101.40	249.96	250.13
1.9	0.10	319.94	319.94	250.01	101.40	249.96	250.14
2.0	0.10	319.94	319.94	250.01	101.40	249.96	250.15
2.1	0.10	319.94	319.93	250.02	101.40	249.95	250.16
2.2	0.10	319.93	319.93	250.02	101.40	249.95	250.16
2.3	0.10	319.93	319.93	250.02	101.40	249.95	250.17
2.4	0.10	319.93	319.92	250.02	101.40	249.95	250.18
2.5	0.10	319.92	319.92	250.02	101.40	249.95	250.19
2.6	0.10	319.92	319.92	250.02	101.40	249.94	250.19
2.7	0.10	319.92	319.91	250.02	101.40	249.94	250.20
2.8	0.10	319.91	319.91	250.02	101.40	249.94	250.21
2.9	0.10	319.91	319.91	250.03	101.40	249.94	250.22
3.0	1.00	319.91	319.90	250.03	101.41	249.93	250.22
4.0	1.00	319.89	319.87	250.04	101.41	249.91	250.30
5.0	1.00	319.87	319.84	250.06	101.41	249.89	250.37
6.0	1.00	319.84	319.81	250.08	101.42	249.87	250.44
7.0	1.00	319.81	319.78	250.10	101.42	249.85	250.52
8.0	1.00	319.78	319.75	250.13	101.43	249.83	250.59
9.0	1.00	319.75	319.71	250.16	101.43	249.80	250.66
10.0	1.00	319.71	319.68	250.19	101.44	249.78	250.74
11.0	0.03	319.68	319.65	250.22	101.44	249.76	250.81
12.0	0.06	345.57	319.62	250.27	101.44	249.74	250.88

UWMAK-III TWO CELL TEST CASES WITH CRACK=0.01 CM**2
USING VERSION OF LITFIRE: "AKEXX" IN SI UNITS
DATE: 12 august, 1982

TIME	DELT	TCZF	TLIF	TGPF	PAP	TSPF	TSBF
13.0	0.07	359.26	319.59	250.32	101.45	249.72	250.96
14.0	0.08	368.12	319.57	250.39	101.45	249.70	251.03
15.1	0.08	374.71	319.56	250.47	101.46	249.67	251.11
16.0	0.09	379.72	319.55	250.56	101.47	249.65	251.17
17.0	0.10	384.55	319.53	250.65	101.48	249.63	251.25
18.0	0.10	388.93	319.52	250.75	101.48	249.61	251.32
19.1	0.11	393.40	319.51	250.87	101.50	249.59	251.39
20.1	0.12	397.56	319.51	250.99	101.51	249.57	251.47
21.1	0.12	401.39	319.50	251.11	101.52	249.55	251.54
22.1	0.13	405.37	319.50	251.24	101.53	249.53	251.61
23.1	0.14	409.51	319.49	251.39	101.55	249.51	251.68
24.1	0.14	413.27	319.49	251.54	101.56	249.49	251.75
25.1	0.15	417.18	319.49	251.71	101.58	249.46	251.83
30.2	0.19	435.67	319.50	252.63	101.67	249.36	252.18
35.1	0.22	452.73	319.54	253.74	101.79	249.26	252.53
40.1	0.26	469.50	319.60	255.09	101.94	249.16	252.88
45.2	0.30	485.35	319.69	256.64	102.11	249.06	253.23
50.0	0.34	499.66	319.80	258.28	102.30	248.96	253.56
55.1	0.39	513.96	319.93	260.18	102.51	248.86	253.91
60.4	0.43	528.07	320.09	262.33	102.75	248.76	254.27

THIS OUTPUT CORRESPONDS TO TWO CELL GEOMETRY
TEST CASE: UWMAK-III LARGE SPILL COMPARISON.
DATE: 12 august 1982

TIME	TGSF	TSSF	PAP	PAS	XMDOT
0.0	0.2700E+02	0.2700E+02	0.1014E+03	0.1014E+03	0.0000E+00
0.1	0.2700E+02	0.2700E+02	0.1014E+03	0.1014E+03	0.0000E+00
0.2	0.2700E+02	0.2700E+02	0.1014E+03	0.1014E+03	0.0000E+00
0.3	0.2700E+02	0.2700E+02	0.1014E+03	0.1014E+03	0.0000E+00
0.4	0.2700E+02	0.2700E+02	0.1014E+03	0.1014E+03	0.0000E+00
0.5	0.2700E+02	0.2700E+02	0.1014E+03	0.1014E+03	0.0000E+00
0.6	0.2700E+02	0.2700E+02	0.1014E+03	0.1014E+03	0.0000E+00
0.7	0.2700E+02	0.2700E+02	0.1014E+03	0.1014E+03	0.0000E+00
0.8	0.2700E+02	0.2700E+02	0.1014E+03	0.1014E+03	0.0000E+00
0.9	0.2700E+02	0.2700E+02	0.1014E+03	0.1014E+03	0.0000E+00
1.0	0.2700E+02	0.2700E+02	0.1014E+03	0.1014E+03	0.0000E+00
1.1	0.2701E+02	0.2700E+02	0.1014E+03	0.1014E+03	0.0000E+00
1.2	0.2701E+02	0.2700E+02	0.1014E+03	0.1014E+03	0.0000E+00
1.3	0.2701E+02	0.2700E+02	0.1014E+03	0.1014E+03	0.0000E+00
1.4	0.2701E+02	0.2700E+02	0.1014E+03	0.1014E+03	0.0000E+00
1.5	0.2701E+02	0.2700E+02	0.1014E+03	0.1014E+03	0.0000E+00
1.6	0.2701E+02	0.2700E+02	0.1014E+03	0.1014E+03	0.0000E+00
1.7	0.2701E+02	0.2700E+02	0.1014E+03	0.1014E+03	0.0000E+00
1.8	0.2701E+02	0.2700E+02	0.1014E+03	0.1014E+03	0.0000E+00
1.9	0.2701E+02	0.2700E+02	0.1014E+03	0.1014E+03	0.0000E+00
2.0	0.2701E+02	0.2700E+02	0.1014E+03	0.1014E+03	0.0000E+00
2.1	0.2701E+02	0.2700E+02	0.1014E+03	0.1014E+03	0.0000E+00
2.2	0.2701E+02	0.2700E+02	0.1014E+03	0.1014E+03	0.0000E+00
2.3	0.2701E+02	0.2700E+02	0.1014E+03	0.1014E+03	0.0000E+00
2.4	0.2701E+02	0.2700E+02	0.1014E+03	0.1014E+03	0.0000E+00
2.5	0.2701E+02	0.2700E+02	0.1014E+03	0.1014E+03	0.0000E+00
2.6	0.2701E+02	0.2700E+02	0.1014E+03	0.1014E+03	0.0000E+00
2.7	0.2701E+02	0.2700E+02	0.1014E+03	0.1014E+03	0.0000E+00
2.8	0.2701E+02	0.2700E+02	0.1014E+03	0.1014E+03	0.0000E+00
2.9	0.2701E+02	0.2700E+02	0.1014E+03	0.1014E+03	0.0000E+00
3.0	0.2701E+02	0.2700E+02	0.1014E+03	0.1014E+03	0.0000E+00
4.0	0.2702E+02	0.2700E+02	0.1014E+03	0.1014E+03	0.0000E+00
5.0	0.2702E+02	0.2700E+02	0.1014E+03	0.1014E+03	0.0000E+00
6.0	0.2703E+02	0.2700E+02	0.1014E+03	0.1014E+03	-0.2792E-05
7.0	0.2703E+02	0.2700E+02	0.1014E+03	0.1014E+03	-0.3411E-05
8.0	0.2704E+02	0.2700E+02	0.1014E+03	0.1014E+03	-0.4016E-05
9.0	0.2704E+02	0.2700E+02	0.1014E+03	0.1014E+03	-0.4609E-05
10.0	0.2705E+02	0.2700E+02	0.1014E+03	0.1014E+03	-0.5192E-05
11.0	0.2705E+02	0.2700E+02	0.1014E+03	0.1014E+03	-0.5766E-05
12.0	0.2706E+02	0.2700E+02	0.1014E+03	0.1014E+03	-0.5796E-05

THIS OUTPUT CORRESPONDS TO TWO CELL GEOMETRY
TEST CASE: UWMAK-III LARGE SPILL COMPARISON.
DATE: 12 august 1982

TIME	TGSF	TSSF	PAP	PAS	XMDOT
13.0	0.2706E+02	0.2701E+02	0.1014E+03	0.1014E+03	-0.6051E-05
14.0	0.2707E+02	0.2701E+02	0.1015E+03	0.1014E+03	-0.6447E-05
15.1	0.2707E+02	0.2701E+02	0.1015E+03	0.1014E+03	-0.6936E-05
16.0	0.2708E+02	0.2701E+02	0.1015E+03	0.1014E+03	-0.7436E-05
17.0	0.2708E+02	0.2701E+02	0.1015E+03	0.1014E+03	-0.8016E-05
18.0	0.2709E+02	0.2701E+02	0.1015E+03	0.1014E+03	-0.8613E-05
19.1	0.2709E+02	0.2701E+02	0.1015E+03	0.1014E+03	-0.9280E-05
20.1	0.2710E+02	0.2701E+02	0.1015E+03	0.1014E+03	-0.9943E-05
21.1	0.2710E+02	0.2701E+02	0.1015E+03	0.1014E+03	-0.1059E-04
22.1	0.2711E+02	0.2701E+02	0.1015E+03	0.1014E+03	-0.1128E-04
23.1	0.2711E+02	0.2701E+02	0.1015E+03	0.1014E+03	-0.1203E-04
24.1	0.2712E+02	0.2701E+02	0.1016E+03	0.1014E+03	-0.1273E-04
25.1	0.2712E+02	0.2701E+02	0.1016E+03	0.1014E+03	-0.1348E-04
30.2	0.2715E+02	0.2701E+02	0.1017E+03	0.1014E+03	-0.1729E-04
35.1	0.2717E+02	0.2701E+02	0.1018E+03	0.1015E+03	-0.2113E-04
40.1	0.2719E+02	0.2702E+02	0.1019E+03	0.1015E+03	-0.2516E-04
45.2	0.2722E+02	0.2702E+02	0.1021E+03	0.1015E+03	-0.2919E-04
50.0	0.2724E+02	0.2702E+02	0.1023E+03	0.1015E+03	-0.3298E-04
55.1	0.2727E+02	0.2702E+02	0.1025E+03	0.1016E+03	-0.3689E-04
60.4	0.2729E+02	0.2702E+02	0.1028E+03	0.1015E+03	-0.4085E-04

THIS IS THE PAN OUTPUT FILE
UWHAK-III SPILL TWO CELL CODE
DATE: 7 august 1982

TIME	MNIP	MOXP	RN2	CMBRH	LIBP
0.0	0.4909E+03	0.1480E+03	0.0000E+00	0.8042E-03	0.0000E+00
0.1	0.4909E+03	0.1480E+03	0.0000E+00	0.1151E-01	0.0000E+00
0.2	0.4909E+03	0.1480E+03	0.0000E+00	0.2218E-01	0.0000E+00
0.3	0.4909E+03	0.1480E+03	0.0000E+00	0.3282E-01	0.0000E+00
0.4	0.4909E+03	0.1480E+03	0.0000E+00	0.4342E-01	0.0000E+00
0.5	0.4909E+03	0.1480E+03	0.0000E+00	0.5398E-01	0.0000E+00
0.6	0.4909E+03	0.1480E+03	0.0000E+00	0.6451E-01	0.0000E+00
0.7	0.4909E+03	0.1480E+03	0.0000E+00	0.7500E-01	0.0000E+00
0.8	0.4909E+03	0.1480E+03	0.0000E+00	0.8546E-01	0.0000E+00
0.9	0.4909E+03	0.1480E+03	0.0000E+00	0.9588E-01	0.0000E+00
1.0	0.4909E+03	0.1480E+03	0.0000E+00	0.1063E+00	0.0000E+00
1.1	0.4909E+03	0.1480E+03	0.0000E+00	0.1166E+00	0.0000E+00
1.2	0.4909E+03	0.1480E+03	0.0000E+00	0.1269E+00	0.0000E+00
1.3	0.4909E+03	0.1480E+03	0.0000E+00	0.1372E+00	0.0000E+00
1.4	0.4909E+03	0.1480E+03	0.0000E+00	0.1475E+00	0.0000E+00
1.5	0.4909E+03	0.1480E+03	0.0000E+00	0.1577E+00	0.0000E+00
1.6	0.4909E+03	0.1480E+03	0.0000E+00	0.1679E+00	0.0000E+00
1.7	0.4909E+03	0.1480E+03	0.0000E+00	0.1780E+00	0.0000E+00
1.8	0.4909E+03	0.1480E+03	0.0000E+00	0.1881E+00	0.0000E+00
1.9	0.4909E+03	0.1480E+03	0.0000E+00	0.1982E+00	0.0000E+00
2.0	0.4909E+03	0.1480E+03	0.0000E+00	0.2082E+00	0.0000E+00
2.1	0.4909E+03	0.1480E+03	0.0000E+00	0.2183E+00	0.0000E+00
2.2	0.4909E+03	0.1480E+03	0.0000E+00	0.2282E+00	0.0000E+00
2.3	0.4909E+03	0.1480E+03	0.0000E+00	0.2382E+00	0.0000E+00
2.4	0.4909E+03	0.1480E+03	0.0000E+00	0.2481E+00	0.0000E+00
2.5	0.4909E+03	0.1480E+03	0.0000E+00	0.2580E+00	0.0000E+00
2.6	0.4909E+03	0.1480E+03	0.0000E+00	0.2678E+00	0.0000E+00
2.7	0.4909E+03	0.1480E+03	0.0000E+00	0.2776E+00	0.0000E+00
2.8	0.4909E+03	0.1480E+03	0.0000E+00	0.2874E+00	0.0000E+00
2.9	0.4909E+03	0.1480E+03	0.0000E+00	0.2971E+00	0.0000E+00
3.0	0.4909E+03	0.1480E+03	0.0000E+00	0.3068E+00	0.0000E+00
4.0	0.4909E+03	0.1480E+03	0.0000E+00	0.4025E+00	0.0000E+00
5.0	0.4909E+03	0.1480E+03	0.0000E+00	0.4950E+00	0.0000E+00
6.0	0.4909E+03	0.1480E+03	0.0000E+00	0.5844E+00	0.0000E+00
7.0	0.4909E+03	0.1480E+03	0.0000E+00	0.6709E+00	0.0000E+00
8.0	0.4909E+03	0.1480E+03	0.0000E+00	0.7544E+00	0.0000E+00
9.0	0.4909E+03	0.1480E+03	0.0000E+00	0.8352E+00	0.0000E+00
10.0	0.4909E+03	0.1480E+03	0.0000E+00	0.9133E+00	0.0000E+00
11.0	0.4909E+03	0.1480E+03	0.2693E-01	0.9887E+00	0.0000E+00
12.0	0.4909E+03	0.1479E+03	0.3099E-01	0.1091E+01	0.4383E-01

THIS IS THE PAN OUTPUT FILE
UWHAK-III SPILL TWO CELL CODE
DATE: 7 august 1982

TIME	MNIP	MOXP	RN2	CMBRH	LIBP
13.0	0.4909E+03	0.1479E+03	0.3330E-01	0.1194E+01	0.9149E-01
14.0	0.4909E+03	0.1478E+03	0.3487E-01	0.1298E+01	0.1446E+00
15.1	0.4909E+03	0.1478E+03	0.3609E-01	0.1403E+01	0.2029E+00
16.0	0.4909E+03	0.1477E+03	0.3704E-01	0.1499E+01	0.2601E+00
17.0	0.4909E+03	0.1476E+03	0.3797E-01	0.1600E+01	0.3258E+00
18.0	0.4908E+03	0.1476E+03	0.3884E-01	0.1699E+01	0.3940E+00
19.1	0.4908E+03	0.1475E+03	0.3975E-01	0.1804E+01	0.4712E+00
20.1	0.4908E+03	0.1474E+03	0.4062E-01	0.1903E+01	0.5497E+00
21.1	0.4908E+03	0.1474E+03	0.4143E-01	0.1997E+01	0.6273E+00
22.1	0.4908E+03	0.1473E+03	0.4228E-01	0.2094E+01	0.7133E+00
23.1	0.4908E+03	0.1472E+03	0.4319E-01	0.2197E+01	0.8085E+00
24.1	0.4908E+03	0.1471E+03	0.4403E-01	0.2291E+01	0.9003E+00
25.1	0.4908E+03	0.1470E+03	0.4492E-01	0.2389E+01	0.1001E+01
30.2	0.4907E+03	0.1465E+03	0.4934E-01	0.2858E+01	0.1552E+01
35.1	0.4906E+03	0.1460E+03	0.5377E-01	0.3298E+01	0.2180E+01
40.1	0.4905E+03	0.1453E+03	0.5848E-01	0.3739E+01	0.2924E+01
45.2	0.4903E+03	0.1446E+03	0.6329E-01	0.4163E+01	0.3757E+01
50.0	0.4902E+03	0.1439E+03	0.6795E-01	0.4553E+01	0.4631E+01
55.1	0.4900E+03	0.1431E+03	0.7295E-01	0.4950E+01	0.5636E+01
60.4	0.4897E+03	0.1422E+03	0.7823E-01	0.5349E+01	0.6772E+01

CONCRETE NODAL TEMPERATURE PROFILES.

TIME	TBF(1)	TBF(2)	TBF(8)	TCF(1)	TCF(8)
0.0	0.2700E+02	0.2700E+02	0.2700E+02	0.2700E+02	0.2700E+02
0.1	0.2700E+02	0.2700E+02	0.2700E+02	0.2700E+02	0.2700E+02
0.2	0.2700E+02	0.2700E+02	0.2700E+02	0.2700E+02	0.2700E+02
0.3	0.2700E+02	0.2700E+02	0.2700E+02	0.2700E+02	0.2700E+02
0.4	0.2700E+02	0.2700E+02	0.2700E+02	0.2700E+02	0.2700E+02
0.5	0.2700E+02	0.2700E+02	0.2700E+02	0.2700E+02	0.2700E+02
0.6	0.2700E+02	0.2700E+02	0.2700E+02	0.2700E+02	0.2700E+02
0.7	0.2700E+02	0.2700E+02	0.2700E+02	0.2700E+02	0.2700E+02
0.8	0.2700E+02	0.2700E+02	0.2700E+02	0.2700E+02	0.2700E+02
0.9	0.2700E+02	0.2700E+02	0.2700E+02	0.2700E+02	0.2700E+02
1.0	0.2700E+02	0.2700E+02	0.2700E+02	0.2700E+02	0.2700E+02
1.1	0.2700E+02	0.2700E+02	0.2700E+02	0.2700E+02	0.2700E+02
1.2	0.2700E+02	0.2700E+02	0.2700E+02	0.2700E+02	0.2700E+02
1.3	0.2700E+02	0.2700E+02	0.2700E+02	0.2700E+02	0.2700E+02
1.4	0.2700E+02	0.2700E+02	0.2700E+02	0.2700E+02	0.2700E+02
1.5	0.2700E+02	0.2700E+02	0.2700E+02	0.2700E+02	0.2700E+02
1.6	0.2700E+02	0.2700E+02	0.2700E+02	0.2700E+02	0.2700E+02
1.7	0.2700E+02	0.2700E+02	0.2700E+02	0.2700E+02	0.2700E+02
1.8	0.2700E+02	0.2700E+02	0.2700E+02	0.2700E+02	0.2700E+02
1.9	0.2700E+02	0.2700E+02	0.2700E+02	0.2700E+02	0.2700E+02
2.0	0.2700E+02	0.2700E+02	0.2700E+02	0.2700E+02	0.2700E+02
2.1	0.2700E+02	0.2700E+02	0.2700E+02	0.2700E+02	0.2700E+02
2.2	0.2700E+02	0.2700E+02	0.2700E+02	0.2700E+02	0.2700E+02
2.3	0.2700E+02	0.2700E+02	0.2700E+02	0.2700E+02	0.2700E+02
2.4	0.2700E+02	0.2700E+02	0.2700E+02	0.2700E+02	0.2700E+02
2.5	0.2700E+02	0.2700E+02	0.2700E+02	0.2700E+02	0.2700E+02
2.6	0.2700E+02	0.2700E+02	0.2700E+02	0.2700E+02	0.2700E+02
2.7	0.2700E+02	0.2700E+02	0.2700E+02	0.2700E+02	0.2700E+02
2.8	0.2700E+02	0.2700E+02	0.2700E+02	0.2700E+02	0.2700E+02
2.9	0.2700E+02	0.2700E+02	0.2700E+02	0.2700E+02	0.2700E+02
3.0	0.2700E+02	0.2700E+02	0.2700E+02	0.2700E+02	0.2700E+02
4.0	0.2700E+02	0.2700E+02	0.2700E+02	0.2700E+02	0.2700E+02
5.0	0.2700E+02	0.2700E+02	0.2700E+02	0.2700E+02	0.2700E+02
6.0	0.2700E+02	0.2700E+02	0.2700E+02	0.2700E+02	0.2700E+02
7.0	0.2700E+02	0.2700E+02	0.2700E+02	0.2700E+02	0.2700E+02
8.0	0.2700E+02	0.2700E+02	0.2700E+02	0.2700E+02	0.2700E+02
9.0	0.2700E+02	0.2700E+02	0.2700E+02	0.2700E+02	0.2700E+02
10.0	0.2700E+02	0.2700E+02	0.2700E+02	0.2700E+02	0.2700E+02
11.0	0.2700E+02	0.2700E+02	0.2700E+02	0.2700E+02	0.2700E+02
12.0	0.2700E+02	0.2700E+02	0.2700E+02	0.2700E+02	0.2700E+02

CONCRETE NODAL TEMPERATURE PROFILES.

TIME	TBF(1)	TBF(2)	TBF(8)	TCF(1)	TCF(8)
13.0	0.2700E+02	0.2700E+02	0.2700E+02	0.2700E+02	0.2700E+02
14.0	0.2700E+02	0.2700E+02	0.2700E+02	0.2700E+02	0.2700E+02
15.1	0.2700E+02	0.2700E+02	0.2700E+02	0.2700E+02	0.2700E+02
16.0	0.2700E+02	0.2700E+02	0.2700E+02	0.2700E+02	0.2700E+02
17.0	0.2700E+02	0.2700E+02	0.2700E+02	0.2700E+02	0.2700E+02
18.0	0.2700E+02	0.2700E+02	0.2700E+02	0.2700E+02	0.2700E+02
19.1	0.2700E+02	0.2700E+02	0.2700E+02	0.2700E+02	0.2700E+02
20.1	0.2700E+02	0.2700E+02	0.2700E+02	0.2700E+02	0.2700E+02
21.1	0.2700E+02	0.2700E+02	0.2700E+02	0.2700E+02	0.2700E+02
22.1	0.2700E+02	0.2700E+02	0.2700E+02	0.2700E+02	0.2700E+02
23.1	0.2700E+02	0.2700E+02	0.2700E+02	0.2700E+02	0.2700E+02
24.1	0.2700E+02	0.2700E+02	0.2700E+02	0.2700E+02	0.2700E+02
25.1	0.2700E+02	0.2700E+02	0.2700E+02	0.2700E+02	0.2700E+02
30.2	0.2700E+02	0.2700E+02	0.2700E+02	0.2700E+02	0.2700E+02
35.1	0.2700E+02	0.2700E+02	0.2700E+02	0.2700E+02	0.2700E+02
40.1	0.2700E+02	0.2700E+02	0.2700E+02	0.2700E+02	0.2700E+02
45.2	0.2700E+02	0.2700E+02	0.2700E+02	0.2700E+02	0.2700E+02
50.0	0.2700E+02	0.2700E+02	0.2700E+02	0.2700E+02	0.2700E+02
55.1	0.2700E+02	0.2700E+02	0.2700E+02	0.2700E+02	0.2700E+02
60.4	0.2700E+02	0.2700E+02	0.2700E+02	0.2700E+02	0.2700E+02

APPENDIX F

LITFIRE Glossary

```
C
C
C  ACTVTY  CALULATES ACTIVITY OF LITHIUM IN LIPB
C  AEHCP   SURFACE AREA OF PRIMARY EXTRANEOUS HEAT CAPACITY  FT2.
C  AEHCS   SURFACE AREA OF SECONDARY EXTRANEOUS HEAT CAPACITY  FT2.
C  AFP     AREA OF THE PRIMARY STEEL FLOOR THAT IS OF INTEREST IN HEAT
C              TRANSFER CALCULATIONS.  USUALLY EQUAL TO "ASLI" WHEN
C              LITHIUM IS SPILLED DIRECTLY ONTO FLOOR.
C  AFS     SURFACE AREA OF SECONDARY STEEL FLOOR LINER  FT2.
C  AHT     SURFACE AREA OR HEAT TRANSFER BETWEEN LITHIUM POOL AND PAN FT2.
C  AINS    OUTSIDE EXPOSED AREA OF INSULATING LAYER ON PAN  (FT2)
C  AKLEAD  THERMAL CONDUCTIVITY OF LEAD  BTU/FT.-SEC. DEG. F
C              INPUT AS BTU/FT. HR. DEG. F
C  AKLI    THERMAL CONDUCTIVITY OF LITHIUM   BTU/FT.-SEC. DEG. F
C              INPUT AS BTU/FT. HR. DEG. F
C  AK1,AK2,AK3ES,AK3EP,AK4H,AK5   PROD. OF THERMAL COND. AND PRANDTL NO.
C              BTU/SEC-FT-DEG. F  SEE RELATED FILM TEMPS. "T"
C  ALLOYI  INITIAL ATOM PERCENT OF LI IN LIPB SPILLED
C  ALPHA   USED IN DETERMINING IF LILP SHOULD BE FIXED AT A MINIMUM
C              EQUAL TO AKLI/(RHLI*CPLI)
C  ALPHA2  USED IN DETERMING PYU TESTS CONDUCTION LIMIT OF THE PAN OR
C              STEEL LINER ON TIM STEP
C  AMIN1   A FORTRAN SUPPLIED STATEMENT THAT DETERMINES THE MINIMUM
C              VALUE OF THE ARGUMENTS LISTED.
C  AMLI    ATOMIC   MASS OF BREEDER
C  AMPB    ATOMIC   MASS OF ALLOY METAL
C  APAN    PAN EXTERNAL AREA FOR HEAT TRANSFER
C  ARE     SURFACE AREA OF BREEDER ELEMENT
C  ASLI    SURFACE AREA OF LITHIUM      FT2
C  ATI     INNER SURFACE AREA OD COOLANT TUBES IN ELEMENT
C  ATO     OUTER SURFACE AREA OF COOLANT TUBES IN ELEMENT
C  AWP     PRIMARY CONTAINMENT EXPOSED WALL AREA    FT2
C  AWS     SECONDARY CONTAINMENT EXPOSED WALL AREA  FT2
C  B       USED IN CALC. THERMAL RESIST. OF LINER-GAP-CONC.   FT.
C  BB      ANALOGOUS TO B , ONLY FOR FLOOR CONCRETE
C  B1,B2,B3EP,B3ES,B4,B4H,B5   COEFFICIENT OF GAS EXPANSION     1/DEG. F
C              SEE RELATED FILM TEMPS.  "T"
C  BETA    THE INVERSE STICKING COEFFICIENT FOR PARTICLES IMPACTING
C              ON A WALL  SEC.
C  BIL     FRACTION CHANGE BETWEEN BILGE AND DELT   USED IN DETERMINING
C              MINIMUM TIME STEP.
C  BILGE   EQUAL TO THE MINIMUM VALUE OF DT1, DT2, DT3, DT4, OR DT5
C              USED IN CALCULATING THE TIME STEP
C  BLIN    TIME AFTER SPILL AT WHICH INERT GAS FLOODING AND
C              EXHAUST BEGINS   SEC
C  BLOUT   TIME AFTER SPILL AT WHICH FLOODING AND EXHAUST STOPS  SEC
C  BLOWR   INERT GAS INPUT RATE  LB/SEC
C  BLOWV   INERT GAS INPUR RATE   FT3/MIN
C  BREAKS  OUTER CELL TEMP. RATE OF CHANGE DUE TO CELL GAS LEAKAGE
C  BREDTH  LENGTH AROUND THE SIDE OF THE SPILL PAN   IN FEET
C
C**** "C" IS THE INITIAL USED FOR INDICATIONG A THERMAL DIFFUSIVITY.  I.E., A
C  CONDUCTIVITY BETWEEN TWO NODES DIVIDED BY THE HEAT CAPACITY OF ONE OF
C  THOSE NODES
C  C1      CONTAINMENT GAS TO WALL STEEL          IN GAS
C  C2      PAN TO CONT GAS                        IN GAS
C  C3      STEEL LINER TO CONCRETE WALL           IN WALL
C  C4(I)   CONCRETE NODE I TO NODE I+1            IN WALL CONCRETE
C  C5      CONCRETE WALL TO AMBIENT               IN CONCRETE
C  C6      CONTAINMENT GAS TO WALL STEEL          IN STEEL
C  C7      STEEL LINER TO CONCRETE WALL           IN STEEL
C  C8      STEEL LINER TO CONCRETE FLOOR          IN STEEL
C  C9      STEEL LINER TO CONCRETE FLOOR          IN CONCRETE
C  C10(I)  CONCRETE FLOOR NODE I TO NODE I+1      IN FLOOR CONCRETE
C  C11     STEEL WALL LINER TO AMBIENT (NO CONCRETE OPTION)  IN STEEL
C  C12     STEEL FLOOR LINER TO AMBIENT (NO CONCRETE OPTION) IN STEEL
C  C13     PAN TO GAS                             IN PAN
C  C14     SECONDARY STEEL FLOOR TO SECONDARY GAS IN STEEL
C  C15     SECONDARY STEEL FLOOR TO SECONDARY GAS IN GAS
C  C16     PRIMARY STEEL FLOOR TO PRIMARY GAS     IN STEEL
C  C17     PRIMARY STEEL FLOOR TO PRIMARY GAS     IN GAS
C  C18     PRIMARY STEEL FLOOR TO SECONDARY GAS   IN STEEL
```

```
C  C19      PRIMARY STEEL FLOOR TO SECONDARY GAS   IN GAS
C  C20      PRIMARY STEEL WALL TO SECONDARY GAS    IN STEEL
C  C21      SECONDARY STEEL LINER TO SECONDARY CELL GAS   IN STEEL
C  C22      PRIMARY STEEL WALL TO SECONDARY GAS           IN GAS
C  C23      SECONDARY STEEL LINER TO SECONDARY CELL GAS   IN GAS
C  CCZ      AMOUNT OF HEAT BEING DEVELOPED IN THE COMB. ZONE  (BTU/SEC)
C  CCZG     COMBUSTION ZONE TO CONTAINMENT GAS     IN GAS
C  CCZP     POOL TO COMBUSTION ZONE                IN POOL
C  CD       COEFFICIENT OF DISCHARGE  (NEAR UNITY)
C  CEHCGP   THERMAL DIFFUSIVITY BETWEEN PRIMARY EXTR. HEAT CAPACITY
C              AND PRIMARY GAS                    IN PRIMARY GAS
C  CEHCGS   THERMAL DIFFUSIVITY BETWEEN SECONDARY EXTR. HEAT CAPACITY
C              AND SECONADRY GAS                  IN SECONDARY GAS
C  CF       THERMAL IMPEDANCE BETWEEN BREEDER ELEMENTS   IN INNER ELEMENT
C  CGCZ     COMBUSTION ZONE TO CONTAINMENT GAS     IN COMBUSTION ZONE
C  CGLI     POOL TO CONTAINMENT GAS (NO COMBUSTION)  IN POOL
C  CGPEHC   THERMAL DIFFUSIVITY BETWEEN PRIMARY GAS AND PRIMARY
C              EXTRANEOUS HEAT CAPACITY    IN EXTR. HEAT CAPACITY
C  CGSEHC   THERMAL DIFFUSIVITY BETWEEN SECONDARY GAS AND SECONDARY
C              EXTRANEOUS HEAT CAPACITY    IN EXTR. HEAT CAPACITY
C  CHP      PRIMARY CONTAINMENT HEIGHT      FT
C  CHS      SECONDARY CONTAINMENT HEIGHT .    FT
C  CIN1PN   STEEL PAN TO INNER INSULATION            IN INSULATION
C  CIN12    INNER TO OUTER INSULATION          IN INNER INSULATION
C  CIN21    INNER TO OUTER INSULATION          IN OUTER INSULATION
C  CLIG     POOL TO CONTAINMENT GAS (NO COMBUSTION)  IN GAS
C  CLIPAN   POOL TO SPILL PAN   IN POOL     (SUSP PAN OPTION)
C  CLIST    LITHIUM POOL TO FLOOR STEEL        IN LITHIUM
C  CMBR     TOTAL COMBUSTION RATE     LB. LI/SEC.-FT2
C  CMBRH    TOTAL COMBUSTION RATE     LB. LI/HR.-FT2
C  CMBRHI   INITIAL COMBUSTION RATE   LB. LI/HR-FT2
C  CMBRN    COMB. RATE FOR NITROGEN REACTION  LB. LI/SEC.-FT2
C  CMBRO    COMB. RATE FOR OXYGEN REACTION   LB. LI/SEC.-FT2
C  CMBRW    COMB. RATE FOR WATER VAPOR REACTION   LB. LI/SEC.-FT2
C  CPA      INERT GAS SPECIFIC   HEAT  BTU/LB.-DEG. F
C  CPAB     SPEC. HEAT OF FLOODING GAS  BTU/LB-DEG.F
C  CPANLI   POOL TO PAN          IN PAN
C  CPAP     SPECIFIC HEAT OF PRIMARY CELL INERT GAS  (BTU/LB DEG F)
C  CPAS     SPECIFIC HEAT OF SECONDARY CELL INERT GAS  (BTU/LB DEG F)
C  CPCON    HEAT CAPACITY OF FLOOR AND WALL CONCRETE
C  CPCZ     LITHIUM POOL TO COMBUSTION ZONE    IN COMBUSTION ZONE
C  CPEHCP   SPECIFIC HEAT OF PRIMARY EXTRANEOUS HEAT CAPACITY (BTU/LB DEG F)
C  CPEHCS   SPECIFIC HEAT OF SECONDARY EXTRANEOUS HEAT CAPACITY (BTU/LB DEG F)
C  CPFAC    used in calculating cpli (cpfac=.004938**tli-6.20741)
C  CPH2      SPECIFIC HEAT OF HYDROGEN GAS
C            SET TO 3.76 BTU/LB-DEG F. IN PROGRAM
C  CPINS     SPECIFIC HEAT OF INSULATION   BTU/LB DEG F
C  CPLEAD    SPECIFIC HEAT OF PURE LEAD
C  CPLI      SPECIFIC HEAT OF LI      BTU/LB. -DEG. F
C  CPLIH     SPECIFIC HEAT OF LITH. HYDROXIDE IN CONT.
C            SET TO 0.67 BTU/LB-DEG. F IN PROGRAM.
C  CPLIN     SPECIFIC HEAT OF LITHIUM NITRIDE        BTU/LB.-DEG. F
C  CPLINP    SPECIFIC HEAT OF LITH. NITRIDE IN PRIMARY CONT.  BTU/LB-DEG. F
C  CPLINS    SPECIFIC HEAT OF LITH. NITRIDE IN SECONDARY CONT. BTU/LB-DEG. F
C  CPLIO     SPECIFIC HEAT OF LITHIUM OXIDE   BTU/LB.-DEG. F
C  CPLIOH    SPECIFIC HEAT OF LIOH          BTU/LB-MOLE F
C  CPLIOP    SPECIFIC HEAT OF LITHIUM OXIDE IN PRIMARY  BTU/LB-DEG F.
C  CPLIOS    SPECIFIC HEAT OF LITHIUM OXIDE IN SECONDARY  BTU/LB-DEG F.
C  CPLI1     MEAN HEAT CAPACITY OF BREEDER AS SOLID    BTU/LB MOLE-R
C  CPMCZ     EFFECTIVE HEAT CAPACITY OF COMB. ZONE   BTU/DEG F
C  CPMH2     HEAT CAPACITY OF HYDROGEN IN CONTAINMENT   BTU/DEG. F
C  CPMLOS    HEAT CAP. OF LITHIUM OXIDE IN PRIMARY CONT.   BTU/DEG. F
C  CPMLOP    HEAT CAP. OF LITHIUM OXIDE IN SECONDARY CONT.  BTU/DEG. F
C  CPMNIP    HEAT CAPACITY OF NITROGEN IN PRIMARY CONT.    BTU/DEG. F
C  CPMNIS    HEAT CAPACITY OF NITROGEN IN SECONDARY CONT.   BTU/DEG. F
C  CPMOXP    HEAT CAPACITY OF OXYGEN IN PRIMARY CONTAINMENT   BTU/DEG. F
C  CPMOXS    HEAT CAPACITY OF OXYGEN IN SECONDARY CONTAINMENT   BTU/DEG. F
C  CPMWA     HEAT CAP. OF WATER VAP. IN CONTAINMENT    BTU/DEG. F
C  CPNIN1    THERMAL DIFFUSIVITY OF STEEL PAN TO INNER INSULATION   IN PAN
C  CPN2P     SPECIFIC HEAT OF NITROGEN GAS IN PRIMARY CONT. BTU/LB-DEG F.
C  CPN2S     SPECIFIC HEAT OF NITROGEN GAS IN SECONDARY CONT. BTU/LB-DEG F.
C  CPO2P     SPECIFIC HEAT OF OXYGEN GAS IN PRIMARY CONT.  BTU/LB-DEG F.
```

```
C  CPO2S    SPECIFIC HEAT OF OXYGEN GAS IN SECONDARY CONT.  BTU/LB-DEG F.
C  CPPAN    SPECIFIC   HEAT OF SPILL PAN      BTU/LB-DEG F
C  CPPB     HEAT CAPACITY OF ALLOY METAL IN BREEDER ZONE   BTU/LB-F
C  CPPB1    MEAN HEAT CAPACITY OF ALLOY METAL SOLID    BTU/LB MOLE-R
C  CPPL     LIQUID HEAT CAPACITY OF ALLOY METAL      BTU/LB R
C  CPPZ     HEAT CAPACITY OF ALLOY METAL IN REACTION ZONE   BTU/LM F
C  CPSTL    HEAT CAPACITY OF STEEL LINER    (BTU/LB-DEG F)
C  CPWA     SPEC. HEAT OF WATER VAPOR  (SET TO 0.44 BTU/LB.-DEG. F)
C  CP1      USED TO CALCULATE CP CHANGE OF ALLOY METAL     BTU/LB R
C  CP2      USED TO CALCULATE CP CHANGE OF ALLOY METAL   BTU/LB R
C  CRACON   AREA OF CONCRETE EXPOSED TO LITHIUM IN CONCRETE
C              COMBUSTION MODEL FT**2
C  CRACK    AREA OF ORRIFICE BETWEEN PRIMARY AND SECONDARY CONTAINMENTS
C              THE UNITS OF CRACK ARE SQUARE INCHES!!!  CONVERTED TO FT2 IN
C              PROGRAM
C  CSBLI    THERMAL DIFFUSIVITY OF LITHIUM POOL TO FLOOR STEEL   IN STEEL
C  CT       THERMAL IMPEDANCE BETWEEN BREEDER ELEMENTS   IN OUTER ELEMENT
C  DELH     STANDARD HEAT OF HYDROLSIS OF BREEDER      BTU/LB MOLE
C  DELMP    FRACTIONAL EXCHANGE RATE OF PRIMARY GAS  (IN SEC)  USED IN
C              DETERMINING THE MINIMUM TIME STEP
C  DELMS    FRACTIONAL EXCHANGE RATE OF SECONDARY GAS  (IN SEC)  USED IN
C              DETERMINING THE MINIMUM TIME STEP
C  DELOUT   OUT TIME STEP   SEC.
C  DELT     INTEGRATION TIME STEP    SEC.
C  DFILM    LITHIUM VAPOR FILM THICKNESS      FT
C  DFLIPB   DIFFUSION COEFFICIENT FOR LITHIUM THROUGH LEAD  FT**2/SEC
C  DIFF     DIFFUSION  COEFF. TO COMB. ZONE    FT2/SEC.
C  DIFFLI   LITHIUM VAPOR DIFFUSION COEFFICIENT    FT2/SEC
C  DMPBDT   MASS RATE OF CHANGE OF LEAD IN LEAD LAYER   LB/SEC
C  DPROD    ENTHALPY CHANGE OF REACTION PRODUCTS IN REACTION ZONE
C  DP1,DP2,DP3      PSIA INCREASE IN CONTAINMENT PRESSURE DUE TO EACH INJECT
C  DREAC  ENTHALPY CHANGE OF REACTANTS IN REACTION ZONE
C  DTRDT(I) CONC. FLOOR TEMP. RATE OF CHANGE, NODE I   DEG. F/SEC.
C  DTCDT(I) CONC. WALL TEMP. RATE OF CHANGE, NODE I   DEG. F/SEC.
C  DTMIN    MINIMUM TIME STEP TO BE USED   SEC.
C  DT1,... .DT4   USED IN CALCULATING TIME STEP   SEC.
C  DT1      POOL TIME STEP     (TEMP./RATE OF CHANGE OF TEMP.)
C  DT2      CONT. GAS TIME STEP
C  DT3      STEEL WALL TIME STEP
C  DT4      COMBUSTION RATE TIME STEP
C  DT5      COMBUSTION ZONE TEMP. TIME STEP
C  DYNAMI   SUBROUTINE USED IN CONTROLLING INTEGRATION LOOPS
C  D1,D2,D3EP,D3ES,D4,D4H,D5  KINEMATIC   VISCOSITY OF CELL GAS (SQUARED)
C              (FT4/SEC2)  SEE RELATED FILM TEMPS "T"
C  EFILM    FILM DEPTH OF DEPLETED ZONE ABOVE COMB. ZONE (IN INCHES)
C  EMCONC   THERMAL EMISSIVITY OF CONCRETE
C  EMCZ     THERMAL EMISSIVITY OF COMBUSTION ZONE
C  EMF      USED IN FIXING MINIMUM THERMAL EMISSIVITY OF LI POOL
C             SET EQUAL TO .9 IN PROGRAM
C  EMGP     THERMAL EMISSIVITY OF PRIMARY CELL GAS
C             MINIMUM VALUE OF .005 IN PROGRAM
C  EMGS     THERMAL EMISSIVITY OF SECONDARY CELL GAS
C             MINIMUM VALUE OF .005 IN PROGRAM
C  EMINS    THERMAL EMISSIVITY OF INSULATION AROUND PAN
C  EMLI     THERMAL EMISSIVITY OF LITHIUM POOL
C  EMSTL    THERMAL EMISSIVITY OF STEEL LINER
C  ESCR     HEAT REMOVAL RATE BY EMERGENCY SPACE COOLING   BTU/SEC
C  ESCTIN   TIME AFTER SPILL WHEN ESCR BEGINS   SEC
C  EXHSTR   RATE OF CONTAINMENT GAS EXHAUST  LB/SEC
C  EXHSTV   RATE OF CONTAINMENT GAS EXHAUST   FT3/SEC
C  EXX      USED IN CALC. MASS & HEAT TRANSF. COEFF.   1/FT3
C  EX1,EX2,EX3EP,EX3ES,EX4H,EX5  USED IN CALCULATING MASS
C              & HEAT TRANSF. COEFF.  1/FT  SEE RELATED FILM TEMPS  "T"
C  FCT1,FCT2,FCT3     FRACTION OF NITROGEN PRESENT IN EACH INJECTION(BY NO.)
C  FF1,FF2  USED IN HEAT BALANCE EQS. FOR SPRAY FIRE   BTU
C  FMLEAK   FRACT. OF MASS LEAKED OUT OF CONTAINMENT
C  FMLEFT   FRACTION OF MASS STILL WITHIN CONTAINMENT
C  FNIP     WT. FRACTION OF NITROGEN IN PRIMARY CELL GAS
C  FNIS     WT. FRACTION OF NITROGEN IN SECONDARY CELL GAS
C  FOUTP    LOSS RATE OF PRIMARY CONT. GAS WHICH EITHER LEAKS OR IS EXHAUSTED
C  FOUTS    LOSS RATE OF SECONDARY CONT. GAS WHICH EITHER LEAKS OR IS EXHAUSTED
C  FOUTT    TOTAL LEAKAGE FROM OUTERMOST CONTAINMENT (FOUTS+LEAK)
```

```
C  FOXP     WT. FRACTION OF OXYGEN IN PRIMARY CELL GAS
C  FOXS     WT. FRACTION OF OXYGEN IN SECONDARY CELL GAS
C  FPG      RADIATIVE VIEW FACTOR FROM POOL TO GAS (1.0 IF NO PAN,0.23 IF PAN)
C  FPW      RAD. VIEW FACTOR FROM POOL TO WALL (1.0 IF NO PAN,0.384 IF PAN)
C  FRA      FRACTION OF COMBUSTION PRODUCTS EVOLVED INTO CELL GAS
C  FWAP     WT. FRACTION OF WATER VAPOR IN PRIMARY CELL GAS
C  FWAS     WT. FRACTION OF WATER VAPOR IN SECONDARY CELL GAS
C  GAP      AIR GAP BETWEEN STEEL LINER AND CONCRETE FLOOR (INPUT AS FT.)
C  GAMMA    RATIO OF SPECIFIC HEATS Cp/Cv  (SET = 1.4)
C  GIN      GRAVITATIONAL CONSTANT     32.2 FT/SEC**2
C  HGWP     INTERIOR FILM COEF.   BTU/SEC-FT**2-DEG. F
C  HA       EXTERIOR FILM COEF.   BTU/SEC. FT**2-DEG. F
C  HB       HEAT TRANSFER COEFFICIENT TO POOL   BTU/SEC-FT2-DEG F
C  HBINF    EQUILIBRIUM VALUE OF HB
C  HCO      HEAT TRANSFER COEFICIENT OF BOILING WATER   BTU/SEC-FT**2-DEG F.
C  HEHCP    HEAT TRANSFER COEFFICIENT OF PRIMARY CELL EXTRANEOUS HEAT
                CAPACITY TO PRIMARY GAS     BTU/SEC-FT**2-DEG F.
C  HEHCS    HEAT TRANSFER COEFFICIENT OF SECONDARY CELL EXTRANEOUS HEAT
                CAPACITY TO SECONDARY CELL GAS     BTU/SEC-FT**2-DEG F.
C  HF       GAS TRANSPORT COEFF. TO POOL    FT/SEC.
C  HFPGP    HEAT TRANSFER COEFFICIENT FROM PRIMARY FLOOR STEEL TO
C             PRIMARY CELL GAS   BTU/SEC-FT**2-DEG F.
C  HFPGAS   HEAT TRANSFER COEFFICIENT FROM PRIMARY FLOOR STEEL TO
C             SECONDARY CELL GAS    BTU/SEC-FT**2-DEG F.
C  HFINF    EQUILIBRIUM VALUE OF HF
C  HIN      CORRELATION FOR HEAT TRANSFER COEFFICIENT  (H, HB, HF)
C  HINECP   CORRELATION FOR HEAT TRANSFER COEFFICIENT  FOR PRIMARY
C             CELL EXTRANEOUS HEAT CAPACITY   DIMENSIONLESS
C  HINECS   CORRELATION FOR HEAT TRANSFER COEFFICIENT  FOR SECONDARY
C             CELL EXTRANEOUS HEAT CAPACITY   DIMENSIONLESS
C  HINFGS   CORRELATION FOR HEAT TRANSFER COEFFICIENT  (HFPGAS)
C  HINGSP   CORRELATION FOR HEAT TRANSFER COEFFICIENT  (HGWP)
C  HINGSS   CORRELATION FOR HEAT TRANSFER COEFFICIENT  (HSEC)
C  HINPS    CORRELATION FOR HEAT TRANSFER COEFFICIENT  (HWPGAS)
C  HINBAM   CORRELATION FOR HEAT TRANSFER COEFFICIENT  (HAWBAM)
C  HINSAM   CORRELATION FOR HEAT TRANSFER COEFFICIENT  (HA)
C  HPAN     HEAT TRANSFER COEFFICIENT TO PAN  BTU/SEC-FT**2-DEG F.
C  HSEC     HEAT TRANSFER COEFFICIENT FROM SECONDARY STEEL WALL LINER
              TO SECONDARY CELL GAS    BTU/SEC-FT**2-DEG F.
C  HTCPGP   HEAT CAPACITY OF PRIMARY CONTAINMENT ATMOSPHERE  BTU/DEG.F
C  HTCPGS   HEAT CAPACITY OF SECONDARY CONTAINMENT ATMOSPHERE  BTU/DEG.F
C  HWPGAS   HEAT TRANSFER COEFFICIENT FROM PRIMARY STEEL WALL TO
C             SECONDARY CELL GAS    BTU/SEC-FT**2-DEG F.
C  I        GENERAL PURPOSE DO LOOP INDEX
C  IAM      DO LOOP INDEX FOR FLOOR AND WALL CONCRETE NODE INITIALIZATION
C  IB       DO LOOP INDEX USED FOR FLOOR CONCRETE ITERATIONS
C  INIT     INITIALIZING SUBROUTINE FOR INTEGRATION CALCULATIONS
C  INJEC1,INJEC2,INJEC3     FLAGS FOR GAS INJECTION ... INJEC=1 INDICATES
C                           THAT THE PARTICULAR INJECTION HAS OCCURRED
C  INTGRL   ARITHMETIC   STATEMENT FUNCTION FOR FINDING INTEGRALS
C  IPAGE    NUMBER OF OUTPUT LINES PER PAGE (BETWEEN HEADINGS)
C  IPASS    SEE SUBROUTINE VARIABLE LIST
C  J1=1     IF LITHIUM IS BREEDER
C  J2=1     IF HYDROGEN IS EVOLVED
C  KLEAK    LEAK RATE CONSTANT FROM CONTAINMENT (INCHES/((LB**0.5)*SEC))
C   NOTE:    UNITS HAVE BEEN INFERRED FROM THE PROGRAM AND MAY NOT
C           BE CORRECT. REFERENCE INPUT VALUE: 2.588E(-09)
C  KCON     THERMAL CONDUCTIVITY OF THE FLOOR AND WALL CONCRETE
C             CONVERTED TO BTU/SEC-FT-DEG F  IN PROGRAM
C  KFILM    THERM. COND. OF LI POOL/COMB. ZONE FILM  BTU/SEC-FT-F
C  KGAP     THERMAL COND. OF THE AIR GAP BETWEEN THE LINER AND CONCRETE
C             CONVERTED TO BTU/SEC-FT-DEG F  IN PROGRAM
C  KIN1     THERMAL CONDUCTIVITY OF INNER INSULATION - CALC. IN PROGRAM
C  KIN2     THERMAL CONDUCTIVITY OF OUTER INSULATION - CALC. IN PROGRAM
C  KPAN     THERMAL CONDUCTIVITY OF LI PAN     BTU/HR-FT-DEG F
C             CONVERTED TO BTU/SEC-FT-DEG F  IN PROGRAM
C  KSTL     THERMAL CONDUCTIVITY OF THE STEEL LINER (BTU/HR-FT-DEG F)
C             CONVERTED TO BTU/SEC-FT-DEG F  IN PROGRAM
C  L        CONCRETE WALL ELEMENT THICKNESS   FT.
C  LBN      DISTANCE BETWEEN TWO BREEDER ELEMENTS
C  LEAK     CELL GAS LEAKAGE RATE FROM OUTERMOST CONTAINMENT   1/SEC.
C  LEAKO    INITIAL CELL GAS LEAKAGE RATE FROM OUTERMOST CONTAINMENT  1/SEC.
```

```
C  LIBP    LITHIUM BURNED IN POOL FIRE       LB.
C  LIL     AMOUNT OF LI LEFT IN POOL , BUT NOT ALLOWED TO BE LESS
C            THAN LIT/10 FOR NUMERICAL STABILITY IN HEAT TRANSFER CALC.
C  LILNI   AMOUNT OF LITHIUM NITRIDE IN POOL  LB.
C  LILOX   AMOUNT OF LITHIUM OXIDE IN POOL  LB.
C  LILP    TRUE AMOUNT OF LITHIUM IN POOL  (LB)
C  LIS     LITHIUM USED IN SPRAY FIRE        LB.
C  LIT     MASS OF LITHIUM IN POOL INITIALLY      LB.
C  L1      CONCRETE FLOOR ELEMENT THICKNESS   FT.
C  MAIP    INITIAL MASS OF INERT GAS IN PRIMARY CONTAINMENT  (LB)
C  MAIS    INITIAL MASS OF INERT GAS IN SECONDARY CONTAINMENT  (LB)
C  MAIRP   WT. OF PRIMARY CELL GAS   LB.
C  MAIRS   WT. OF SECONDARY CELL GAS   LB.
C  MAP     WT. OF INERT GAS IN PRIMARY CELL    LB.
C  MAS     WT. OF INERT GAS IN SECONDARY CELL    LB.
C  MB      MASS OF BREEDER ELEMENT       LB MOLE
C  MCZ     REACTION ZONE MASS        LB MOLES
C  MCZ1    INITIAL REACTION ZONE MASS        LB MOLE
C  MH2P    WT. OF HYDROGEN IN PRIMARY CONT. CELL GAS    LB.
C  MH2S    WT. OF HYDROGEN IN SECONDARY CONT. CELL GAS    LB.
C  MLEAD   MASS OF LEAD IN LEAD LAYER ABOVE LIPB POOL    LB.
C  MLIHP   WT. OF LITHIUM HRYDROXIDE IN PRIMARY CONT. GAS   LB. -
C  MLIHS   WT. OF LITHIUM HRYDROXIDE IN SECONDARY CONT. GAS   LB.
C  MLINIP  INITIAL MASS OF LITHIUM NITRIDE IN PRIMARY CONT.   LB
C  MLINIS  INITIAL MASS OF LITHIUM NITRIDE IN SECONDARY CONT.   LB
C  MLINP   WT. OF LITHIUM NITRIDE IN PRIMARY CONT. GAS CELL     LB.
C  MLINS   WT. OF LITHIUM NITRIDE IN SECONDARY CONT. GAS CELL     LB.
C  MLIOH   MASS OF LIOH PRODUCT IN LB MOLES
C  MLIOIP  INITIAL MASS OF LITHIUM OXIDE IN PRIMARY CONT.   LB
C  MLIOIS  INITIAL MASS OF LITHIUM OXIDE IN SECONDARY CONT.   LB
C  MLIOP   WEIGHT OF LITHIUM OXIDE IN PRIMARY CELL GAS.  ALL OT THE
C             SPRAY FIRE PRODUCT REMAINS IN THE CELL GAS.  A FRACTION
C             OF THE PRODUCTS FROM THE POOL FIRE IS ADDED     LB.
C  MLIOS   WT.  OF LITHIUM OXIDE IN SECONDARY CELL GAS.  LB. (ZERO)
C  MNIINJ  RATE OF INJECTION OF NITROGEN DURING A 60 SEC  INTERVAL
C             USED TO MODEL HEDL PROCEDURE   (LB/SEC)
C  MNIIP   INITIAL WEIGHT OF NITROGEN IN PRIMARY CONTAINMENT   LB
C  MNIIS   INITIAL WEIGHT OF NITROGEN IN SECONDARY CONTAINMENT   LB
C  MNIP    WEIGHT OF NITROGEN IN PRIMARY CONT. CELL GAS     LB.
C  MNIS    WEIGHT OF NITROGEN IN SECONDARY CONT. CELL GAS     LB.
C  MNINJ1,MNINJ2,MNINJ3     MASS OF NITROGEN INJECTED  (LBS)
C  MOINJ1,MOINJ2,MOINJ3     MASS OF OXYGEN INJECTED (LBS.)
C  MOXINJ  RATE OF INJECTION OF OXYGEN USED TO MODEL HEDL EXPERIMENTAL
C              PROCEDURE.   OCCURS DURING A 60 SEC. INTERVAL(LB./SEC.)
C  MOXIP   INITIAL WEIGHT OF OXYGEN IN PRIMARY CONT.   LB.
C  MOXIS   INITIAL WEIGHT OF OXYGEN IN SECONDARY CONT.  LB.
C  MOXP    WEIGHT OF OXYGEN IN PRIMARY CELL GAS    LB.
C  MOXS    WEIGHT OF OXYGEN IN SECONDARY CELL GAS    LB.
C  MPB     MASS OF ALLOY METAL PRODUCT IN LB MOLES
C  MWAP    WEIGHT OF WAT. VAP. IN PRIMARY CONTAINMENT CELL GAS    LB.
C  MWAS    WEIGHT OF WAT. VAP. IN SECONDARY CONTAINMENT CELL GAS    LB.
C  MWAIP   INITIAL MASS OF WATER VAPOR IN PRIMARY CONT. CELL GAS    LB
C  MWAIS   INITIAL MASS OF WATER VAPOR IN SECONDARY CONT. CELL GAS    LB
C  N       INDICE USED TO TRANSFER CONTROL IN SUBROUTINES
C  NA      NUMBER OF ELEMENTS IN BREEDER ZONE
C  NAME(I) INPUT CONTAINING PROGRAM TITLE AND HEADING
C  NL      NUMBER OF CONCRETE WALL NODES
C  NL1     NUMBER OF CONCRETE FLOOR NODES
C  NLM1,NL1M1     WALL AND FLOOR CONCRETE NUMBER OF NODES MINUS ONE
C  NUMCTD  NUMBER OF COOLANT TUBES DAMAGED
C  OUTINT  FRACTION OF THE OUTERMOST CONTAINMENT GAS LEAKED TO AMBIENT
C  OVERP   CONTAINMENT OVER PRESSURE   PSIG
C  OVERPP  PRIMARY CONTAINMENT OVERPRESSURE   PSIG
C  OVERPS  SECONDARY CONTAINMENT OVERPRESSURE  PSIG
C  OXLB    OXYGEN BURNED   LB.
C  OXLBI   OXYGEN BURNED INITIALLY   LB.
C  OXLFS   OXYGEN LEFT AFTER SPRAY FIRE   LB.
C  PAP     GAS PRESSURE IN PRIMARY CELL    PSIA
C  PAPZER  INITIAL PRIMARY CELL PRESSURE  PSIA
C  PAS     GAS PRESSURE IN SECONDARY CELL    PSIA
C  PASZER  INITIAL SECONDARY CELL PRESSURE  PSIA
C  PAZERO  INITIAL CELL PRESSURE   PSIA
```

```
C  PBMELT  MELTING POINT OF ALLOY METAL      R
C  PERCEN  PERCENTAGE BY NUMBER OF PEROXIDE (VS. MONOXIDE) FORMED IN
C             COMBUSTION
C  PLIV    PARTIAL PRESSURE OF LITHIUM VAPOR      PSIA
C  PYU     USED IN SETTING THE MINIMUM TIME STEP  CALCULATED FROM
C              CONDUCTION RATE FROM PAN OR STEEL LINER FROM POOL
C  PZEROP  PRIMARY CONTAINMENT PRESSURE AFTER SPRAY FIRE
C  QC      FORCED CONVECTIVE COOLING HEAT FLOW
C  QCCONC  HEAT OF COMB. FOR CONCRETE REACTION   BTU/LB. LI
C  QCN     HEAT OF COMB. FOR NITROGEN REACTION   BTU/LB. LI
C  QCO     HEAT OF COMBUSTION FOR OXYGEN REACTION    BTU/LB. LI
C  QCO1    HEAT OF COMBUSTION FOR MONOXIDE REACTION     BTU/LB. LI
C  QCO2    HEAT OF COMBUSTION FOR PEROXIDE REACTION     BTU/LB. LI
C  QCW     HEAT OF COMB. FOR REACTION WITH WATER VAPOR    BTU/LB. LI
C  QIN     HEAT ADDITION TO CELL GAS FROM SPRAY FIRE   BTU
C  QLIOH   LATENT HEAT OF MELTING FOR LIOH       BTU/LB-MOLE
C  QMELT   HEAT OF FUSION OF BREEDER       BTU/LB MOLE
C  QMELTP  HEAT OF FUSION OF ALLOY METAL       BYU/LB MOLE
C  QOUT1,2,3,4    USED IN HEAT BALANCE EQS. FOR SPRAY FIRE    BTU
C  QRAD    INDICATES A RADIATIVE HEAT FLOW     BTU/SEC
C  QRAOB   FROM STEEL FLOOR (PAN) TO FLOOR CONC. OR TO AMBIENT
C  QRADC   FROM STEEL WALL TO WALL CONCRETE OR TO AMBIENT
C  QRADCG  FROM SPILL PAN TO CELL GAS
C  QRADFS  FROM PRIMARY STEEL FLOOR TO SECONDARY STEEL WALL
C  QRADG   FROM LI POOL TO GAS (NO COMB.) OR FROM COMB ZONE TO CELL GAS
C  QRADP   FROM COMB. ZONE TO LITHIUM POOL (COMB. ZONE MODEL ONLY)
C  QRADPG  FROM PRIMARY STEEL WALL TO SECONDARY CELL GAS
C  QRADPS  FROM PRIMARY STEEL WALL TO SECONDARY STEEL WALL
C  QRADS   FROM SPILL PAN TO STEEL FLOOR
C  QRADW   FROM COMB ZONE TO WALL STEEL OR FROM LI POOL TO WALL STEEL
C  QVAP    HEAT OF VAPORIZATION OF LITHIUM     BTU/LB
C  QWA     HEAT OF REACTION OF BREEDER WITH WATER
C  RA      MEAN RADIUS OF COMBUSTION PRODUCT PARTICLES    MICRONS
C  RAREA   SURFACE AREA OF REACTION ZONE
C
C   THE SYMBOL "R" DESIGNATES A TEMPERATURE RATE OF CHANGE IN SOME NODE
C   DUE TO RADIATION HEAT TRANSFER BETWEEN THAT NODE AND SOME OTHER NODE
C  RADB    IN FLOOR STEEL DUE TO RAD. TO FLOOR CONC. OR TO AMBIENT
C  RADC    IN WALL STEEL DUE TO RAD. TO CONCRETE OR TO AMBIENT
C  RADCB   IN FLOOR CONCRETE   FROM STEEL FLOOR (PAN)
C  RADCC   IN WALL CONCRETE   FROM STEEL WALL
C  RBREAK  TEMP. RATE OF CHANGE OF PRIMARY CELL GAS DUE TO GAS LEAKAGE
C  RCMBH2  STOICH. COMB. RATIO FOR H2O VAPOR REACT.   LB. LI/LB. H2
C  RCMBN   STOICH. COMB. RATIO OF NITROGEN REACT.   LB. LI / LB. N
C  RCMBO   STOICH. COMB. RATIO FOR OXYGEN REACTION  LB. LI/LB. O
C  RCMBO1  STOICH. COMB. RATIO FOR MONOXIDE REACTION     LB. LI/LB. O
C  RCMBO2  STOICH. COMB. RATIO FOR PEROXIDE REACTION     LB. LI/LB. O
C  RCMBW   STOICH. COMB. RATIO FOR WAT. VAP. REACT.  LB. LI/LB. H2O
C  RCZG    IN GAS    FROM COMBUSTION ZONE
C  RCZP    IN LITHIUM POOL  FROM COMBUSTION ZONE
C  RCZW    IN WALL STEEL   FROM COMBUSTION ZONE
C  RELERR  MAXIMUM ALLOWABLE FRACTIONAL TEMP. CHANGE ACROSS A SINGLE
C                INTEGRATION STEP.  USED TO VARY TIME STEP.
C  RGASPA  IN PAN DUE TO RAD. TO CONTAINMENT GAS
C  RGLI    IN POOL DUE TO RAD. TO GAS  (NO COMB)
C  RHCON   DENSITY OF FLOOR AND WALL CONCRETE
C  RHINS   DENSITY OF INSULATING LAYER ON PAN
C  RHLEAD  DENSITY OF PURE LEAD   LB./FT**3
C  RHLI    DENSITY OF LITHIUM   LB. / FT3
C  RHOAIP  INITIAL DENSITY OF PRIMARY CELL GAS   LB/FT3
C  RHOAIS  INITIAL DENSITY OF SECONDARY CELL GAS   LB/FT3
C  RHOAP   DENSITY PRIMARY CELL GAS LB/FT3
C  RHOAS   DENSITY SECONDARY CELL GAS LB/FT3
C  RHOLIH  DENSITY OF LITHIUM HYDROXIDE   LB/FT3
C  RHOLIN  DENSITY OF LITHIUM NITRIDE    LB/FT3
C  RHOLIO  DENSITY OF LITHIUM OXIDE   LB/FT3
C  RHOLIV  LITHIUM VAPOR DENSITY ABOVE POOL      LB/FT3
C  RHPAN   DENSITY OF LI SPILL PAN          LBS/FT**3
C  RHPB    DENSITY OF ALLOY METAL     ·LB-MOLE/FT3
C  RHSTL   DENSITY OF STEEL LINER  (LB/FT3)
C  RIFCZG  RADIATIVE INTERCHANGE FACTOR BETWEEN COMB. ZONE AND THE
C              PRIMARY CELL GAS
```

```
C  RIFCZP  RADIATIVE INTERCHANGE FACTOR BETWEEN COMB. ZONE AND
C             THE POOL SURFACE
C  RIFCZW  RADIATIVE INTERCHANGE FACTOR BETWEEN COMB. ZONE AND
C             CONTAINMENT WALLS
C  RIFFPS  RADIATIVE INTERCHANGE FACTOR BETWEEN PRIMARY STEEL FLOOR
C             AND SECONDARY STEEL FLOOR
C  RIFPAG  RADIATIVE INTERCHANGE FACTOR      PAN TO GAS
C  RIFPAS  RADIATIVE INTERCHANGE FACTOR      PAN TO STEEL FLOOR
C  RIFPG   RAD. INT. FAC. BETWEEN POOL AND PRIMARY CELL GAS
C  RIFPGA  RAD. INT. FAC. BETWEEN PRIMARY STEEL WALL AND SECONDARY GAS
C  RIFPS   RAD. INT. FAC. BETWEEN PRIMARY AND SECONDARY CELLS
C  RIFPW   RAD. INT. FACT. BETWEEN POOL AND WALL
C  RIFSLC  RADIATIVE INTERCHANGE FACTOR BETWEEN STEEL LINER
C               AND CONCRETE SURFACE
C  RIN     UNIVERSAL GAS CONSTANT   1545 FT. LBF./LB.MOLE-DEG. F
C  RINP    PRIMARY CELL RIN
C  RINS    SECONDARY CELL RIN
C  RLIG    IN GAS DUE TO RAD. FROM POOL  (NO COMBUSTION)
C  RLIW    IN WALL STEEL   FROM LITHIUM POOL  (NO COMB)
C  RNILB   RATE OF NITROGEN CONSUMPTION       LB./ SEC
C  RN2     DEGREE TO WHICH NITROGEN-LI REACTION OCCURS.  VALUE IS
C             BETWEEN ZERO AND ONE (=0 FOR NO REACTION, =1 FOR COMPLETE)
C  ROXLB   RATE OF OXYGEN CONSUMPTION BY POOL FIRE   LB./SEC.
C  RPAGAS  IN CELL GAS DUE TO RAD. FROM LI PAN
C  RPANST  IN WALL STEEL DUE TO RAD. FROM LITHIUM PAN
C  RRAD    INITIAL RADIUS OF REACTION ZONE         FT
C  RSTPAN  IN PAN DUE TO RAD. TO FLOOR STEEL
C
C  RTLI,RTG,RADB,RADW,RADCB,RADCW          VARIOUS RATES OF TEMP.
C             CHANGE OF NODES   DEG. F/SEC.
C
C  RVOL    INITIAL REACTION ZONE VOLUME   FT3
C  RVOL1   REACTION ZONE VOLUME           FT3
C  RWALB   RATE OF WATER VAPOR CONSUMPTION      LB./SEC
C
C  RWCZ,RCZW,RCZG,RADB,RADW,RADCB,RADCW,RLIW,RGLI,RLIG,RSPGS,RWLI,RWPGAS,
C  RWPWS,RWSWP    VARIOUS RATES OF TEMP. CHANGE OF NODES   DEG. F/SEC
C
C  RWLI    IN LITHIUM POOL   FROM RAD. TO WALL STEEL  (NO COMB)
C  R1      COEFFICIENT OF BREEDER IN WATER REACTION EQUATION
C  R2      COEFFICIENT OF ALLOY METAL IN WATER REACTION EQUATION
C  SFLCR   HEAT REMOVAL RATE BY EMERGENCY COOLING OF STEEL
C          FLOOR LINER   BTU/SEC
C  SFLEND  TIME AFTER SPILL WHEN SFLCR ENDS     SEC
C  SFLTIN  TIME AFTER SPILL WHEN SFLCR BEGINS   SEC
C  SIGMA   STEPHAN-BOLTZMAN CONSTANT ...   .1713E-8 BTU/FT**2/HR/R**4
C  SPILL   TOTAL WEIGHT OF LITHIUM SPILLED   LB.
C  SPRAY   WEIGHT FRACTION OF LITHIUM CONSUMED IN THE SPRAY FIRE
C  STICK   RATE AT WHICH AEROSOLS ARE REMOVED FROM PRIMARY DUE TO
C             STICKING TO THE WALL. IF STICK>1.0 EXECUTION IS STOPPED
C             STICK MAY BE DECREASED BY INCREASING "BETA".
C  TA      AMBIENT TEMPERATURE   DEG. F
C  TAU     TIME CONSTANT FOR TRANSIENf NATURAL CONVECTION should
C          be time dependent see marks mail for explanation.
C  TAUCZ   USED TO MODEL COMBUSTION ZONE-POOL COUPLING IN THE RADIATIVE
C          INTERCHANGE FACTORS INSTEAD OF (1.-EMCZ) (DIMENSIONLESS)
C  TB(I)   TEMP. OF ITH NODE OF CONCRETE FLOOR   DEG. R
C  TBIC(I) INITIAL TEMP. OF ITH NODE OF CONCRETE FLOOR   DEG. R
C  TBF, TCF,TGF, ETC.   CORRESPONDING TEMP. IN DEGREES FAHRENHEIT
C  TBLOW   INERT GAS INLET TEMP.  DEG. R
C  TC(I)   TEMP. OF ITH NODE OF CONCRETE WALL   DEG. R
C  TCIC(I) INITIAL TEMP. OF ITH NODE OF CONCRETE WALL   DEG. R
C  TCIGNI  IGNITION TEMPERATURE OF CONCRETE LITHIUM REACTION
C             IN CONCRETE COMBUSTION MODEL   DEG R.
C  TCON    CONCRETE COMBUSTION ZONE TEMPERATURE IN
C             CONCRETE COMBUSTION MODEL    DEG R.
C  TCONF   CONCRETE COMBUSTION ZONE TEMPERATURE IN
C             CONCRETE COMBUSTION MODEL    DEG F.
C  TCZ     COMBUSTION ZONE TEMPERATURE    DEG R
C  TCZF    COMBUSTION ZONE TEMP.  DEG F.
C  TCZI    INITIAL VALUE OF COMB. ZONE TEMP.    DEG R
C  TE      EQUILIBRIUM TEMP. RESULTING FROM SPRAY FIRE   DEG. R
```

```
C  TEHCP    TEMP. OF PRIMARY EXTRANEOUS HEAT CAPACITY NODE DEG R.
C  TEHCPF   TEMP. OF PRIMARY EXTRANEOUS HEAT CAPACITY NODE DEG F.
C  TEHCS    TEMP. OF SECONDARY EXTRANEOUS HEAT CAPACITY NODE DEG R.
C  TEHCSF   TEMP. OF SECONDARY EXTRANEOUS HEAT CAPACITY NODE DEG F.
C  TEHCZP   INITIAL TEMP. OF PRIMARY EXTRANEOUS HEAT CAPACITY NODE DEG R.
C  TEHCZS   INITIAL TEMP. OF SECONDARY EXTRANEOUS HEAT CAPACITY NODE DEG R.
C  TET1     USED IN CALCULATING THERMAL CONDUCTIVITY OF INNER
C               PAN INSULATION   SEE KIN1
C  TET2     USED IN CALCULATING THERMAL CONDUCTIVITY OF OUTER
C               PAN INSULATION   SEE KIN2
C  TEZ      AVERAGE OF COMBUSTION ZONE TEMP. AND LITHIUM POOL TEMP.
C                USED IN TEST FOR COMBUSTION CONDITION
C  TFEFF    NORMALIZED TEMP. OF LI POOL/COMB. ZONE FILM
C  TGF      CONTAINMENT GAS TEMP. IN FARENHEIT
C  TGP      PRIMARY CELL GAS TEMP. AFTER SPRAY FIRE   DEG. R.
C  TGPF     PRIMARY CELL GAS TEMP. DEG F.
C  TGPZER   INITIAL PRIMARY CELL GAS TEMP.     DEG. R.
C  TGS      SECONDARY CONT. CELL GAS TEMP.  DEG R.
C  TGSF     SECONDARY CONT. CELL GAS TEMP.  DEG F.
C  TGSZER   INITIAL SECONDARY CELL GAS TEMP.     DEG. R.
C  THFC     CONCRETE FLOOR THICKNESS   INPUT AS FT.
C  THFP     PRIMARY STEEL FLOOR THICKNESS  INPUT AS FT.
C  THFS     SECONDARY STEEL FLOOR THICKNESS  INPUT AS FT.
C  THKIN1   INNER INSULATION THICKNESS INPUT AS FT.
C  THKIN2   OUTER INSULATION THICKNESS INPUT AS FT.
C  THKPAN   SPILL PAN THICKNESS IN FEET   (INPUT AS FT.)
C  THPB     THICKNESS OF LEAD LAYER ABOVE LIPB POOL
C  THWC     CONCRETE WALL THICKNESS    INPUT AS FT.
C  THWP     PRIMARY STEEL WALL THICKNESS  INPUT AS FT.
C  THWS     SECONDARY STEEL WALL THICKNESS INPUT AS FT.
C  TIME     TIME AFTER SPILL HAS OCCURRED   SEC.
C  TIMEF    STOP INTEGRATION TIME   SEC.
C  TIMEO    OUTPUT TIME INDICATOR    SEC.
C  TINS1    TEMP. OF INNER NODE OF INSULATION   DEG R.
C  TINS1F   TEMP. OF INNER NODE OF INSULATION   DEG F.
C  TINS1I   INITIAL TEMP. OF INNER NODE OF INSULATION   DEG R.
C  TINS2    TEMP. OF OUTER NODE OF INSULATION   DEG R.
C  TINS2F   TEMP. OF OUTER NODE OF INSULATION   DEG F.
C  TINS2I   INITIAL TEMP. OF OUTER NODE OF INSULATION   DEG R.
C  TLEAD    TEMP. OF LEAD LAYER IN POOL   DEG R.
C  TLEADF   TEMP. OF LEAD LAYER IN POOL   DEG F.
C  TLEADI   INITIAL TEMP. OF LEAD LAYER IN POOL   DEG R.
C  TLI      LITHIUM TEMP. IN POOL    DEG. R.
C  TLIBS    LITHIUM TEMPERATURE BEFORE SPRAY FIRE  DEG R.
C  TLIF     LITHIUM POOL TEMP. IN FARENHEIT
C  TLII     INITIAL LITHIUM POOL TEMP.  (DEG R)
C  TLIO     INITIAL LITHIUM POOL TEMP.     DEG. R.
C  TMELT    MELTING TEMP. OF LITHIUM   DEG. R.
C  TN       TEMPERATURE OF BREEDER ZONE ELEMENT  DEG R.
C  TO       TEMP. OF CELL GAS BEFORE SPRAY FIRE   DEG. R.
C  TONE,TTWO,TTHREE     TIME IN SECONDS AT WHICH EACH INJECTION OCCURS
C  TPAN     LITHIUM PAN TEMP  (DEG R)    SUSP PAN OPTION
C  TPANF    LITHIUM PAN TEMP  (DEG F)
C  TPANZO   INITIAL PAN TEMPERATURE IN DEGREES R
C  TSFP     PRIMARY STEEL FLOOR LINER TEMP.  DEG. R
C  TSFPF    PRIMARY FLOOR STEEL LINER TEMPERATURE   DEG F.
C  TSFPI    INITIAL PRIMARY STEEL FLOOR LINER TEMP.   DEG.R
C  TSFSI    INITIAL SECONDARY CELL FLOOR LINER TEMP.   DEG R.
C  TSP      PRIMARY CELL STEEL WALL LINER TEMP.   DEG R.
C  TSPF     PRIMARY CELL STEEL WALL LINER TEMP.   DEG F.
C  TSPZER   INITIAL PRIMARY CELL STEEL WALL LINER TEMP.  DEG. R.
C  TSS      SECONDARY CELL STEEL WALL LINER TEMP.  DEG. R.
C  TSSF     SECONDARY CELL STEEL WALL LINER TEMP.  DEG. F.
C  TSSZER   INITIAL SECONDARY CELL STEEL WALL LINER TEMP.  DEG. R
C  TVAP     BOILING POINT OF LITHIUM     DEG. R
C  T1       FILM TEMP. BETWEEN PRIMARY CELL GAS AND POOL   DEG. R
C  T2       FILM TEMP. BETWEEN PRIMARY CELL GAS AND STEEL WALL LINER  DEG. R
C  T3EP     FILM TEMP. BETWEEN PRIMARY CELL GAS AND EXTR. HEAT CAP.  DEG R.
C  T3ES     FILM TEMP. BETWEEN SECONDARY CELL GAS AND EXTR. HEAT CAP.  DEG R.
C  T4       FILM TEMP. BETWEEN SECONDARY GAS AND SECONDARY STEEL WALL  DEG R.
C  T4H      FILM TEMP. BETWEEN AMBIENT AND OUTSIDE STEEL OR CONCRETE WALL
C               DEPENDING IF THERE IS CONCRETE PRESENT   DEG R.
```

```
C  T5       FILM TEMP. BETWEEN PRIMARY STEEL WALL AND SECONDARY GAS  DEG R.
C  T6       FILM TEMP. BETWEEN SECONDARY CELL GAS AND PRIMARY FLOOR  DEG R.
C  T7       FILM TEMP. BETWEEN AMBIENT AND OUTSIDE STEEL FLOOR OR CONCRETE
C               FLOOR DEPENDING IF THERE IS CONCRETE PRESENT  DEG R.
C  USUBA    HEAT TRANSF. COEFF., CONTAINMENT-AMBIENT  BTU/SEC-FT2-DEG. F
C  VCONC    VOLUME OF CONCRETE IN FIRST NODE OF CONCRETE IN THE CONCRETE
C               COMBUSTION MODEL  FT3
C  VP       PRIMARY CONTAINMENT CELL FREE VOLUME     FT3
C  VS       SECONDARY CONTAINMENT CELL FREE VOLUME     FT3
C  VOL      VOLUME OF BREEDER ELEMENT
C  WAB      WEIGHT FRACTION OF INERT GAS IN FLOODING GAS
C  WAP      WT. FRACTION OF INERT GAS IN PRIMARY ATMOSPHERE
C  WAS      WT. FRACTION OF INERT GAS IN SECONDARY ATMOSPHERE
C  WATER    AMOUNT OF WATER THAT SHOULD BE LEFT IN CONCRETE TOP NODE
C               ACCORDING TO THE CORRELATION USED    LBS/FT3
C  WFP      THICKNESS OF PRIMARY FLOOR STEEL LINER   (INPUT AS FT.)
C  WN2P     WEIGHT FRACTION OF NITROGEN IN PRIMARY ATMOSPHERE
C  WN2S     WEIGHT FRACTION OF NITROGEN IN SECONDARY ATMOSPHERE
C  WN2B     WEIGHT FRACTION OF NITROGEN IN FLOODING GAS
C  WO2P     WEIGHT FRACTION OF OXYGEN IN PRIMARY ATMOSPHERE
C  WO2S     WEIGHT FRACTION OF OXYGEN IN SECONDARY ATMOSPHERE
C  WO2B     WEIGHT FRCTION OF OXYGEN IN FLOODING GAS
C  WP       THICKNESS OF PRIMARY STEEL POOL LINER  (INPUT AS FT.)
C  WS       THICKNESS OF SECONDARY STEEL POOL LINER (INPUT AS FT.)
C  WWAB     WT. FRACTION OF WATER VAPOR IN FLOODING GAS
C  WWAP     WEIGHT FRACTION OF WATER VAPOR IN PRIMARY CONTAINMENT ATMOSPHERE
C  WWAS     WEIGHT FRACTION OF WATER VAPOR IN SECONDARY CONTAINMENT ATMOSPHERE
C  XALLOY   ATOM PERCENT LITHIUM IN LIPB POOL
C  XBLOW    USED IN CONJUNCTION WITH IBLOW
C  XESC     USED IN CONJUNCTION WITH IESC
C  XLI      WEIGHT FRACTION OF LITHIUM IN LIPB ALLOY
C  XLIDOT   MASS FLOW RATE OF LITHIUM THROUGH LEAD LAYER ABOVE LIPB POOL  LB/SEC
C  XMAIRP   AMOUNT OF GAS IN PRIMARY CONTAIMENT AFTER SPRAY   LB.-MOLES
C  XMAIRS   AMOUNT OF GAS IN SECONDARY CONTAIMENT AFTER SPRAY   LB.-MOLES
C  XMDOT    MASS FLOW RATE OF GAS BETWEEN PRIMARY AND SECONDARY CONT. (LB./SEC)
C  XMEHCP   MASS OF PRIMARY EXTRANEOUS HEAT CAPACITY  LBm.
C  XMEHCS   MASS OF SECONDARY EXTRANEOUS HEAT CAPACITY  LBm.
C  XMH2OI   INITIAL MASS OF WATER IN CONCRETE IN CONCRETE COMBUSTION
C               OPTION    LBm.
C  XMOLP    MOL. WEIGHT OF PRIMARY CONTAINMENT GAS   LB./LB.-MOLE
C  XMOLS    MOL. WEIGHT OF SECONDARY CONTAINMENT GAS   LB./LB.-MOLE
C  XMOLA    MOLECULAR WT. OF INERT GAS   LB./LB.-MOLE
C  XMOLAR   MOL. WT. OF INERT FLOODING GAS
C  XPB      WEIGHT FRACTION OF ALLOY METAL
C  XSFL     INDICATES EMERGENCY COOLING OF FLOOR STEEL
C               XSFL=0. FOR NO COOLING , XSFL=1. FOR COOLING
C               (1/SEC.)
C  YALICZ   EFFECTIVE THERMAL ADMITTANCE,  FILM-COMB. ZONE BTU/SEC-DEG. F
C  YALIG    EFFECTIVE THERMAL ADMITTANCE, POOL-CELL GAS BTU/SEC-DEG. F
C  YAPCZ    EFFECTIVE THERMAL ADMITTANCE POOL-COMB. ZONE  BTU/SEC-DEG F
C  YPAGAS   EFFECTIVE THERMAL ADMITTANCE  PAN-PRIMARY CELL GAS BTU/SEC-DEG F
C  ZLI      THICKNESS OF LITHIUM NODE     FT.
C  ZP       USED TO DETERMINE EMLI IF EMLI.LT.0.9
C  ZZ       TEMPERATURE RATE OF CHANGE IN BREEDER ELEMENT
C  ZZ1      POOL TEMP. RATE OF CHANGE   DEG. F/SEC.
C  ZZ2      LI SPILL PAN TEMP. RATE OF CHANGE  (DEG R/SEC)
C  ZZ3      SECONDARY CELL GAS TEMPERATURE RATE OF CHANGE  (DEG. R/SEC)
C  ZZ4      PRIMARY CELL GAS TEMP. RATE OF CHANGE   DEG. F/SEC.
C  ZZ5      STEEL WALL LINER TEMP. RATE OF CHANGE   DEG. F/SEC.
C  ZZ6      COMB. ZONE TEMP. RATE OF CHANGE    DEG. F/SEC
C  ZZ7      FLOOR STRUCTURE TEMP. RATE OF CHANGE   DEG. F/SEC.
C  ZZ8      INNER INSULATION TEMP. RATE OF CHANGE  (SUSP. PAN OPTION)
C  ZZ9      OUTER INSULATION TEMP. RATE OF CHANGE  (SUSP. PAN OPTION)
C  ZZ99     USED TO ENSURE POSITIVE COMBUSTION RATE
C  ZZEP     PRIMARY CELL EXTRANEOUS HEAT CAPACITY TEMP. RATE OF CHANGE
C               DEG R./SEC
C  ZZES     SECONDARY CELL EXTRANEOUS HEAT CAPACITY TEMP. RATE OF CHANGE
C               DEG R./SEC
C  ZZPB     LEAD LAYER ABOVE LIPB POOL TEMPERATURE RATE OF CHANGE    DEG R/SEC
C  ZZS      SECONDARY CONTAINMENT CELL STEEL WALL TEMPERATURE RATE OF
C               CHANGE    DEG R./SEC
C
```

```
C    PROGRAM DECISION FLAGS
C
C  IAROSL= 1  AEROSOL REMOVAL FROM PRIMARY CONTAINMENT DUE TO AEROSOL
C             STICKING TO THE WALL.
C       = 0  NO AEROSOL REMOVAL.
C
C  IBLOW = 1  FLOOD CONTASINMENT WITH INERT GAS
C       = 0  NO CONTAINMENT FLOODING
C
C  ICMB  = 0  NO OXYGEN LEFT AFTER SPRAY FIRE.
C       = 1  THERE IS STILL OXYGEN LEFT AFTER SPRAY FIRE.
C             SET INITIALLY TO 1 AND THEN RESET TO 0 WHEN THE
C             PROGRAM CALCULATES THAT THE OXYGEN HAS RUN OUT.
C
C  ICNI  = 1  NITROGEN REACTIONS POSSIBLE.
C       = 0  NITROGEN REACTIONS NOT POSSIBLE.
C
C  ICZ   = 1  COMBUSTION ZONE MODEL USED
C       = 0  COMBUSTION ZONE MODEL NOT USED
C
C  IESC  = 1  EMERGENCY SPACE COOLING OPTION
C       = 0  NO EMERGENCY SPACE COOLING
C
C  IL1T  = 0  NO LITHIUM LEFT TO BURN.
C       = 1  LITHIUM LEFT TO BURN (INITIAL CONDITION).
C
C  IMETH = 1  RUNGE-KUTTA METHOD OF INTEGRATION USED.
C       = 3  SIMPSON'S RULE METHOD OF INTEGRATION USED.
C
C  ISFLC = 1  EMERGENCY COOLING OF STEEL FLOOR LINER OPTION
C       = 0  NO EMERGENCY COOLING OF STEEL FLOOR LINER
C
C  ISWICH= 1  CRACK SIZE BECOMES ZERO AFTER INNER AND OUTER CELL
C             PRESSURES EQUILIBRATE IN TWO CELL CALCULATION.
C       = 0  CRACK SIZE REMAINS CONSTANT.
C
C  FLAG2 = .TRUE.   TWO CELL CALCULATION (DEFAUALTS TO 1 CELL IF FALSE)
C
C  FLAGAS= .TRUE.   INJECTIONS OF DRY GAS DURING RUN
C
C  FLAGC = .TRUE.   CONCRETE COMBUSTION (BREACH OF STEEL LINER)
C
C  FLAGD = .TRUE.   CONCRETE COMBUSTION HAS STOPPED
C
C  FLAGDF= .TRUE.   LIPB LAYERED POOL COMBUSTION MODEL IN USE
C
C  FLAGF = .TRUE.   FLOOR CONCRETE
C
C  FLAGL = .TRUE.   LILP IS FIXED AT A MINIMUM
C
C  FLAGM = .TRUE.   SONIC FLOW BETWEEN CONTAINMENTS (CALCULATED IN PROGRAM)
C
C  FLAGN = .TRUE.   SETS N=1 IN SUBROUTINES IN ORDER TO PROPERLY TRANSFER
C                   FLOW THROUGH SUBROUTINES
C
C  FLAGPB= .TRUE.   LIPB POOL COMBUSTION MODEL IN USE
C
C  FLAGPN= .TRUE.   YES ON SUSPENDED PAN GEOMETRY
C
C  FLAGSI= .TRUE.   IF USER WISHES INPUT/OUTPUT IN SI UNITS
C
C  FLAGW = .TRUE.   WALL CONCRETE
```